63-5-6

406309

BRL

MEMORANDUM REPORT NO. 1461
MARCH 1963

406 309

THE RESPONSE OF CYLINDRICAL SHELLS TO EXTERNAL BLAST LOADING

William J. Schuman, Jr.

RDT & E Project No. 1M010501A006

BALLISTIC RESEARCH LABORATORIES

ABERDEEN PROVING GROUND, MARYLAND

B A L L I S T I C   R E S E A R C H   L A B O R A T O R I E S

MEMORANDUM REPORT NO. 1461

MARCH 1963

THE RESPONSE OF CYLINDRICAL SHELLS TO EXTERNAL BLAST LOADING

William J. Schuman, Jr.

Terminal Ballistics Laboratory

Funded Under DASA NWER Sub-Task 02.053

RDT & E Project No. 1M010501A006

A B E R D E E N   P R O V I N G   G R O U N D,   M A R Y L A N D

BALLISTIC RESEARCH LABORATORIES

MEMORANDUM REPORT NO. 1461

WJSchuman/cet
Aberdeen Proving Ground, Md.
March 1963

THE RESPONSE OF CYLINDRICAL SHELLS TO EXTERNAL BLAST LOADING

ABSTRACT

A method of predicting permanent deformation of thin-walled unstiffened cylindrical shells to external blast loading from charges of high explosives is presented. Empirical relations are derived from a series of firings conducted at Aberdeen Proving Ground against scaled shells. The average deviation between the predicted and the actual blast pressures required for permanent deformation is 12%.

TABLE OF CONTENTS

INTRODUCTION

The problem of missile vulnerability is quite complex, involving many factors. A quick resumé of these factors will establish the relationship of the present report to the overall problem.

Missile Condition - A missile may be in the storage, transport, launch, in-flight, or re-entry condition. The missile was considered to be in an unhardened, launch condition in this study.

Kill Mechanisms - A missile is vulnerable in varying degrees to fragments, x-rays, thermal inputs and blast. Blast is the mechanism of concern in this study and it may be further divided into: overturning of the complete missile, excess acceleration loading of internal structural and electrical components, and crushing of the basic structure and internal components. This report will be limited to considerations of crushing damage to the basic structure.

Approach - The problem may be treated theoretically or experimentally. A survey of previous work indicated that some analytical studies had been made at Brooklyn Polytechnic Institute[1*] and Columbia University[2] for various loading and boundary conditions. The Space Technology Laboratories[3] have conducted tests on mylar cylinders with uniform compressive loadings and rise times much slower than those obtained from blast. Avco Corporation[4] has used sheet explosive applied to segments of the surface of a cylinder to obtain deformation. Southwest Research Institute[5] is also studying this problem and has conducted some experimental work with flexural type loadings. Suffield Experimental Station[6] is investigating the details of blast loading of various simple structures, including cylinders.

The lack of experimental data, the complexity of the required theoretical analyses and the urgent need for design data were important factors in deciding that both an experimental and theoretical approach be taken, with the experimental phase receiving precedence. Only the experimental phase of the study will be reported at this time.

* Superscripts refer to references listed at end of report.

Targets - There are three types of targets that might be chosen: actual hardware, scaled-models and simplified models. It was decided to utilize simplified models to define the basic parameters and their relationships before proceeding to the more sophisticated models and actual hardware. The simplified model chosen was a right-circular, thin-walled, unstiffened cylinder.

The primary goal of the first phase of this study was to develop an empirical method of predicting the blast parameters necessary to cause permanent deformation of a wide spectrum of cylinder geometries and materials. The secondary goal was to obtain details of loading and response for correlation and to aid in further studies.

TEST ARRANGEMENTS AND PROCEDURES

Preparation of Models

The cylindrical shells were fabricated from steel and aluminum foil, sheet and tubing. The steel shells were formed from 1040 hot-rolled sheet and butt-welded. The aluminum shells were either sections of 6061-T6 seamless tubing or formed from 1100-0 or 5052-H32 foil and fastened by solder or by cloth-backed adhesive tape. The shell diameters varied from 3 to 24 inches, the lengths from 2 to 48 inches, and the thicknesses from 0.003 to 0.136 inches. These dimensions provided shells that were geometrically scaled and have length-to-diameter ratios of 0.7 to 10 and diameter-to-thickness ratios of 60 to 2000. The dimensions of the shells used are presented in Table I.

A few representative shells were instrumented internally with Baldwin-Lima-Hamilton FAB-25-35, 350-ohm foil strain gages for measuring details of response. One gage pattern is shown in Fig. 1. A solid cylinder (non-responsive) was instrumented with flush-mounted piezoelectric gages for measuring details of loading. The gage pattern is shown in Fig. 2.

The shells were fastened to heavy end caps and this assembly then was fastened over a rigid tube. This tube prevented rotation of the end caps about an axis perpendicular to the longitudinal axis of the shell and therefore minimized bending in the shell. A schematic of the shell and support tube assembly is shown in Fig. 3.

TABLE I
Cylindrical Shell Dimensions

Shell Nos.	Diameter D (in.)	Length L (in.)	Thickness t (in.)	L/D	D/t	Material
1, 2	3.0	6.0	0.019	2.0	158	Steel Sheet - 1040
3 - 6	3.0	8.62	0.019	2.87	158	"
7	3.0	9.0	0.019	3.0	158	"
8, 9	3.0	11.62	0.019	3.87	158	"
10, 11	3.0	14.62	0.019	4.87	158	"
12, 13	3.0	18.0	0.019	6.0	158	"
14, 15	3.0	24.0	0.019	8.0	158	"
16, 17	3.0	8.62	0.035	2.87	86	"
18	3.0	9.0	0.035	3.0	86	"
19	3.0	18.0	0.035	6.0	86	"
20, 21	6.0	18.0	0.019	3.0	316	"
22, 23	6.0	17.5	0.035	2.91	172	"
24	6.0	18.0	0.035	3.0	172	"
25, 26	6.0	17.5	0.076	2.91	79	"
27	6.0	18.0	0.076	3.0	79	"
28, 29	12.0	35.38	0.076	2.94	158	"
30	12.0	35.38	0.136	2.94	88	"
31, 32	24.0	47.25	0.136	1.98	176	"
33	3.0	6.0	0.003	2.0	1000	Alum.Foil - 5052 - H38
34 - 36	3.0	9.0	0.003	3.0	1000	"
37	3.0	15.0	0.003	5.0	1000	"
38 - 40	3.0	9.0	0.006	3.0	500	"
41	3.0	15.0	0.006	5.0	500	"
42	3.0	23.0	0.006	7.67	500	"
43	3.0	30.0	0.006	10.0	500	"
44 - 46	3.0	9.0	0.012	3.0	250	"
47 - 49	3.0	9.0	0.024	3.0	125	"
50 - 53	6.0	18.0	0.003	3.0	2000	"
54 - 56	6.0	18.0	0.006	3.0	1000	"
57, 58	3.0	9.0	0.022	3.0	136	Alum.Tubing - 6061 - T6
59, 60	3.0	9.0	0.042	3.0	71	"
61, 62	6.0	18.0	0.042	3.0	143	"
63	3.0	2.0	0.006	0.67	500	Alum.Foil - 1100 - O
64	3.0	2.0	0.006	1.0	500	"
65	3.0	5.0	0.006	1.67	500	"
66	3.0	6.0	0.006	2.0	500	"
67 - 75	3.0	9.0	0.006	3.0	500	"
76	3.0	12.0	0.006	4.0	500	"
77, 78	3.0	15.0	0.006	5.0	500	"
79	3.0	23.0	0.006	7.67	500	"
80 - 82	3.0	9.0	0.010	3.0	300	"
83, 84	3.0	2.0	0.012	0.67	250	"
85 - 87	3.0	3.0	0.012	1.0	250	"
88 - 91	3.0	9.0	0.012	3.0	250	"
92	6.0	9.0	0.006	1.5	1000	"
93	6.0	11.0	0.006	1.83	1000	"
94	6.0	4.0	0.012	0.67	500	"
95	6.0	6.0	0.012	1.0	500	"
96	6.0	9.0	0.012	3.0	500	"
97, 98	6.0	11.0	0.012	1.83	500	"
99	7.5	7.5	0.063	1.0	119	Alum.(Picatinny Arsenal)
100	7.5	7.5	0.125	1.0	60	Alum.(Picatinny Arsenal)

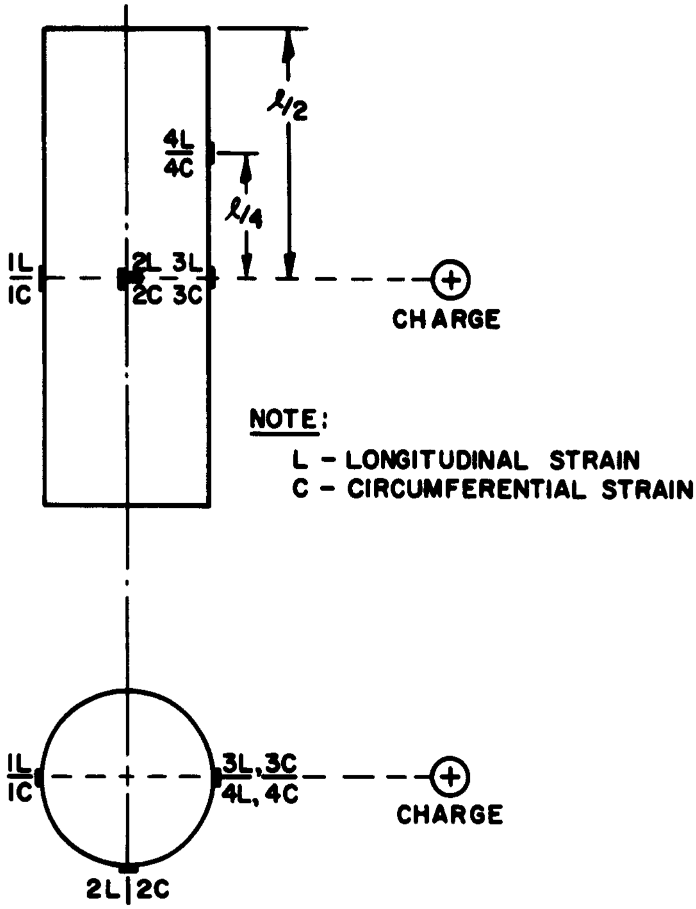

FIG. 1. STRAIN GAGE PATTERN

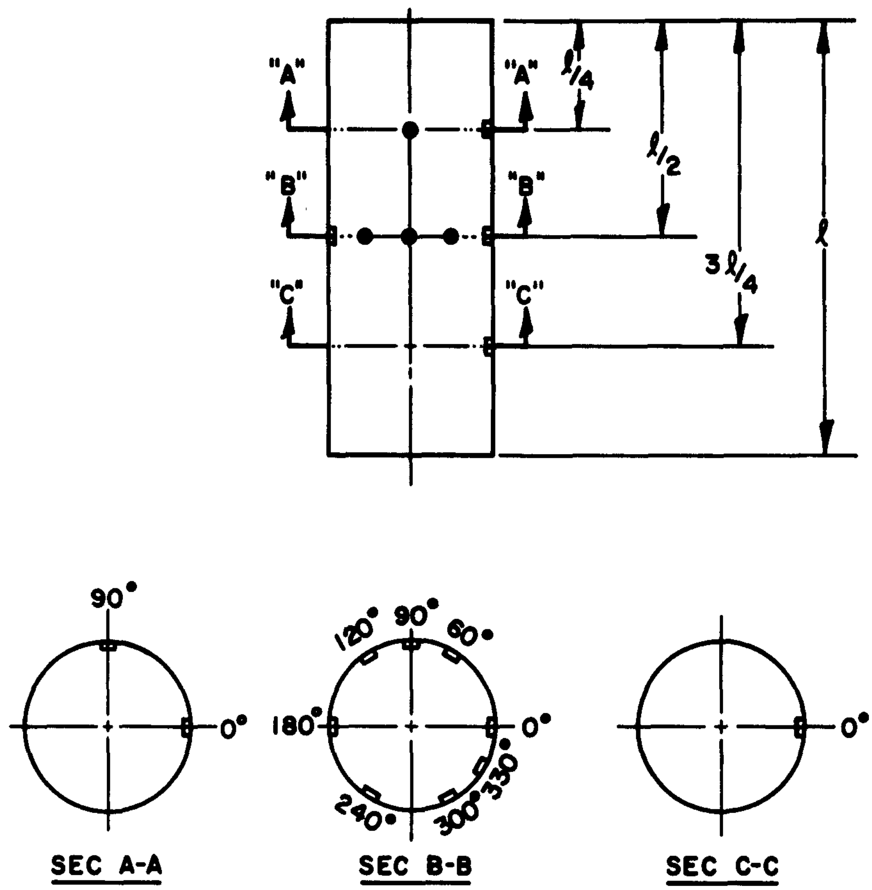

FIG. 2. PRESSURE GAGE PATTERN

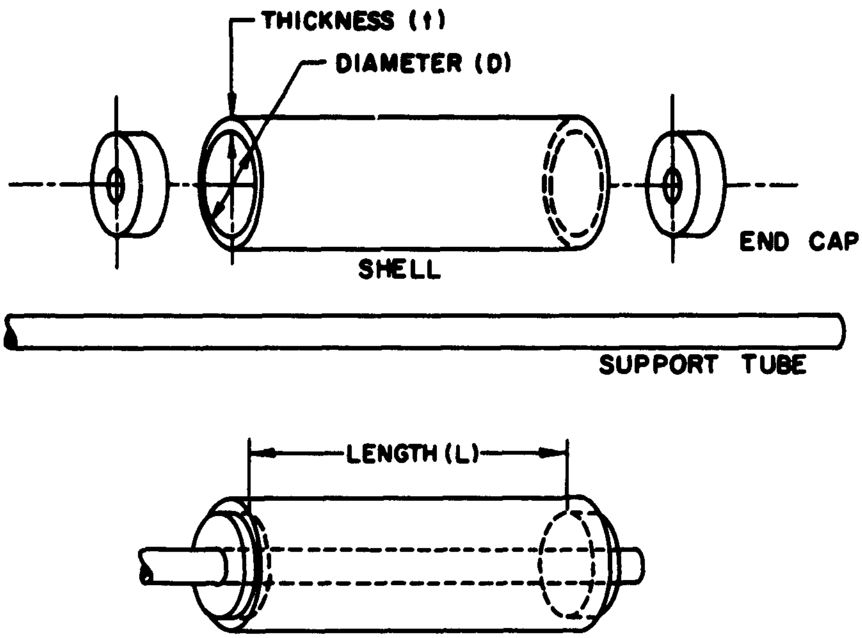

FIG. 3 — TYPICAL SHELL SPECIMEN

Test Arrangements

The blast loading was provided by detonating charges of high explosive (HE) ranging in weight from one pound to 216 pounds. The smaller charges of bare spherical Pentolite was suspended as shown in Fig. 4. The larger charges were placed on the ground. The free air blast parameters; overpressure, impulse, and duration are determined by use of tabulated data[7,8]. (References 9 and 10 define and discuss the various blast parameters.)

The shell and support tube assemblies were mounted on portable stands at a height of 6 feet to minimize ground effects as shown in Figs. 4 and 5. They were oriented with respect to the charge so that the blast impinges on the shells either along a line perpendicular to the longitudinal axis (lateral loading) or along an extension of the longitudinal axis (longitudinal loading). A nose cone was added to the shell for the longitudinal loading orientation to minimize the disturbance of the flow.

Test Procedure

A group of uninstrumented shells were positioned about an explosive charge at various distances such that the pressure levels would be below that required to cause permanent deformation. The shells were then repositioned in increments until optimum deformation - defined in this study as approximately 5% to 10% of the original diameter - was obtained.

The instrumented cylinders were fired on individually because of instrumentation requirements. The signals from the strain gages were recorded by a 16 channel CEC Miller Recording Oscillograph that has a maximum writing speed of 400 in/sec and a frequency response of DC to 200 KC. The signals from the pressure gages were amplified, presented on cathode ray tubes and recorded by General Radio streak cameras. This system has a maximum writing speed of 2500 in/sec and a frequency response of DC to 100 KC.

TEST RESULTS AND DISCUSSION

Uninstrumented Shells

Values of overpressure and impulse for the shells fired on are listed in Tables II and III for the lateral and longitudinal loading orientations.

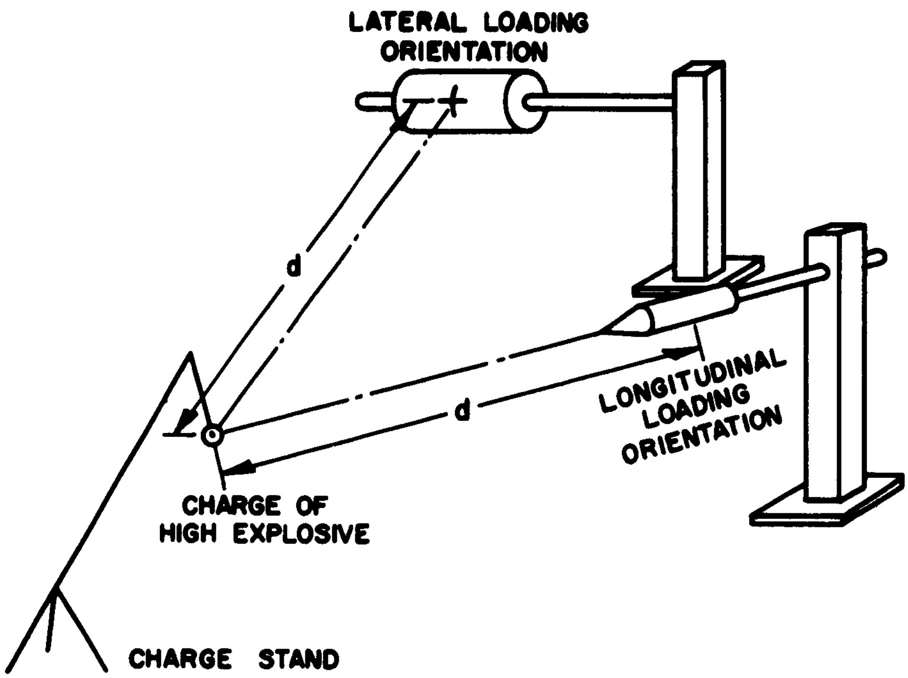

FIG. 4 –TYPICAL FIELD ARRANGEMENT

FIG. 5 — TYPICAL FIELD ARRANGEMENT

TABLE II

Blast Parameters for the Lateral Loading Orientation

Shell No.	Explosive Weight W (lbs)	Explosive Distance d (ft)	Pressure Incident pi (psi)	Pressure Reflected pr (psi)	Impulse Incident Ii (psi-msec)	Impulse Reflected Ir (psi-msec)	Figure* No.	Permanent Deformation
1	9.4	6.0	117	662	28.8	112	1	Optimum
2	389	29.0	60.3	198	89.0	299	2	Greater Than Optimum
4	1.1	2.5	159	1070	15.5	69.5	3, 4	Optimum
5	8.4	7.0	82.4	331	26.9	95.8	5, 6	"
6	64	16.0	58	185	48.8	160	7, 8	"
7	389	33.8	39.7	112	83.2	250	9	"
8	1.1	3.0	118	625	14.5	56.1	10, 11	"
9	8.4	8.0	60.3	199	25.4	83.2	12, 13	"
10	1.1	3.5	82.4	331	13.4	47.9	14, 15	"
11	8.3	9.0	44.8	129	21.6	72.7	16	"
12	8.4	10.0	36.0	97.0	22.6	67.3	17	"
13	389	46.0	19.8	46.3	68.4	190	18, 19	"
14	8.4	11.0	27.9	70.6	20.3	59.9	20	"
15	389	128	2.9	5.95	23.4	50.4	-	None
16	8.4	4.5	213	1590	32.6	153	21	Optimum
17	64	10.0	166	1160	60.8	268	-	None
18	389	23.9	96.7	419	98.5	380	22	Optimum
19	8.4	5.0	172	1240	31.1	138	23	"
20	8.4	10.0	36.0	97.0	22.8	67.3	24	"
21	389	44.0	21.8	320	69.4	182	25 - 27	Greater Than Optimum
22	8.4	5.8	130	706	29.6	116	28, 29	Optimum
23	64	13.0	91.3	419	64.0	200	30, 31	Greater Than Optimum
24	389	28.0	63.6	213	92.0	307	32	Optimum
25	8.4	3.0	463	3680	35.5	254	33	"
26	64	9.0	209	1600	64.0	304	-	Less Than Optimum
27	389	18.0	174	1205	119	489	34, 35	Greater Than Optimum
28	389	25.0	83.7	338	98.8	344	36, 37	Optimum
30	389	15.0	257	1985	118	592	38	"
31	389	25.0	83.7	338	98.8	344	39	Less Than Optimum
33	389	178	1.87	3.75	17.5	32.3	40	Optimum
34	1.0	12.5	5.05	10.4	4.6	10.8	41, 42	"
35	8.4	35.0	3.04	6.17	7.55	14.7	43	"
36	389	200	1.62	3.20	16.1	28.6	44	"

*Figure Number - Appendix A

TABLE II (Cont'd)

Shell No.	Explosive Weight W (lbs)	Explosive Distance d (ft)	Pressure (psi) Incident Pi	Pressure (psi) Reflected Pr	Impulse (psi-m sec) Incident Ii	Impulse (psi-m sec) Reflected Ir	Figure No.	Permanent Deformation
37	389	197	1.65	3.26	16.2	29.2	45	Greater Than Optimum
38	1.0	8.0	12.1	27.8	7.3	19.0	46, 47	Optimum
39	8.5	20.0	7.94	17.2	12.0	30.2	48	"
40	389	106	4.26	7.94	29.2	65.7	49, 50	"
41	389	128	2.94	5.95	24.1	51.1	-	None
42	389	285	1.06	2.19	11.6	18.2	-	"
43	389	172	2.0	3.97	18.2	35.0	-	Optimum
44	1.0	6.0	22.1	54.4	9.4	26.0	51	"
45	8.4	15.0	13.5	33.8	15.4	40.6	52	"
46	389	59.6	11.5	25.9	51.1	131	53, 54	"
47	1.0	4.0	58.8	176	12.5	40.0	55	"
48	8.4	9.0	45.6	135.2	23.4	73.5	56	"
49	389	35.8	35.0	97.0	81.8	230	-	"
50	1.1	20.0	2.50	5.07	2.99	6.19	57	"
51	8.4	60.0	1.5	2.94	5.08	7.30	58	"
53	389	350	0.82	1.73	9.60	13.9	59	"
54	1.1	10.0	7.94	17.2	6.02	15.1	60	"
55	8.3	25.0	5.14	10.7	9.54	22.1	61, 62	"
56	389	150	2.47	4.78	21.2	40.2	63	"
57	1.0	4.0	57.5	184	12.0	40.0	-	No Deformation
58	8.5	9.0	45.6	135	23.4	73.5	64	Optimum
59	1.0	2.0	264	2060	16.5	84	65	"
60	8.4	6.0	116	625	28.4	1.10	66	"
61	1.0	3.0	112	588	14.2	55.0	67	"
62	8.5	8.0	57.5	184	24.0	80.0	68	"
63	1.0	8.0	12.4	27.9	7.55	19.6	69, 70	Excessive
64	1.1	10.0	7.80	16.2	5.92	14.8	71, 72	"
65	1.1	10.0	7.80	16.2	5.92	14.8	73	"
66	1.1	15.0	3.97	7.95	4.08	8.77	74, 75	Optimum
67	1.1	16.0	3.53	7.05	3.90	8.20	76, 77	"
68	15.0	60.0	1.91	3.75	5.93	11.4	78, 79	"
69	8.3	16.0	11.9	27.2	14.7	39.2	80, 81	Excessive
70	66	40.0	7.65	16.5	23.4	58.5	-	"
71	115	70.0	4.18	8.66	21.1	46.8	82, 83	"
72	389	275	1.07	2.28	11.7	19.0	84, 85	Optimum

TABLE II (Cont'd)

Shell No.	Explosive Weight W (lbs)	Explosive Distance d (ft)	Pressure Incident pi (psi)	Pressure Reflected pr (psi)	Impulse Incident Ii (psi-msec)	Impulse Reflected Ir (psi-msec)	Figure No.	Permanent Deformation
75	-	-	-	-	-	-	-	(Static Test)
76	1.0	20.0	2.57	5.80	3.06	6.22	86, 87	Optimum
77	1.1	13.0	4.85	10.2	4.60	10.4	88	Excessive
78	8.4	40.0	2.50	5.0	5.84	12.9	89	"
79	1.1	25.0	1.91	3.82	2.90	4.70	90	Optimum
80	1.1	10.1	7.80	16.2	5.92	14.8	91, 92	Optimum
81	8.2	24.0	5.68	11.5	9.66	23.2	93	"
82	15.0	40.7	3.24	6.48	8.58	18.1	94	"
8[illegible]	15.0	20.0	11.5	25.7	17.7	44.7	-	None
[illegible]4	389	65.0	9.4	20.85	49.64	124.8	95	Optimum
85	1.1	8.0	12.4	27.9	7.55	19.6	-	None
86	15.0	25.0	7.35	15.7	13.8	34.4	-	"
87	389	75.0	7.20	15.42	43.8	105.8	96	Optimum
88	1.1	10.0	7.80	16.2	5.92	14.8	97. 98	"
89	8.2	20.0	7.65	16.3	11.7	28.8	99, 100	Excessive
90	15.0	35.2	3.97	8.10	10.1	22.1	101, 102	Optimum
91	389	160	2.16	4.30	19.7	38.0	-	None
92	14.8	75.5	1.40	2.79	4.66	8.08	103, 104	Optimum
93	15.0	70.1	1.54	3.10	5.05	9.10	105, 106	"
94	389	150	2.32	4.73	21.2	42.3	-	None
95	389	160	2.16	4.30	19.7	38.0	-	"
96	15.0	30.0	5.28	11.0	11.8	26.6	107, 108	Excessive
97	15.0	30.0	5.28	11.0	11.8	26.6	109, 110	"
98	389	200	1.76	3.23	15.7	29.2	111, 112	Optimum
99	389	25.0	83.7	338	98.8	344	113, 114	"
100	389	16.0	218	1660	118	562	-	"

3

TABLE III

Blast Parameters for the Longitudinal Loading Orientation

Shell No.	Explosive Weight W (lbs)	Explosive Distance d (ft)	Pressure Incident Pi (psi)	Pressure Reflected Pr (psi)	Impulse Incident Ii (psi-msec)	Impulse Reflected Ir (psi-msec)	Figure* No.	Permanent Deformation
3a	1.1	1.5	448	3600	17.0	119	-	None
b	8.3	3.0	463	3680	35.5	254	1, 2	Optimum
29a	389	9.0	617	5000	130	1200	-	None
b	66	5.5	544	4260	71.9	566	-	None
32	389	11.0	404	3010	124	73.0	3	Less Than Optimum
52	389	180.0	1.84	37.0	17.5	32.8	4, 5	Optimum
73	1.1	4.5	46.3	132	11.8	36.8	6	Excessive
74	64	20.0	34.5	91.0	42.5	130	7	"

* Figure Number - Appendix B

Plots of incident impulse (I_1) vs. incident pressure (p_1) for the shells listed in Table II as having approximately the optimum deformation are presented in Fig. 6. Iso-damage curves are drawn through these points that represent the various combinations of pressure and impulse for equivalent deformation of a given shell material and configuration (see points 4-5-6-7, 54-55-56, etc., Fig. 6). These curves form the boundaries between regimes of deformation and non-deformation.

The effect of variations of explosive weight on the blast parameters can easily be determined from these curves. As the explosive weight increases, moving from right to left along one of these curves, the impulse increases but the pressure decreases. For very large explosive weights the pressure-time histories will approach a step function (long durations, high impulse values) and the iso-damage curves should approach asymptotically some minimum value of pressure that will cause deformation.

If curves are drawn through different sets of points (i.e., 4-8-10, etc.) the effects of changes in length of the shells can be determined. In this case, the curve appears as a straight line. As length is increased, moving from right to left (all other parameters constant) the required values of pressure and impulse decrease. It is expected that an increase in length beyond a certain minimum value will not produce a further reduction in pressure and impulse values. At this point, the shell can be considered infinite and end conditions will not influence the deformation at the center. This minimum length has not been determined at this time.

In like manner, the variation of pressure and impulse values for changes only in diameter, thickness or type of material can be determined. As expected, an increase in pressure and impulse values is required if either the thickness is increased or the diameter decreased.

Having a family of iso-damage curves and the variation of the significant parameters, it is possible to generate a method of predicting deformation of cylindrical shells. The details of the method will be presented in the next section, "Prediction of Deformation."

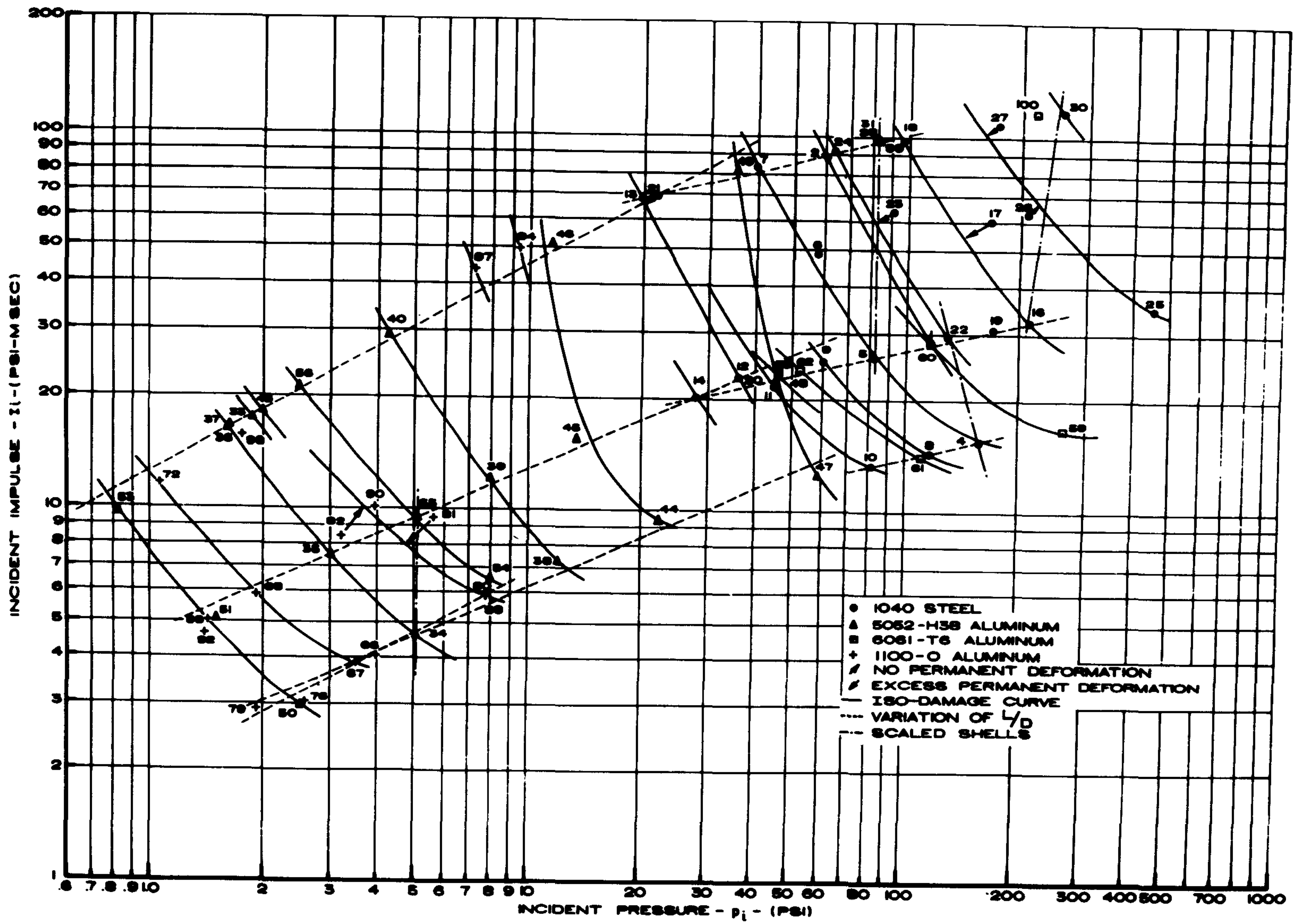

FIG. 6. ISO-DAMAGE CURVES FOR LATERALLY LOADED SHELLS

The nearly vertical, dotted lines on Fig. 6 show that shells of different configurations will be deformed at the same pressure level by unlike explosive weights. A close examination of the connected points indicates that "geometrical" modeling laws apply for these large deformations. For example, refer to Fig. 6 and Fig. 7 - Scaling Parameters, and Table II: Point 5 on Fig. 6 represents a cylinder of given geometry (3 in. diameter, 8.62 in. length, 0.019 in. thickness) laterally loaded by an explosive weight of 8.4 lbs. positioned at a distance of seven feet. The equivalent deformation of a shell whose geometry has been scaled by the factor K = 2 (Point 23 - 6 in. diameter, 17.50 in. length, 0.035 in. thickness) exposed to an explosive weight of 64 lbs. (i.e., $W \propto D_W^3$ or $D_W \propto \sqrt[3]{W}$ or $D_W \propto \sqrt[3]{8.4} \propto 2$ and, therefore, $W_2 \propto K^3 \cdot D_W^3 \propto (2)^3 \cdot (2)^3 \propto 64$) located at a distance of 2d = 2 x 7 = 14 ft. validates this conclusion as do the other sets of points.

There are two general deformation patterns arising from lateral loadings: a single transverse crease or multiple longitudinal lobes. Typical transverse and longitudinal patterns are shown in Figs. 8 - 10 and 11 and 12. A typical deformation pattern resulting from longitudinal loading is shown in Fig. 13. Photographs of all shells are presented in Appendices A and B for the lateral and longitudinal loadings respectively.

The two lateral loading patterns seem to be primarily a function of the shell geometry. The thicker shells deform with a transverse crease while the thinner form a lobe pattern. However, one of the shells deformed in a compound pattern when the explosive weight was increased. (See Fig. 14.) Further investigation is required to define the applicable parameters and their variation.

One shell was tested statically to compare its pattern with those shown in Figs. 8 - 10. The shell and support tube assembly was mounted on v-blocks in a testing machine. The line load was applied perpendicular to the centerline of the shell at the center with a 1/4 x 4 inch striker plate. The deformation pattern is similar to that of the transverse crease (see Figs. 15 and 16). The shell commenced to deform at 3 lb. load and the load increased

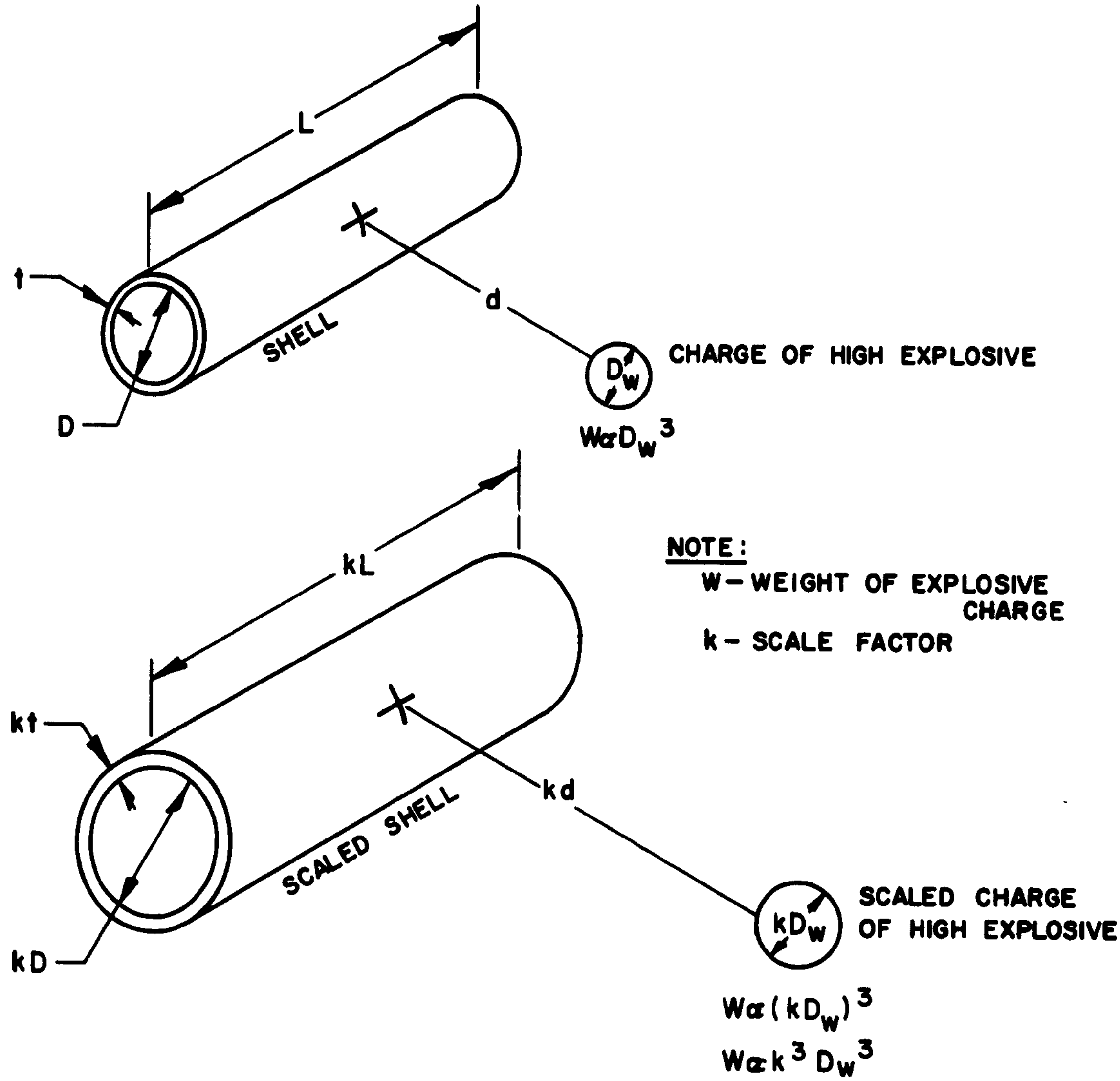

FIG. 7 – SCALING PARAMETERS

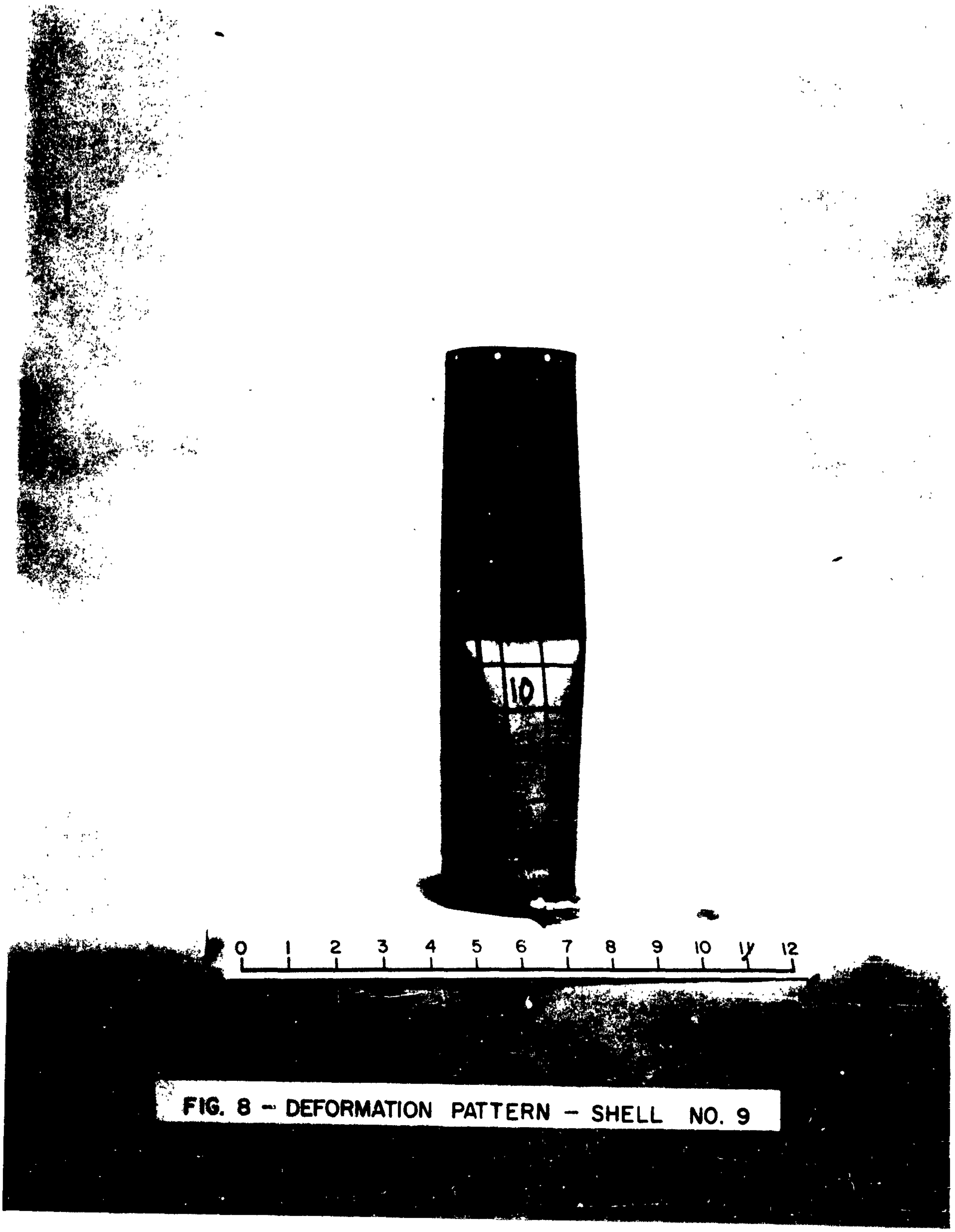

FIG. 8 – DEFORMATION PATTERN – SHELL NO. 9

FIG. 9 – DEFORMATION PATTERN – SHELL NO. 22

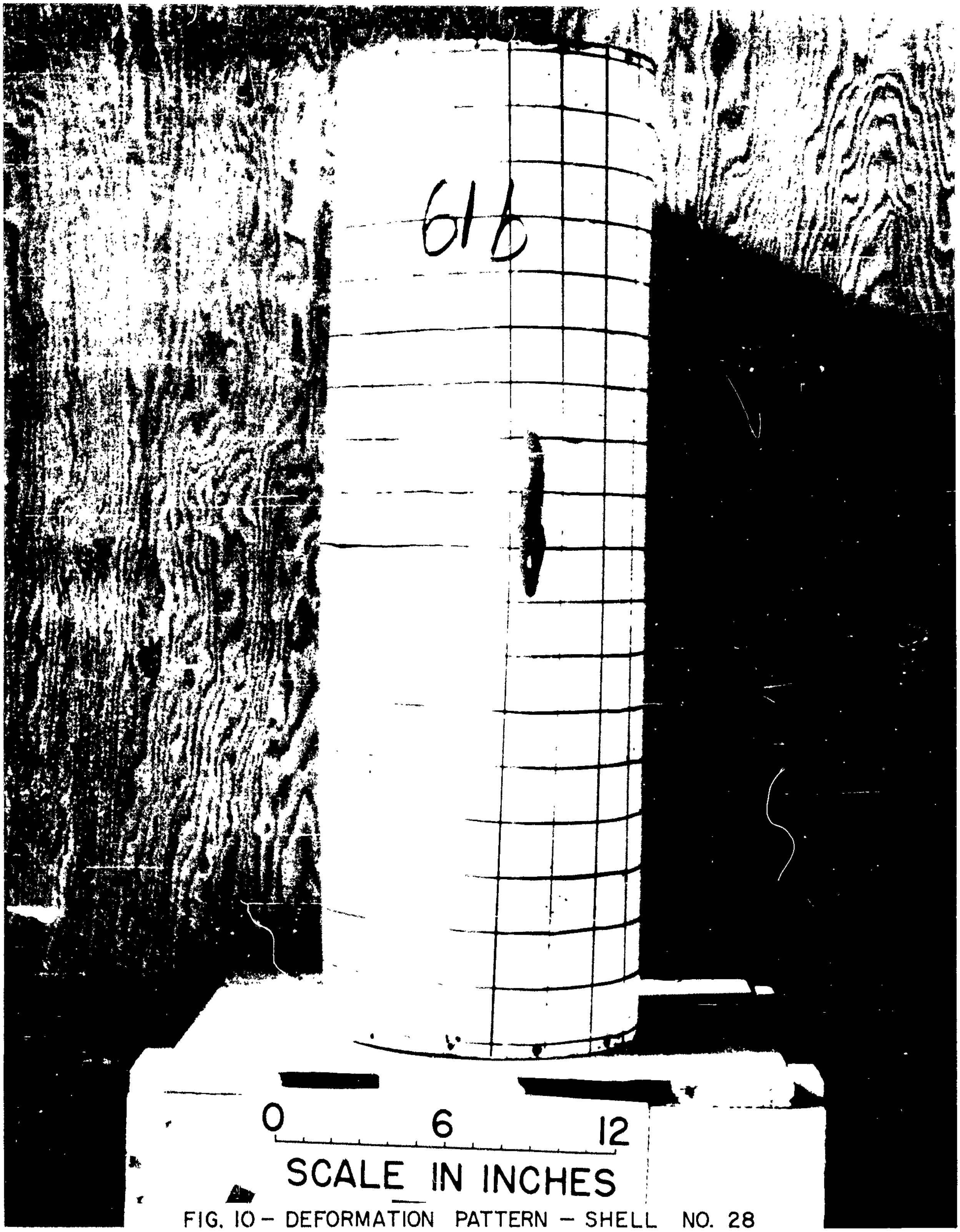

FIG. 10 – DEFORMATION PATTERN – SHELL NO. 28

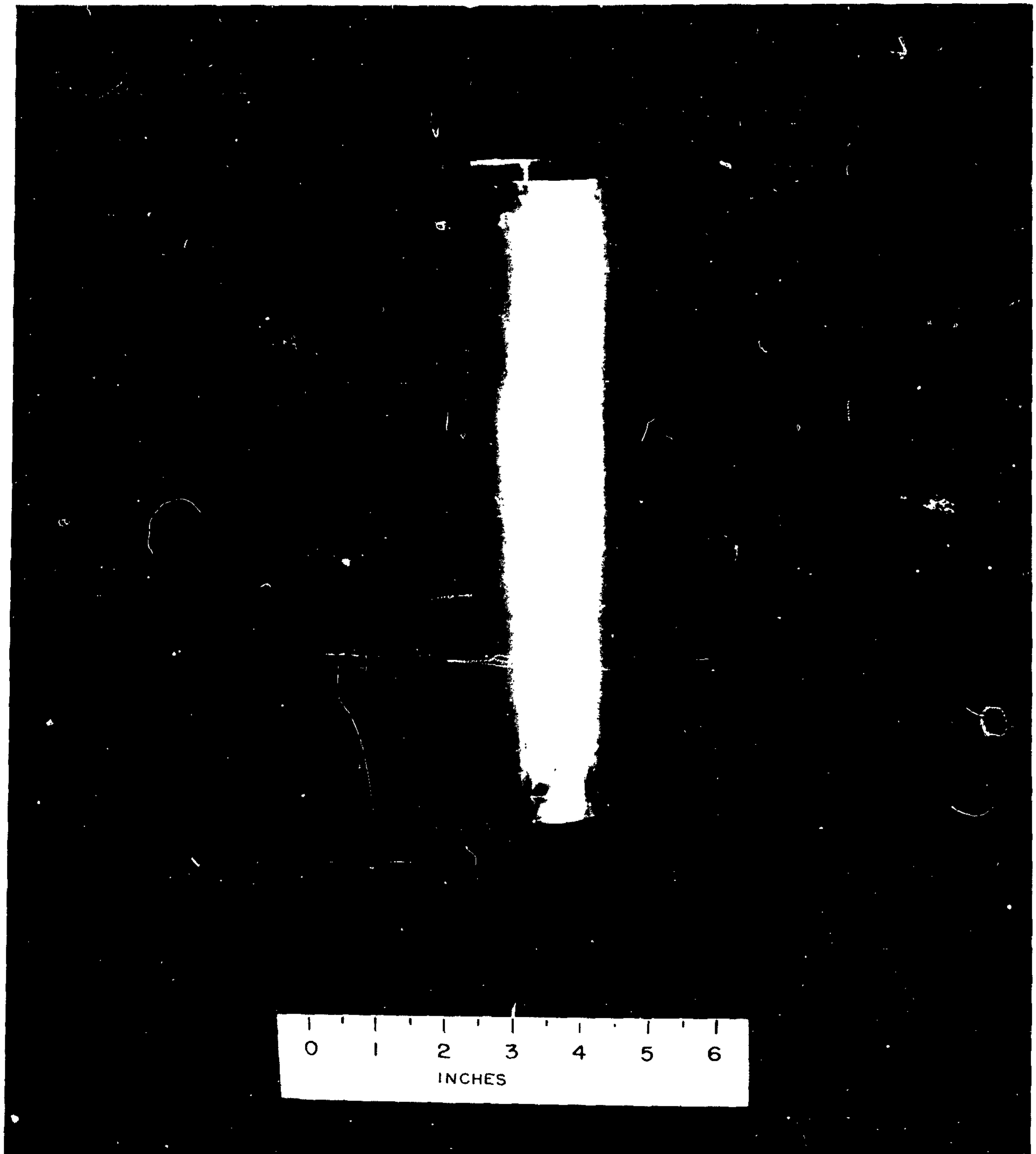

FIG. 11 – DEFORMATION PATTERN – SHELL NO. 88

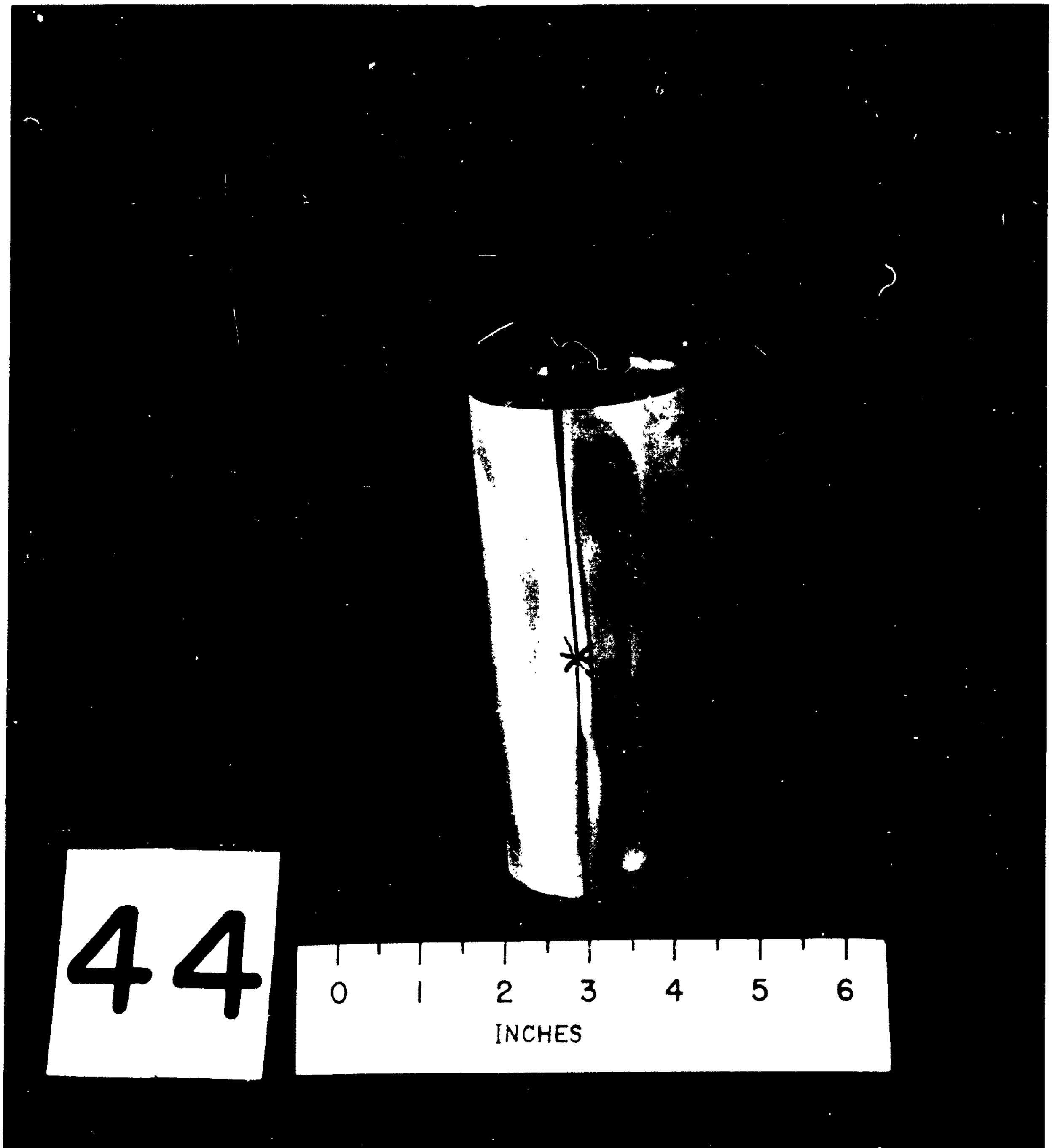

FIG. 12 – DEFORMATION PATTERN – SHELL NO. 66

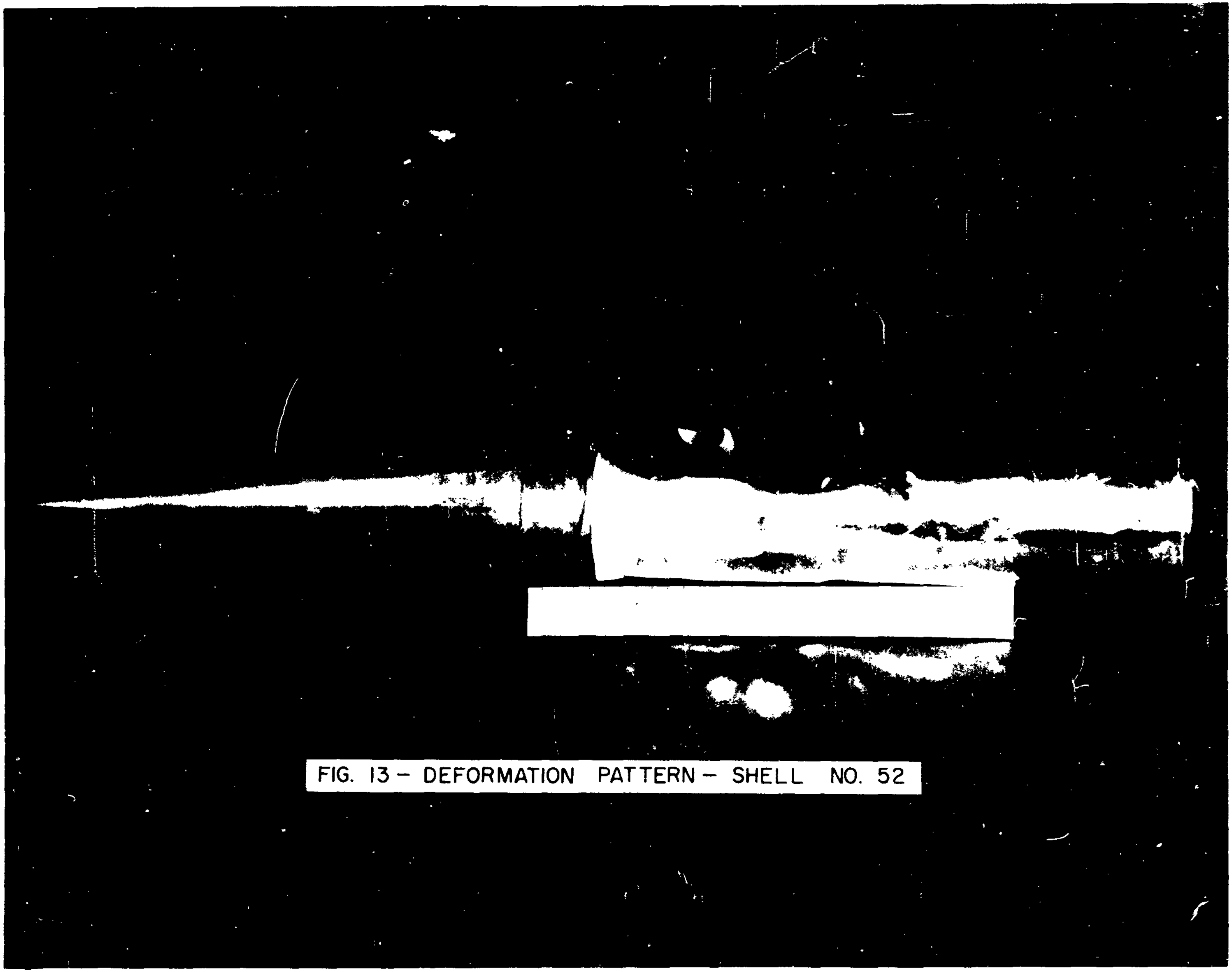

FIG. 13 – DEFORMATION PATTERN – SHELL NO. 52

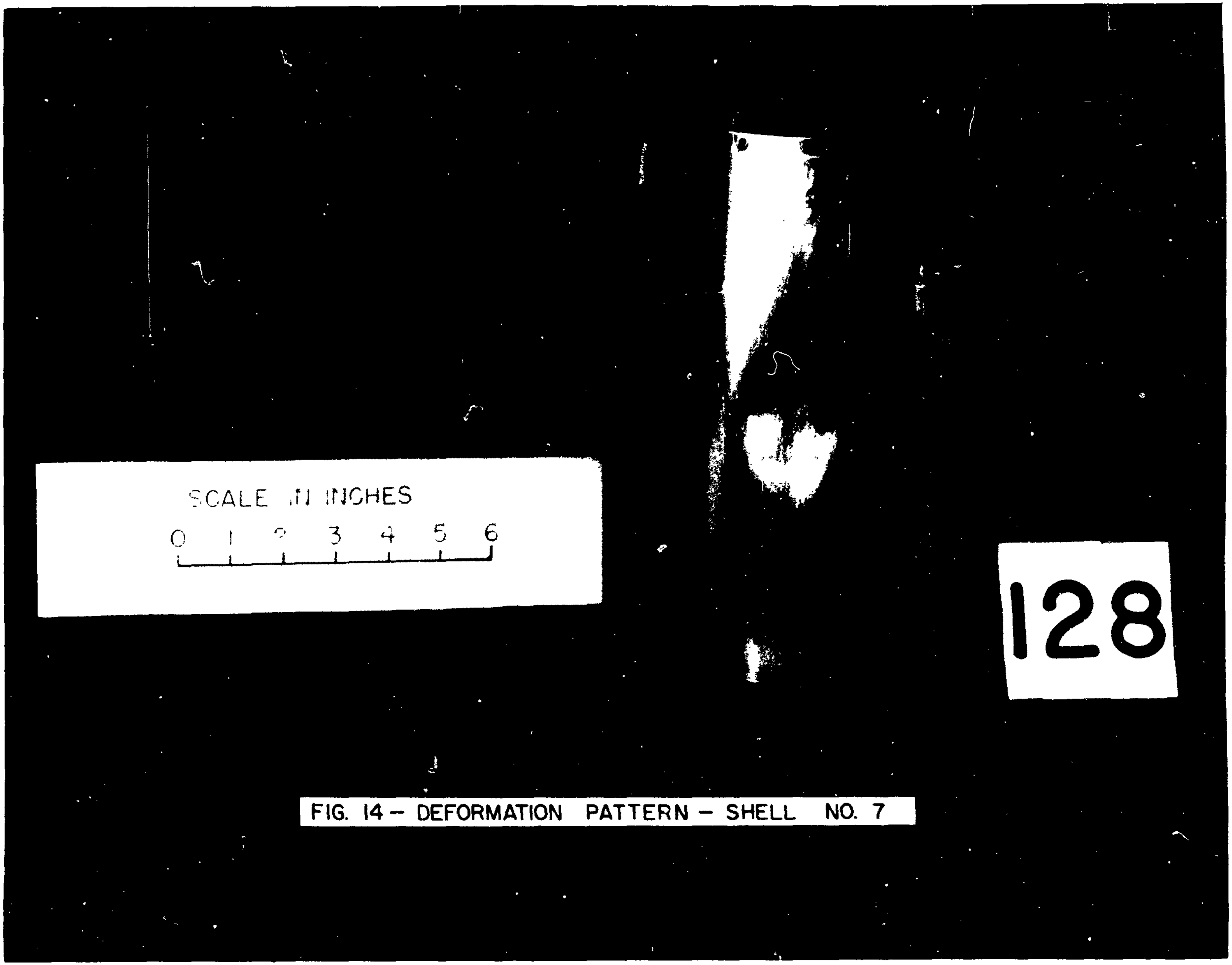

FIG. 14 – DEFORMATION PATTERN – SHELL NO. 7

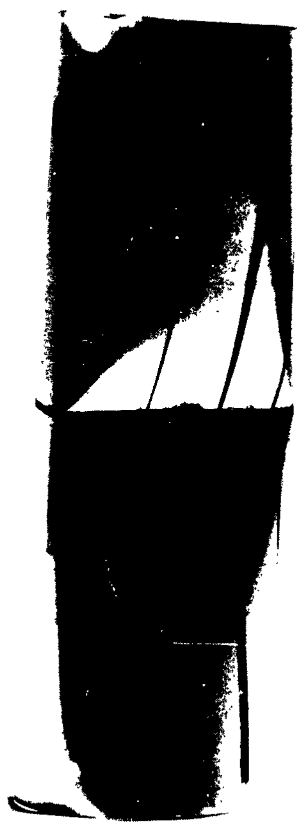

FIG. 15 – DEFORMATION PATTERN – SHELL NO. 75

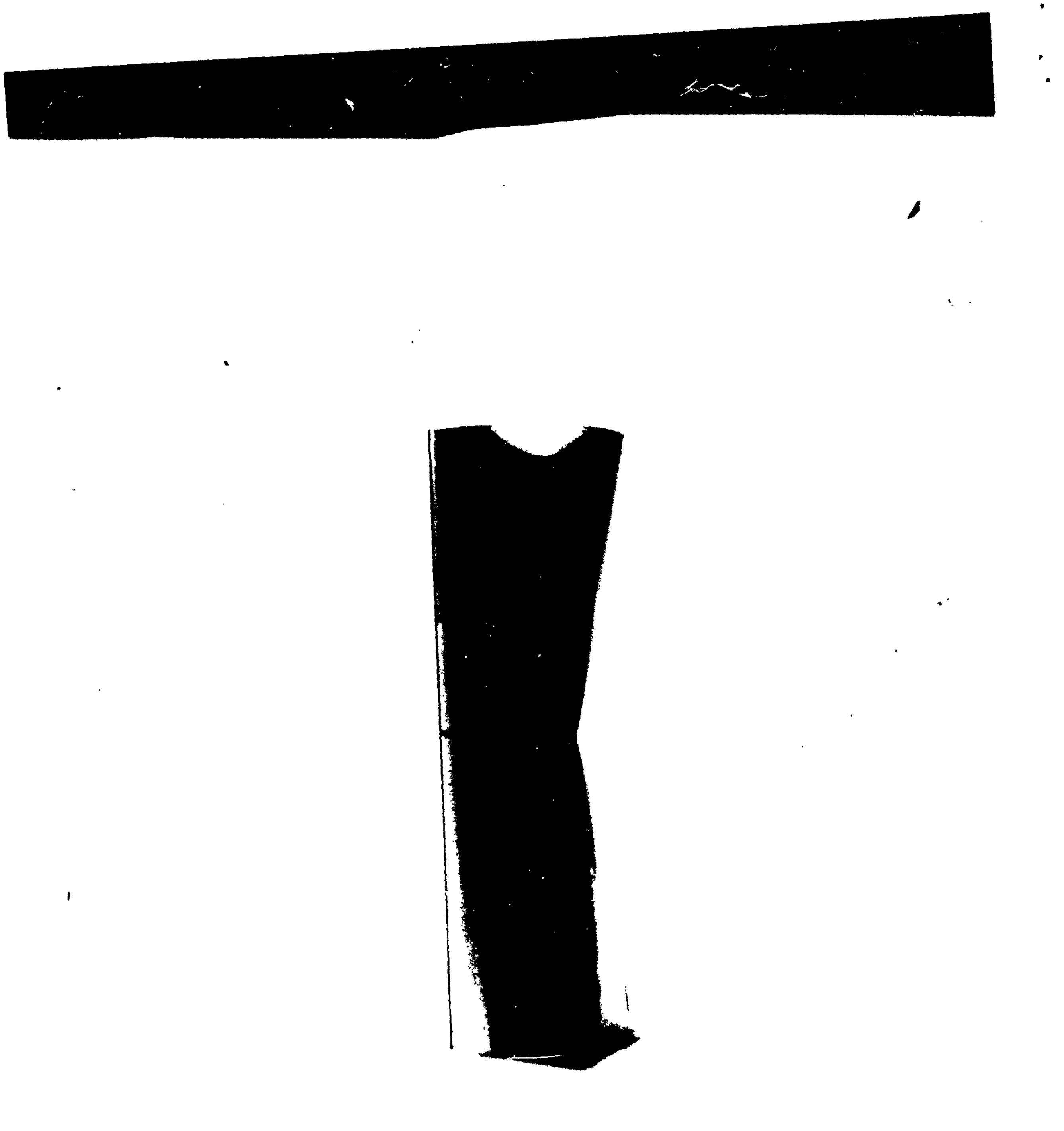

FIG. 16 – DEFORMATION PATTERN – SHELL NO. 75

continuously as the deformation increased. The load was increased to a maximum value of 10 lb. and then removed. This requirement that the load must be increased in order to increase the deformation also agrees with the blast loading results.

Instrumented Shells

The results of exploratory firings for checking out the strain gage recording system are presented in Table IV. Only peak strains were read. Additional firings will be conducted and the results coordinated with similar investigations being carried out at the Suffield Experimental Station.

A number of firings have been made against the solid loading cylinder, but calibration difficulties preclude presenting the data at this time.

PREDICTION OF DEFORMATION

A semi-graphical method for predicting the critical incident pressure required to cause permanent deformation for a cylindrical shell in the lateral loading orientation has been generated. The necessary curves are shown in Figs. 17 - 20.

The four curves of Fig. 17 are plots of the length-to-diameter ratio - L/D - vs. critical incident pressure p_{cr} for the four materials tested: steel and the three types of aluminum alloy. Each of these curves is based on a change of L/D for a constant explosive weight of one pound, a diameter of three inches and a thickness of 0.019 in. for steel and 0.006 in. for aluminum.

If the explosive weight, diameter, or thickness are different from the above standard values, the value of critical incident pressure p_{cr} must be adjusted. The necessary correction factors have been determined from the independent effect of each of these factors on the critical pressure and are given in Figs. 18 - 20. The required pressure is then:

$$P_{cr} = p_{cr} \; K_D \, K_t \, K_w$$

where P_{cr} = Critical Incident Pressure for lateral loading

p_{cr} = Critical Incident Pressure (for standard conditions) (Fig. 17)

K_w = Correction factor for explosive weight (Fig. 18)

TABLE IV

Strain Data for Lateral Loading of Shell*

Round No.	106	107		109		110	111
Explosive Wt. (lb)	1.06	1.06		1.07		8.19	8.19
Explosive Dist. (ft)	3.75	3.75		3.5		8.0	8.0
Press. p_i (psi)	69.2	69.2		82.4		58.8	58.8
Gage Position	Maximum Strain (μ in/in)						
1L	603	551		611		--	--
1C	1635	1281		1749		1923	--
2L	559	536		752		581	633
2C	790	752		1112		656	894
3L	909	668		1308		726	983
3C	1065	663		646		1749	1543
4L	577	574		745		612	656
4C	641	514		790		734	1013

*Shell Dimensions - Diameter - 3", Length - 9", Thickness - .019", Material - Steel

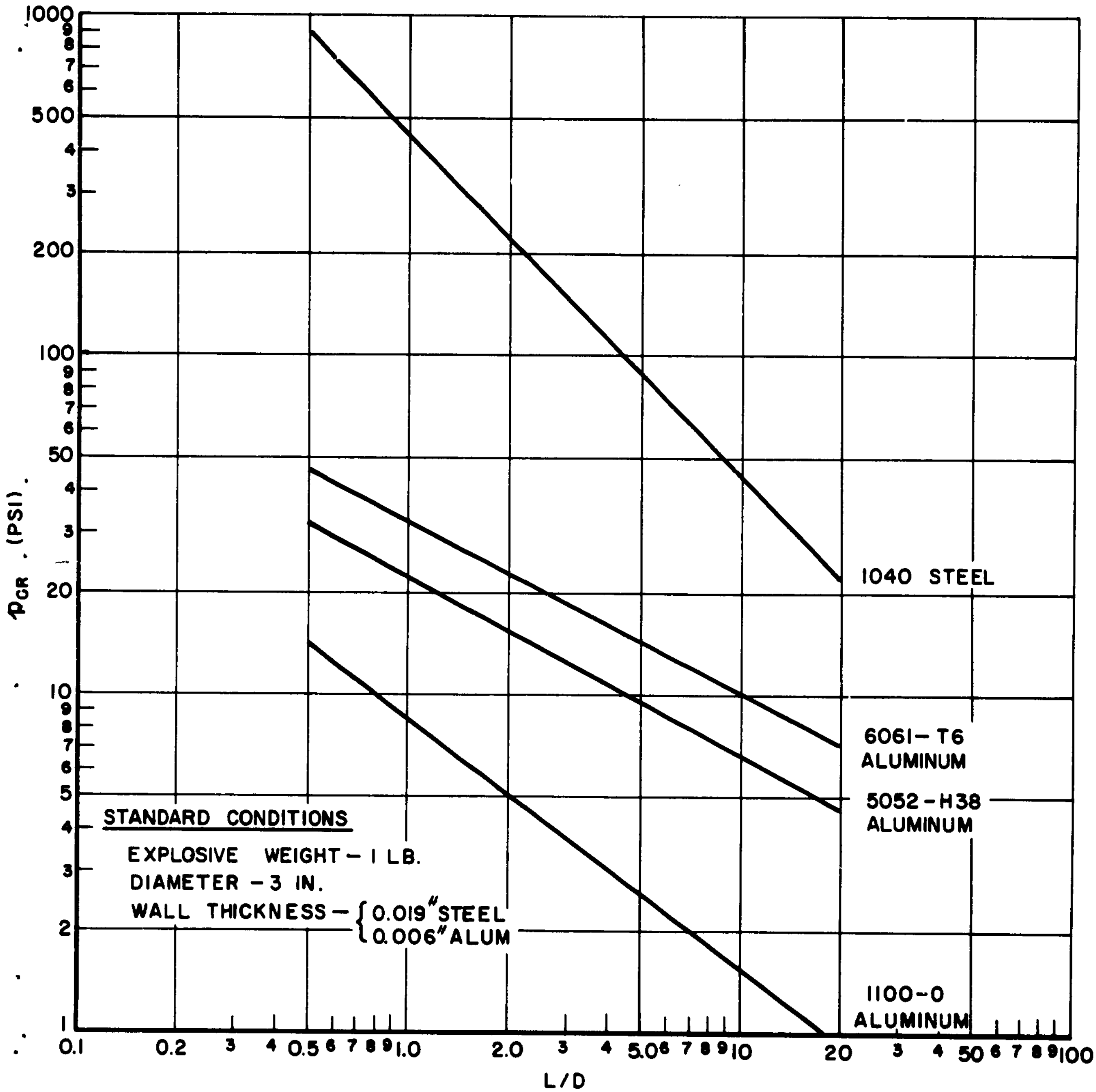

FIG. 17 LENGTH-TO-DIAMETER RATIO
VS
CRITICAL INCIDENT PRESSURE FOR STANDARD CONDITIONS

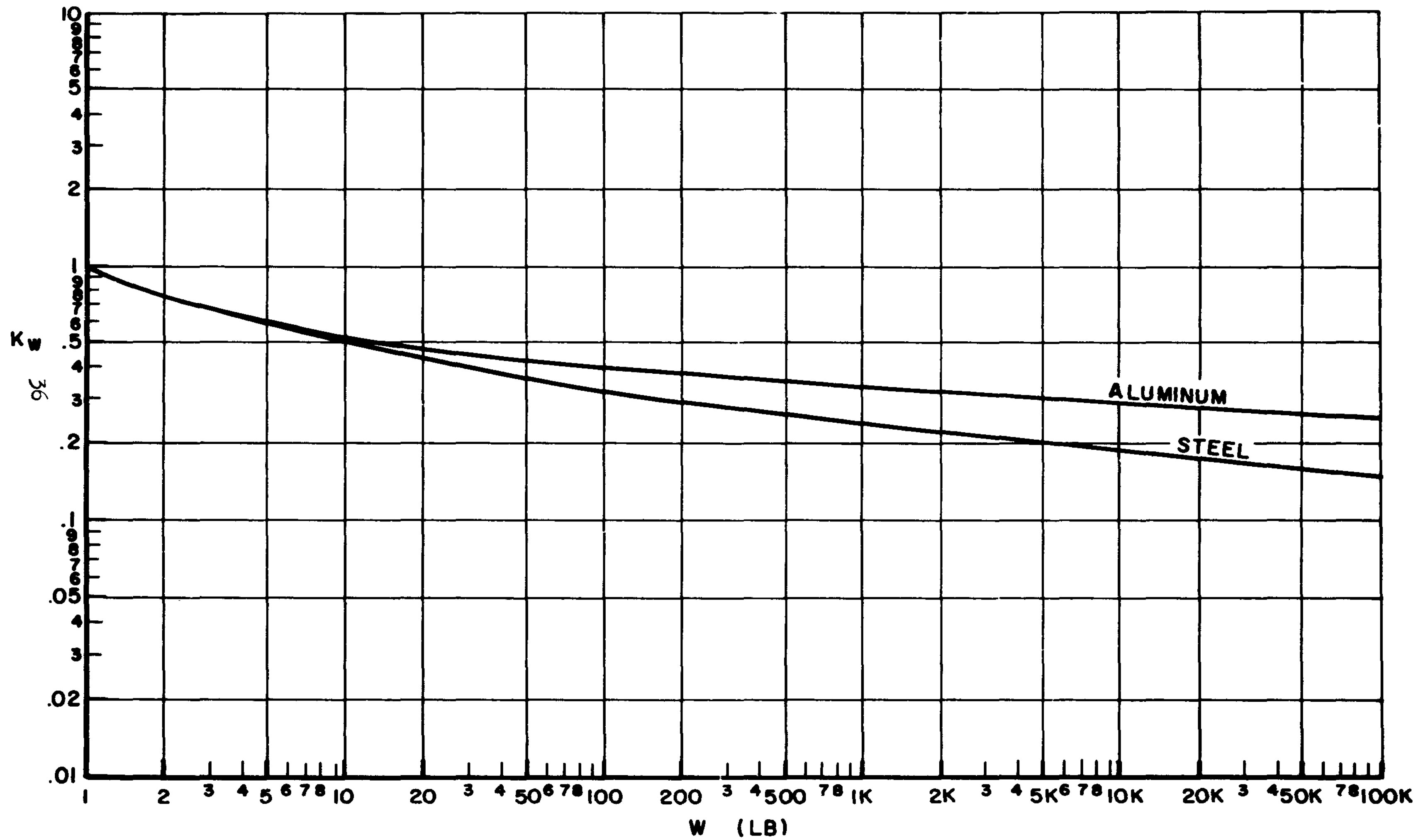

FIG. 18 CORRECTION FACTOR FOR VARIATIONS OF EXPLOSIVE WEIGHT

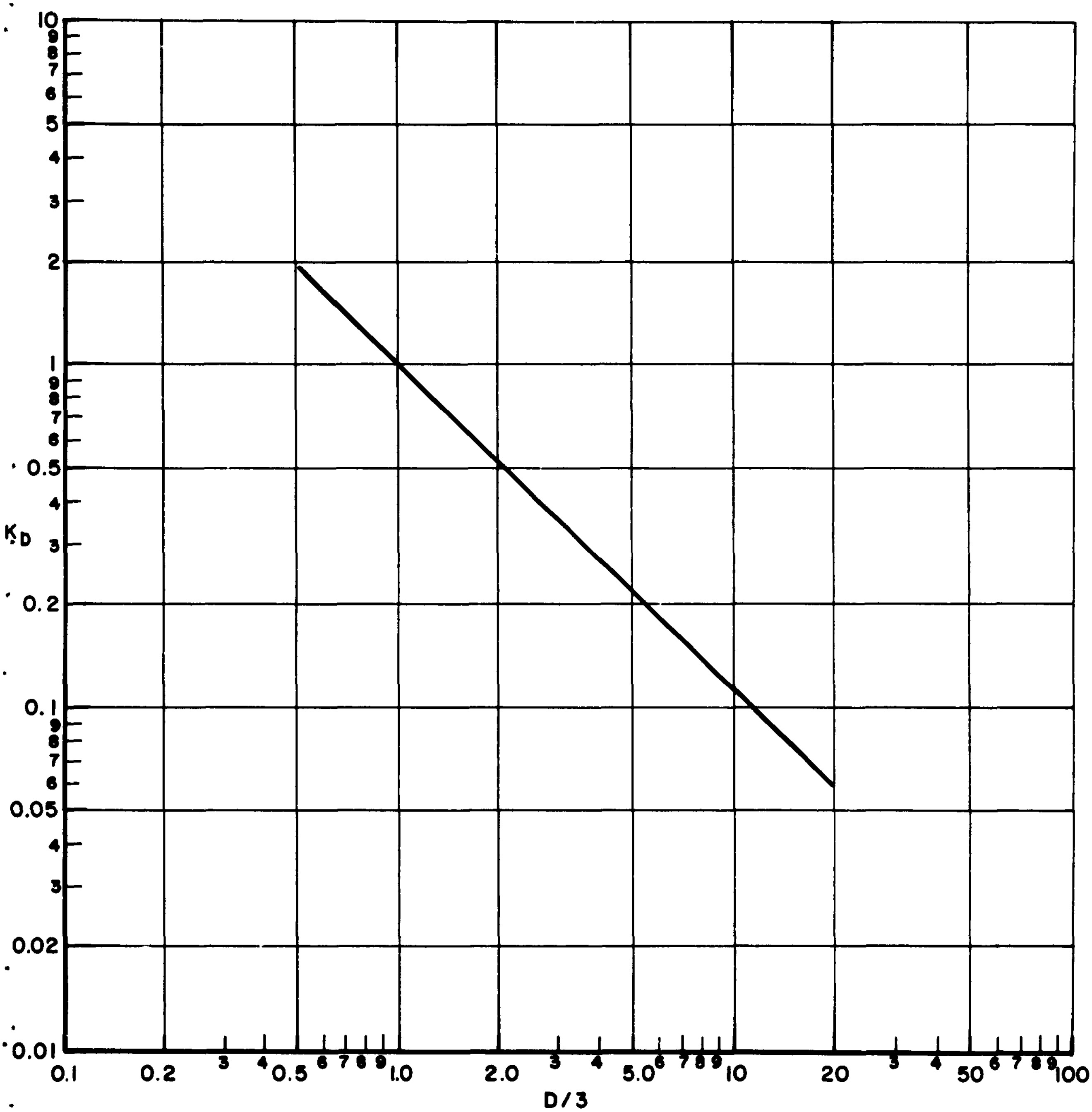

FIG. 19. CORRECTION FACTOR FOR VARIATIONS OF DIAMETER

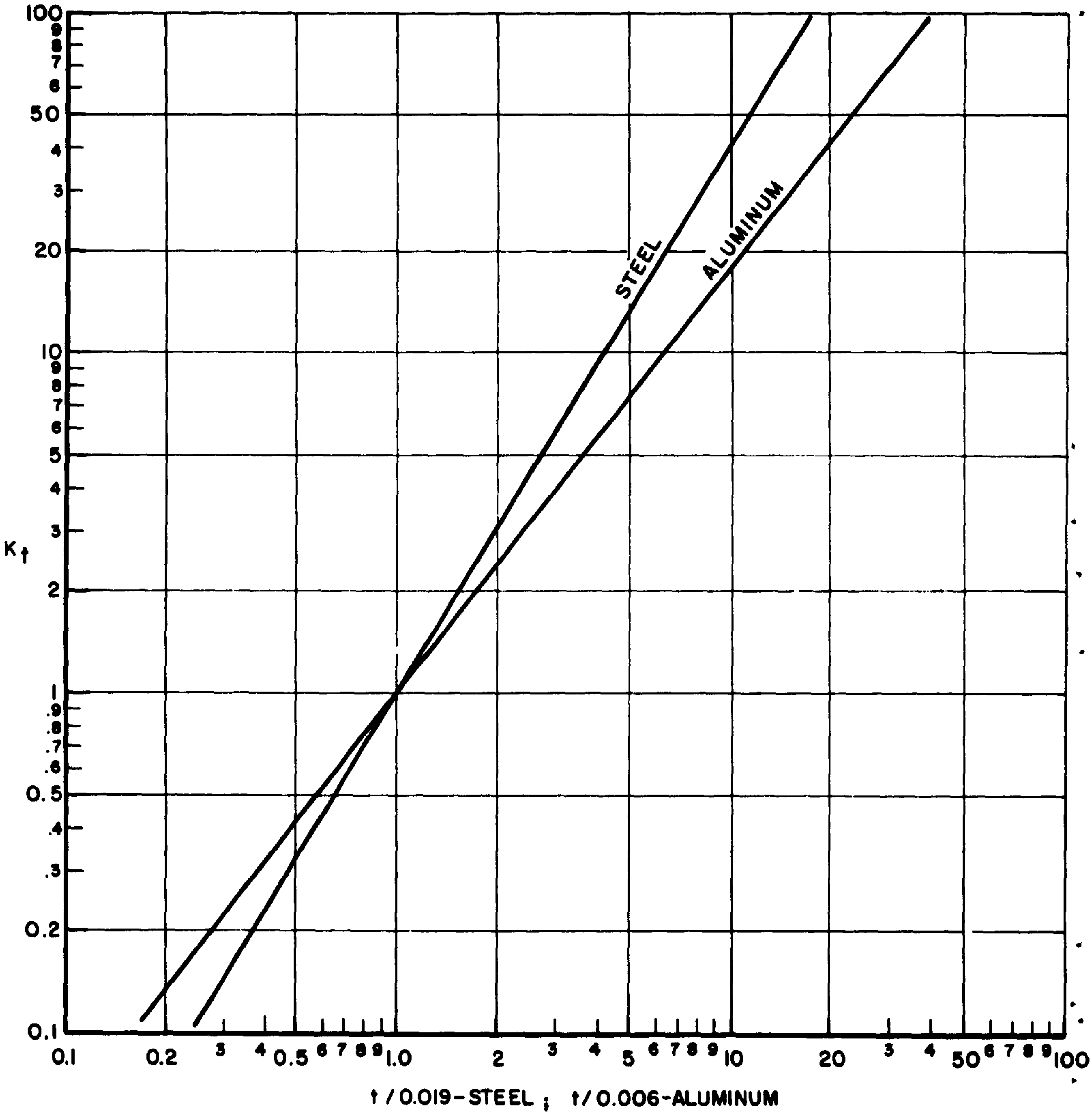

FIG. 20. CORRECTION FACTOR FOR VARIATIONS OF WALL THICKNESS

K_D = Correction Factor for Diameter (Fig. 19)

K_t = Correction Factor for Thickness (Fig. 20)

As an example, consider Shell No. 30. It is steel and $L/D = 2.94$ (Table I).

Therefore $p_{cr} = 150$ psi

also $D = 12.0$ in., $\frac{D}{3} = 4$ and $K_D = 0.27$

$t = 0.136$ in., $\frac{t}{0.019} = 7.17$ and $K_t = 24.2$

$W = 389$ lb., $K_W = 0.265$

Therefore $P_{cr} = p_{cr} K_D K_t K_W$

$= (150)(0.27)(24.2)(0.265)$

$P_{cr} = 260$ psi

The actual pressure was $p_i = 257$ psi. Therefore, the deviation of the predicted value from the actual value is + 1.2%.

The average deviation between predicted and actual pressures for the laterally-loaded cylinders listed in Table V is 12% with a spread of -40% to + 40%.

If the shell is exposed to longitudinal loading, the pressure required for deformation is higher. The data presently available seem to follow the general trend of the other set of iso-damage curves. Therefore, the critical pressure for the lateral loading should be determined and multiplied by a factor of λ where $\lambda \approx 6.0$ for steel, and $\lambda \approx 2.0$ for aluminum.

CONCLUSIONS

The primary goal of the first phase of an investigation of the response of thin walled cylinders exposed to external blast loading has been achieved. An empirical method of predicting the critical incident blast pressure required to cause permanent deformation has been presented. The correlation of predicted and actual pressure values is satisfactory (average deviation of 12%). However, there are several areas requiring further investigation. It is planned to conduct a series of firings in the 1000 lb. to 30,000 lb. explosive weight range at the Yuma Test Station the early part of 1963. This will help define the iso-damage curves at much higher impulse levels.

TABLE V

Comparison of Actual and Predicted Pressures for Optimum Deformation

Shell No.	Incident Pressure* Pi (psi)	Predicted Critical Pressure Pcr (psi)	Deviation (%)	Remarks
1	117	114	-2.6	
2	48.5	58.2	+20.0	
3a**	448	894***	-	No Deformation
3b**	463	484***	+4.6	
4	159	149	-6.3	
5	82.4	80.6	-2.2	
6	58	52.6	-9.3	
7	39.7	39.7	0	
8	118	111	-5.9	
9	60.3	59.8	-0.8	
10	82.4	86.5	+5.0	
11	44.8	46.8	+4.5	
12	36.0	37.9	+5.3	
13	17.4	19.3	+11.0	
14	27.9	28.6	+2.5	
15	2.9	14.5	-	No Deformation
16	213	217	+1.9	
17	166	143	-16.1	
18	96.7	107	+12.1	
19	172	103	-40.0	
20	36.0	40.6	+12.8	
21	21.8	20.7	-5.0	
22	130	112	-13.8	
23	91.3	73.0	-20.1	
24	63.6	55.9	-11.3	
25	463	389	-16.0	
26	209	254	-	No Deformation
27	174	195	+12.0	
28	83.7	102	+22.1	
29a**	617	612***	-	No Deformation
29b**	544	786***	-	No Deformation
30	257	260	+1.2	
31	83.7	196	-	Less Than Optimum
32**	404	1176***	-	" Deformation
33	1.87	2.21	+18.2	
34	5.05	5.06	+0.2	
35	3.04	2.74	-9.9	
36	1.62	1.80	+11.1	
37	1.65	1.37	-16.9	Greater Than Optimum
38	12.1	12.2	+0.8	Deformation
39	7.94	6.59	-17.0	
40	4.26	4.33	+1.6	
41	2.94	3.30	-	No Deformation
42	1.06	2.63	-	No Deformation
43	2.0	2.27	+13.5	
44	22.1	29.2	+40.0	
45	13.5	15.8	+17.0	
46	11.5	10.4	-9.6	
47	58.8	69.5	+18.2	

TABLE V (Cont'd)

Shell No.	Incident Pressure* Pi (psi)	Predicted Critical Pressure Pcr (psi)	Deviation (%)	Remarks
48	45.6	37.6	-17.5	
49	35.0	24.7	-30.6	
50	2.50	2.53	+1.2	
51	1.50	1.42	-4.5	
52**	1.84	1.87***	+1.6	
53	0.82	.935	+16.5	
54	7.94	6.30	-20.7	
55	5.14	3.40	-33.9	
56	2.47	2.24	-9.3	
57	57.5	92.0	-	No Deformation
58	45.6	49.6	+8.8	
59	264	205	-22.4	
60	107	115	+7.5	
61	113	107	-5.3	
62	57.5	57.5	0	
63	12.4	11.0	-	Excess Deformation
64	7.80	7.88	+1.0	
65	7.80	5.38	-	Excess Deformation
66	3.97	4.61	+16.1	
67	3.53	3.46	-2.0	
68	1.91	1.76	-7.8	
69	11.9	1.95	-	Excess Deformation
70	7.65	1.49	-	Excess Deformation
71	4.18	1.42	-	"
72	1.07	1.28	+19.6	
73**	46.3	6.92***	-	Excess Deformation
74**	34.5	3.00***	-	"
75	-	-	-	Static Test
76	2.57	2.95	+14.8	
77	4.85	2.40	-	Excess Deformation
78	2.50	1.35	-	"
79	1.91	1.73	-9.4	
80	7.80	6.40	-17.9	
81	5.68	3.60	-36.6	
82	3.24	3.27	+1.0	
83	11.5	12.9	-	No Deformation
84	9.4	9.38	-0.3	
85	12.4	18.8	-	No Deformation
86	7.35	9.63	-	"
87	7.20	6.99	-2.9	
88	7.80	8.3	+6.4	
89	7.65	4.65	-	Excess Deformation
90	3.97	4.23	+6.5	
91	2.16	3.07	-	No Deformation
92	1.40	1.55	+10.7	
93	1.54	1.33	-13.6	
94	2.32	4.86	-	No Deformation
95	2.16	3.63	-	"
96	5.28	2.20	-	Excess Deformation

TABLE V (Cont'd)

Shell No.	Incident Pressure* Pi (psi)	Predicted Critical Pressure Pcr (psi)	Deviation (%)	Remarks
97	5.28	3.18	-	Excess Deformation
98	1.76	2.30	+30.7	
99	83.7	91.0	+8.7	
100	218	217	-0.5	

* From Tables II & III

** Longitudinal Loading Orientation (all others are lateral loading orientation)

*** Predicted Critical Pressures for Lateral Loading Orientation have been Multiplied by 6.0 for Steel, 2.0 for Aluminum

Shells are being fabricated with greater lengths to determine at what point end conditions may be neglected. The variation in deformation patterns will be studied further. The iso-damage curves for the longitudinal loading orientation will be defined more accurately. The effects of free-body motion of the shell are now being studied.

Continuation of study of the instrumented shells will provide valuable data for analytical correlation of the loading and response.

Future work with actual hardware will determine the degree of applicability of these simplified models.

This is an interim report released at this time so that Government and private agencies may integrate these results into overall vulnerability analyses.

ACKNOWLEDGMENTS

The assistance afforded the author by Professor Norman Davids, Department of Mechanics, the Pennsylvania State University in the planning of these tests and in the preparation of this report is gratefully acknowledged.

Acknowledgment is also made of the assistance of Miles Lampson, Harry Goldstein and the many members of the BRL field crew in conducting experiments at BRL ranges.

William J. Schuman, Jr.

WILLIAM J. SCHUMAN, JR.

APPENDIX A

DEFORMATION OF LATERALLY LOADED SHELLS

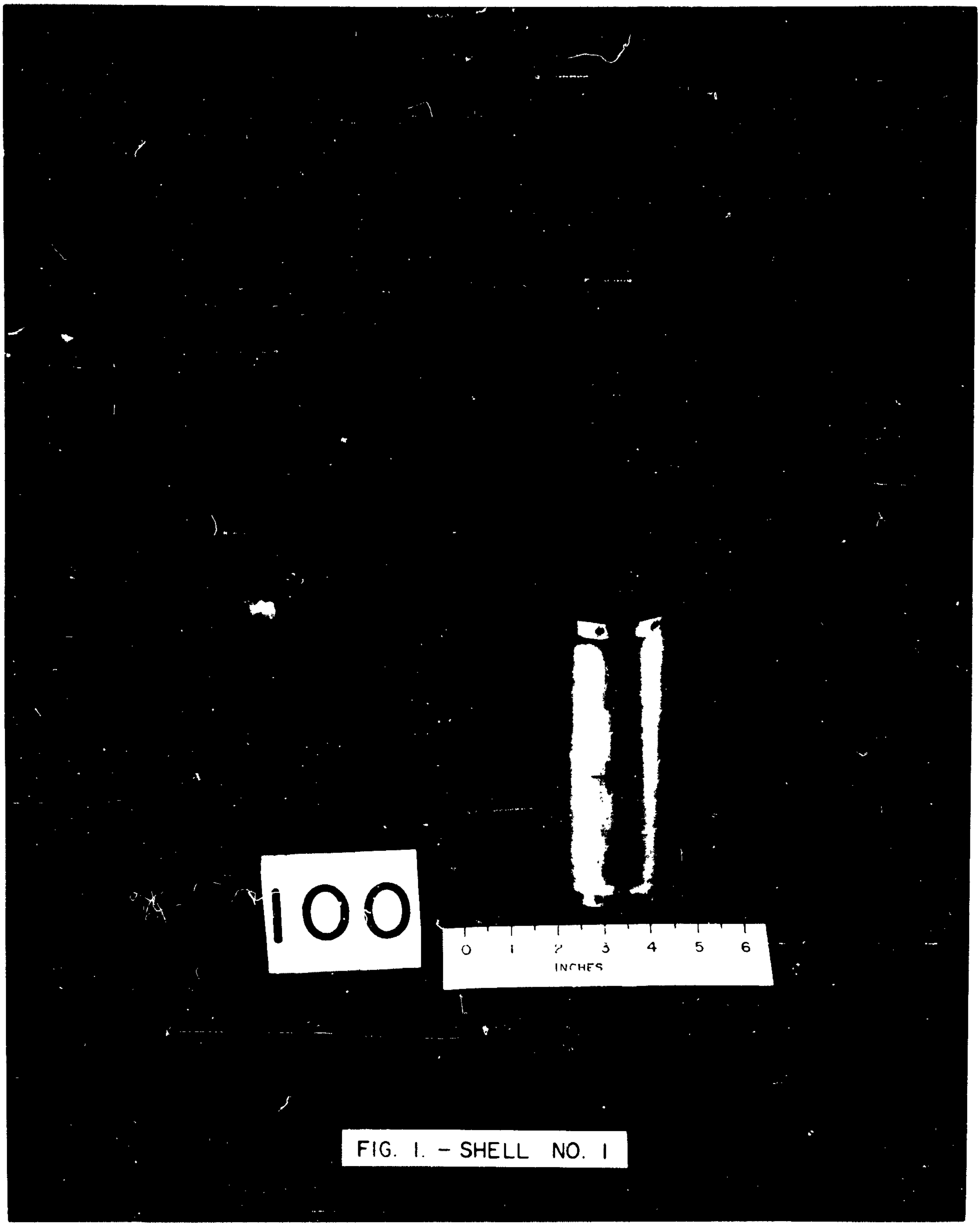

FIG. 1. - SHELL NO. 1

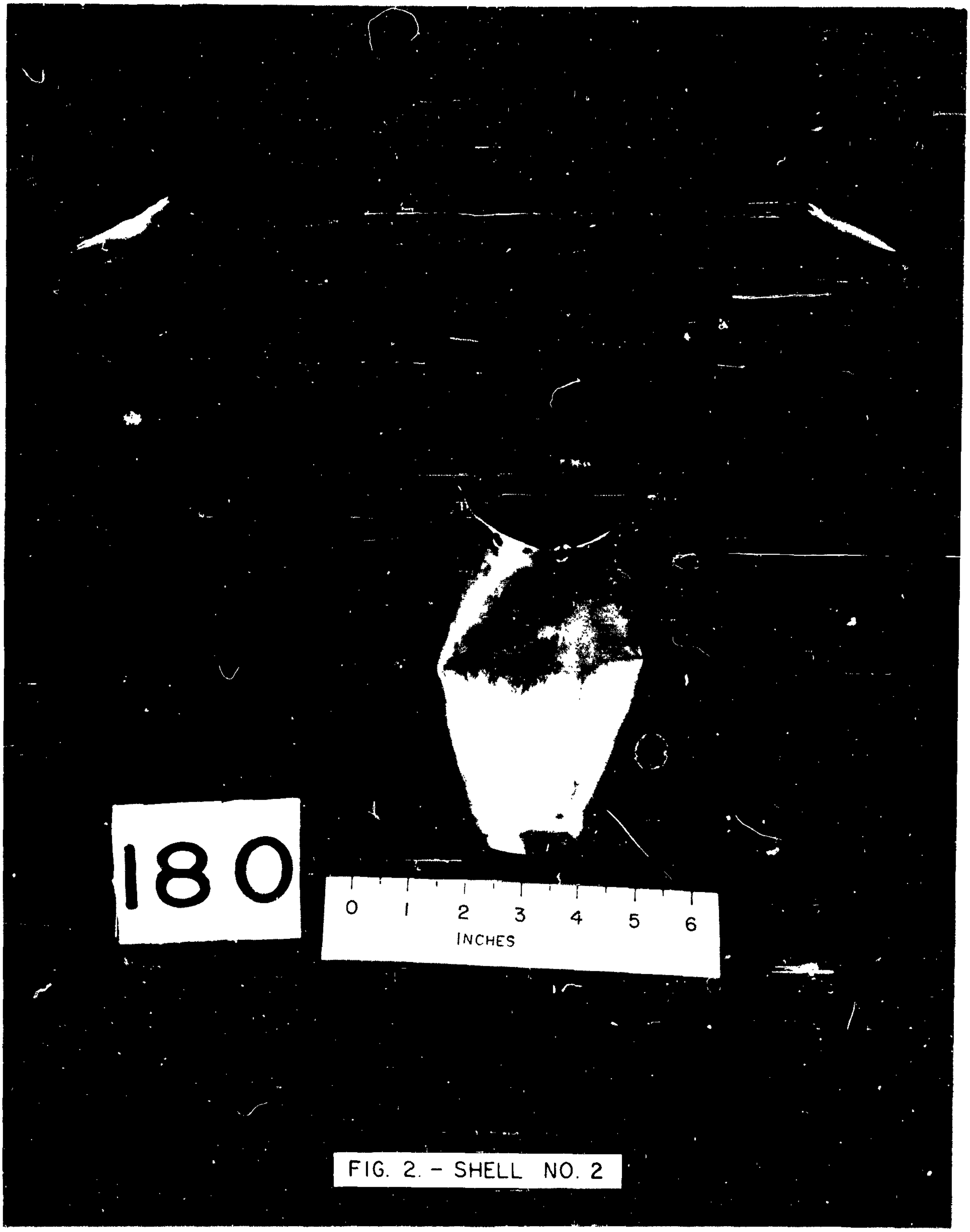

FIG. 2. - SHELL NO. 2

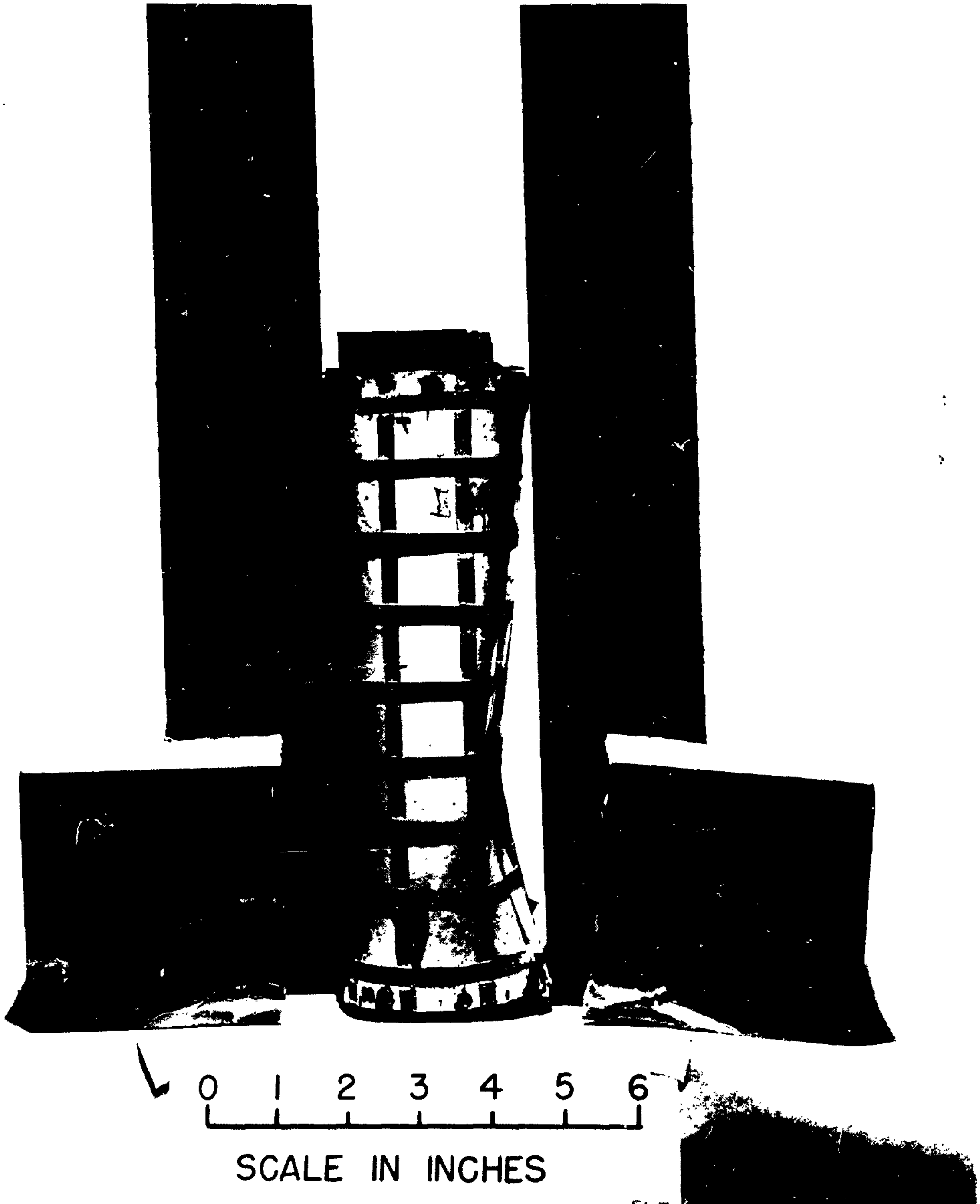

FIG. 3 - SHELL NO. 4 — SIDE VIEW

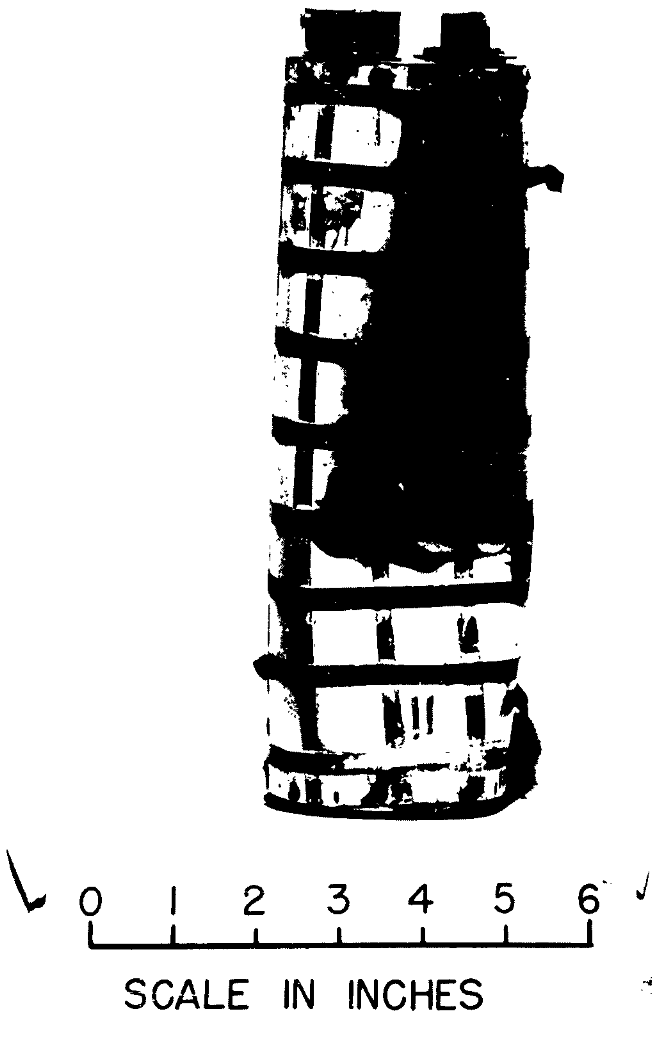

FIG. 4 — SHELL NO. 4 — FRONT VIEW

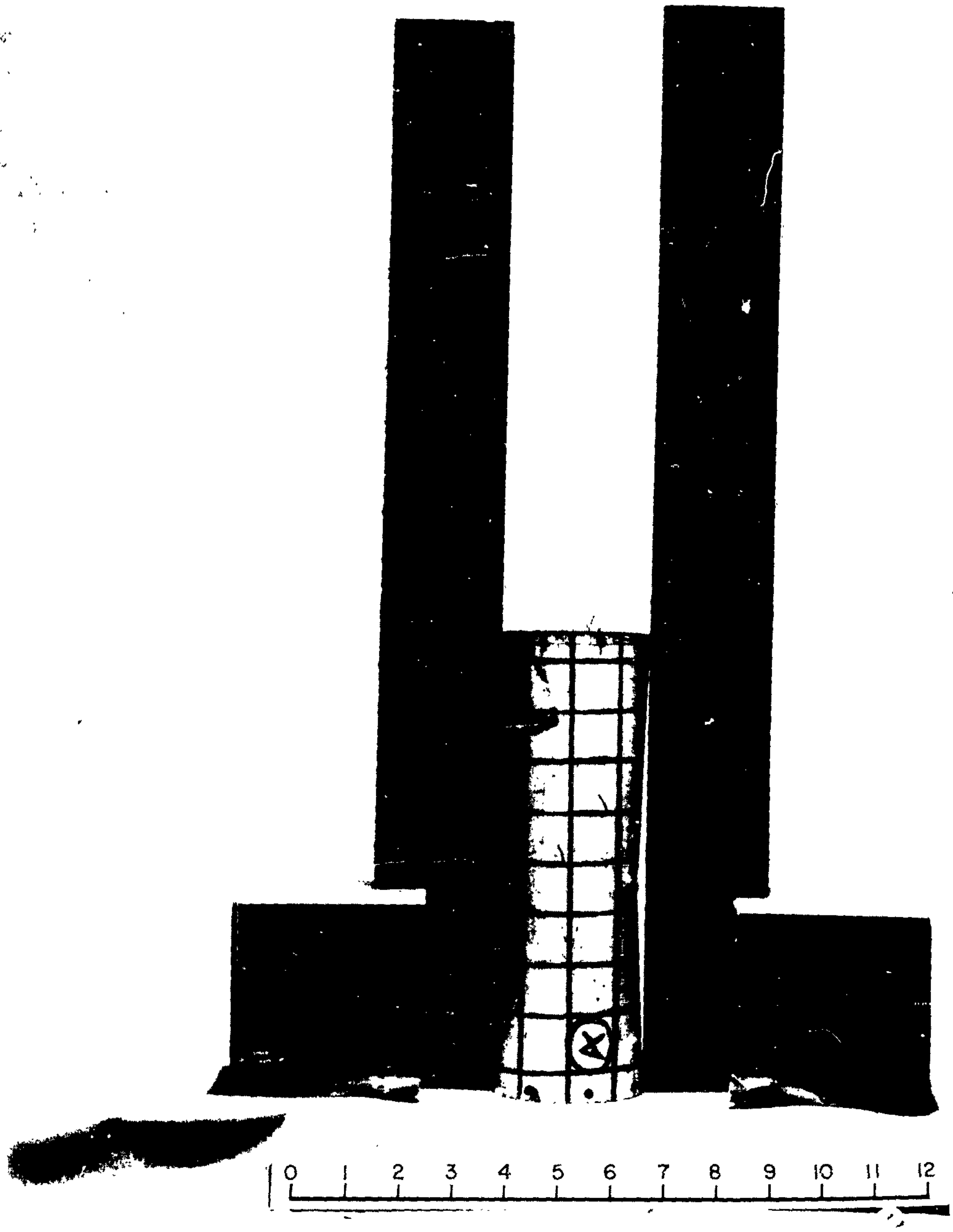

FIG. 5 — SHELL NO. 5 — SIDE VIEW

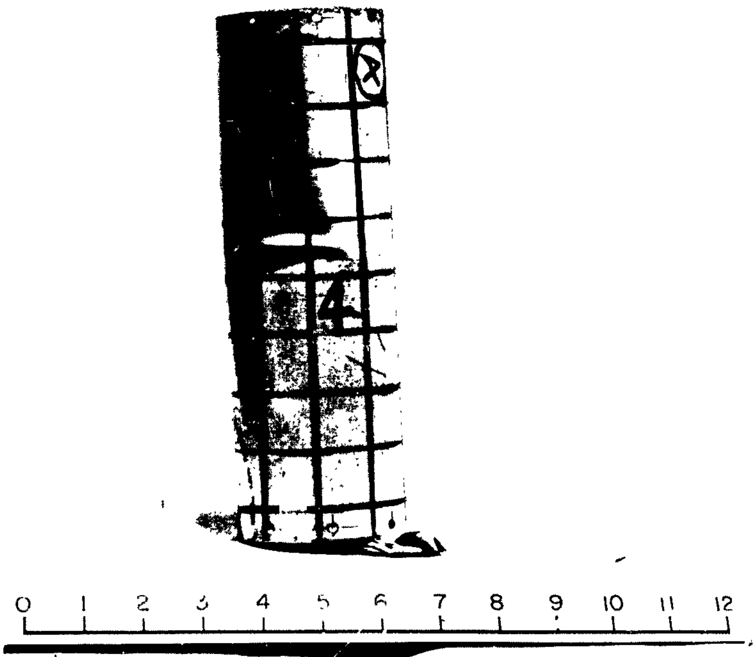

FIG. 6 - SHELL NO. 5 - FRONT VIEW

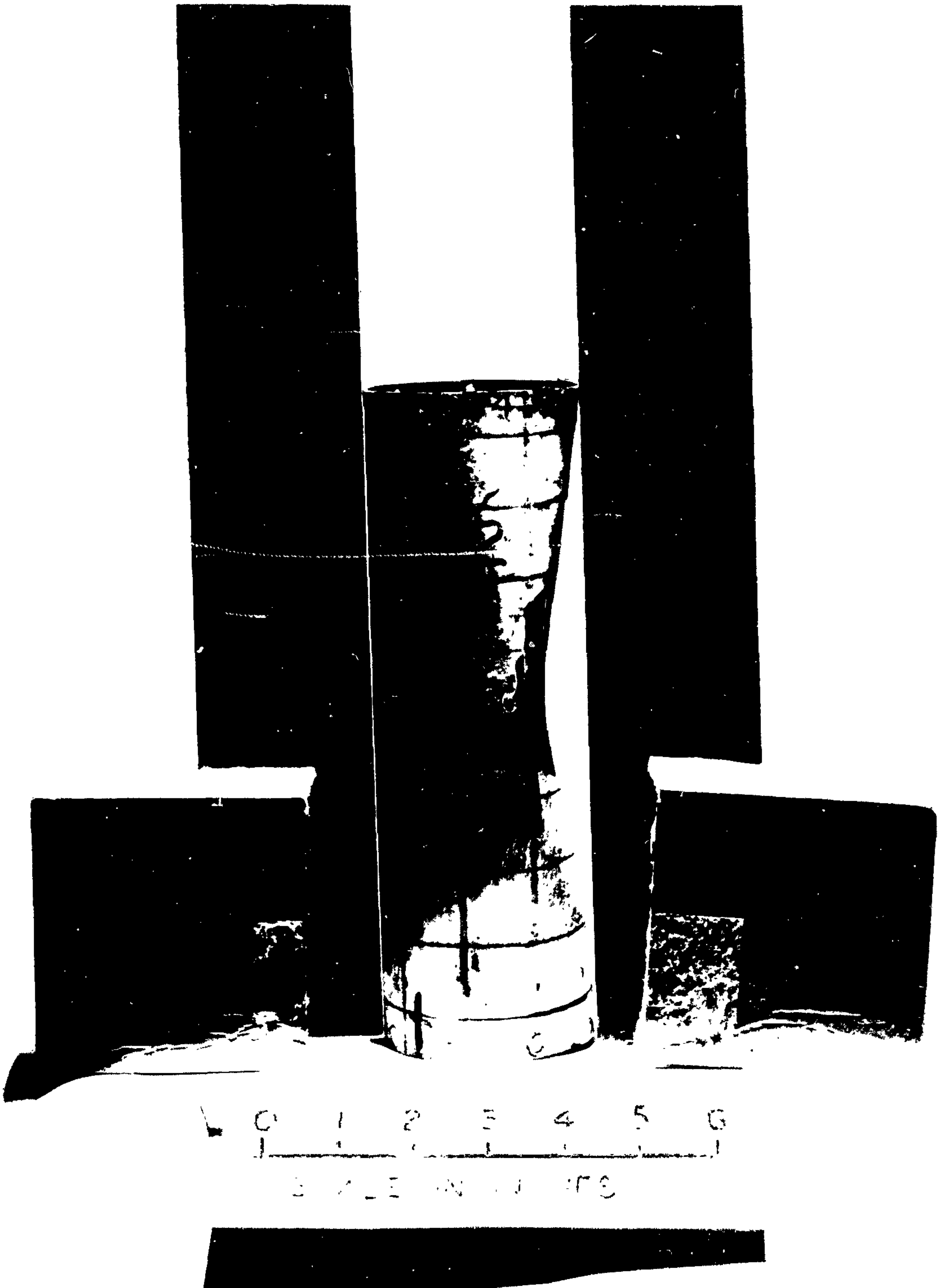

FIG. 7 – SHELL NO. 6 – SIDE VIEW

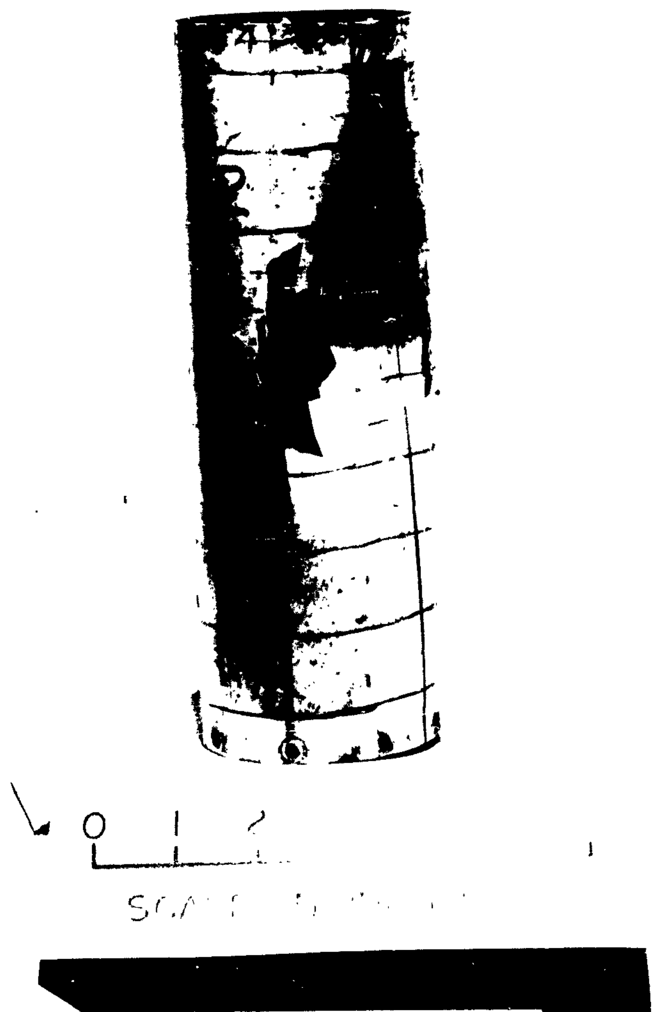

FIG. 8 – SHELL NO. 6 – FRONT VIEW

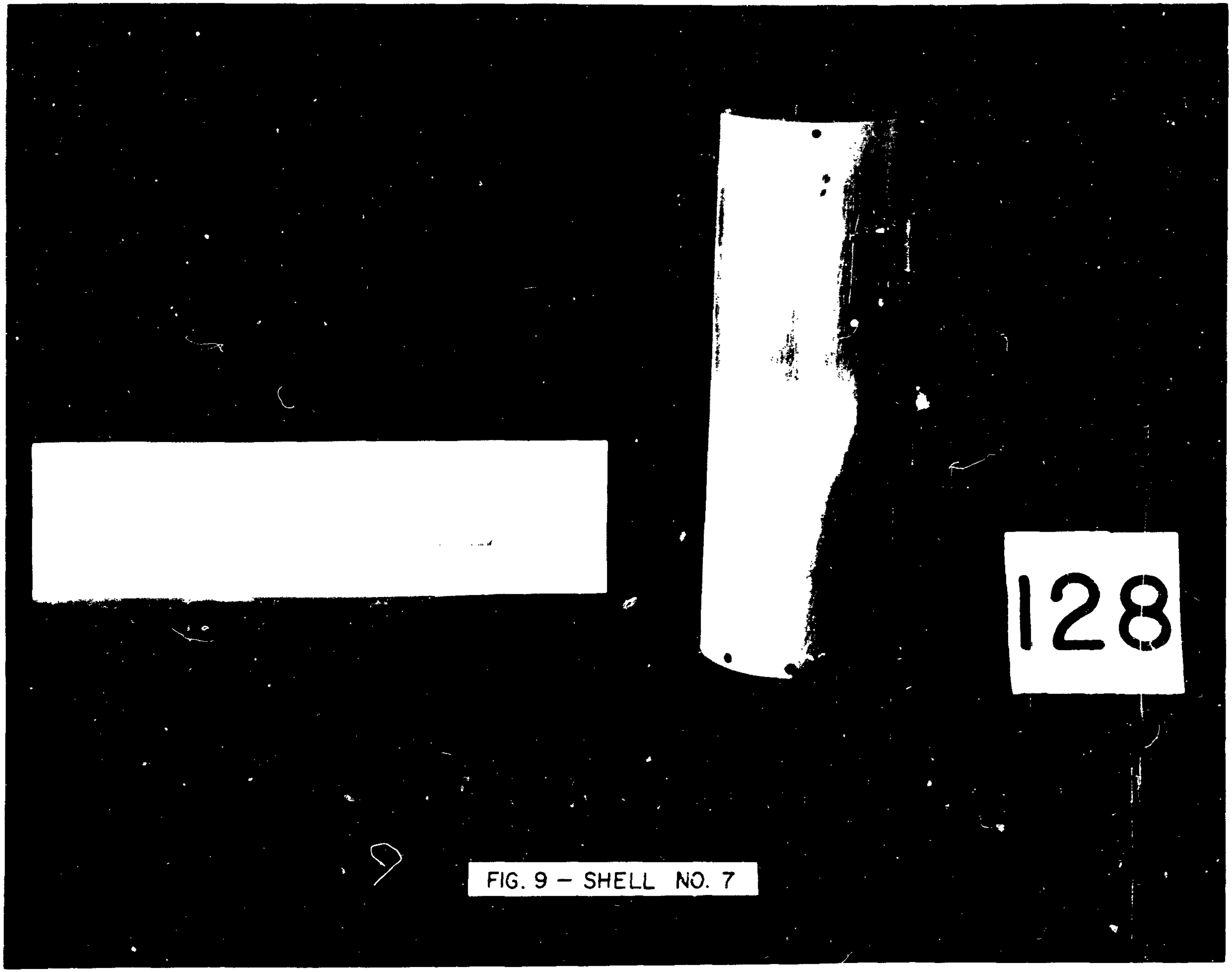

FIG. 9 – SHELL NO. 7

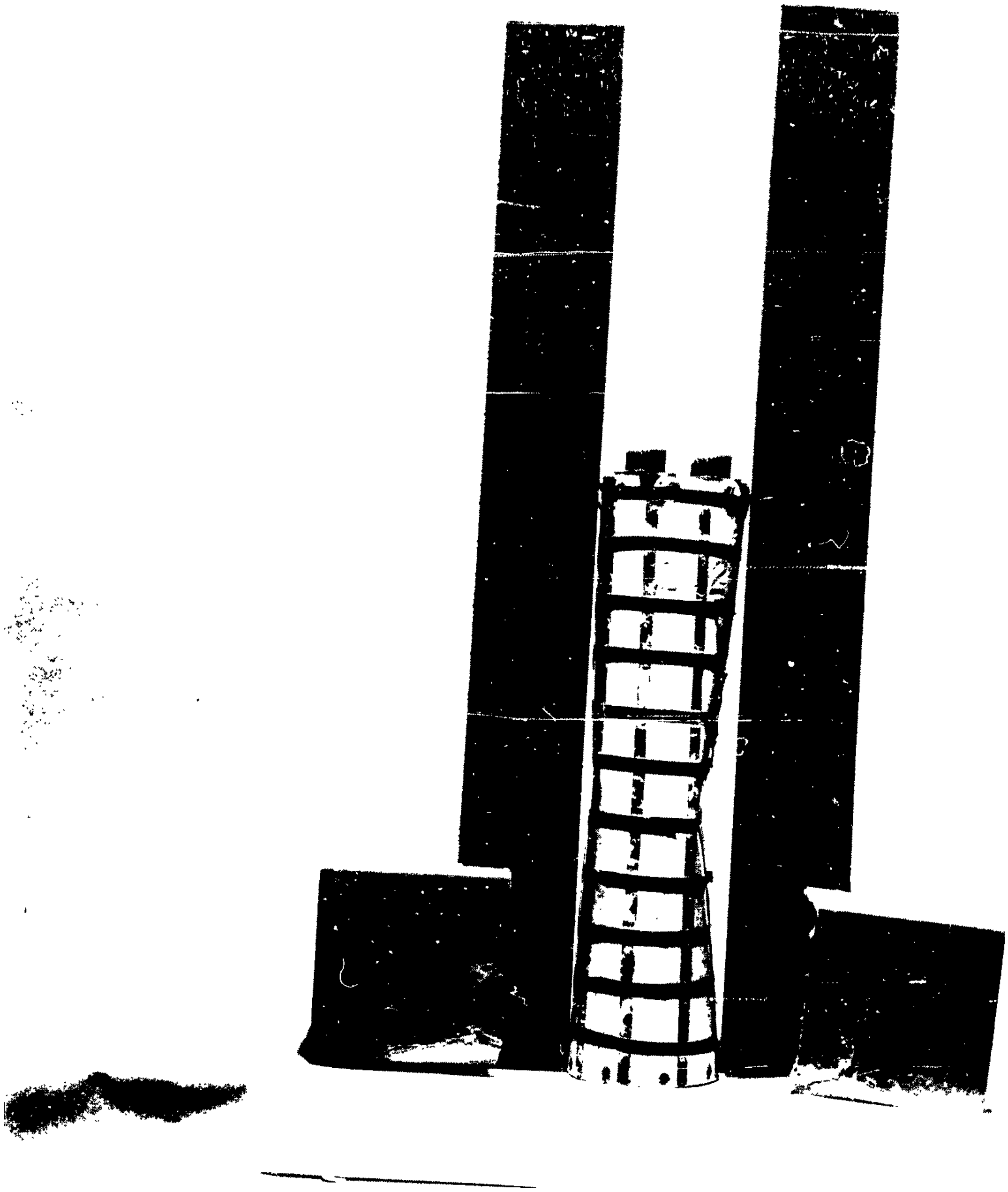

FIG. 10 – SHELL NO. 8 – SIDE VIEW

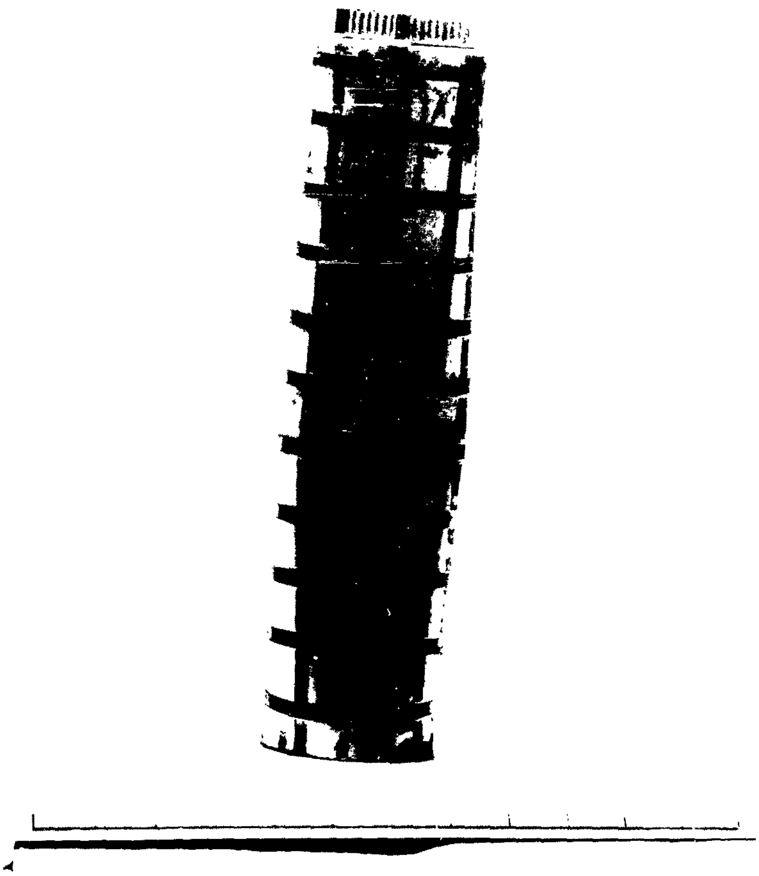

FIG. 11 – SHELL NO. 8 – FRONT VIEW

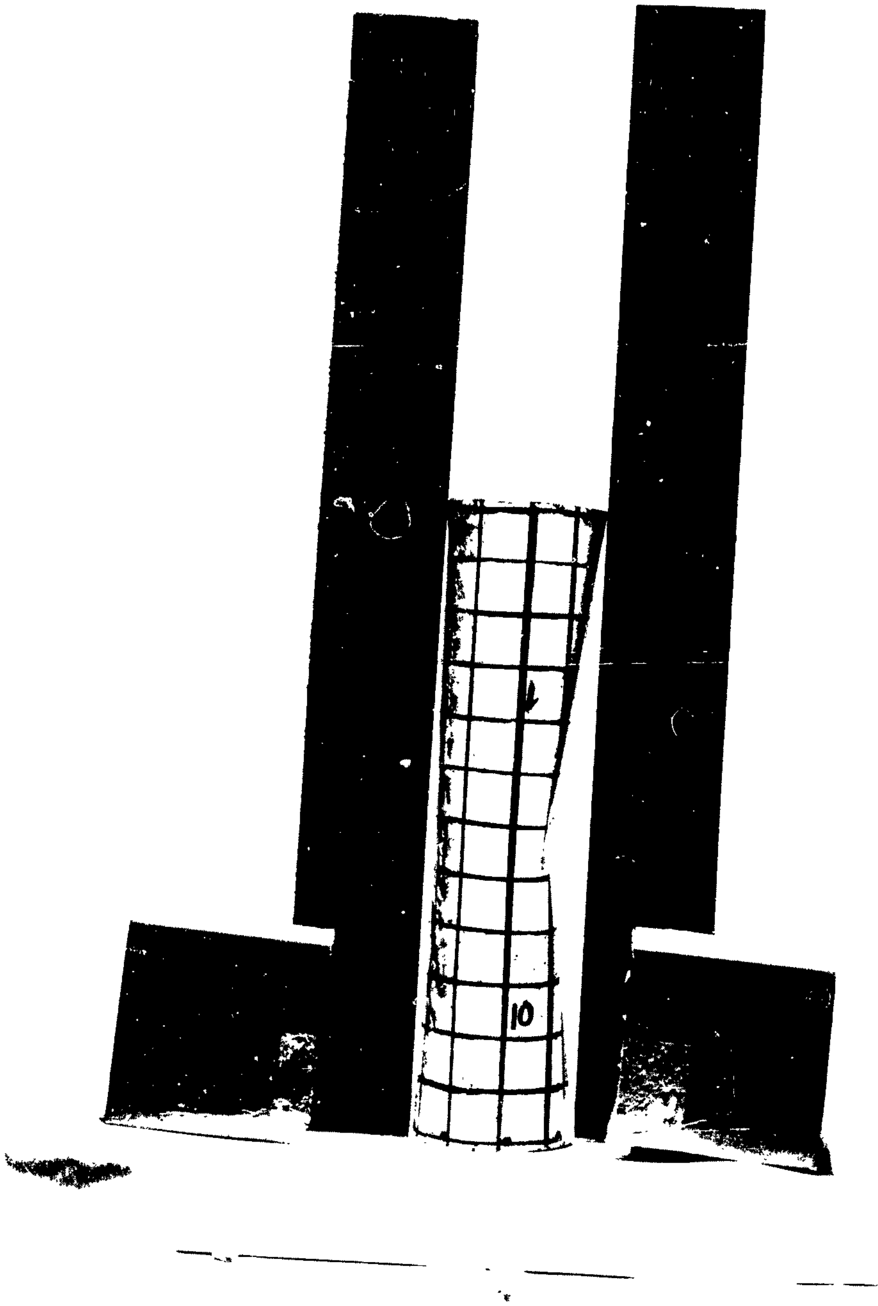

FIG. 12 — SHELL NO. 9 — SIDE VIEW

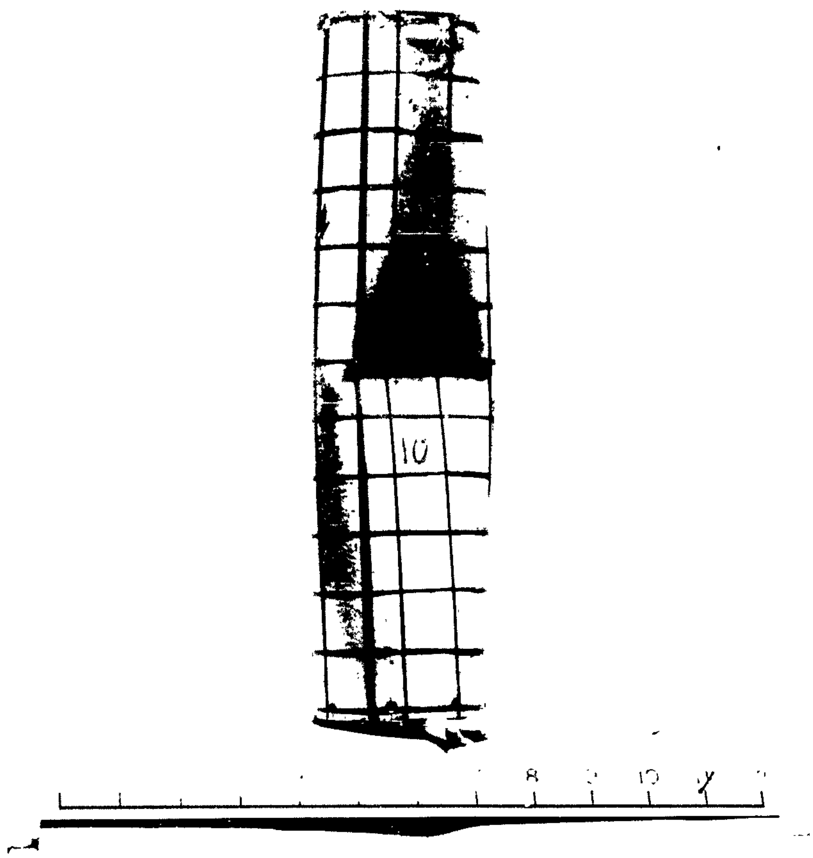

FIG. 13 – SHELL NO. 9 – FRONT VIEW

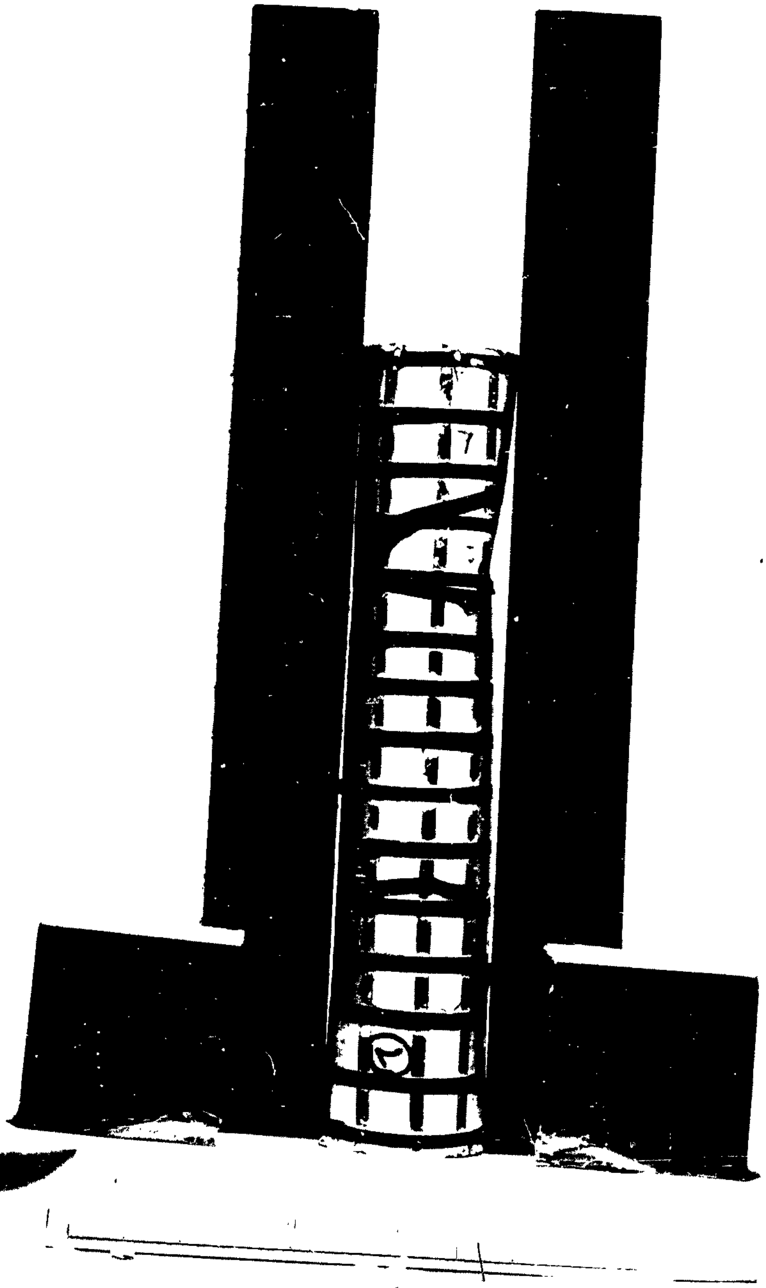

FIG. 14 — SHELL NO. 10 — SIDE VIEW

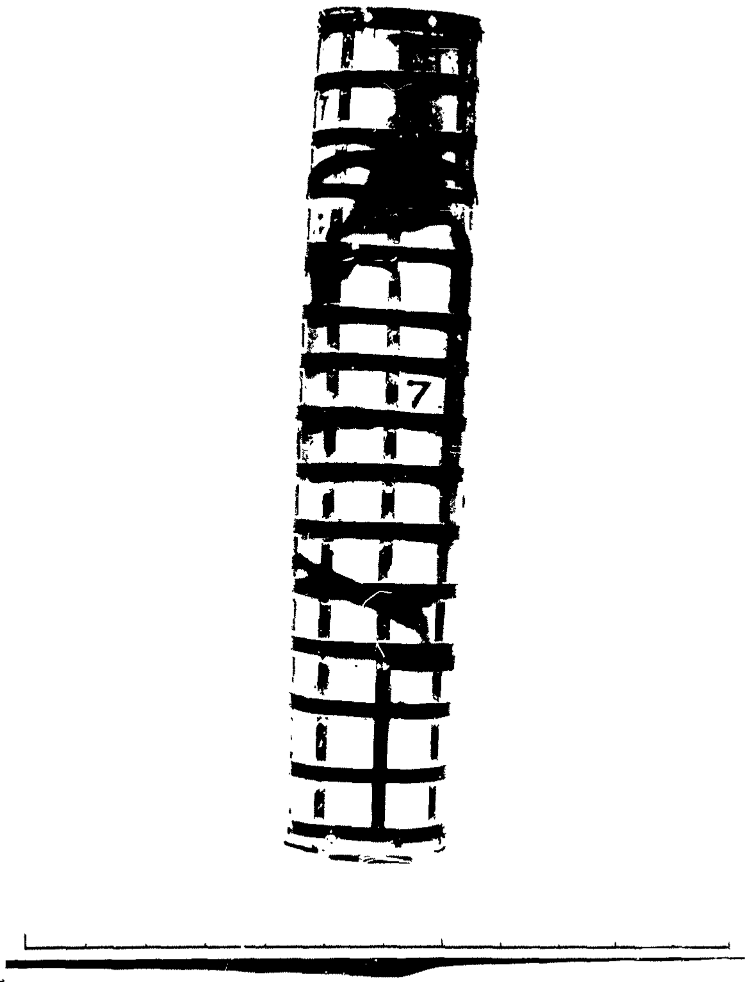

FIG. 15 – SHELL NO. 10 – FRONT VIEW

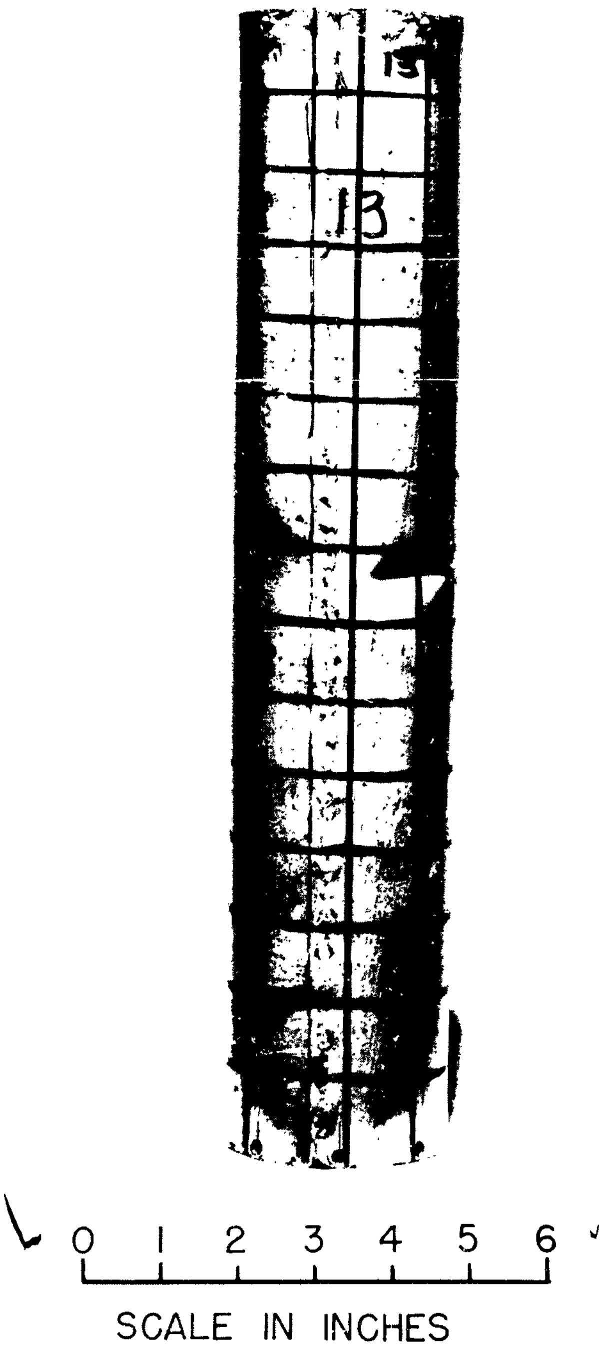

FIG. 16 – SHELL NO. 11

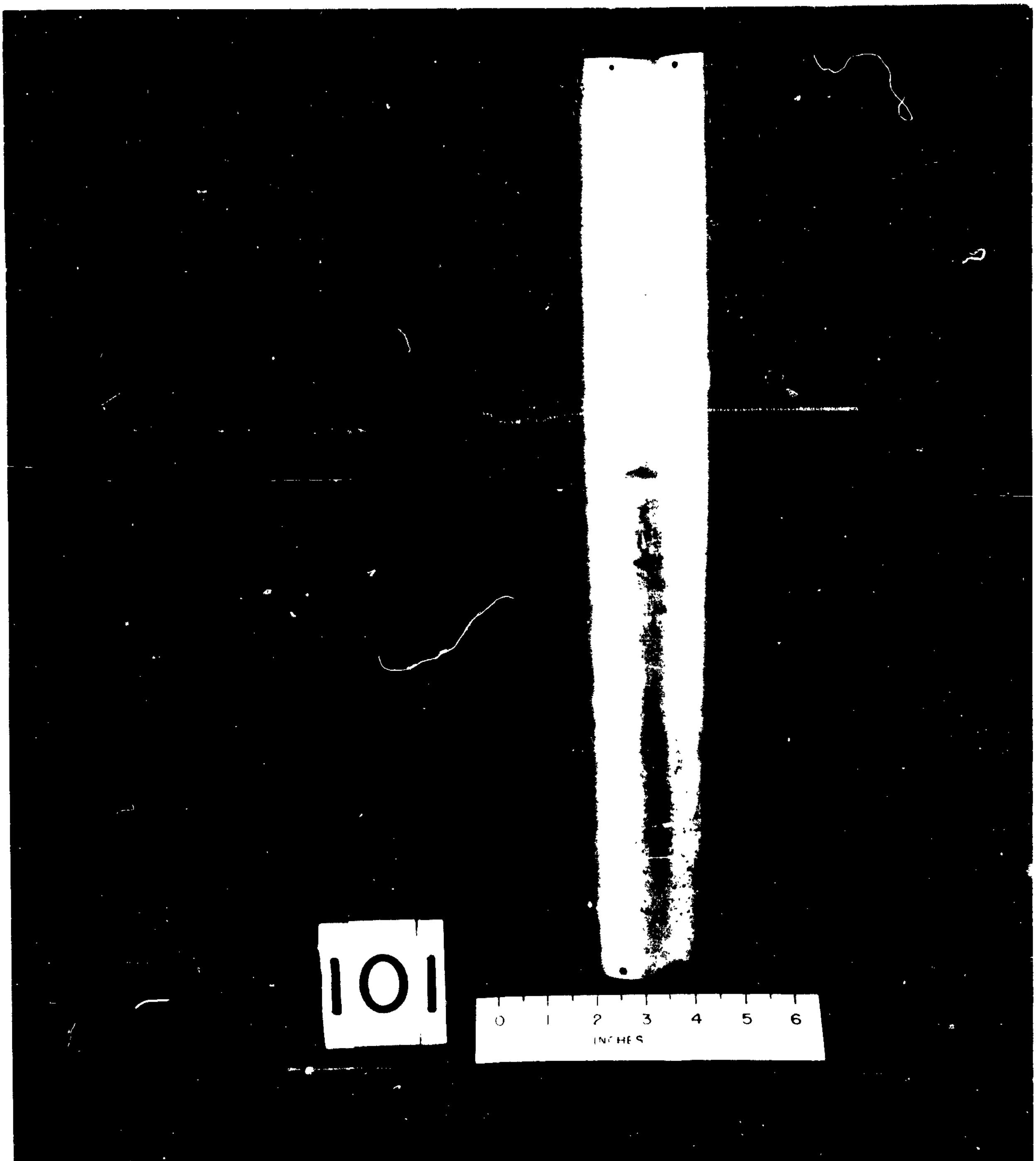

FIG. 17 – SHELL NO. 12

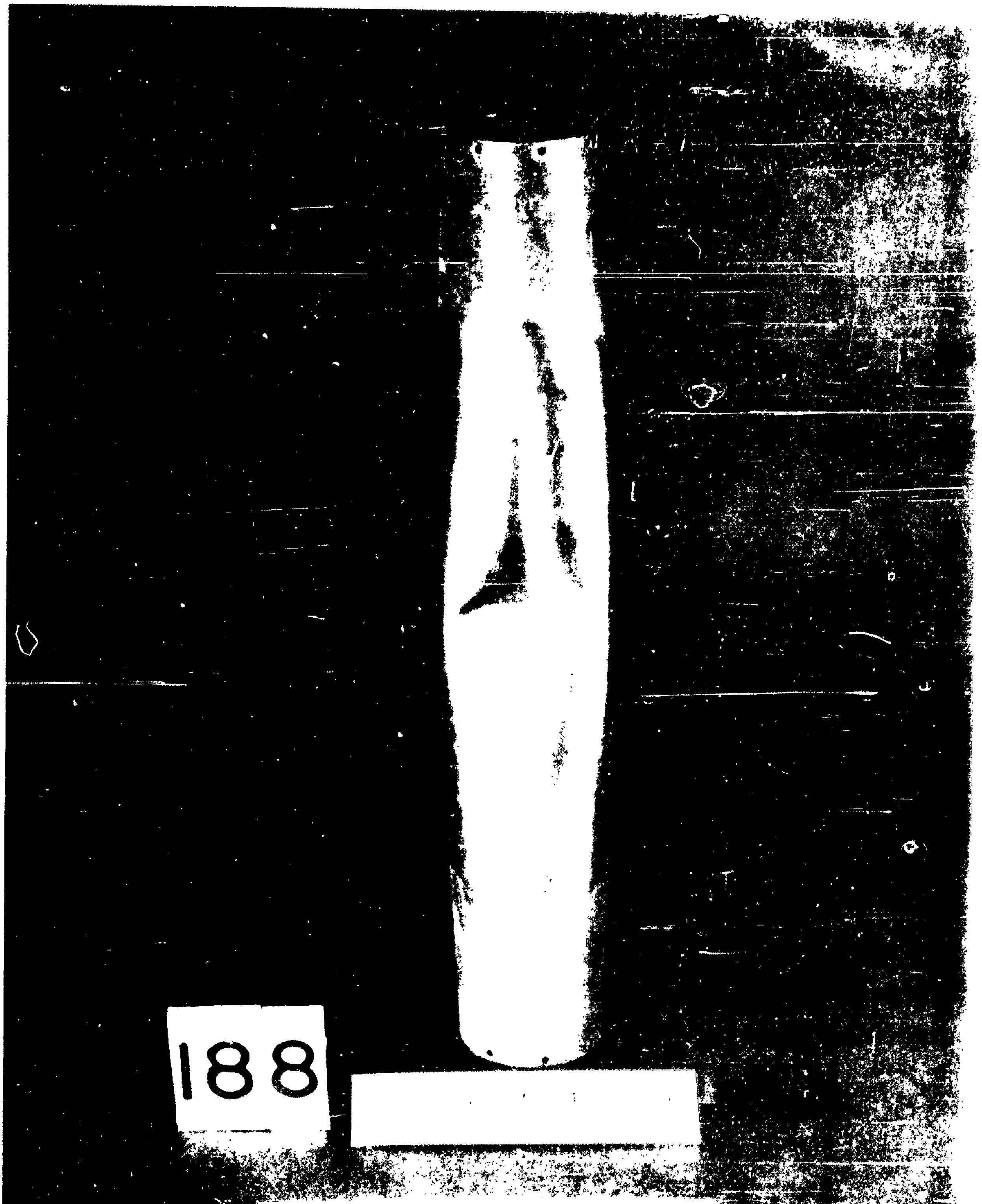

FIG. 18 – SHELL NO. 13 – FRONT VIEW

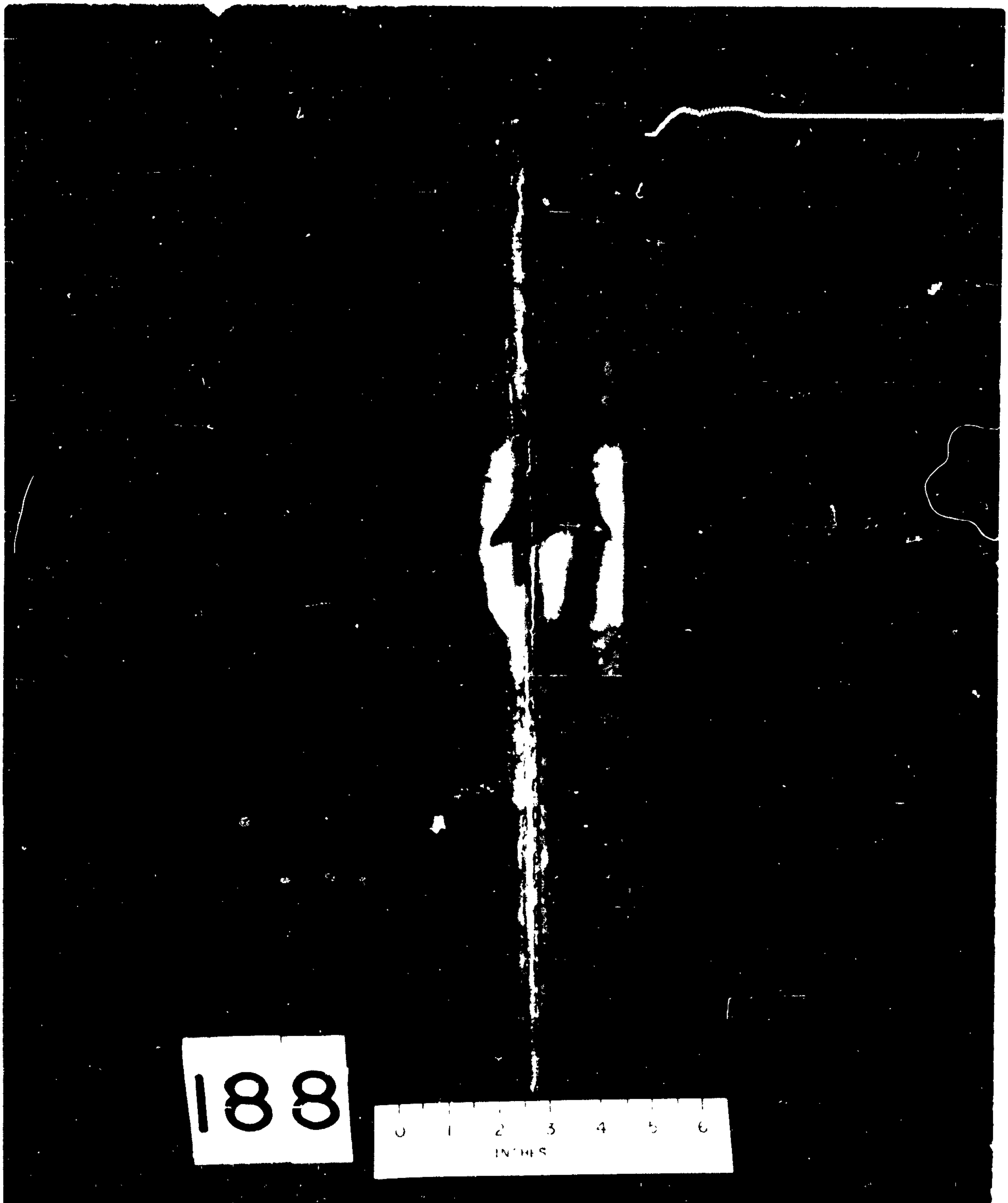

FIG. 19 – SHELL NO. 13 REAR VIEW

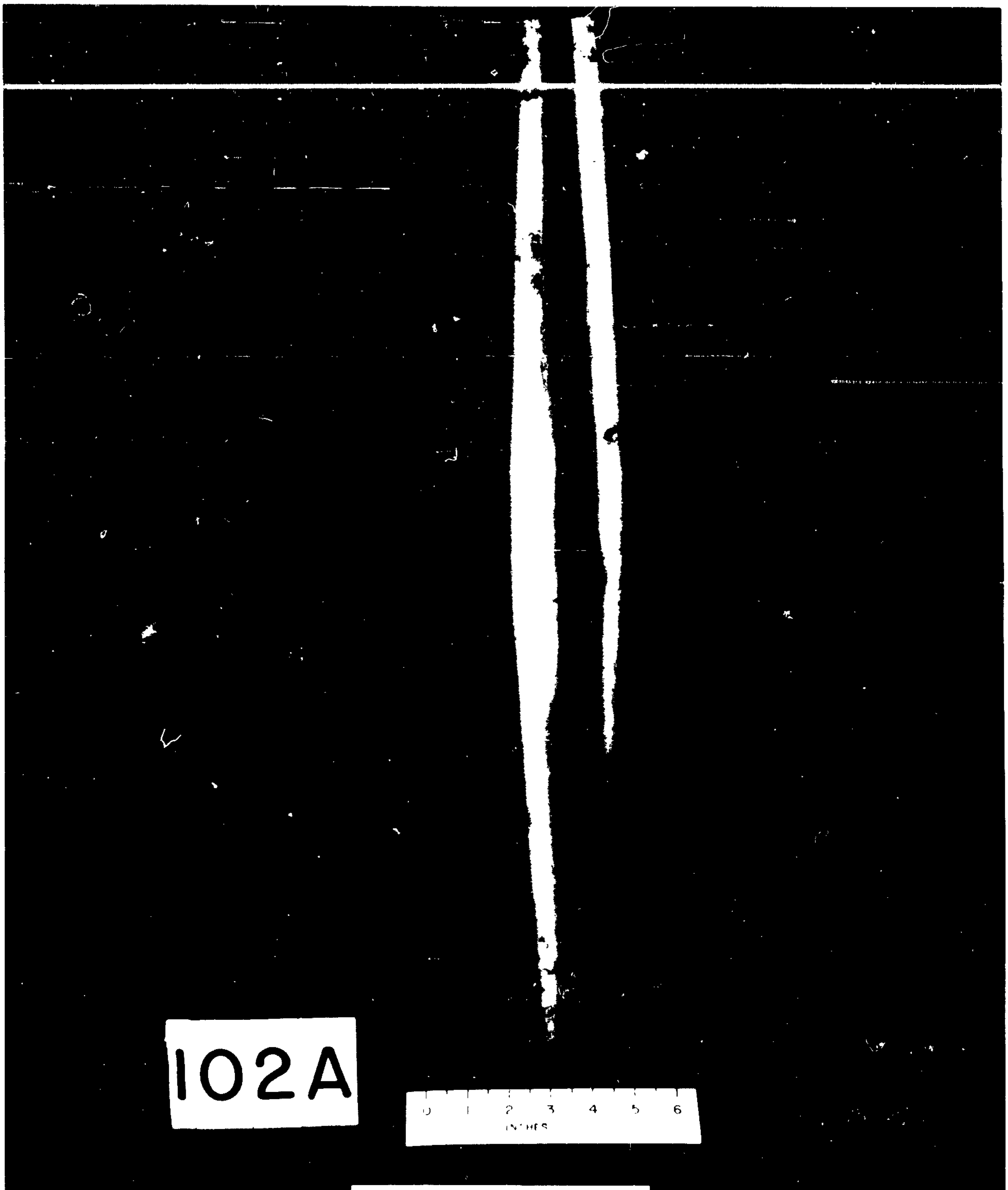

FIG. 20 — SHELL NO. 14

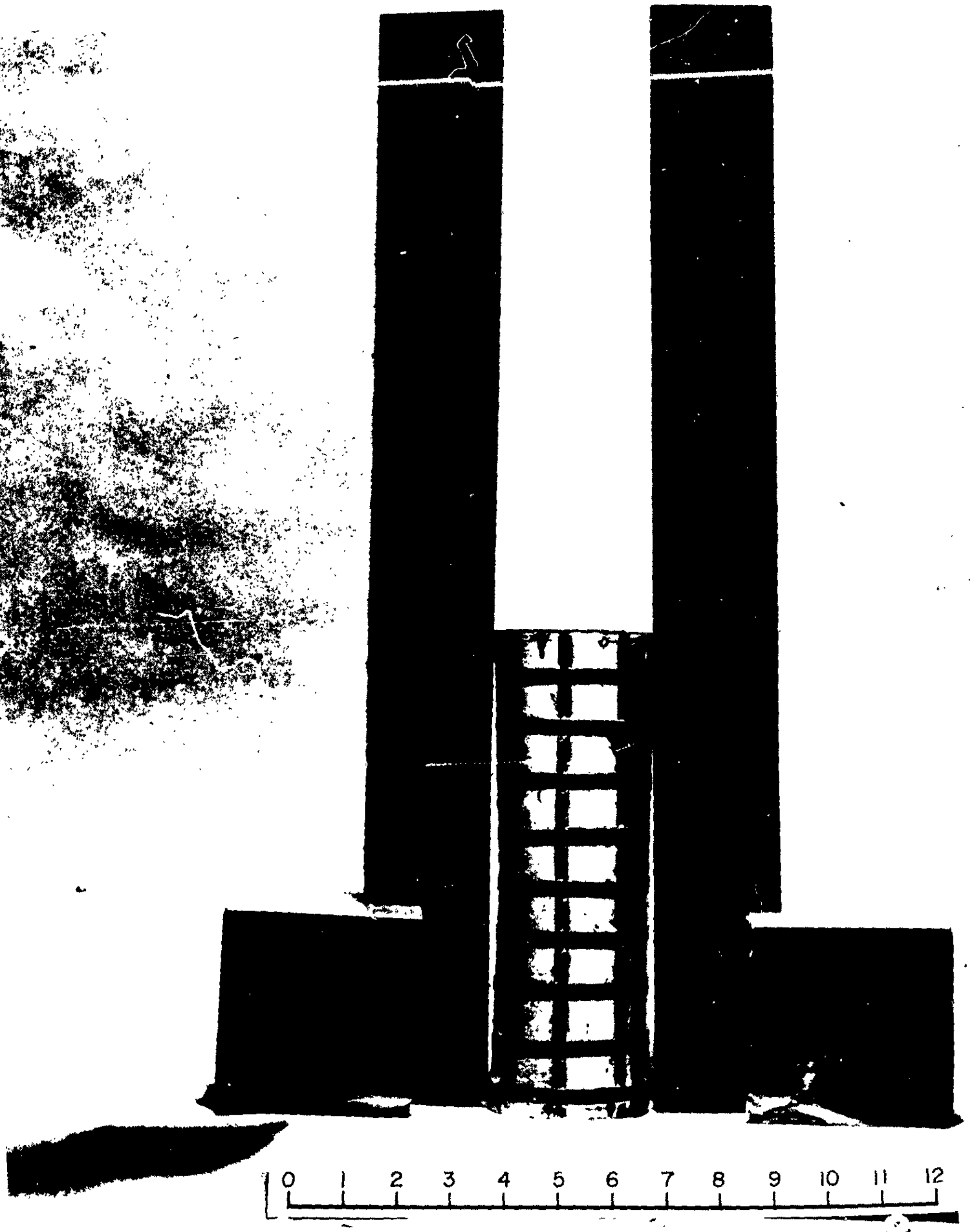

FIG. 21 - SHELL NO. 16

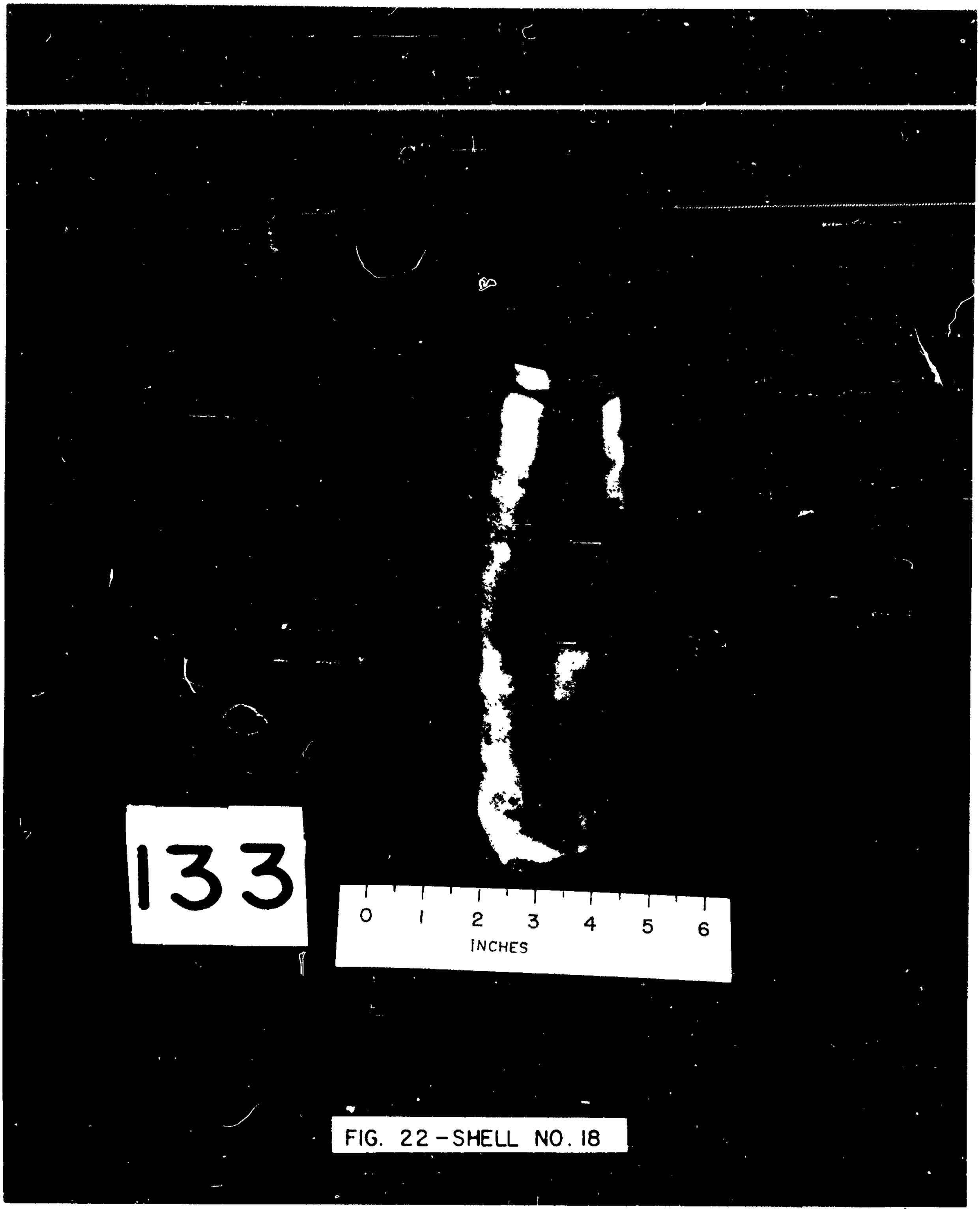

FIG. 22 - SHELL NO. 18

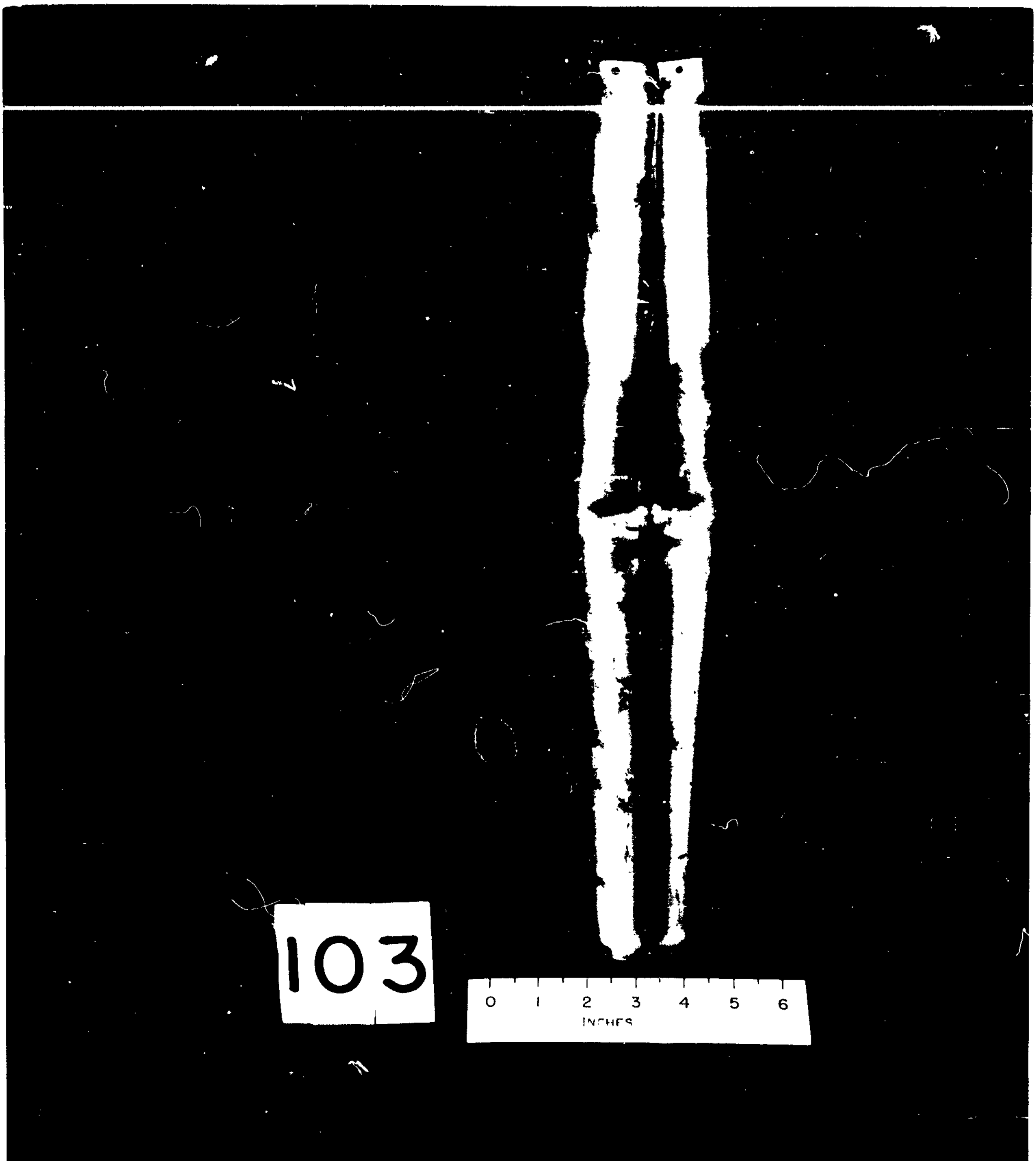

FIG. 23 – SHELL NO. 19

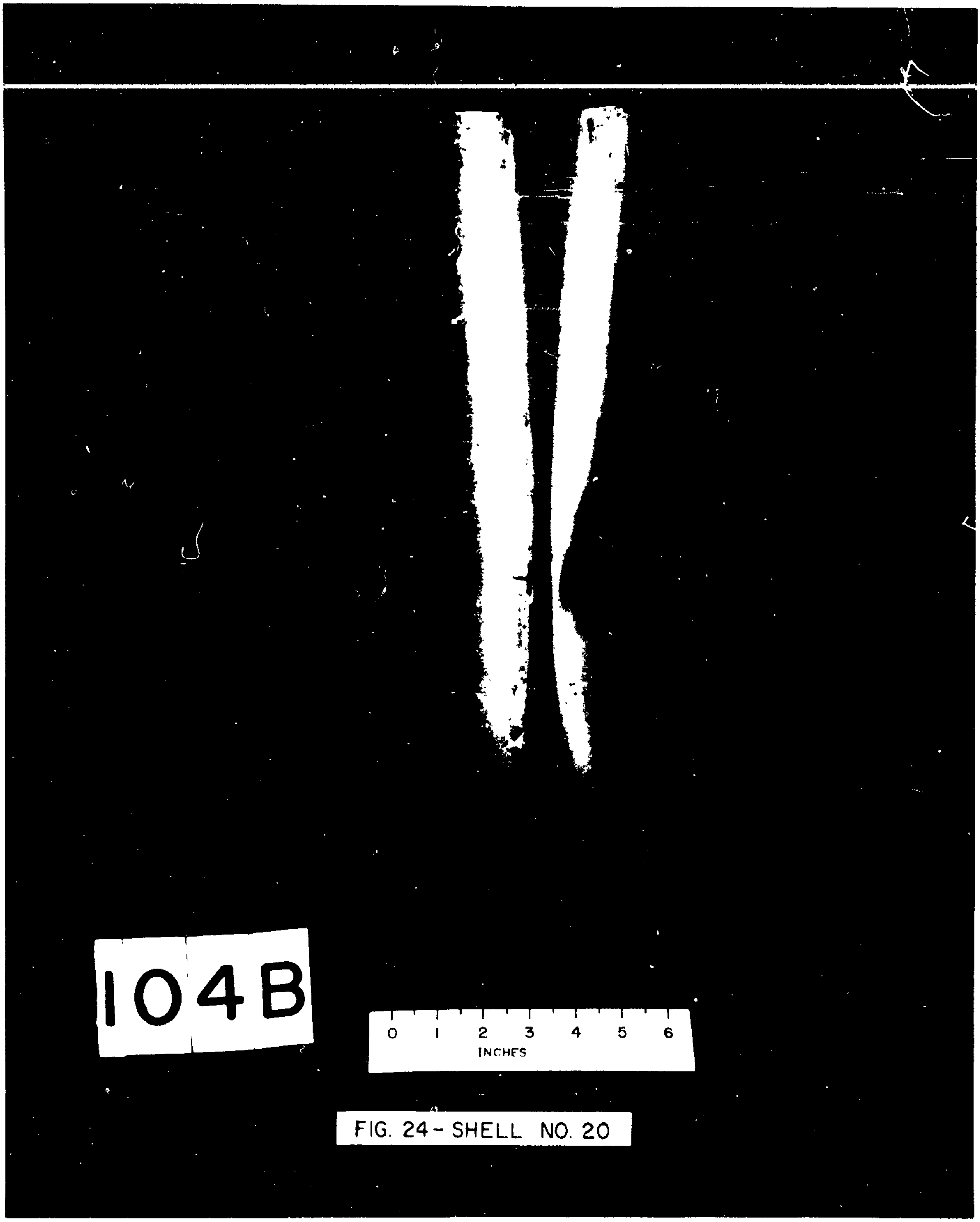

FIG. 24 - SHELL NO. 20

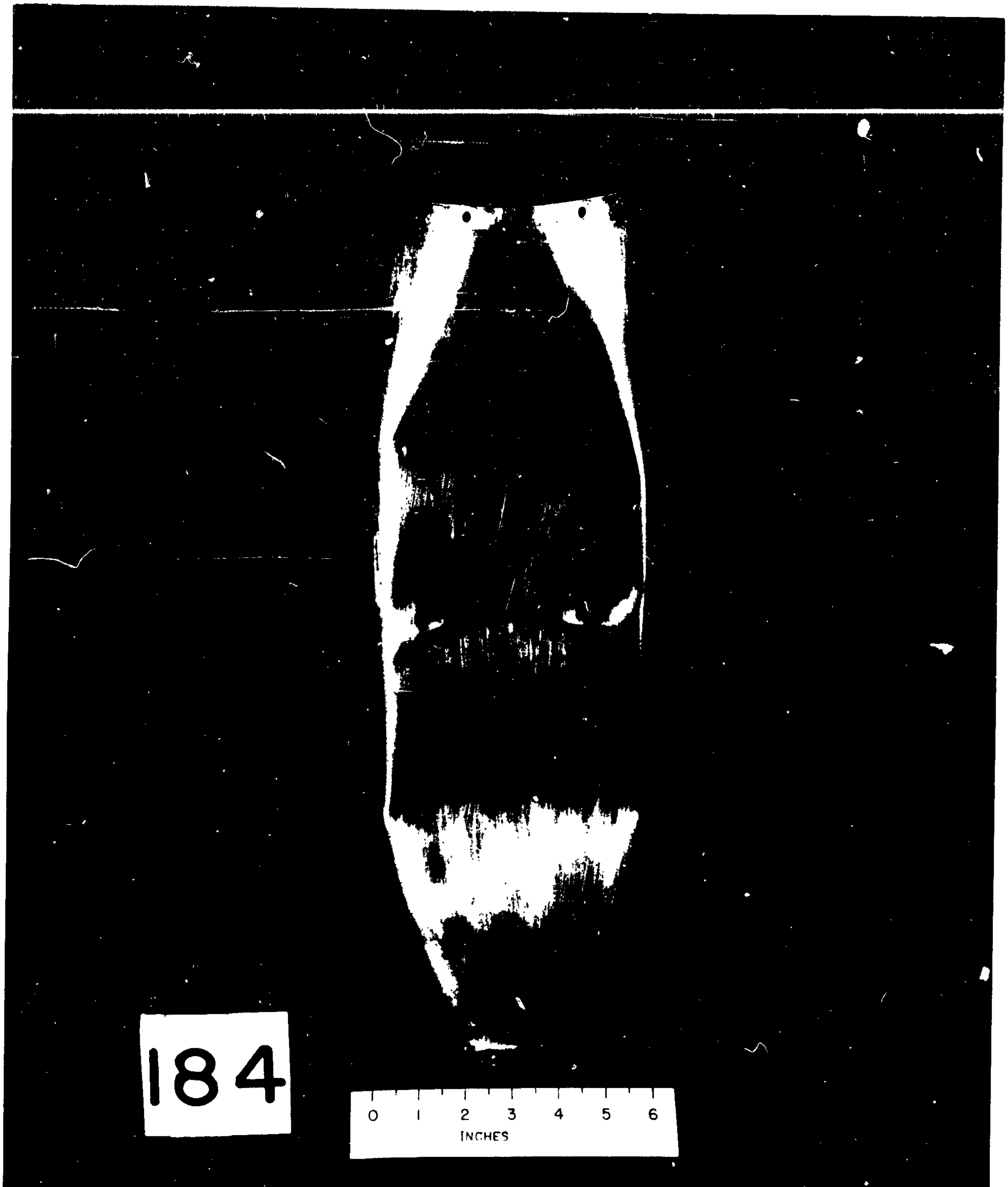

FIG. 25 – SHELL NO. 21 – FRONT VIEW

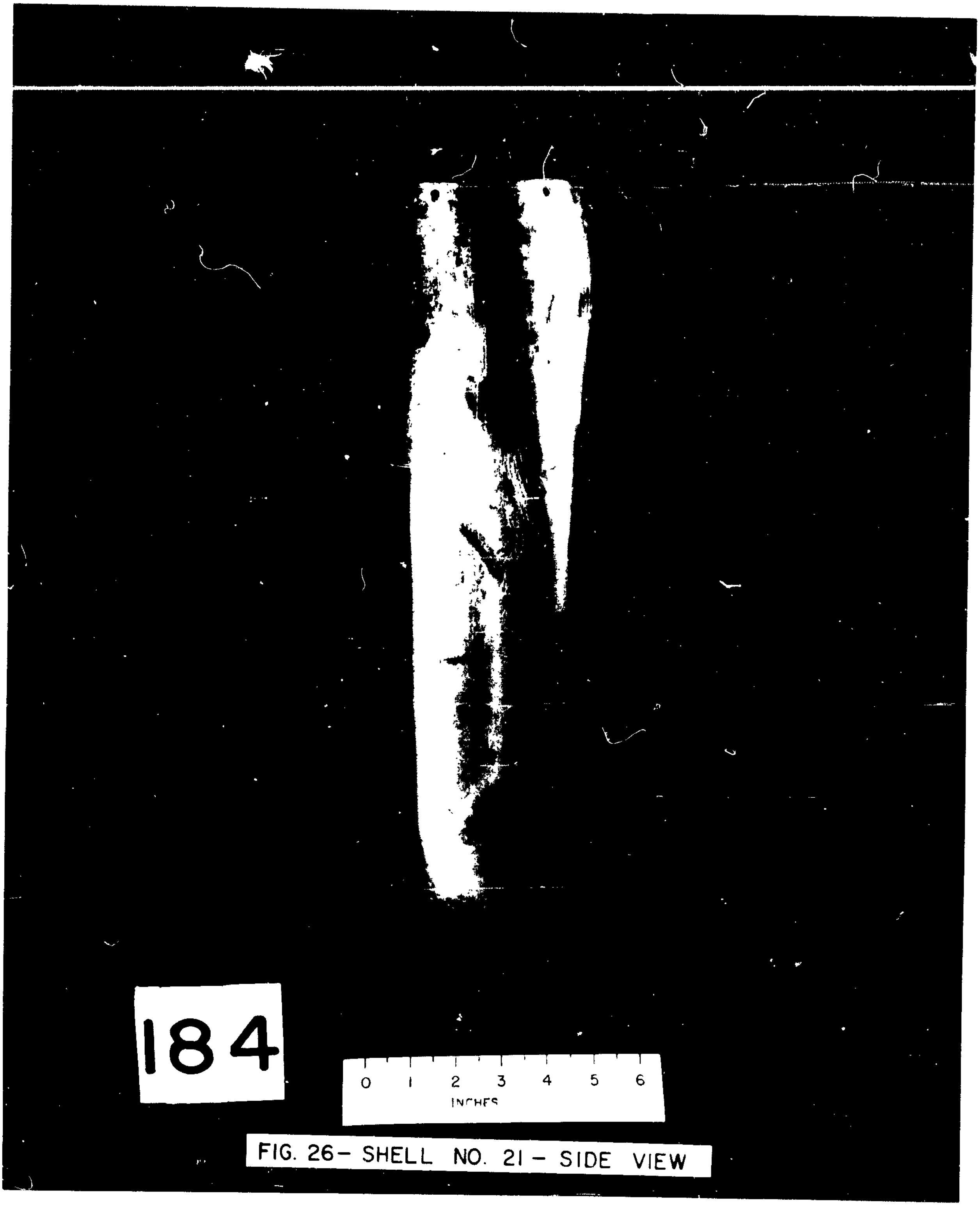

FIG. 26– SHELL NO. 21 – SIDE VIEW

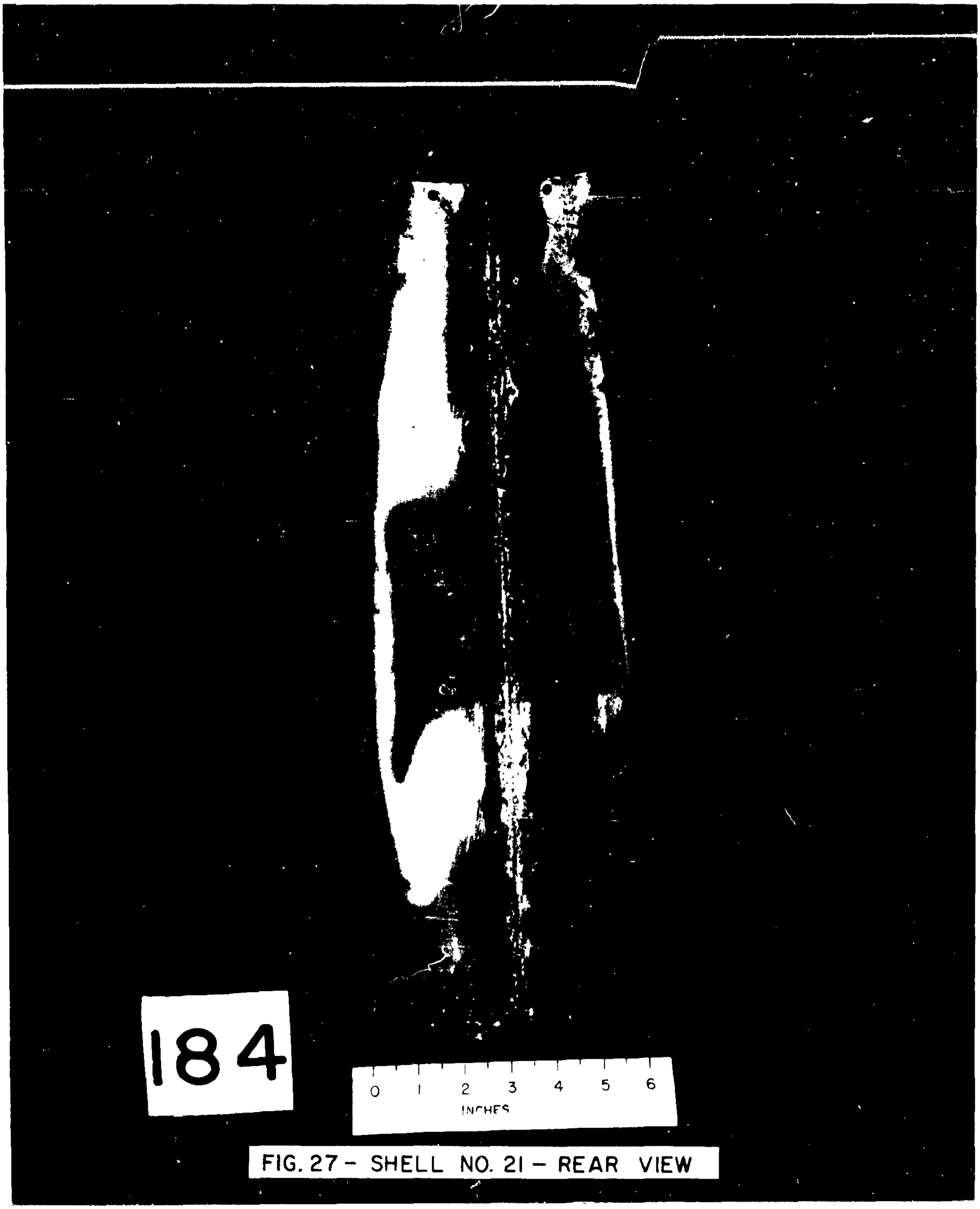

FIG. 27 - SHELL NO. 21 - REAR VIEW

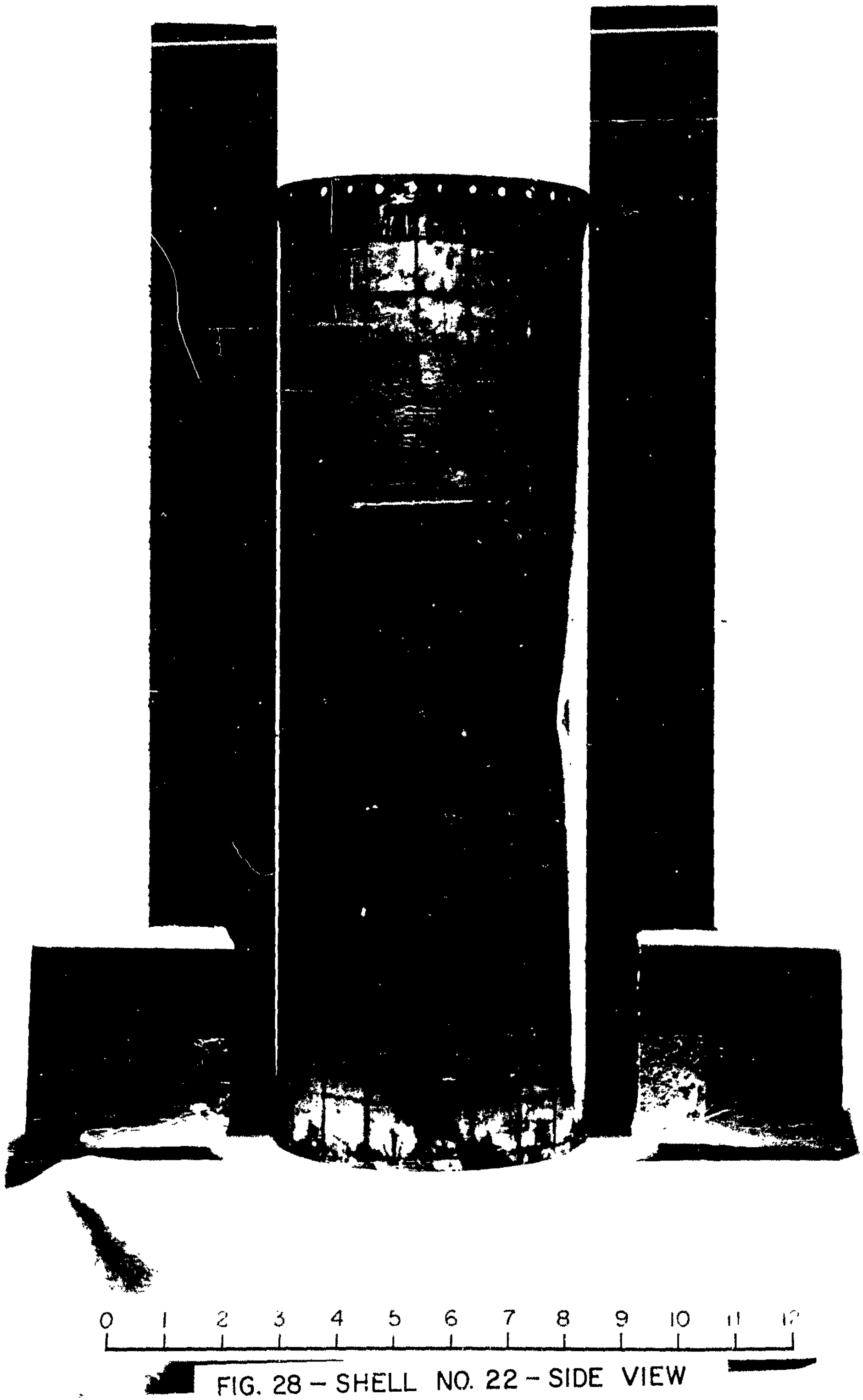

FIG. 28 – SHELL NO. 22 – SIDE VIEW

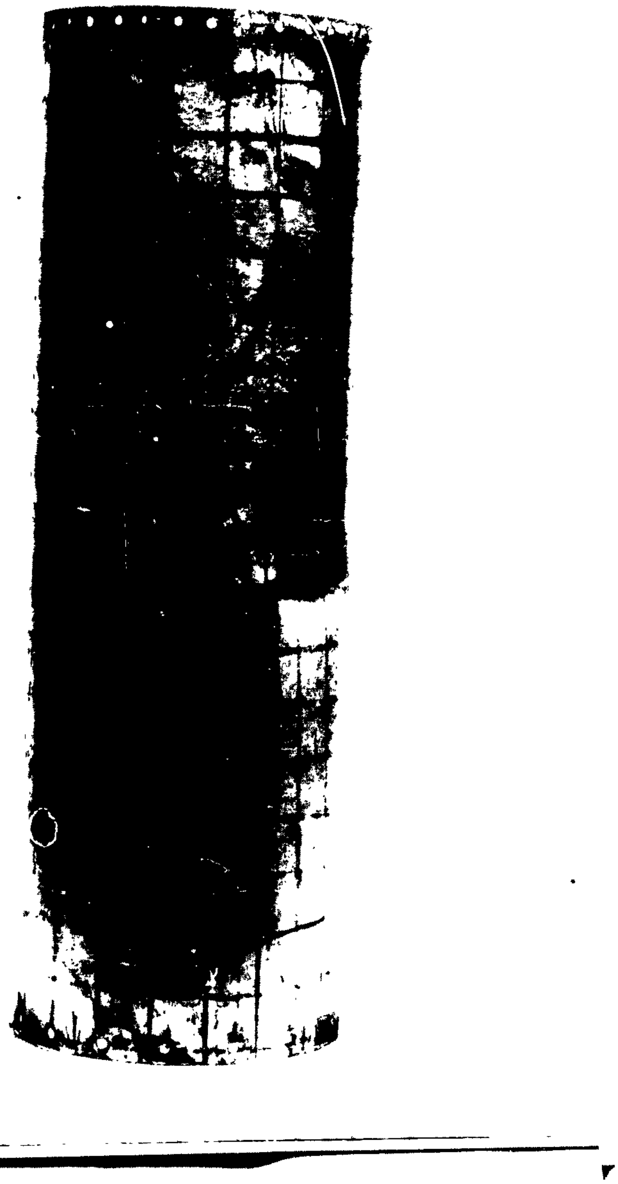

FIG. 29—SHELL NO. 22-FRONT VIEW

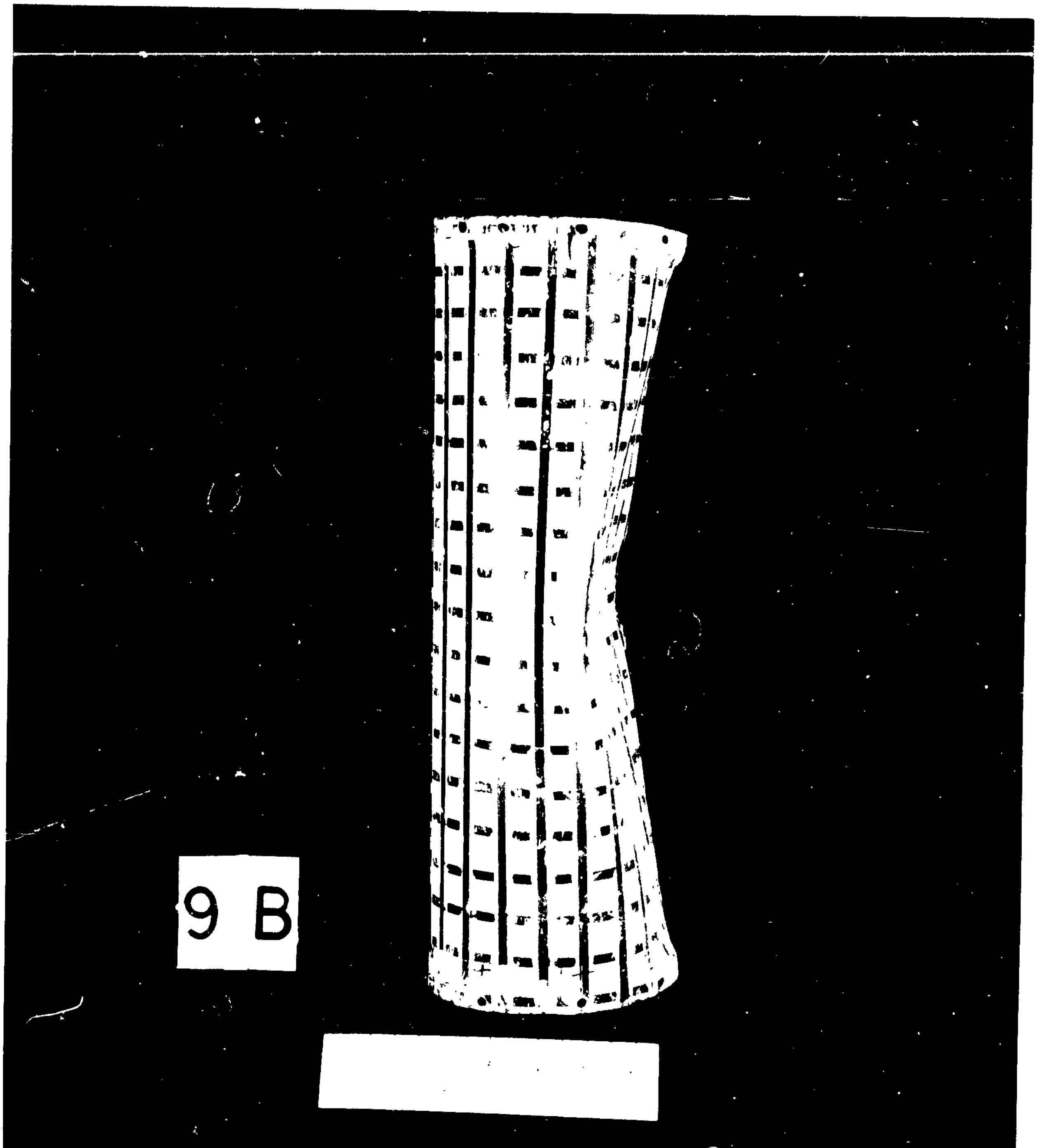

FIG. 30 – SHELL NO. 23 – SIDE VIEW

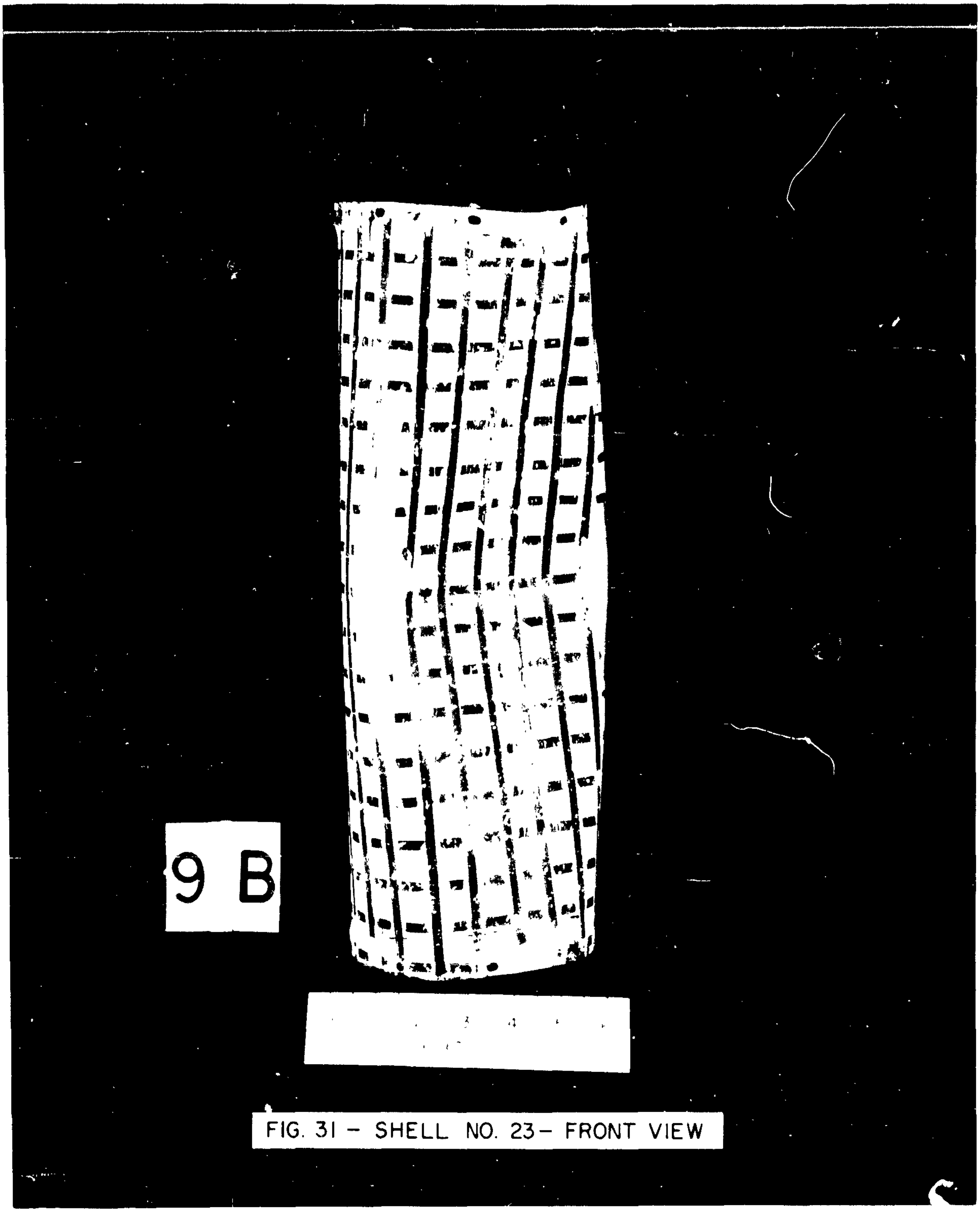

FIG. 31 – SHELL NO. 23– FRONT VIEW

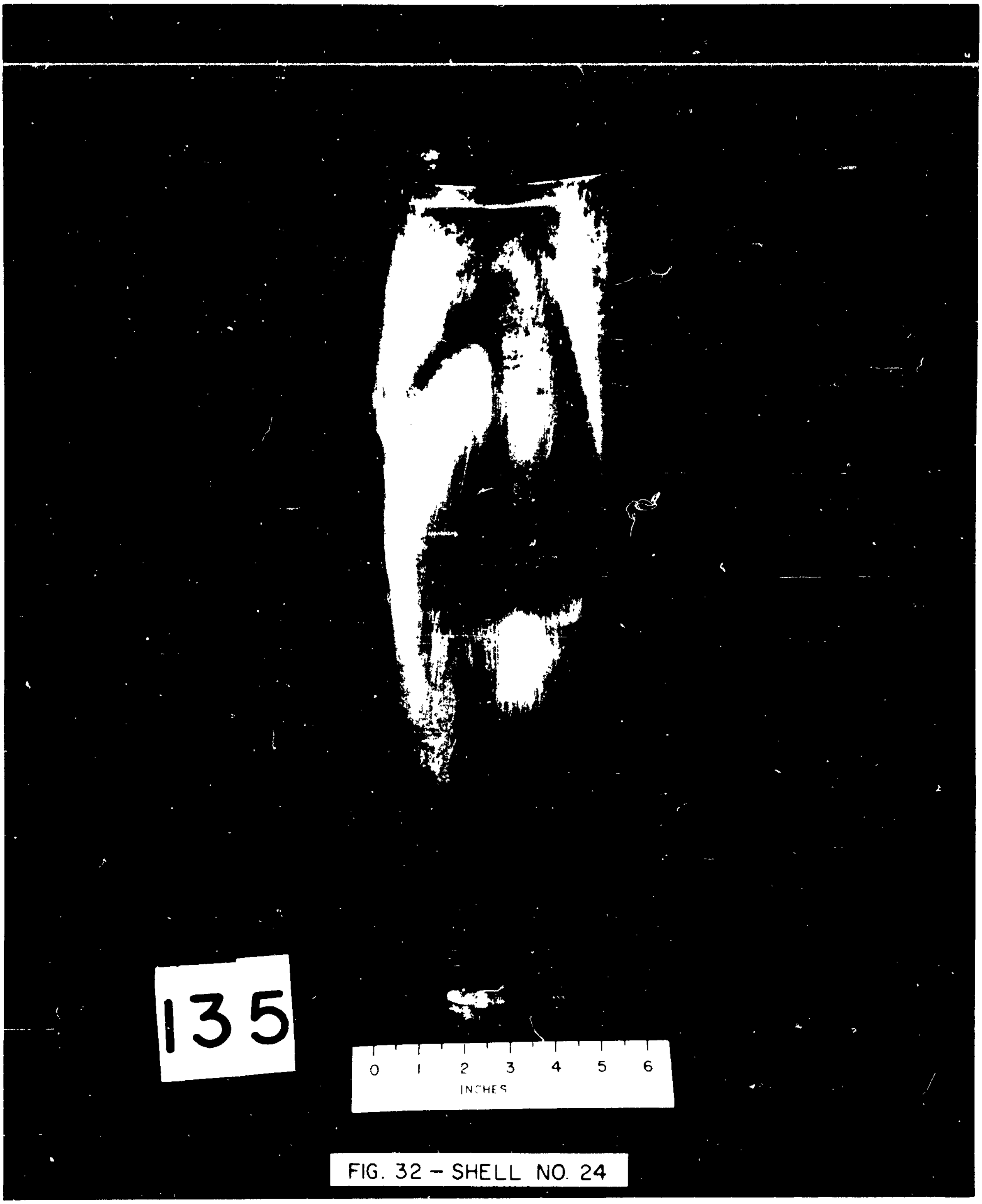

FIG. 32 – SHELL NO. 24

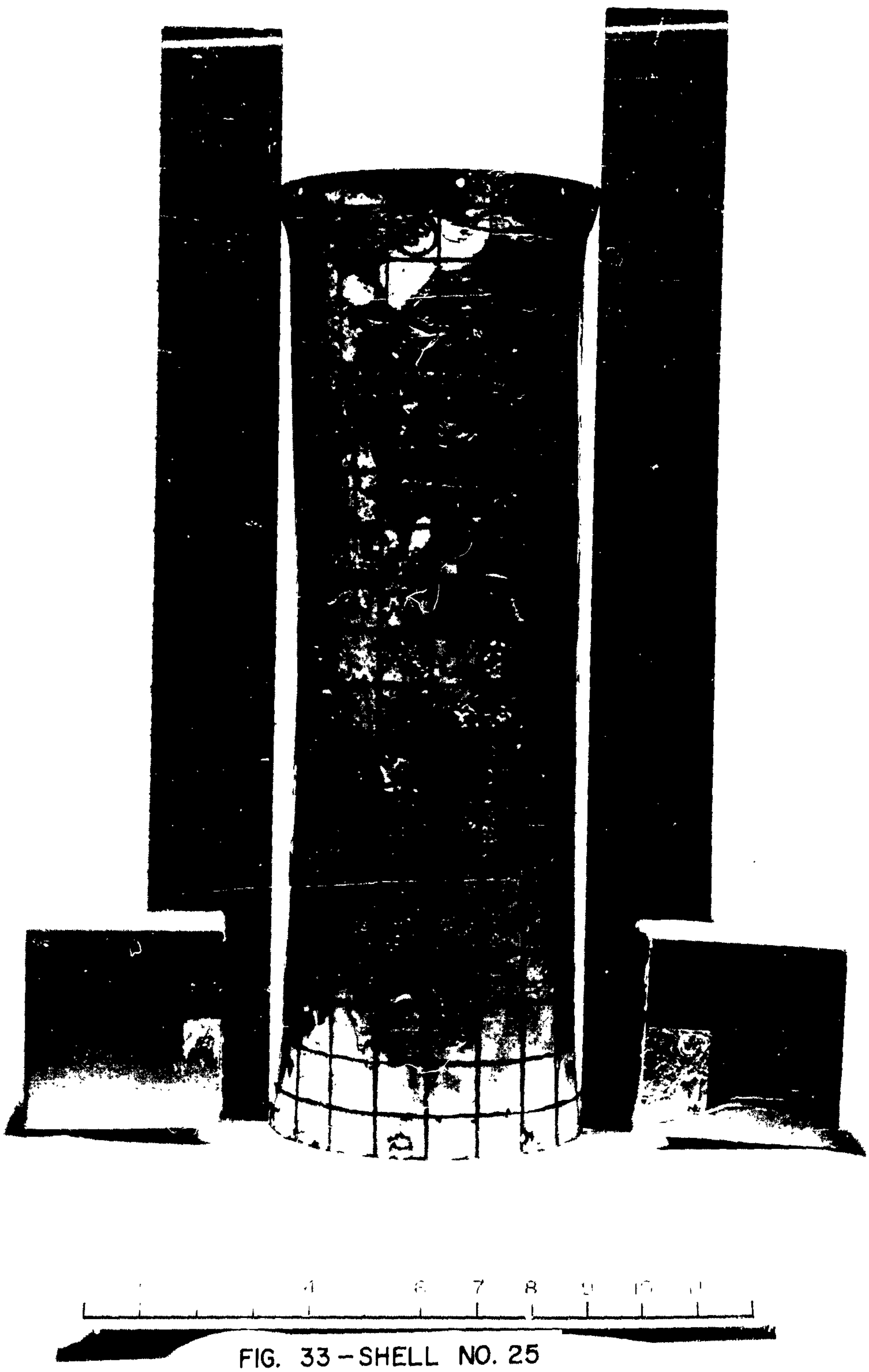

FIG. 33 - SHELL NO. 25

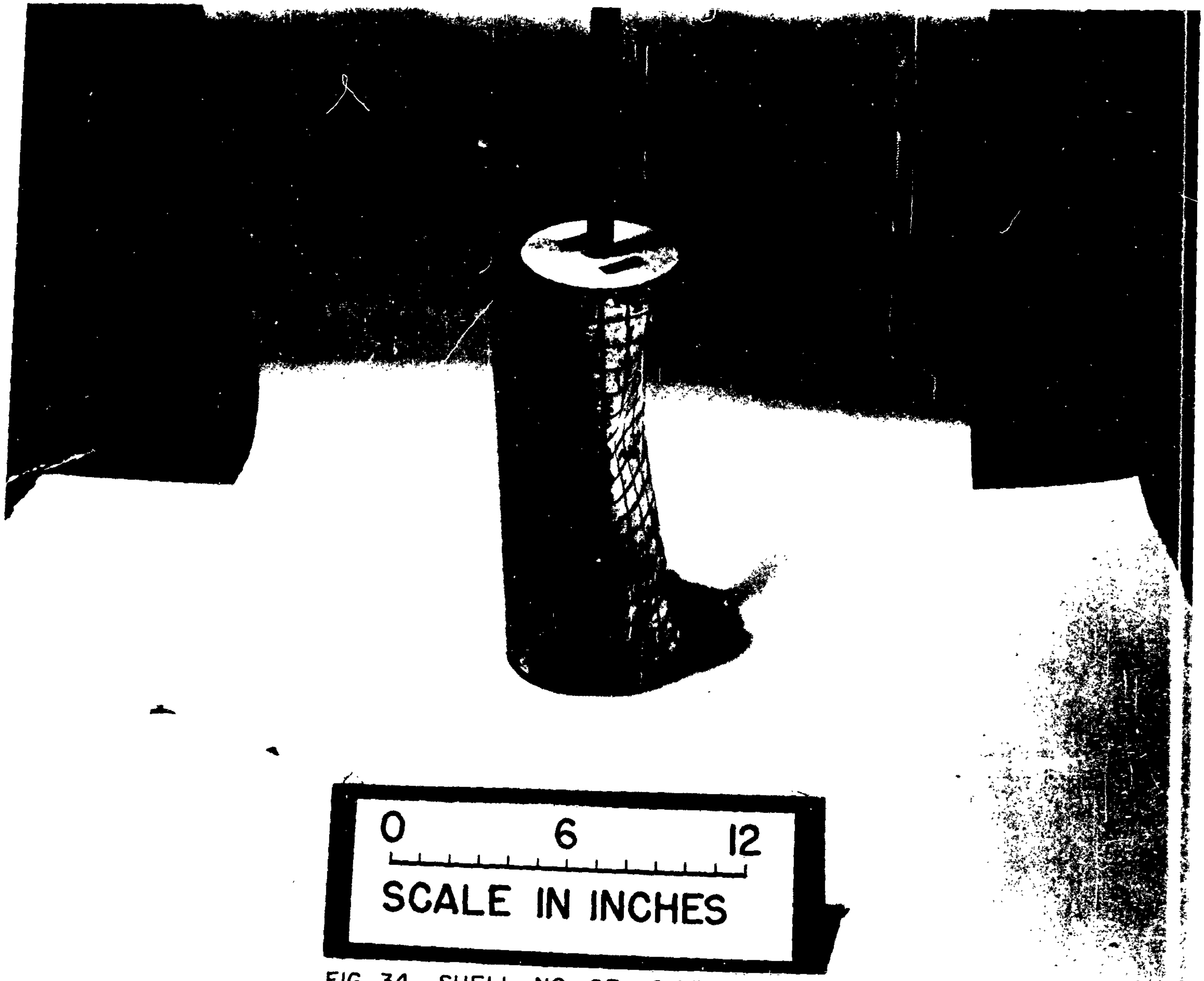

FIG. 34 – SHELL NO. 27 – SIDE VIEW

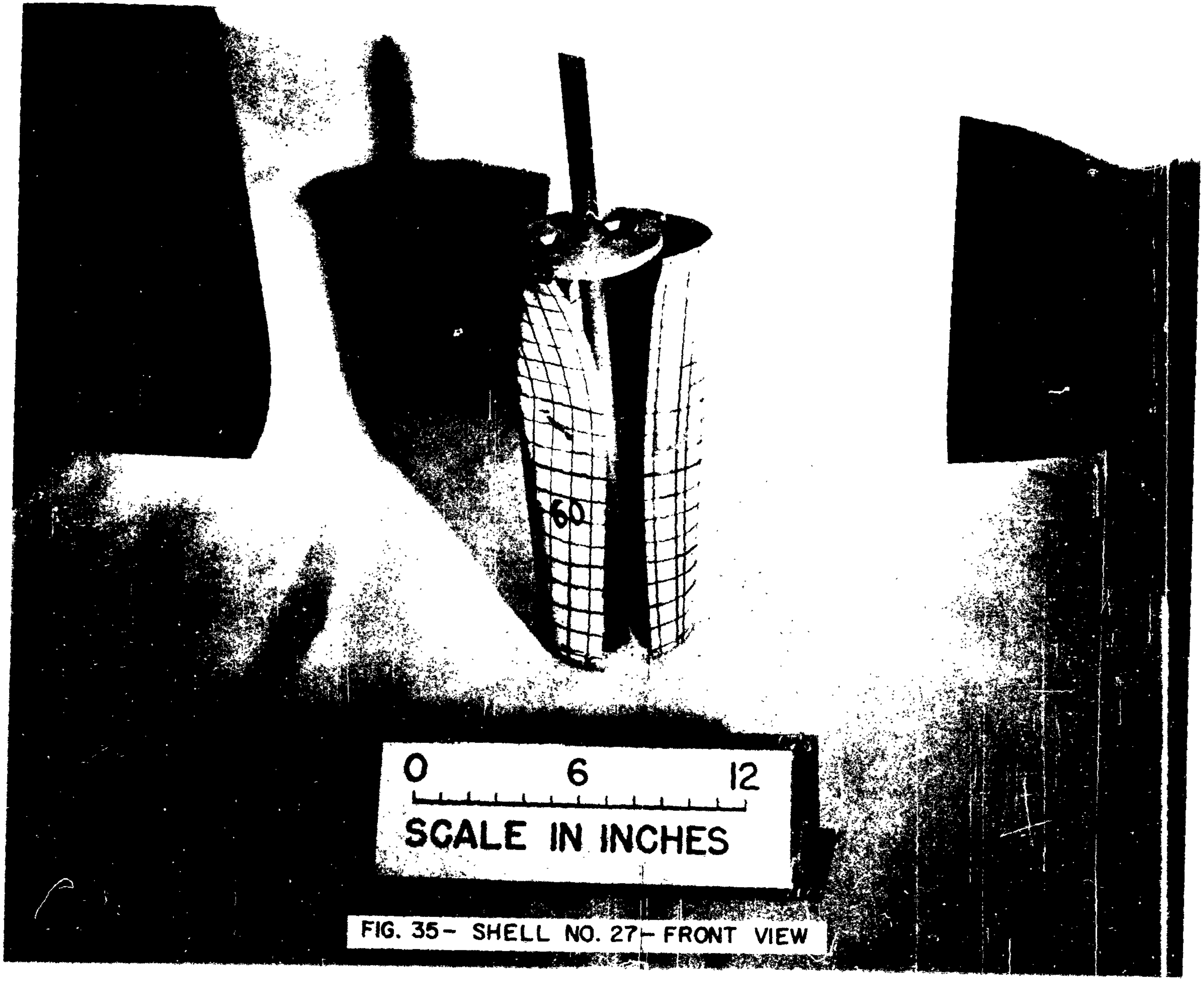

FIG. 35– SHELL NO. 27– FRONT VIEW

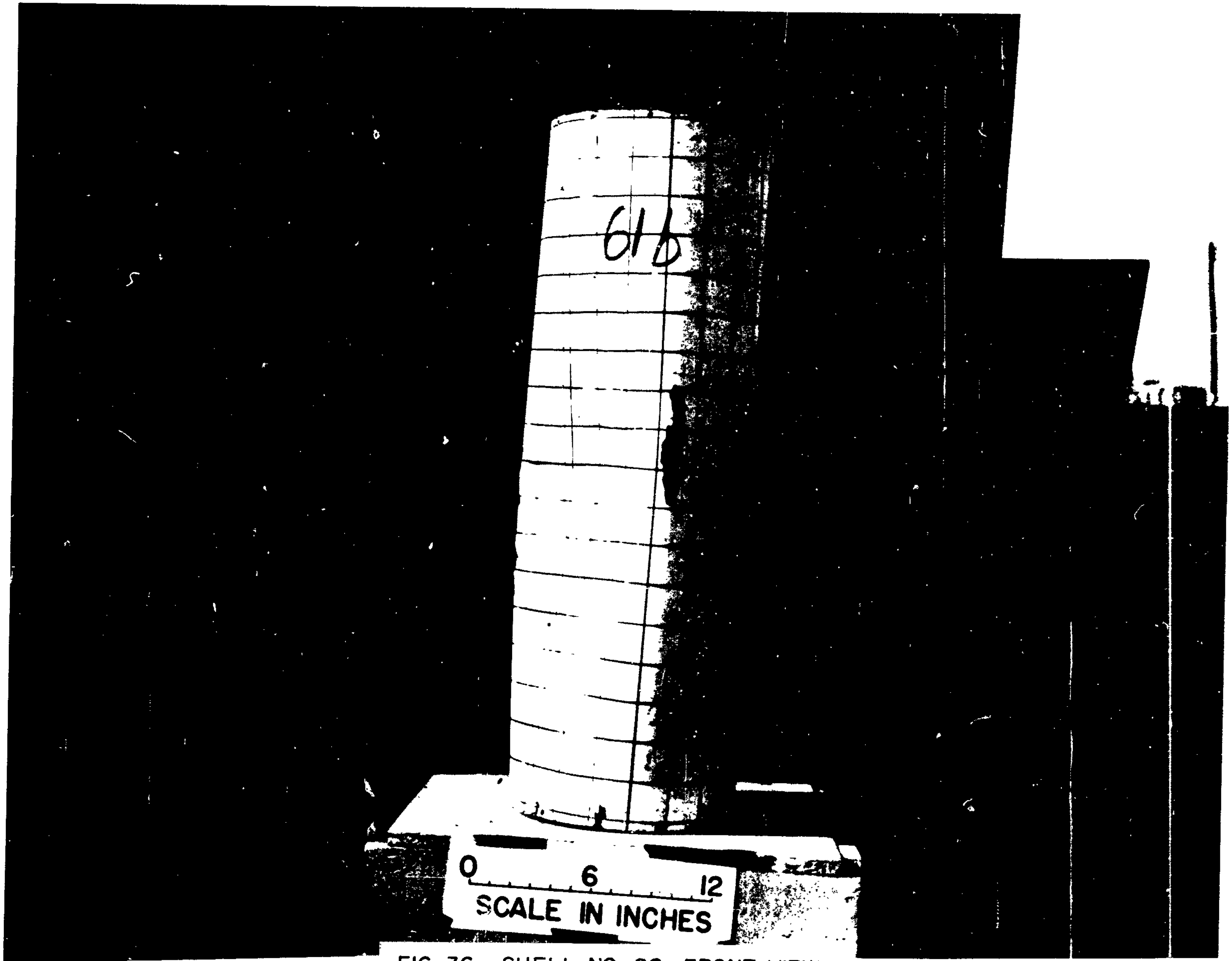

FIG. 36 – SHELL NO. 28 – FRONT VIEW

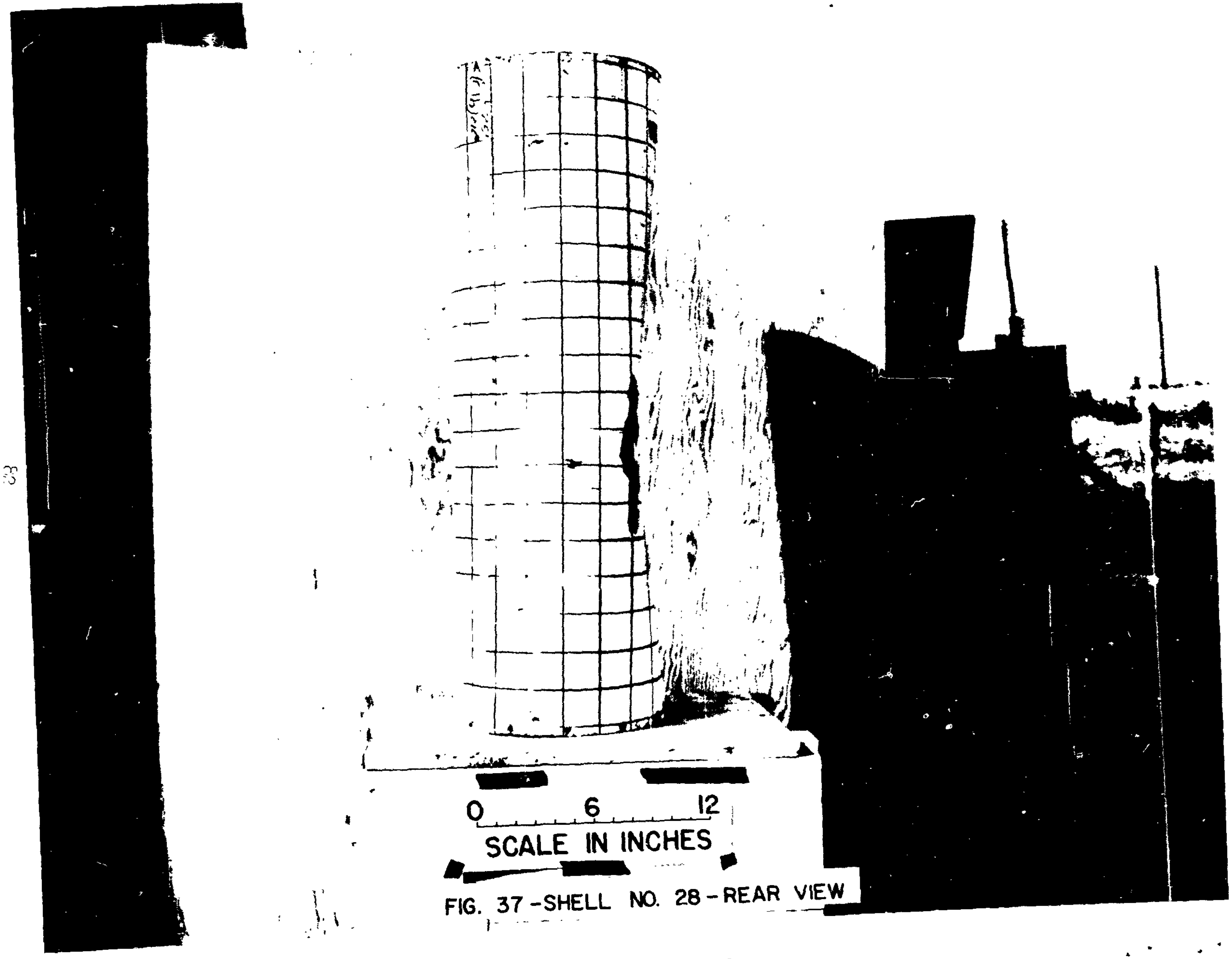

FIG. 37 - SHELL NO. 28 - REAR VIEW

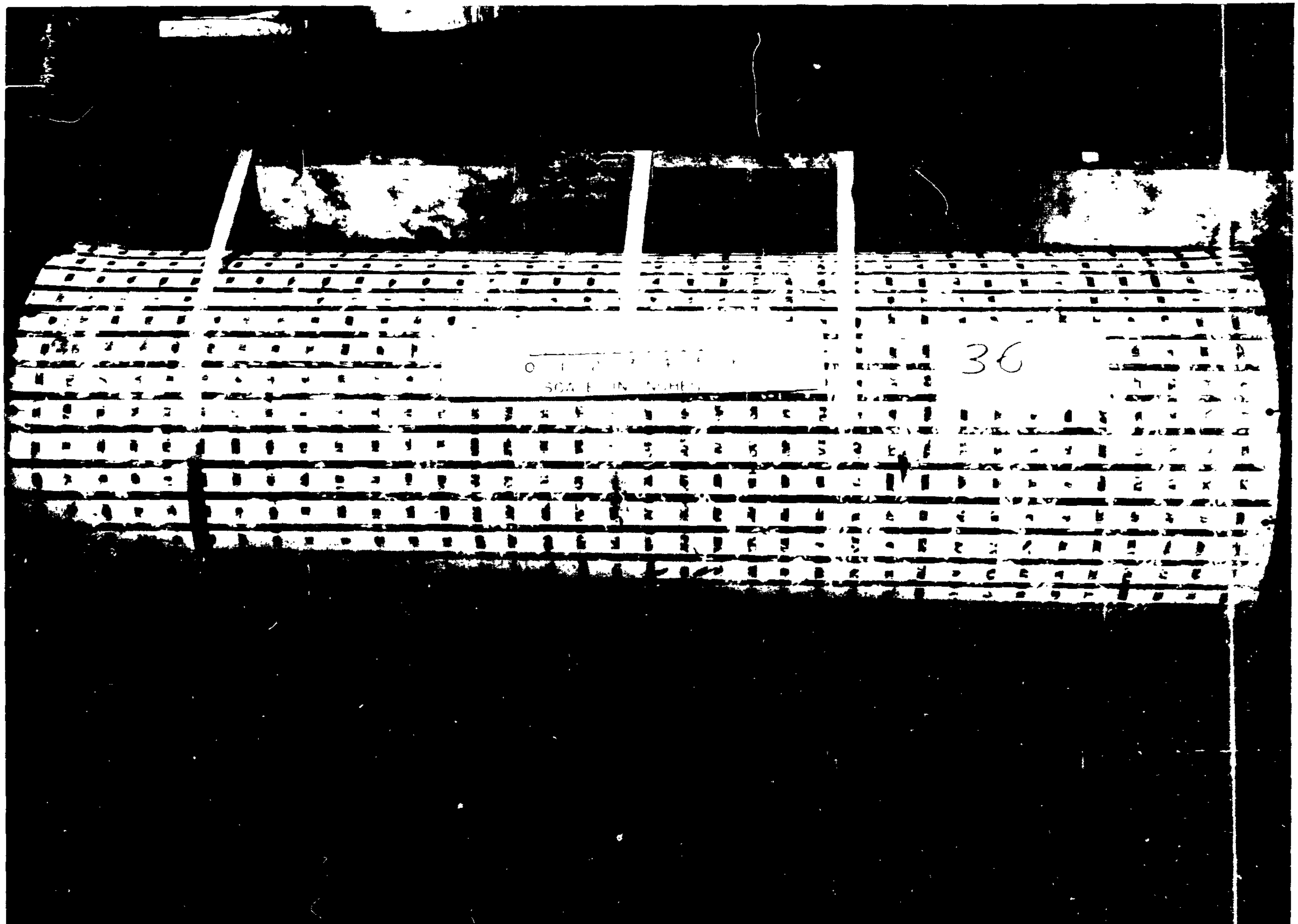

FIG. 38 - SHELL NO. 30

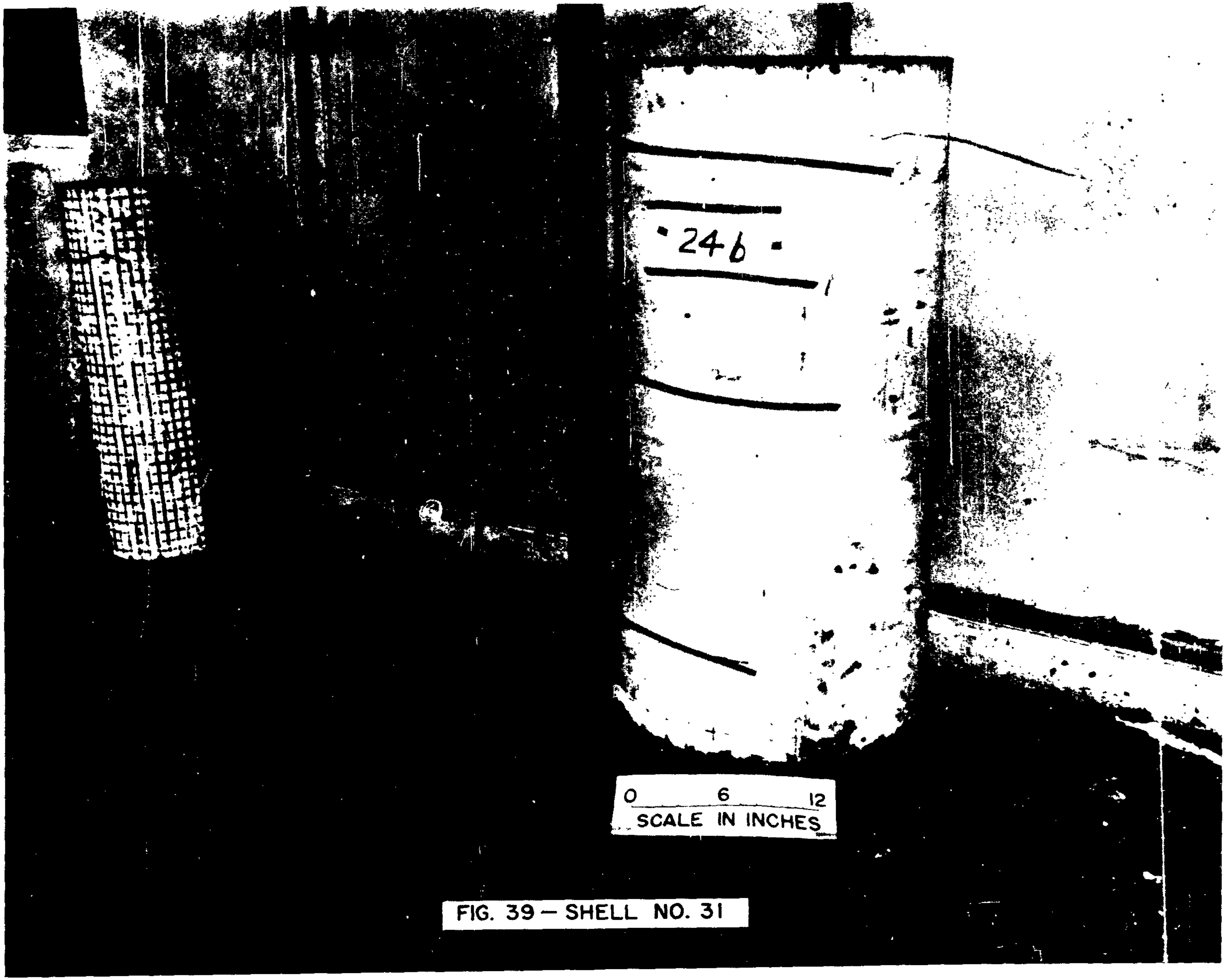

FIG. 39 — SHELL NO. 31

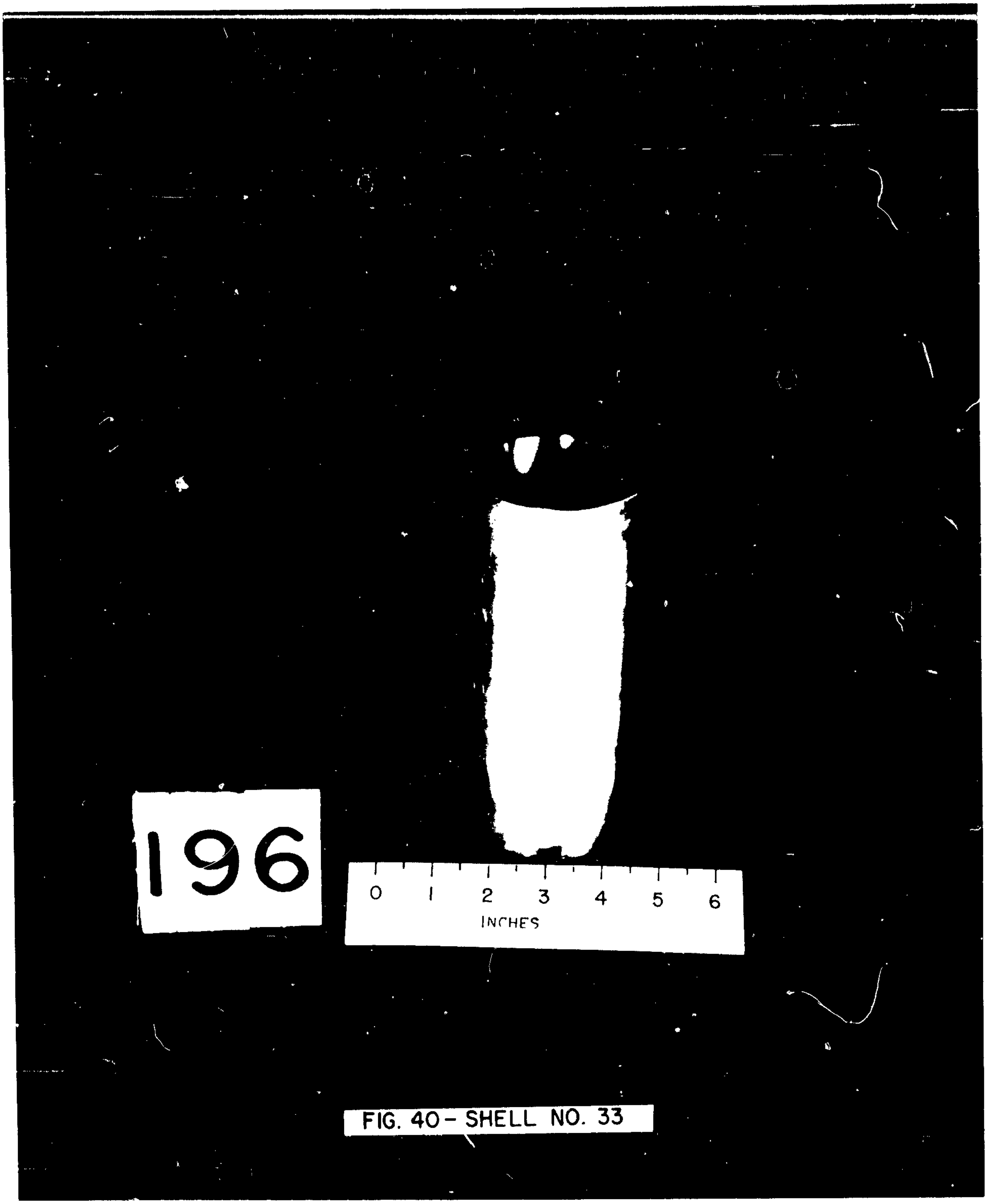

FIG. 40 - SHELL NO. 33

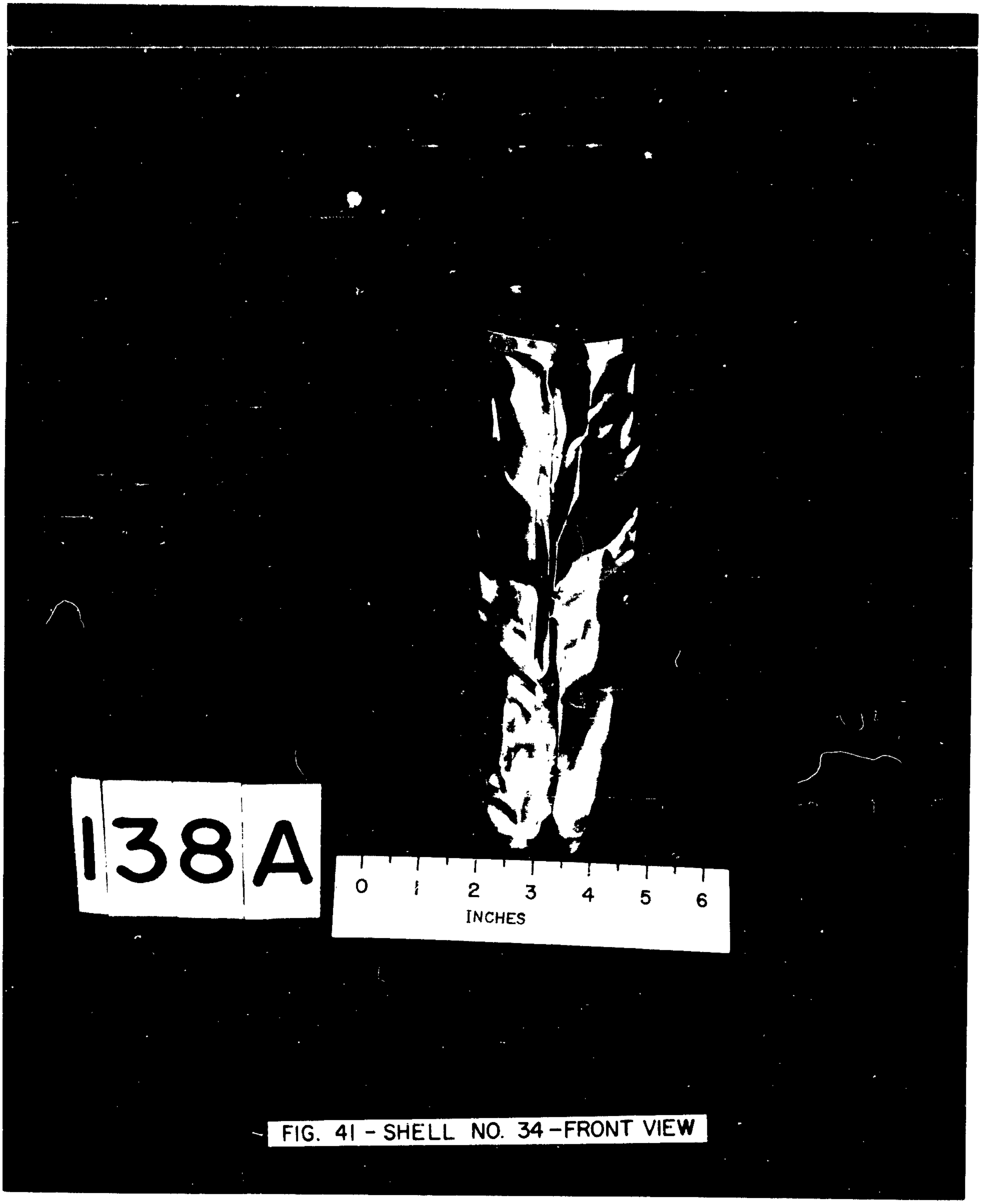

FIG. 41 - SHELL NO. 34 - FRONT VIEW

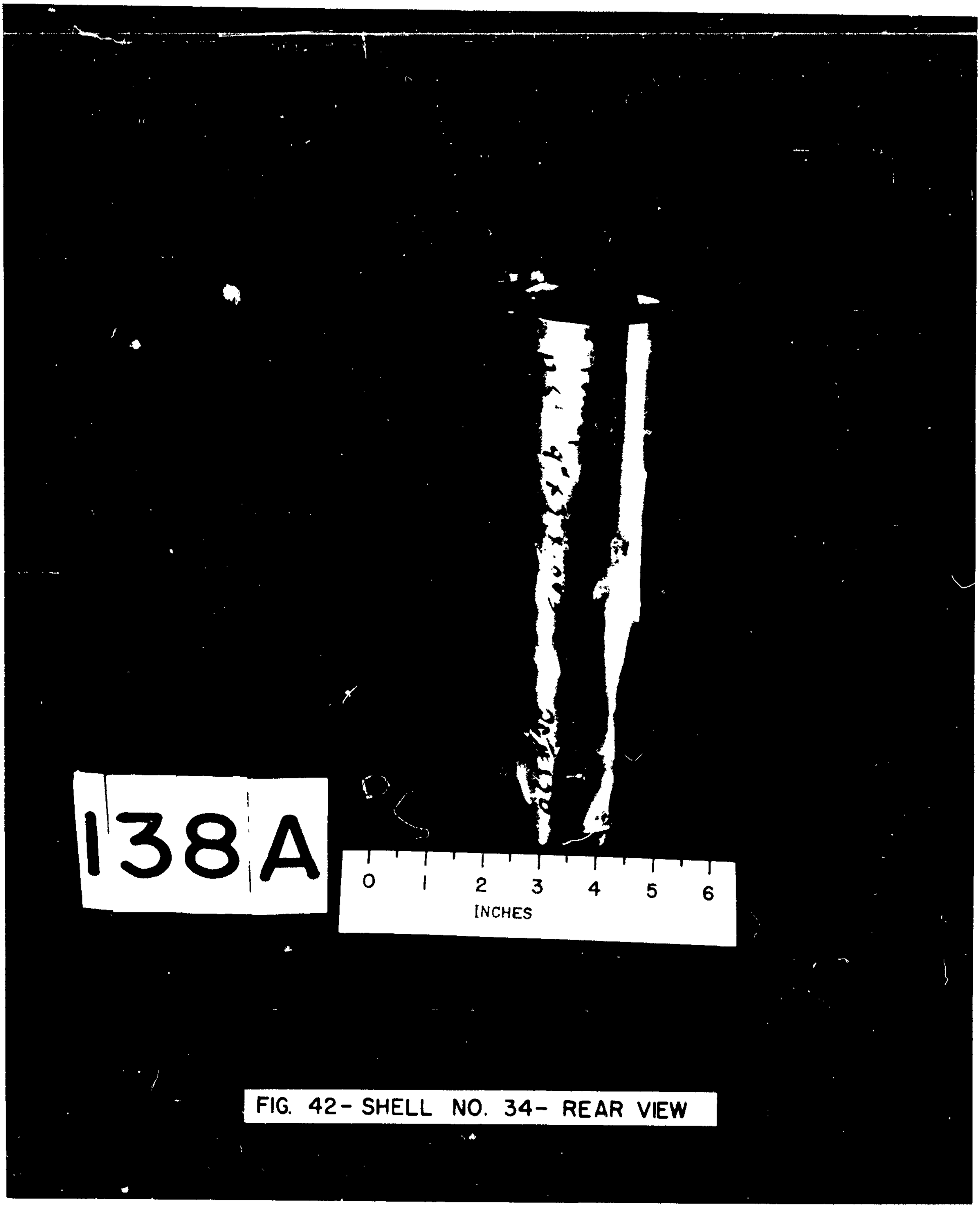

FIG. 42 - SHELL NO. 34 - REAR VIEW

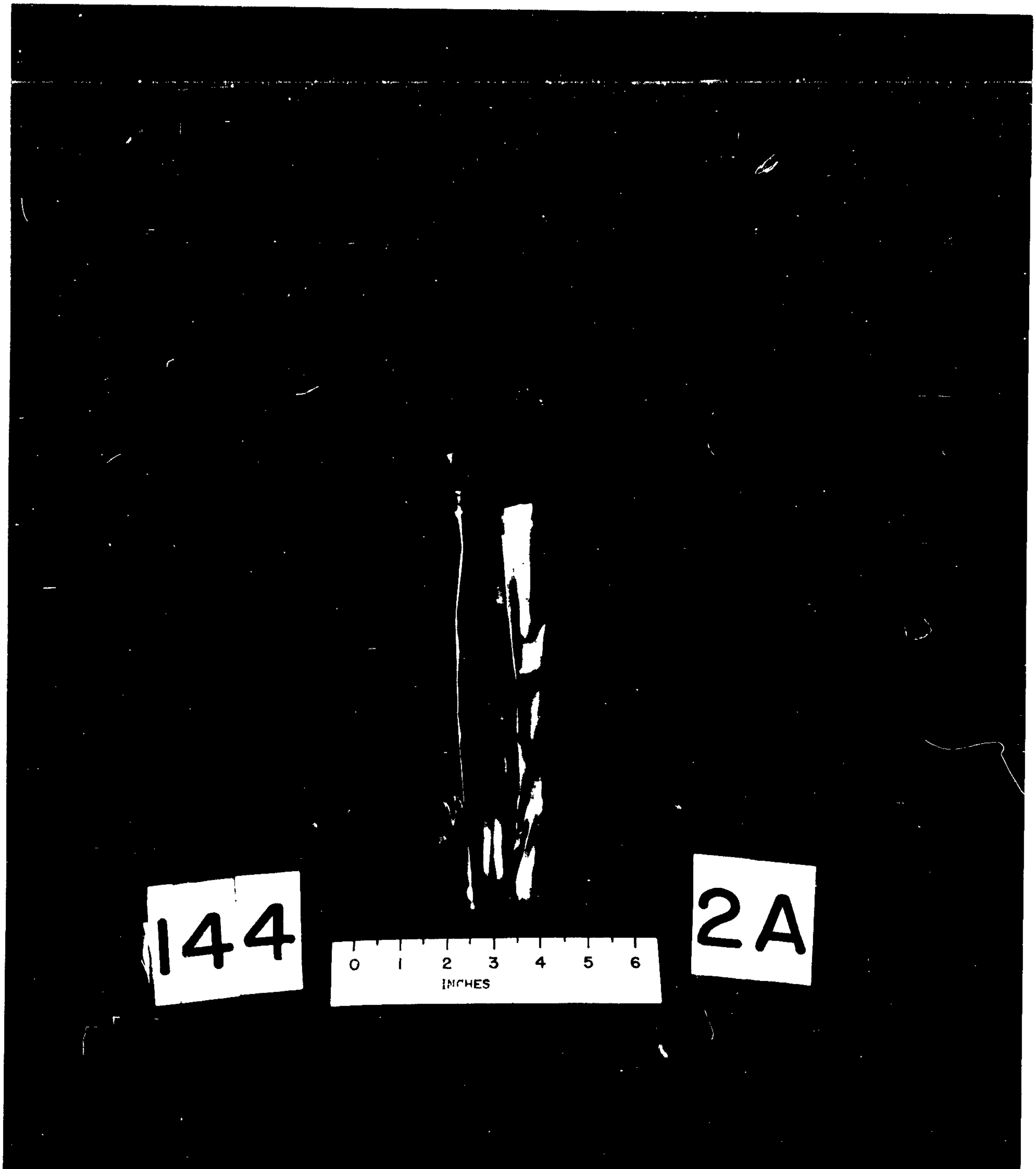

FIG. 43- SHELL NO. 35

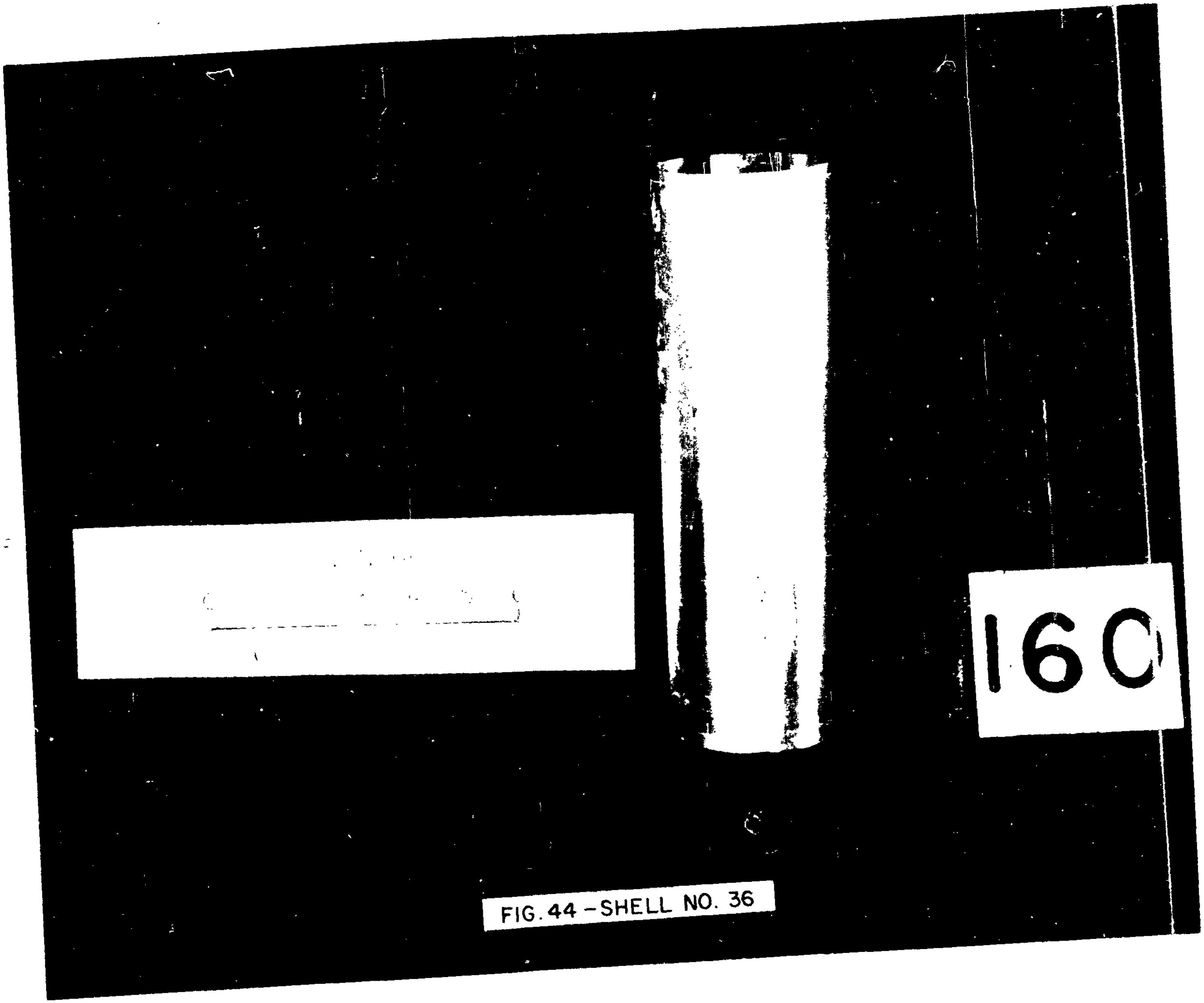

FIG. 44 - SHELL NO. 36

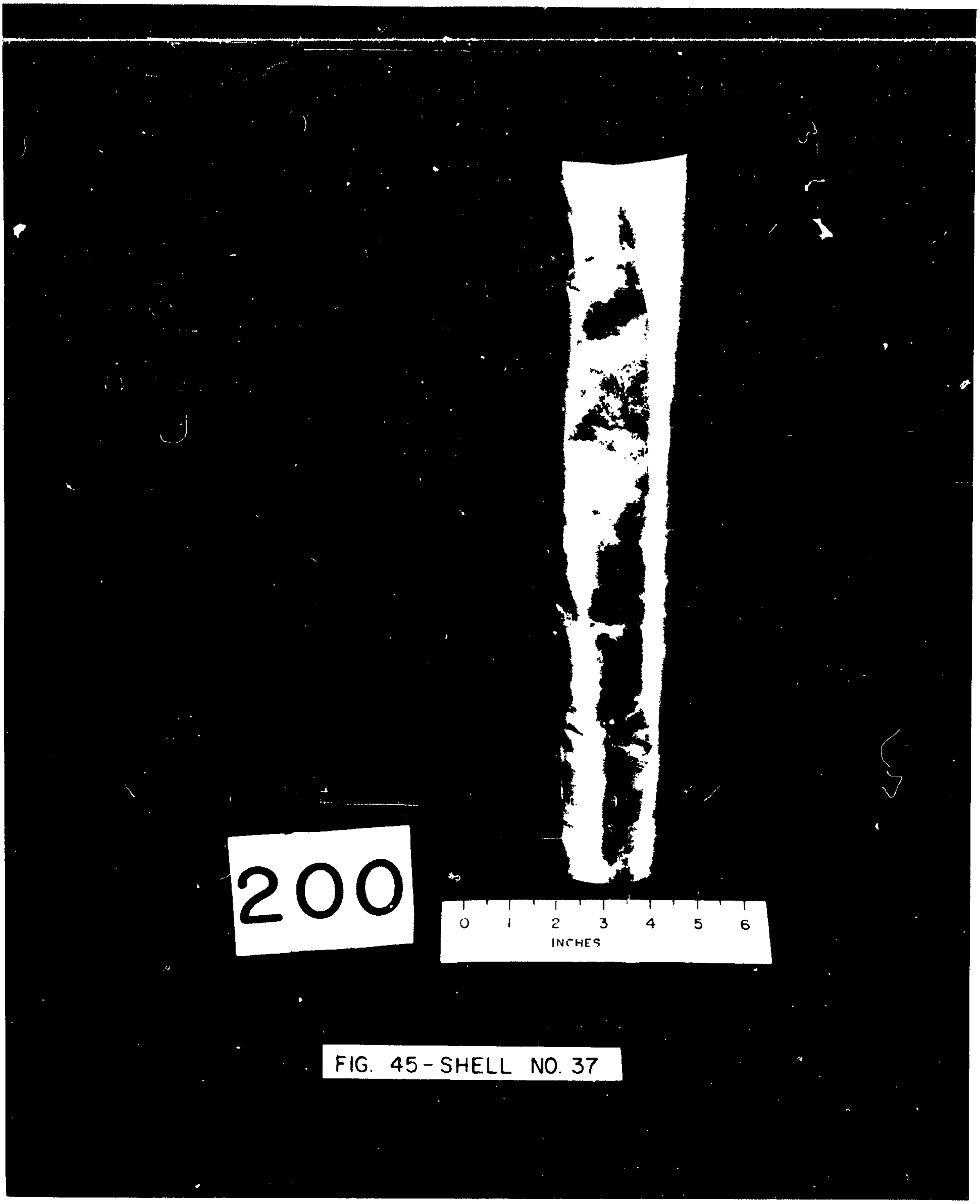

FIG. 45 - SHELL NO. 37

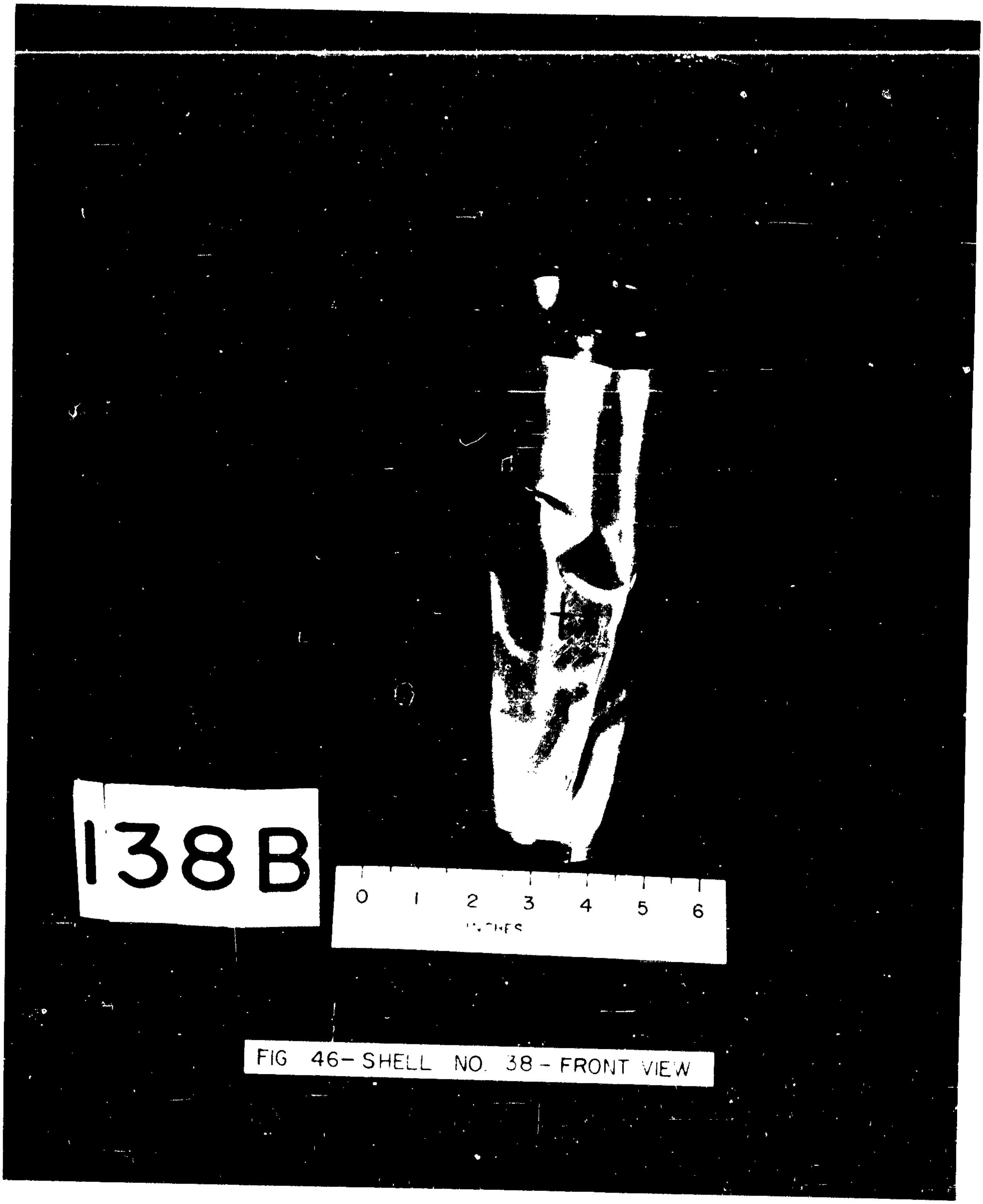

FIG 46- SHELL NO. 38 - FRONT VIEW

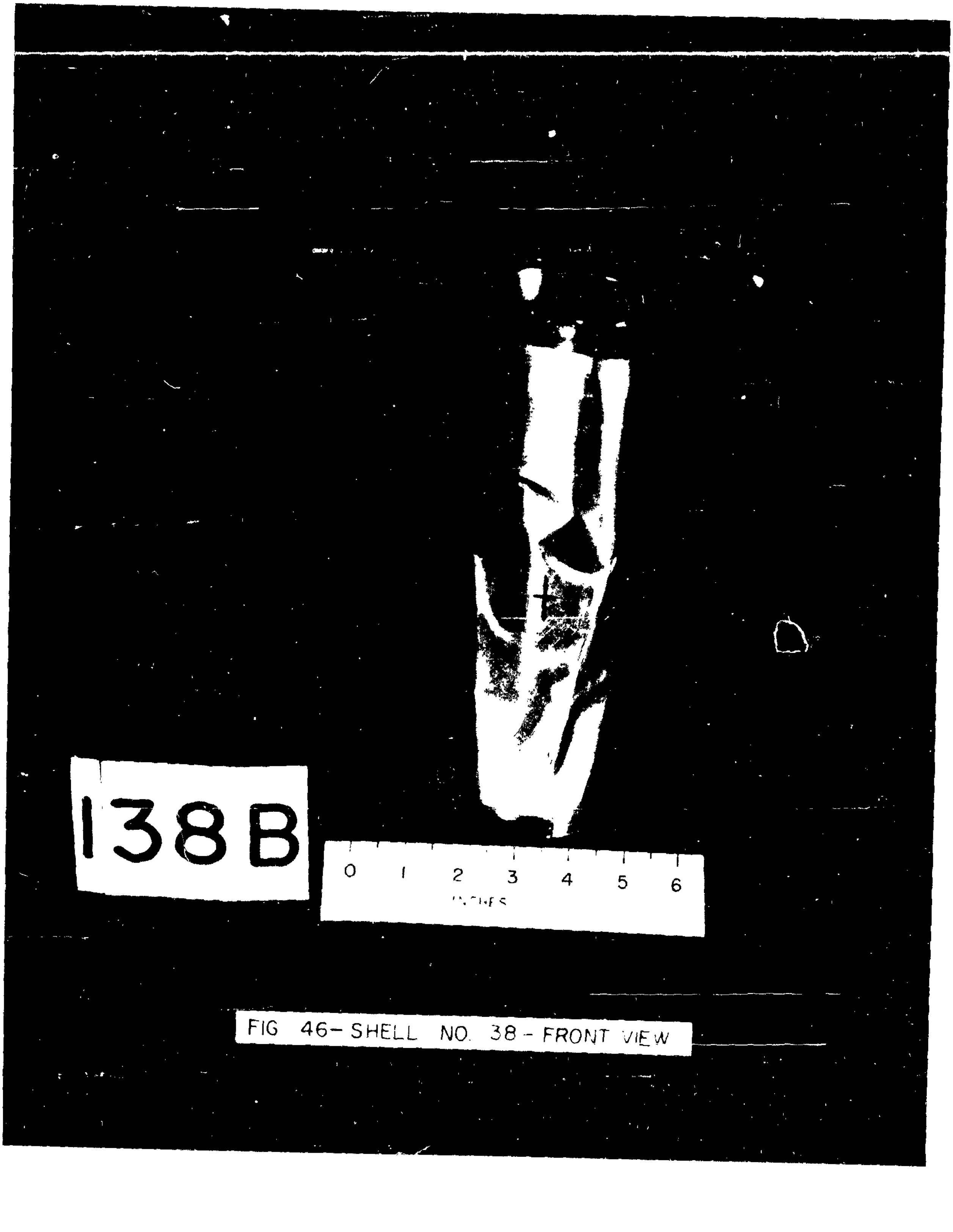

FIG 46 - SHELL NO. 38 - FRONT VIEW

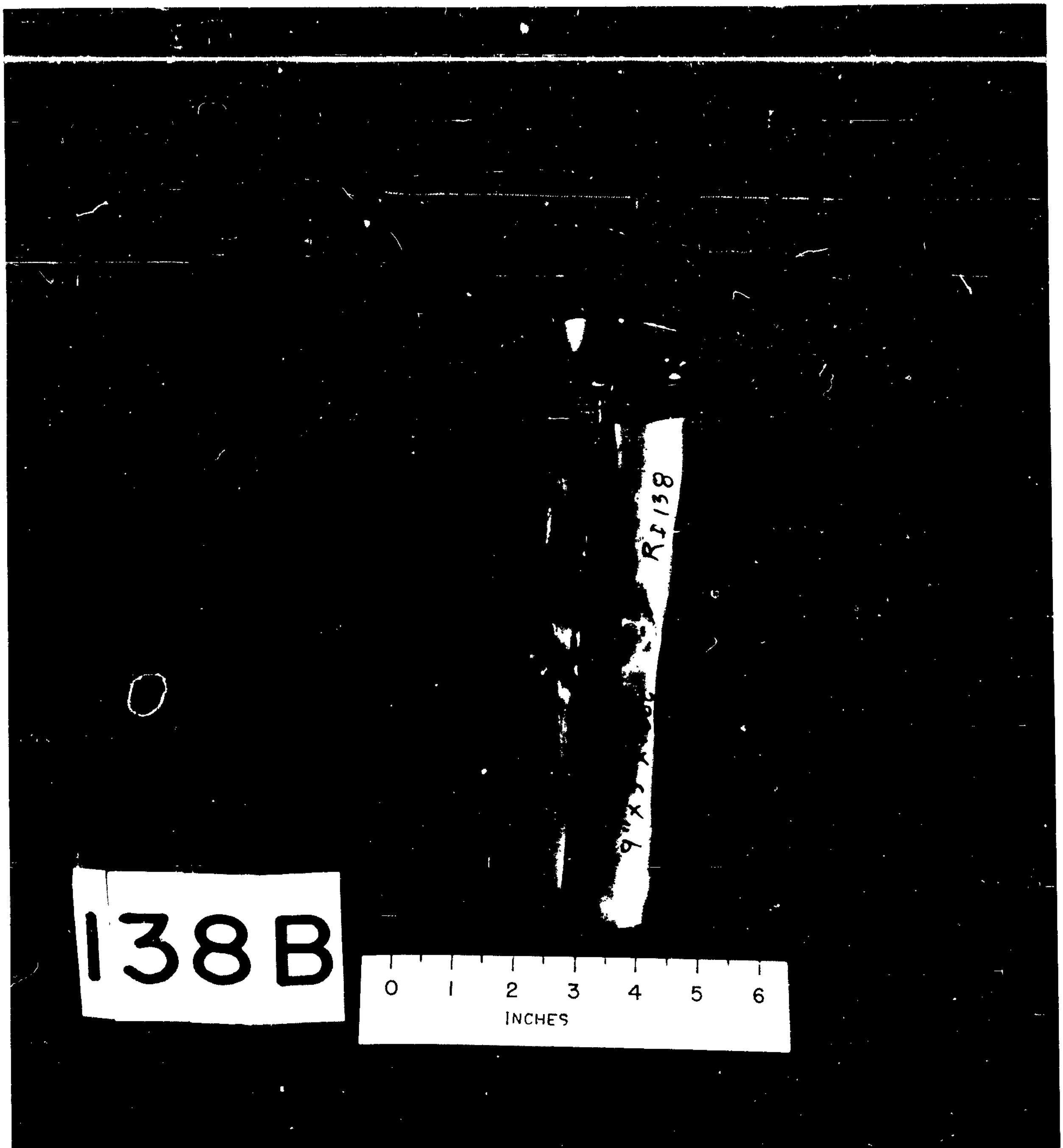

FIG. 47 – SHELL NO. 38 – REAR VIEW

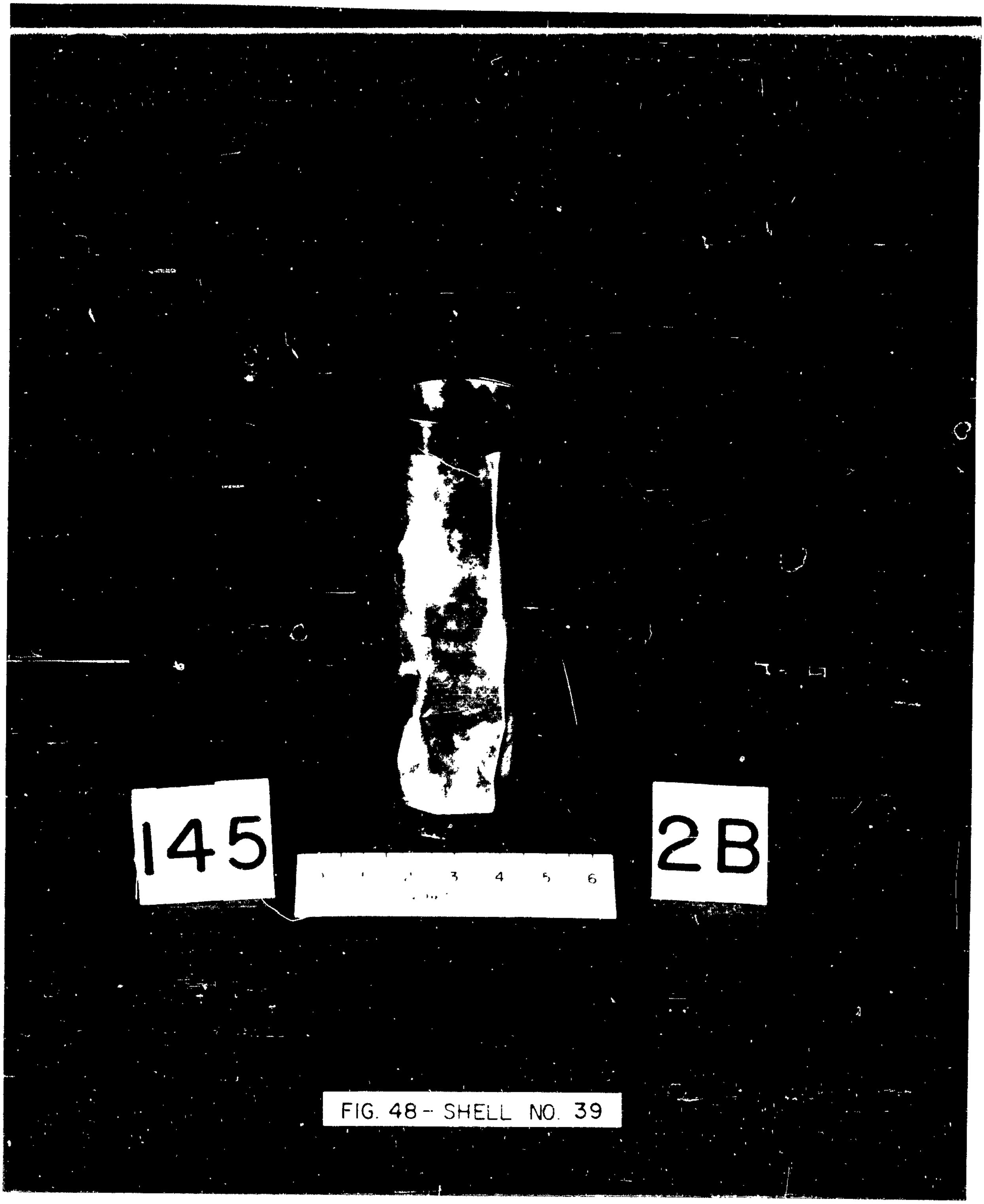

FIG. 48 -- SHELL NO. 39

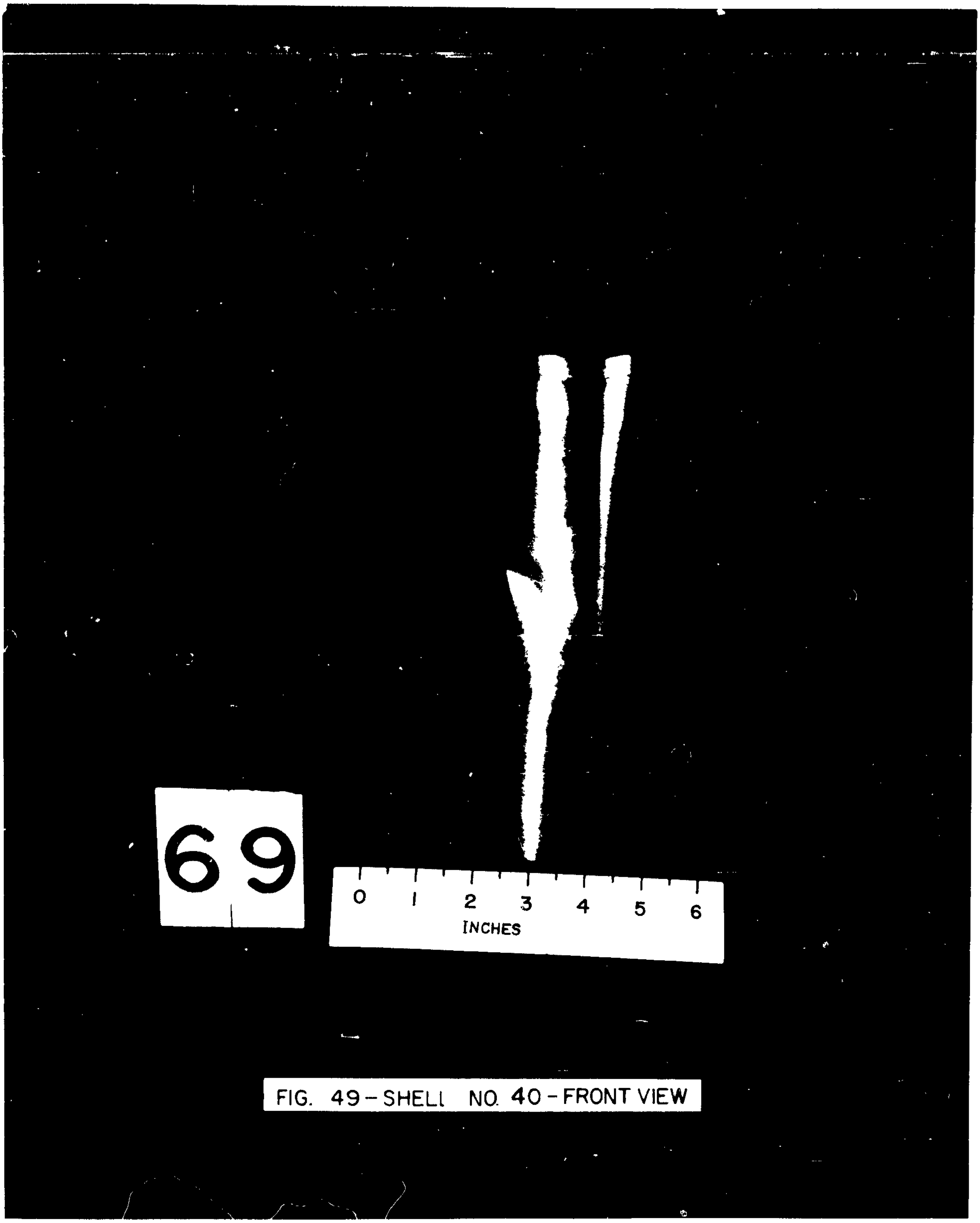

FIG. 49 - SHELL NO. 40 - FRONT VIEW

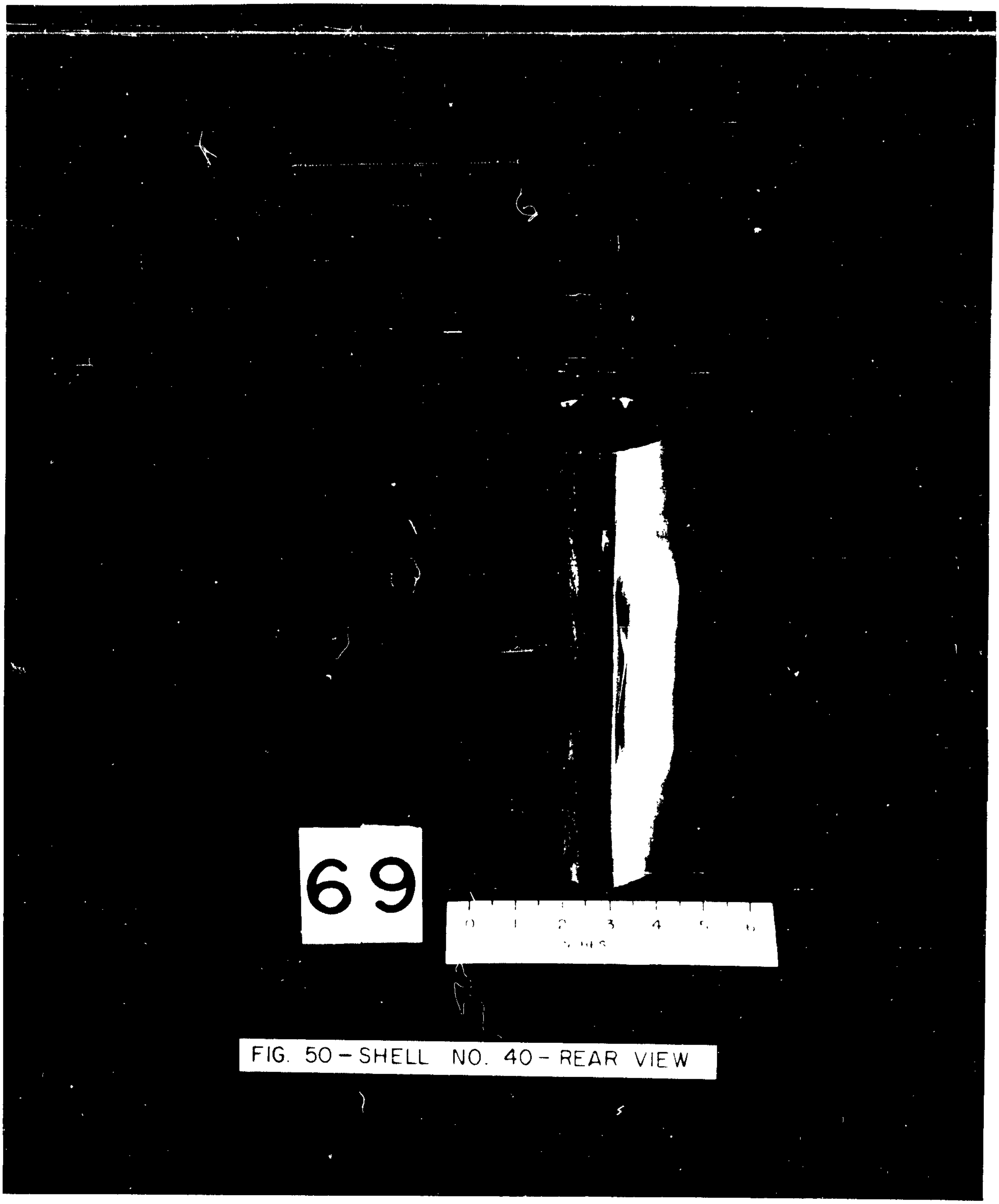

FIG. 50 - SHELL NO. 40 - REAR VIEW

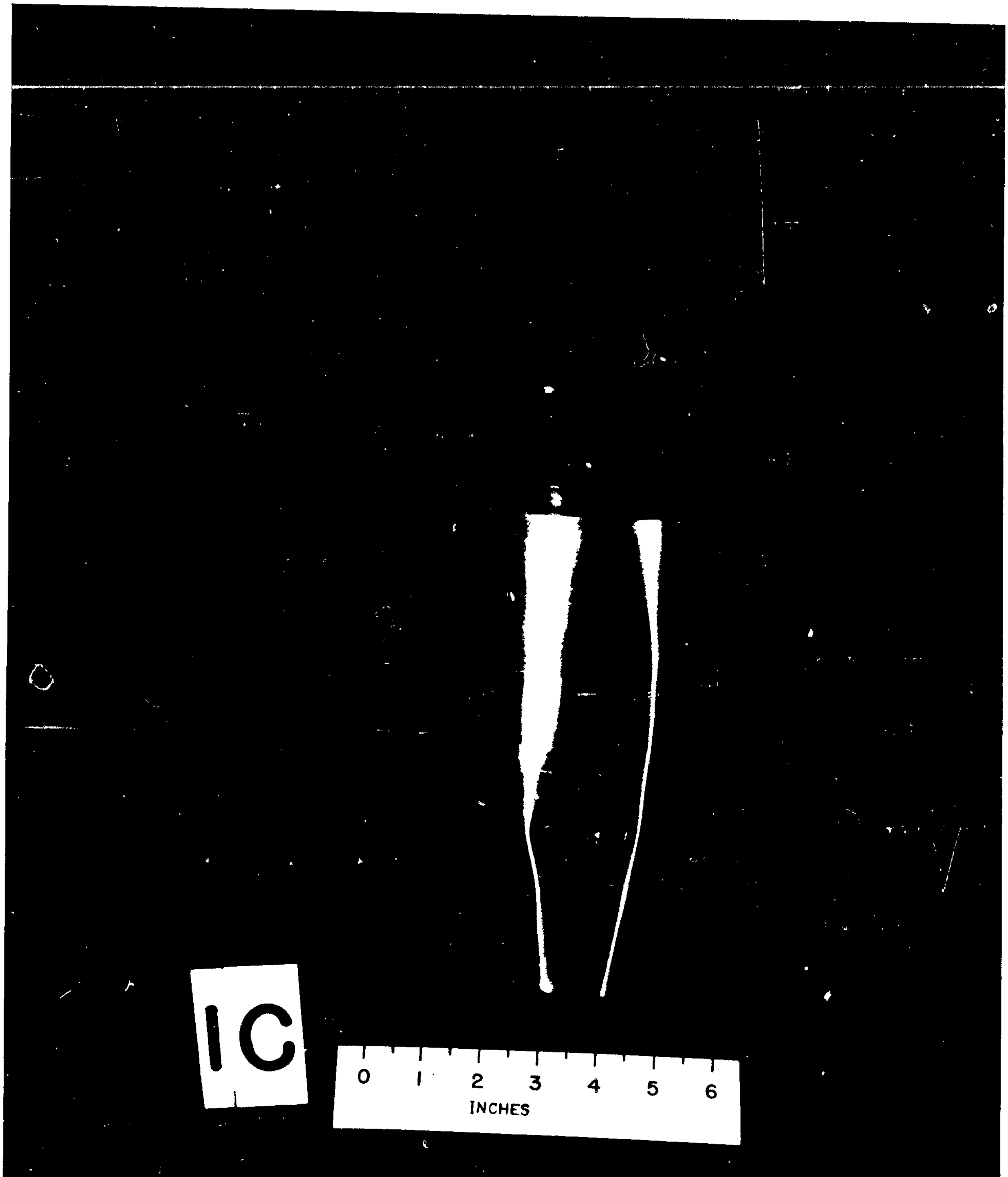

FIG. 51 – SHELL NO. 44

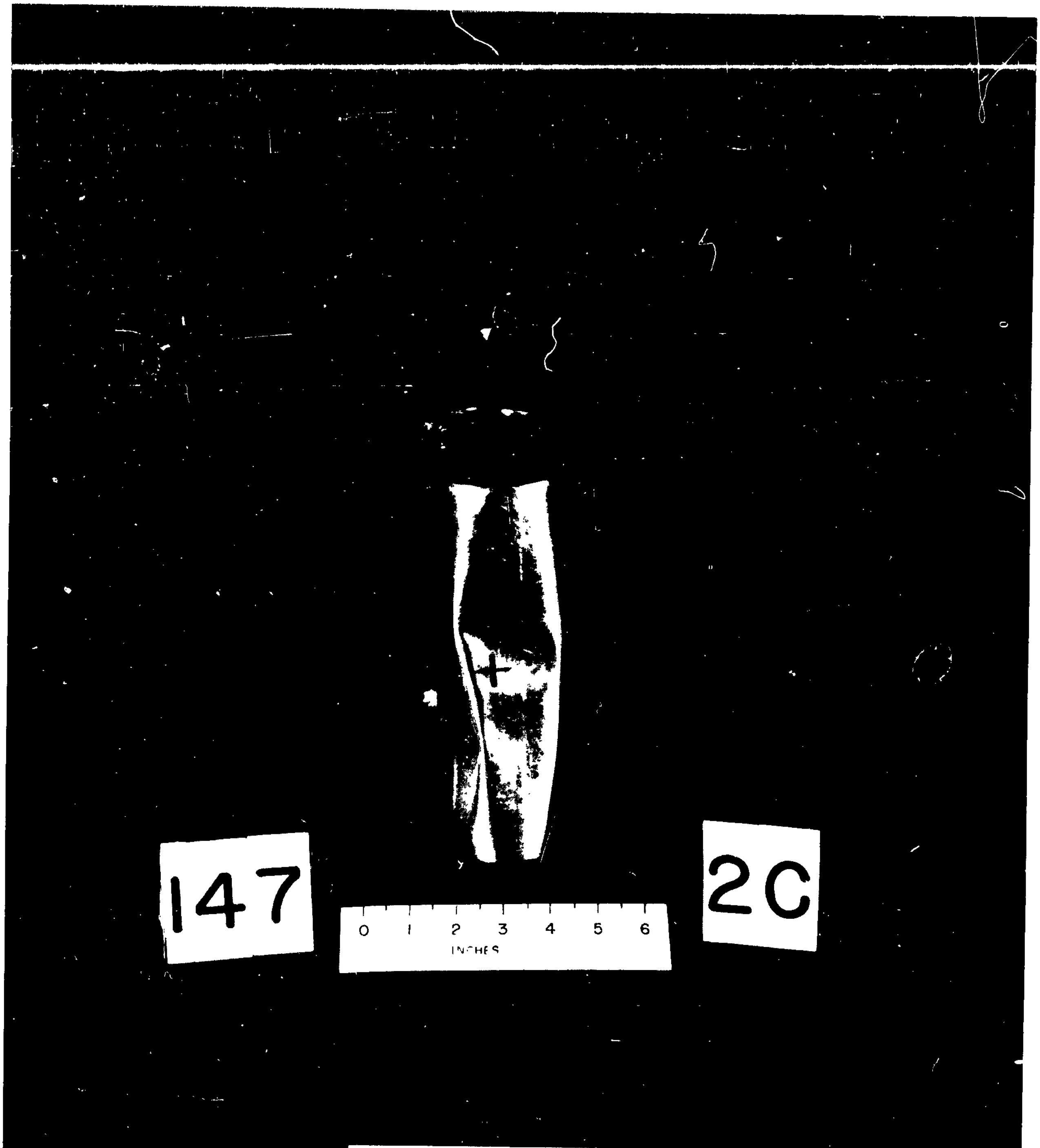

FIG. 52 – SHELL NO. 45

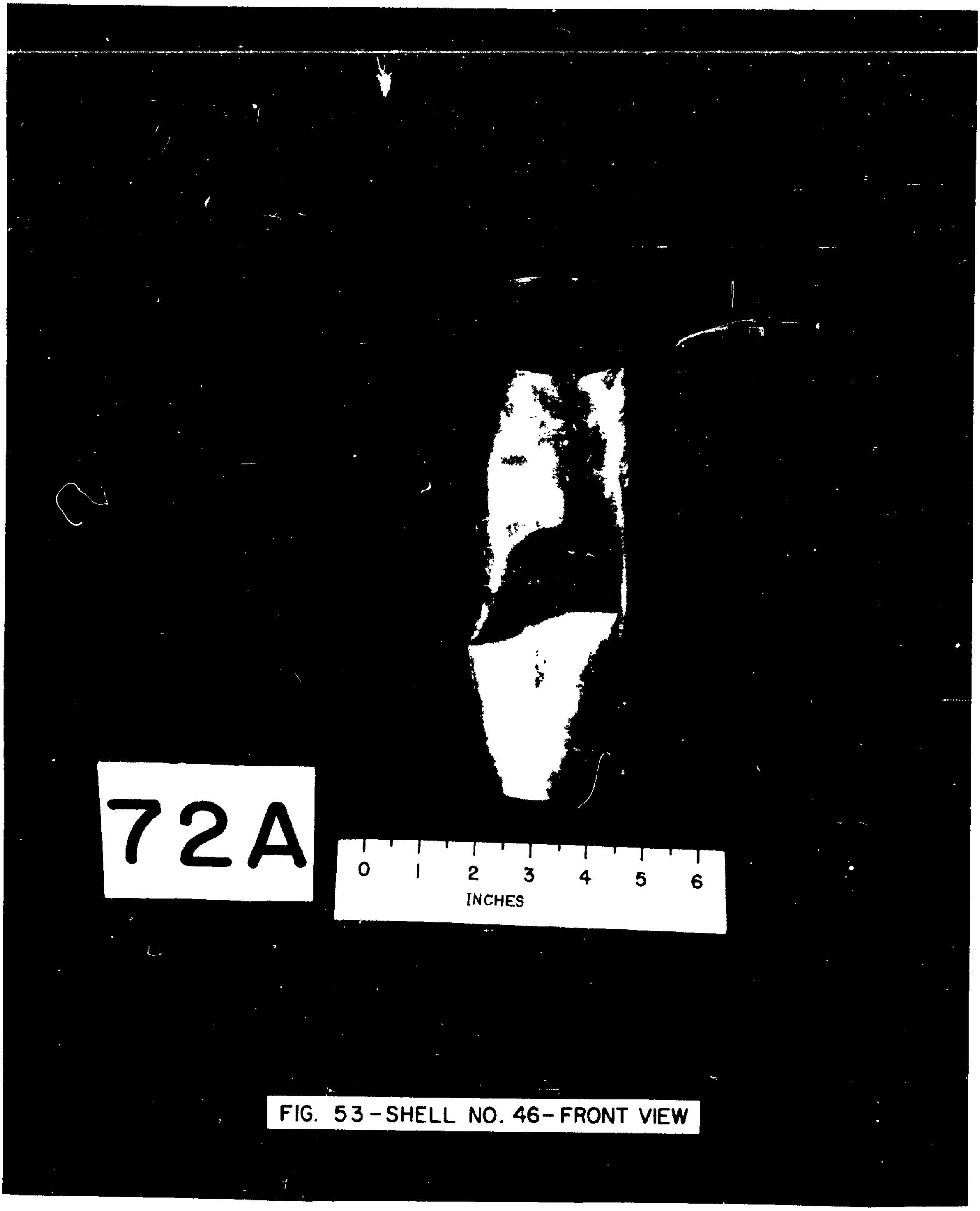

FIG. 53-SHELL NO. 46-FRONT VIEW

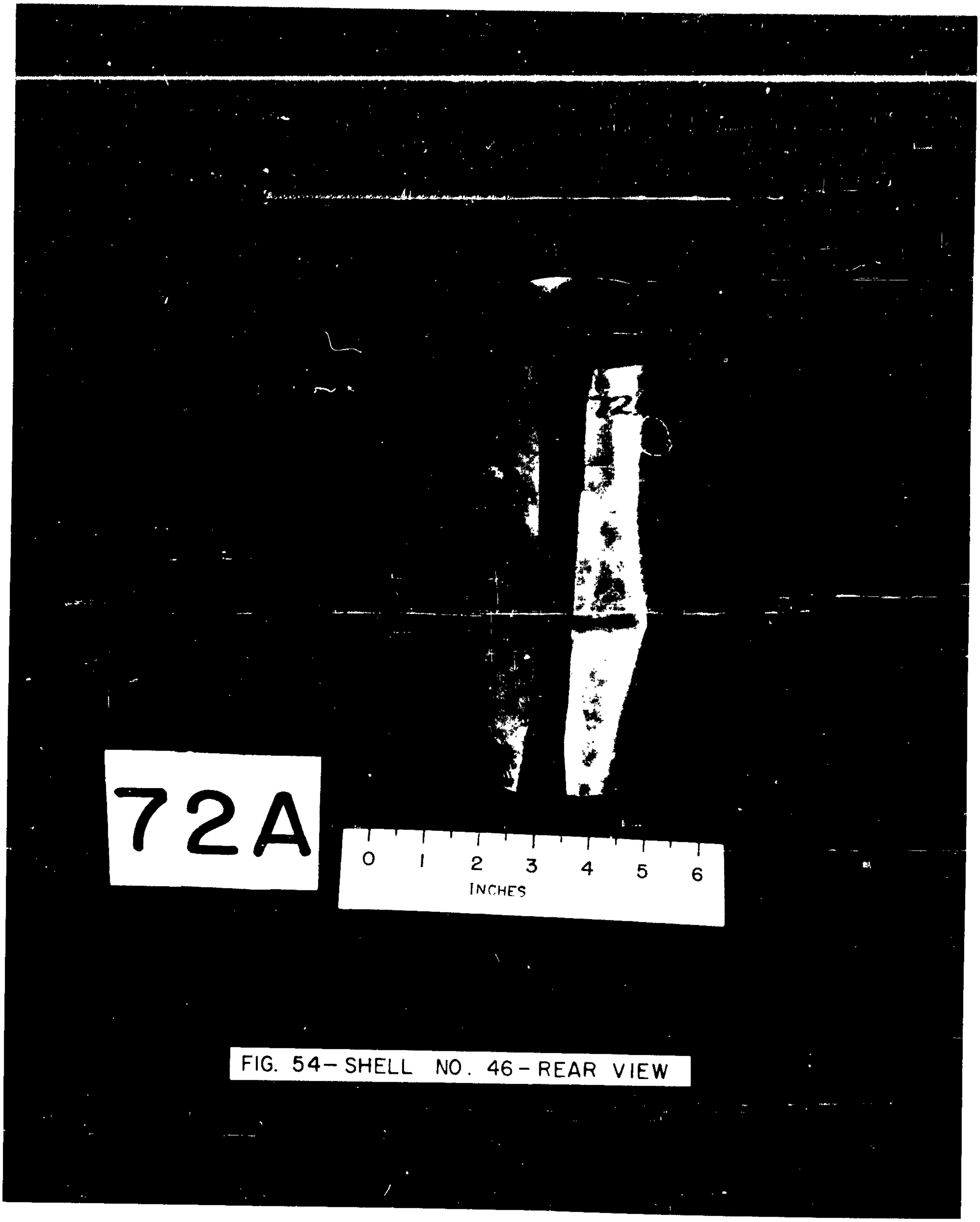

FIG. 54- SHELL NO. 46- REAR VIEW

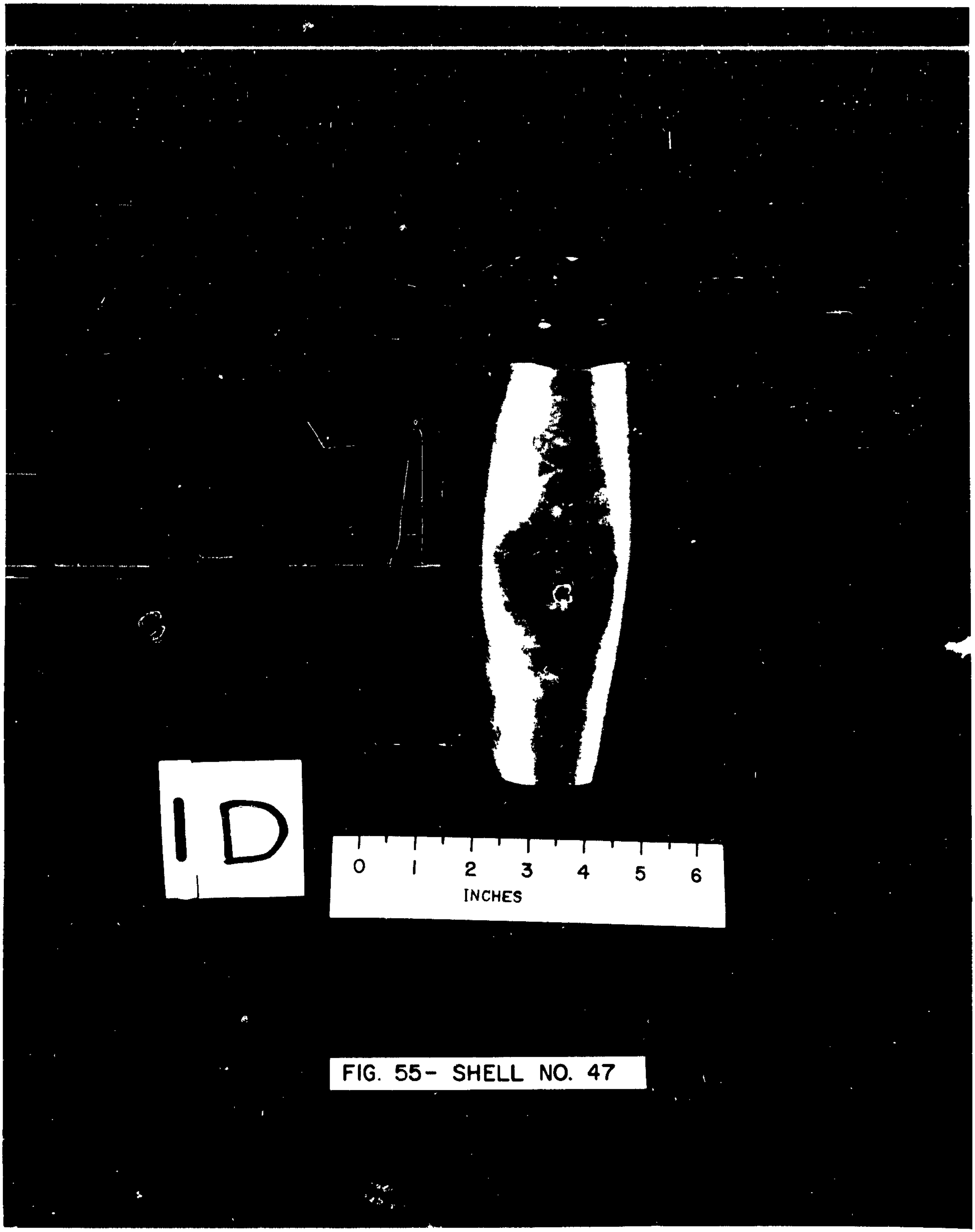

FIG. 55- SHELL NO. 47

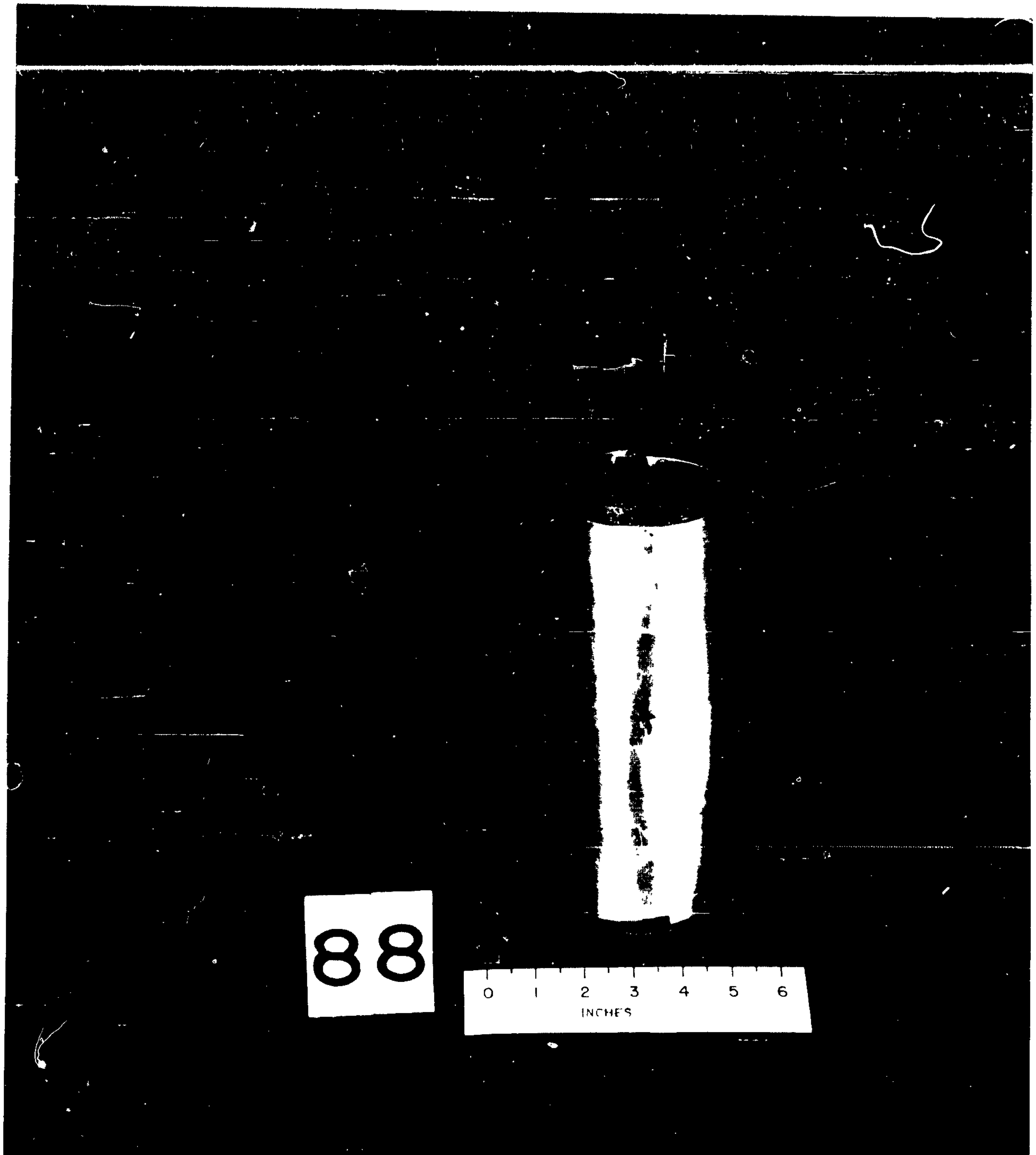

FIG. 56 — SHELL NO. 48

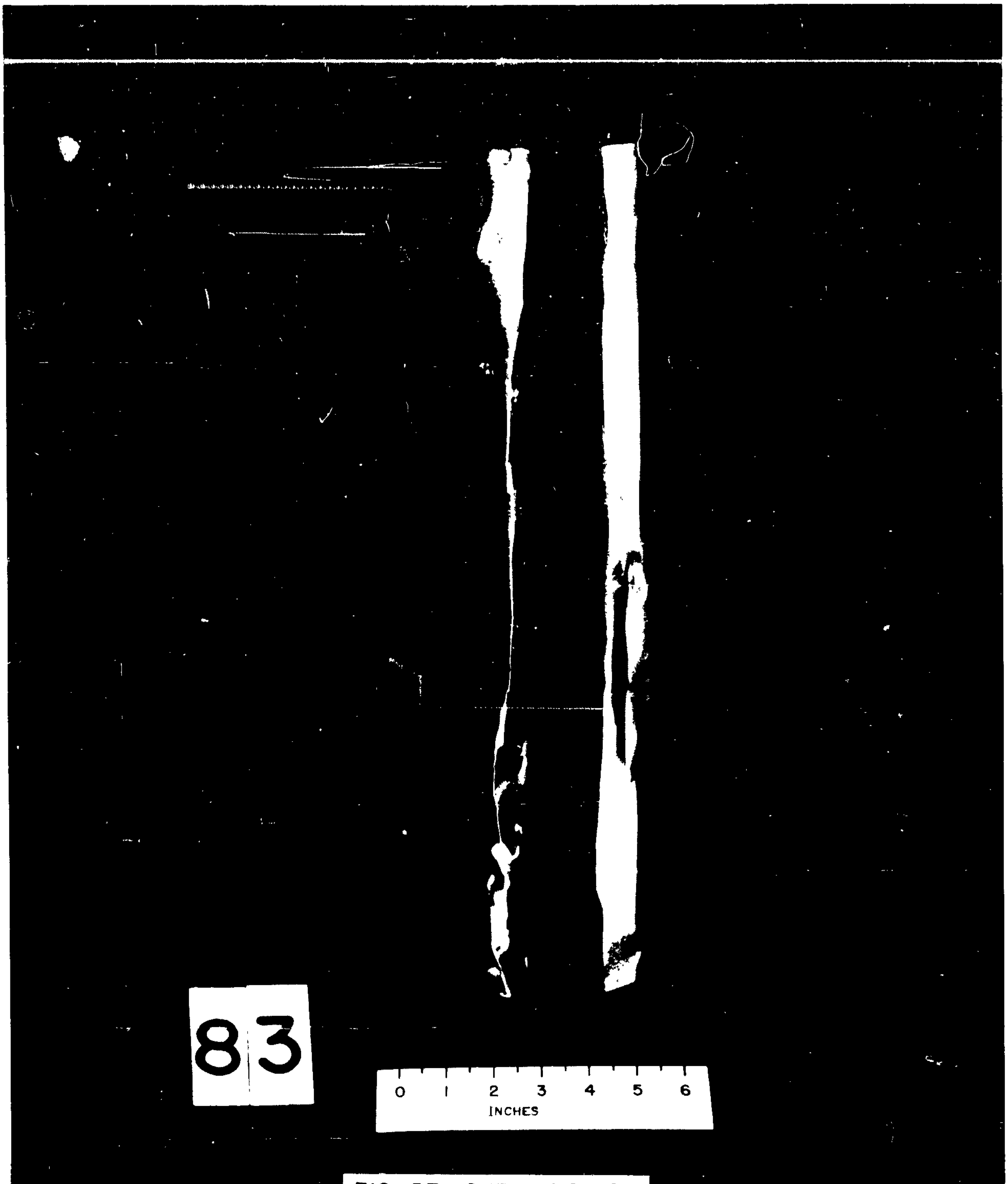

FIG. 57 - SHELL NO. 50

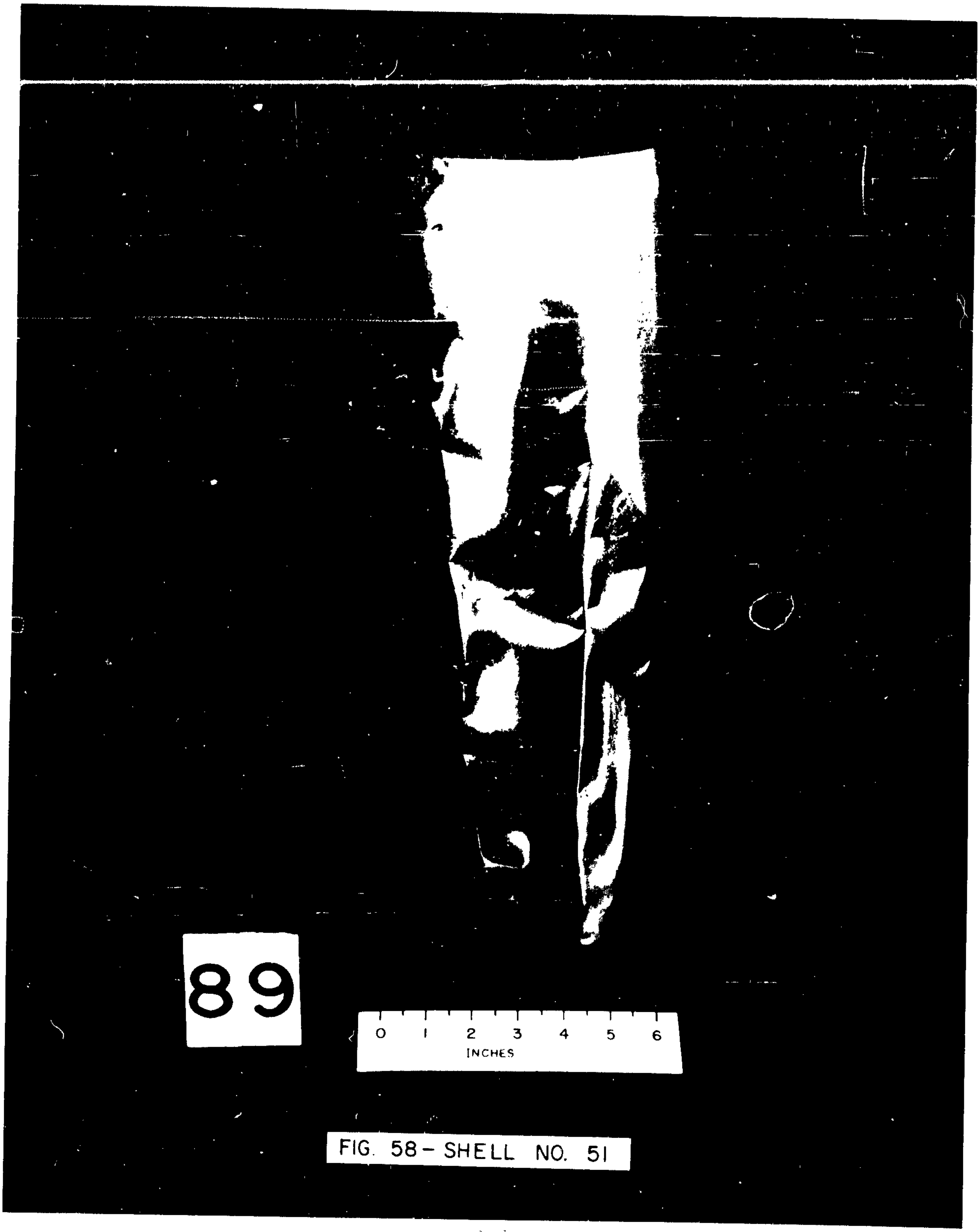

FIG. 58 - SHELL NO. 51

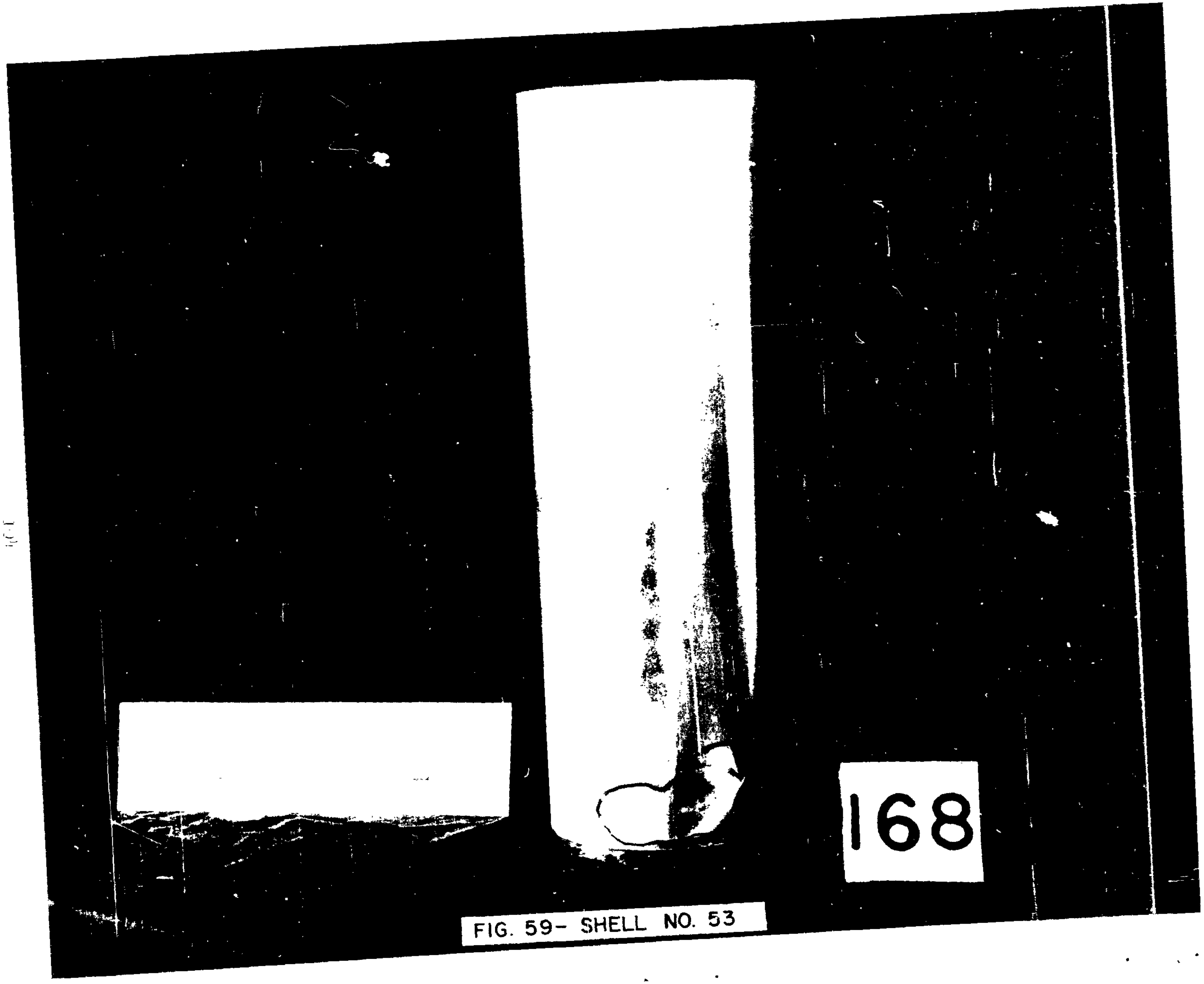

FIG. 59- SHELL NO. 53

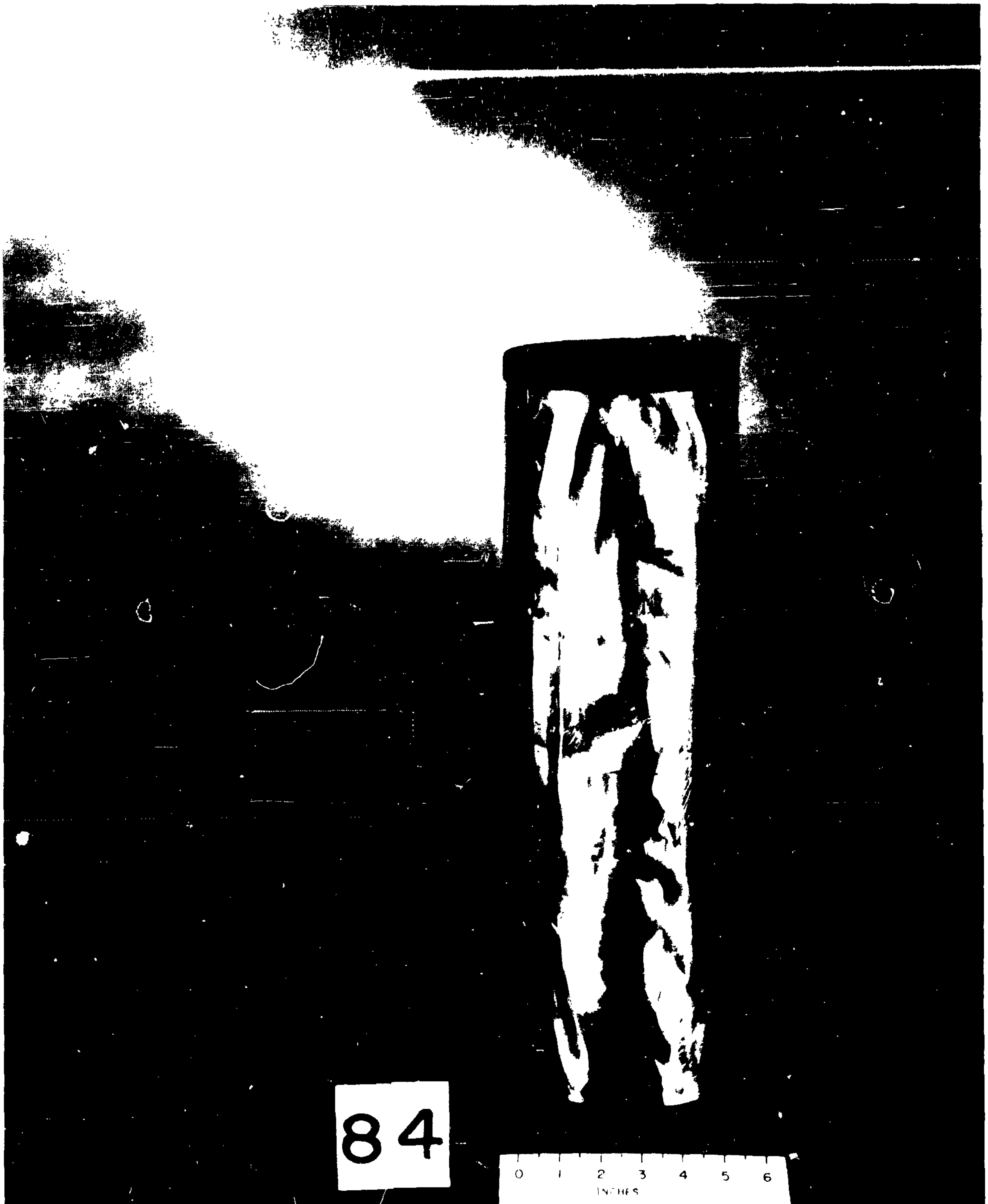

FIG. 60 – SHELL NO. 54

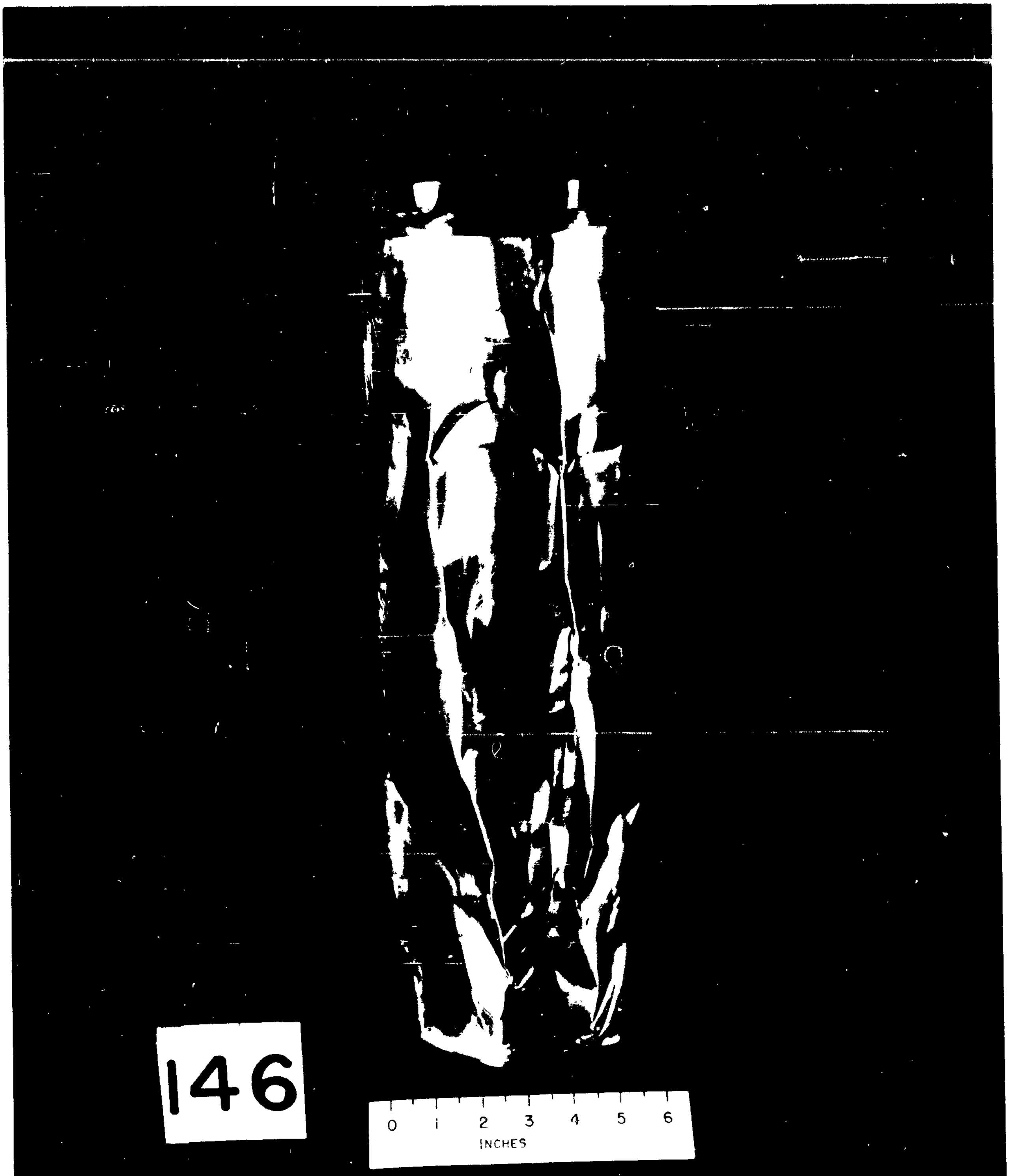

FIG. 61 - SHELL NO. 55-FRONT VIEW

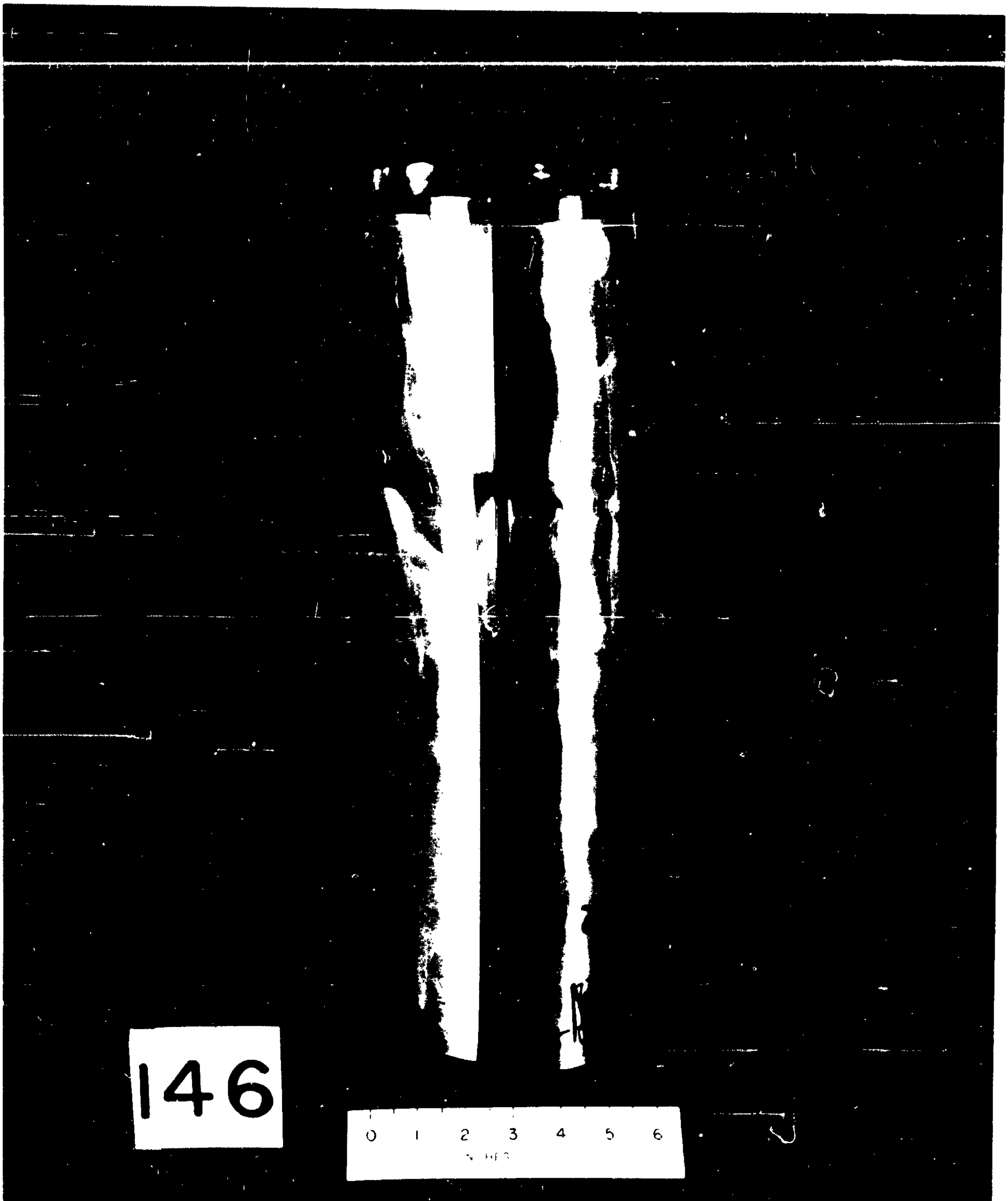

FIG. 62 - SHELL NO. 55 - REAR VIEW

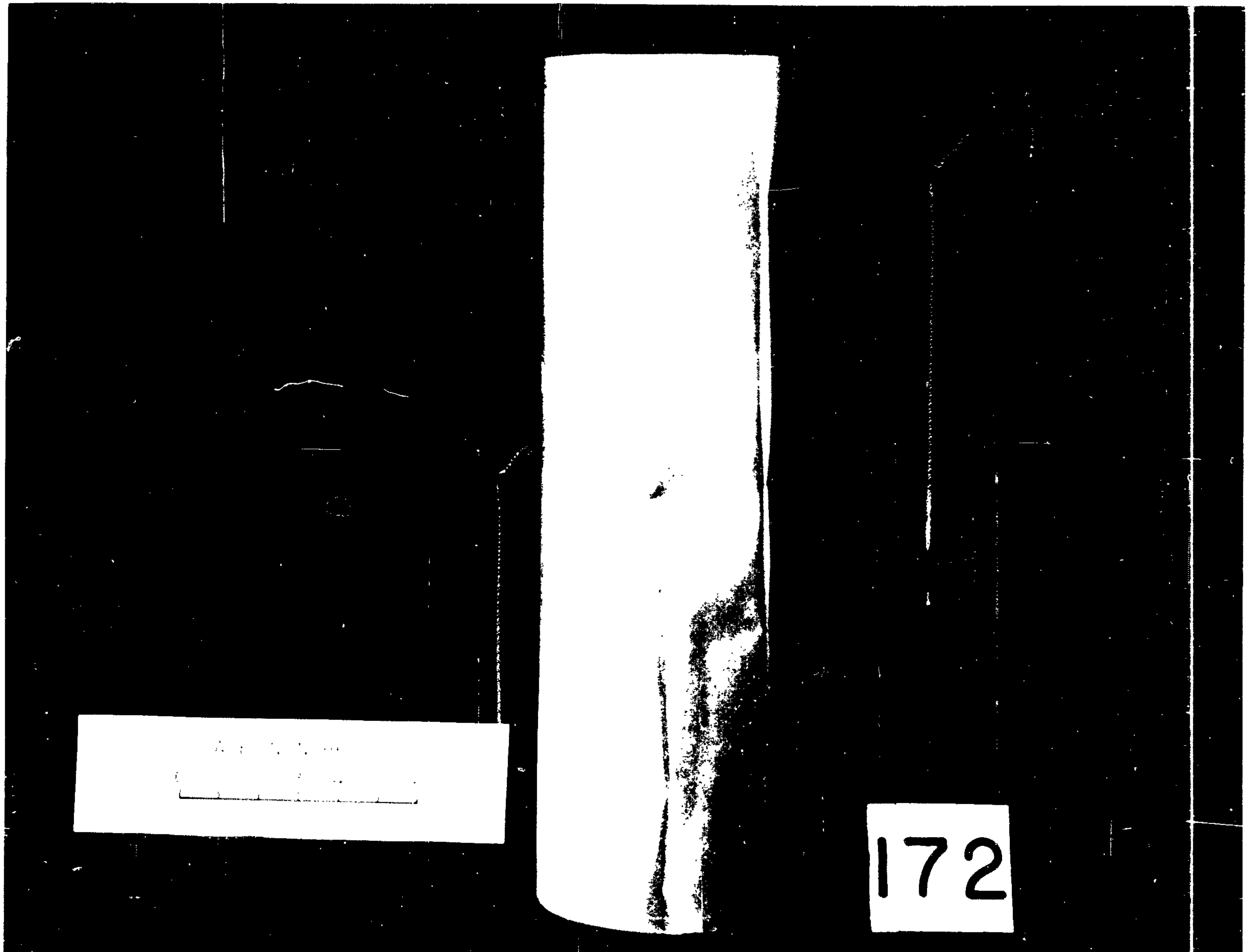

FIG. 63 – SHELL NO. 56

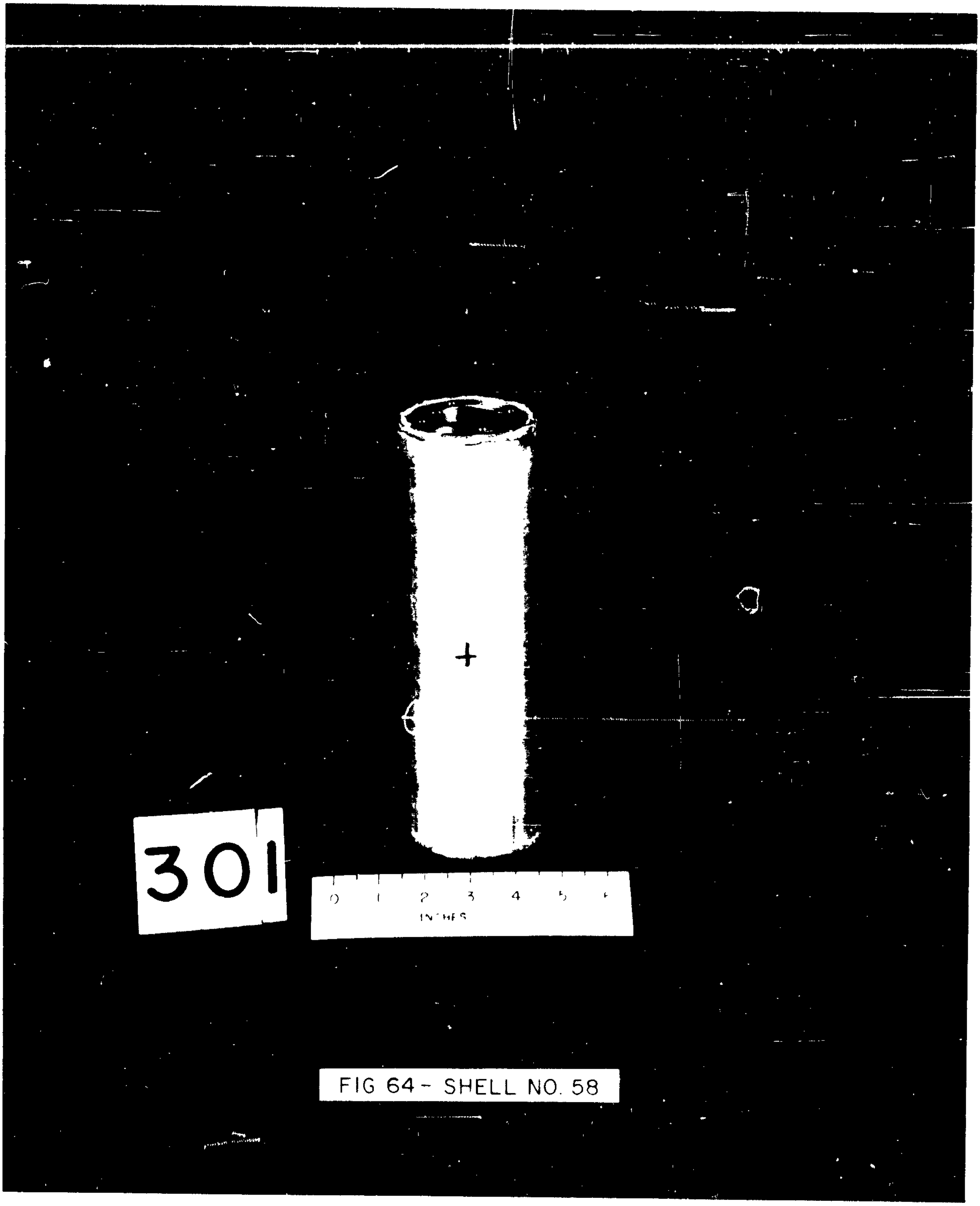

FIG 64 - SHELL NO. 58

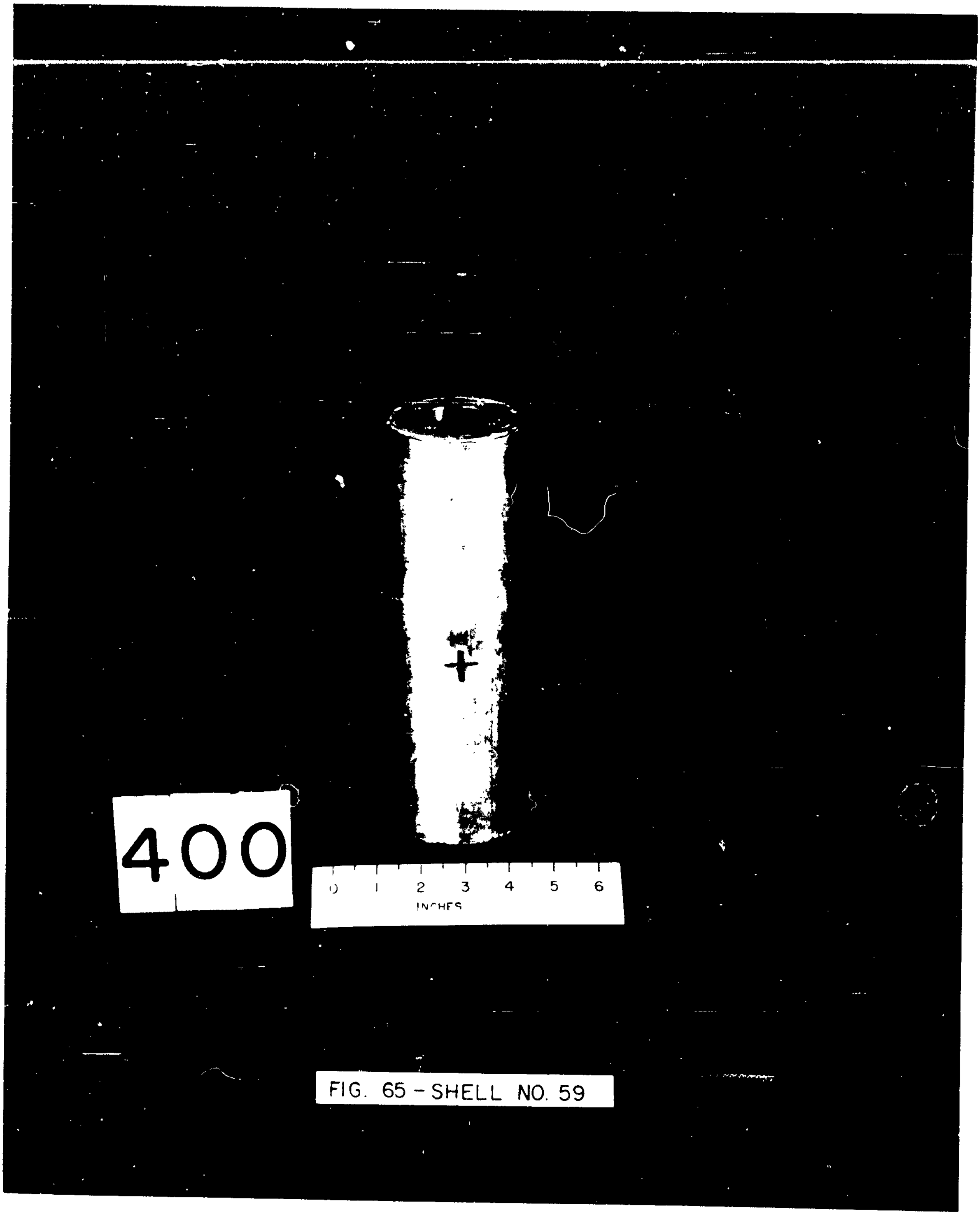

FIG. 65 - SHELL NO. 59

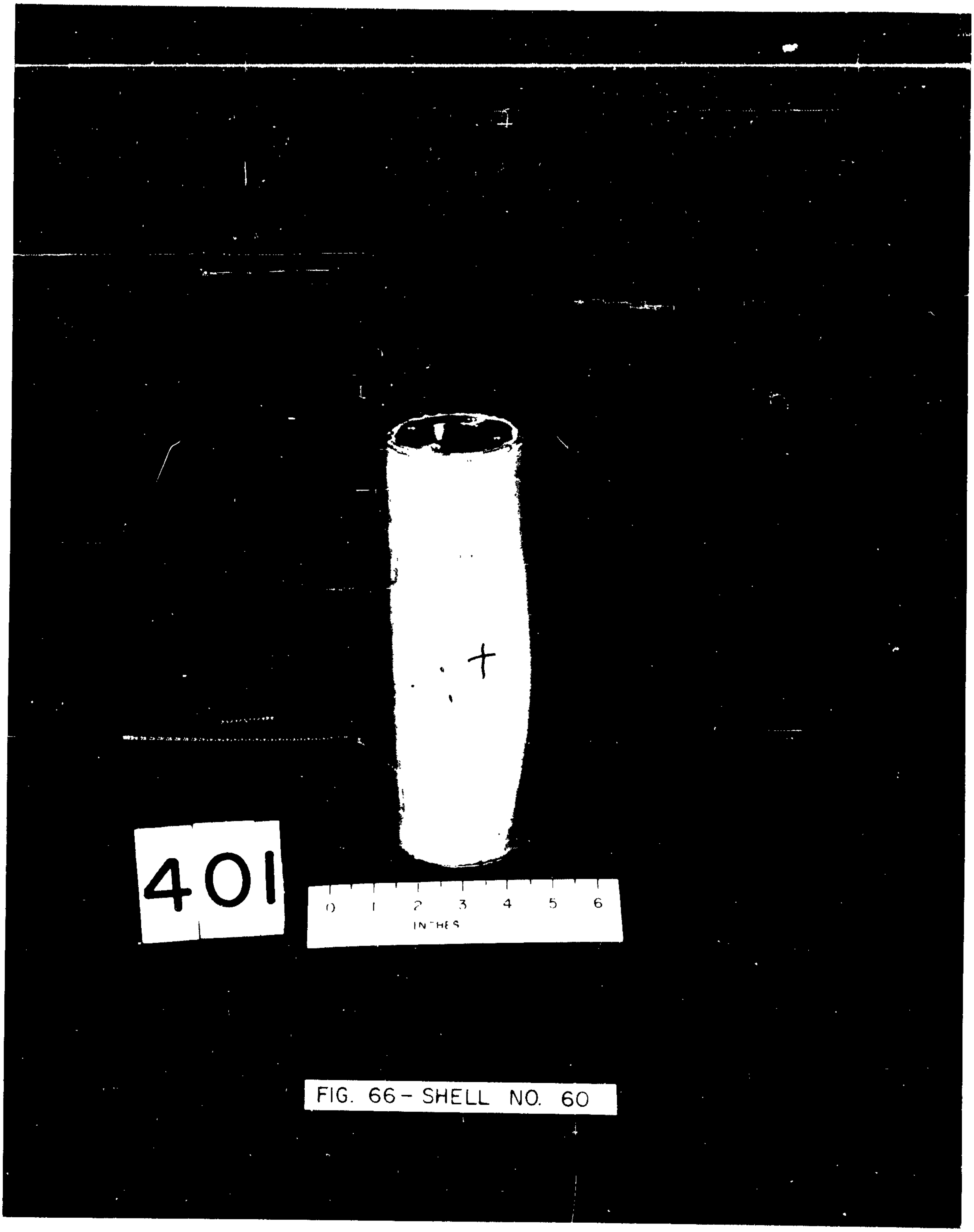

FIG. 66 - SHELL NO. 60

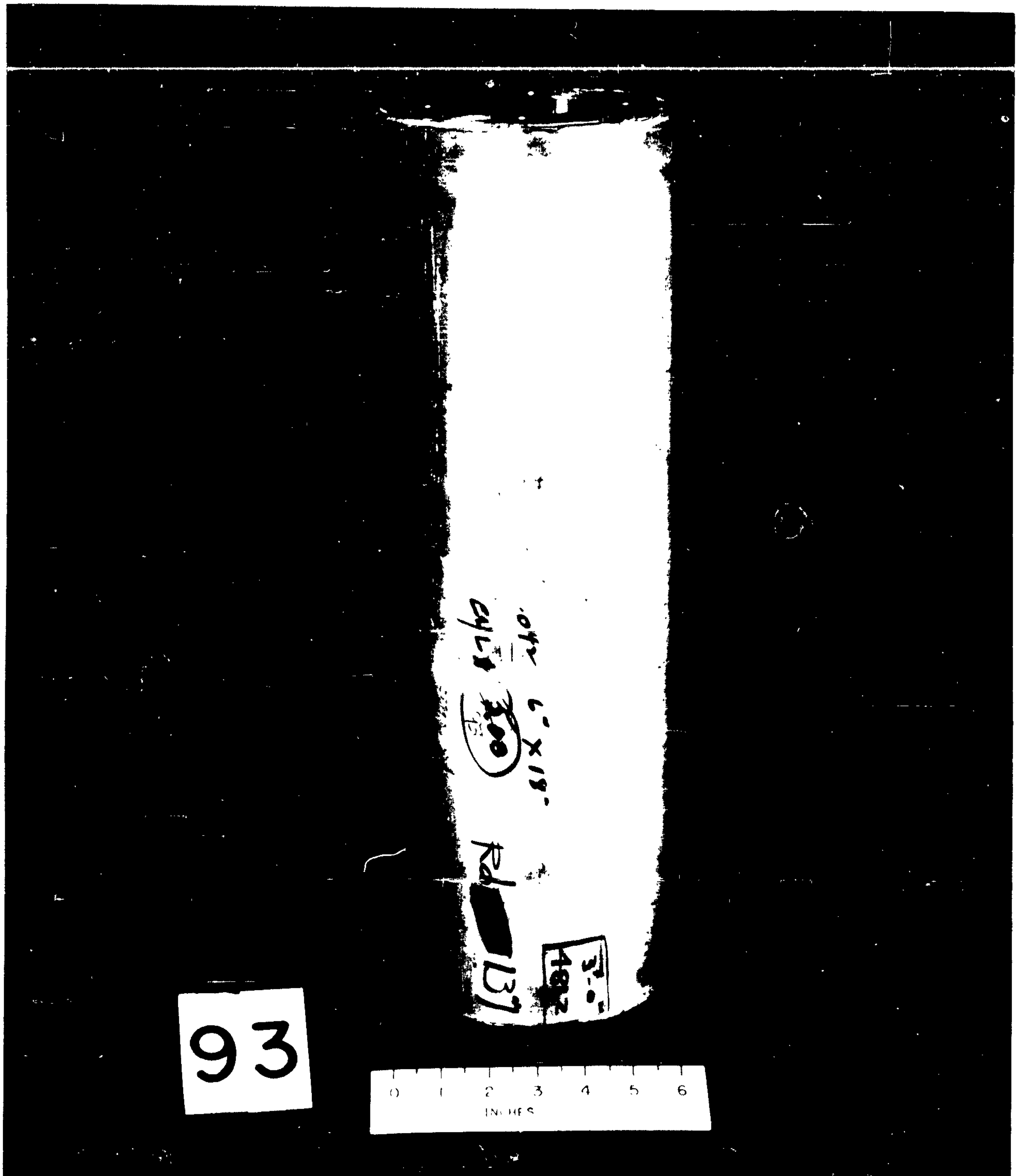

FIG. 67- SHELL NO. 61

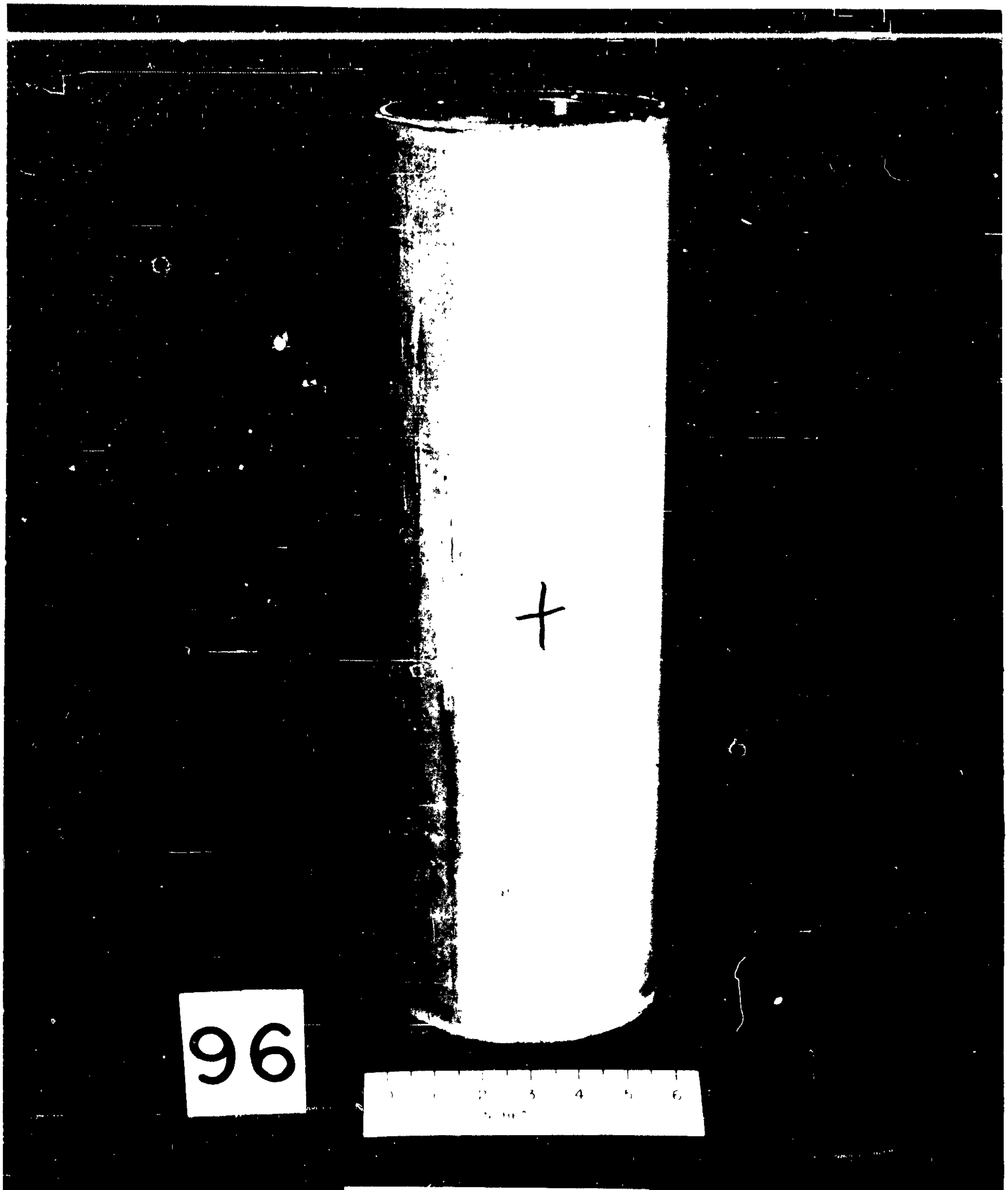

FIG 68 - SHELL NO. 62

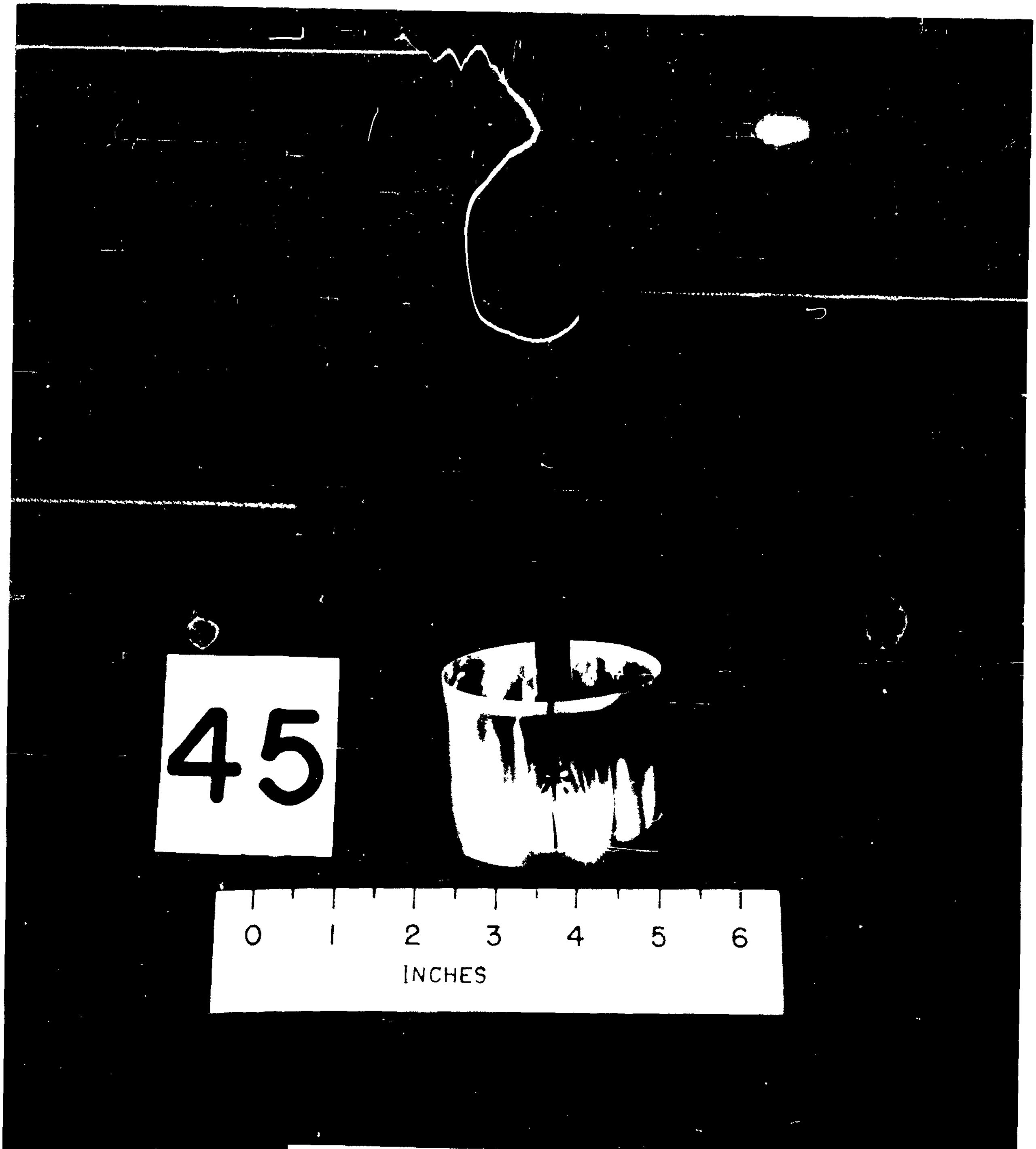

FIG. 69- SHELL NO. 63-FRONT VIEW

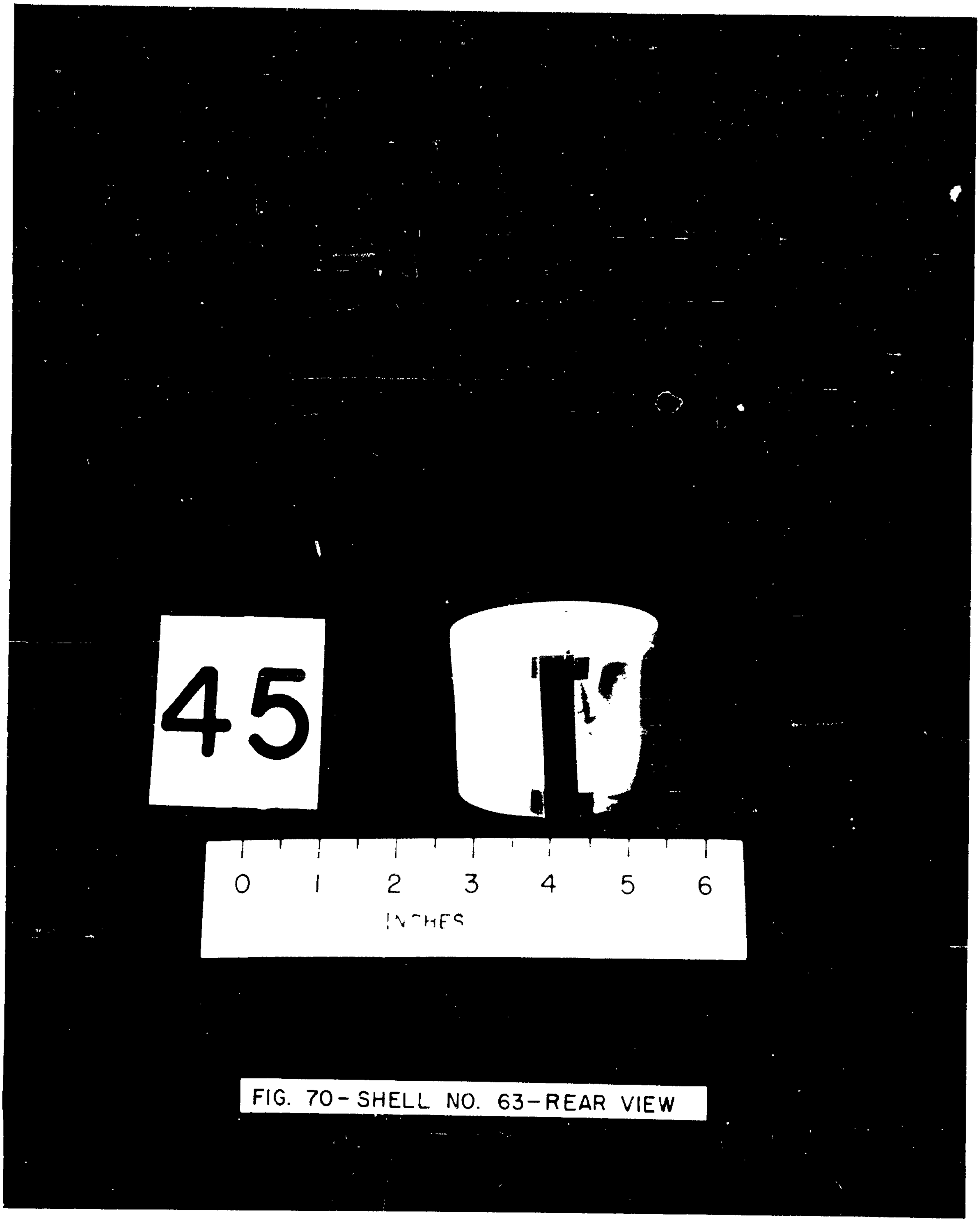

FIG. 70-SHELL NO. 63-REAR VIEW

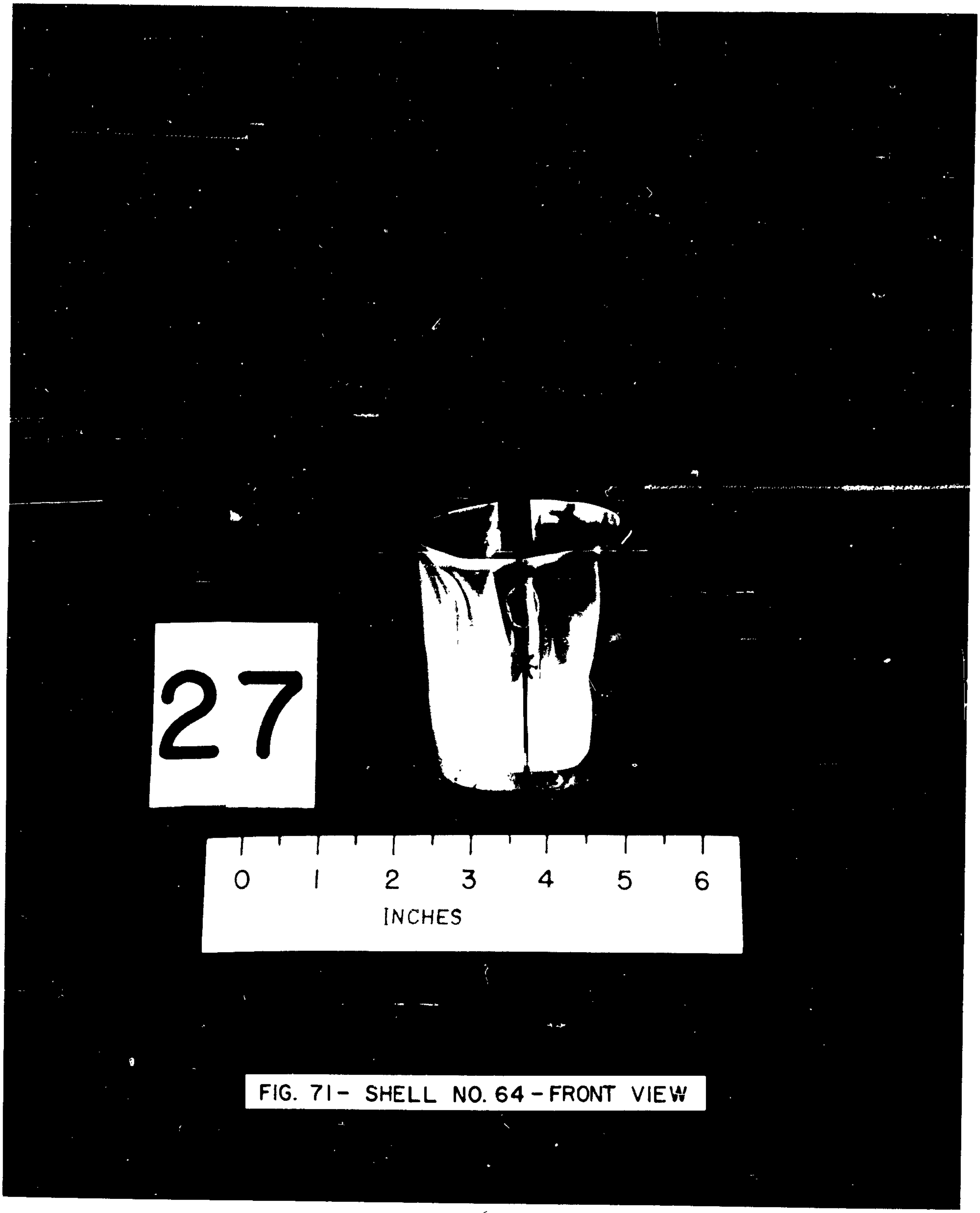

FIG. 71 - SHELL NO. 64 - FRONT VIEW

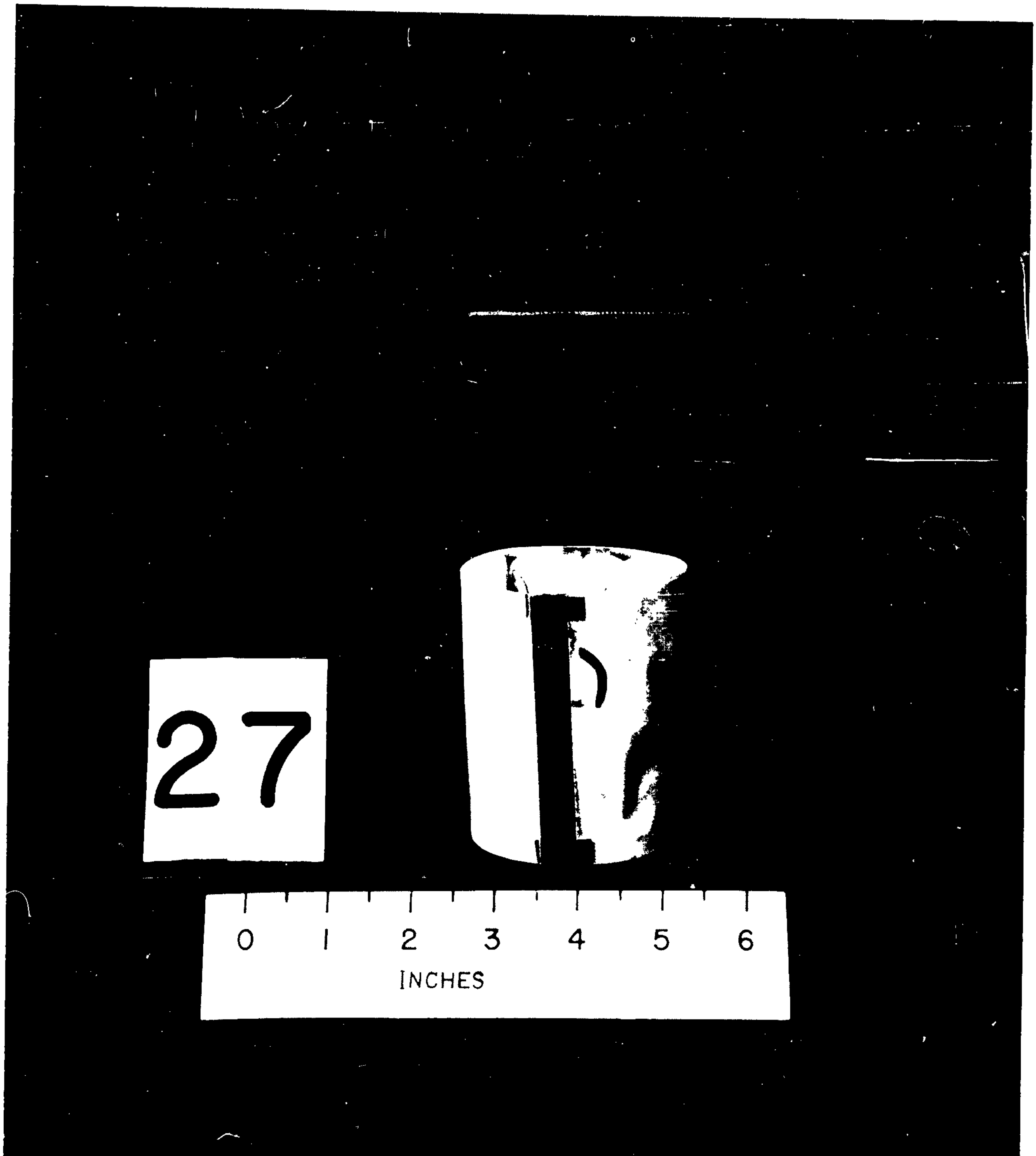

FIG. 72- SHELL NO. 64-REAR VIEW

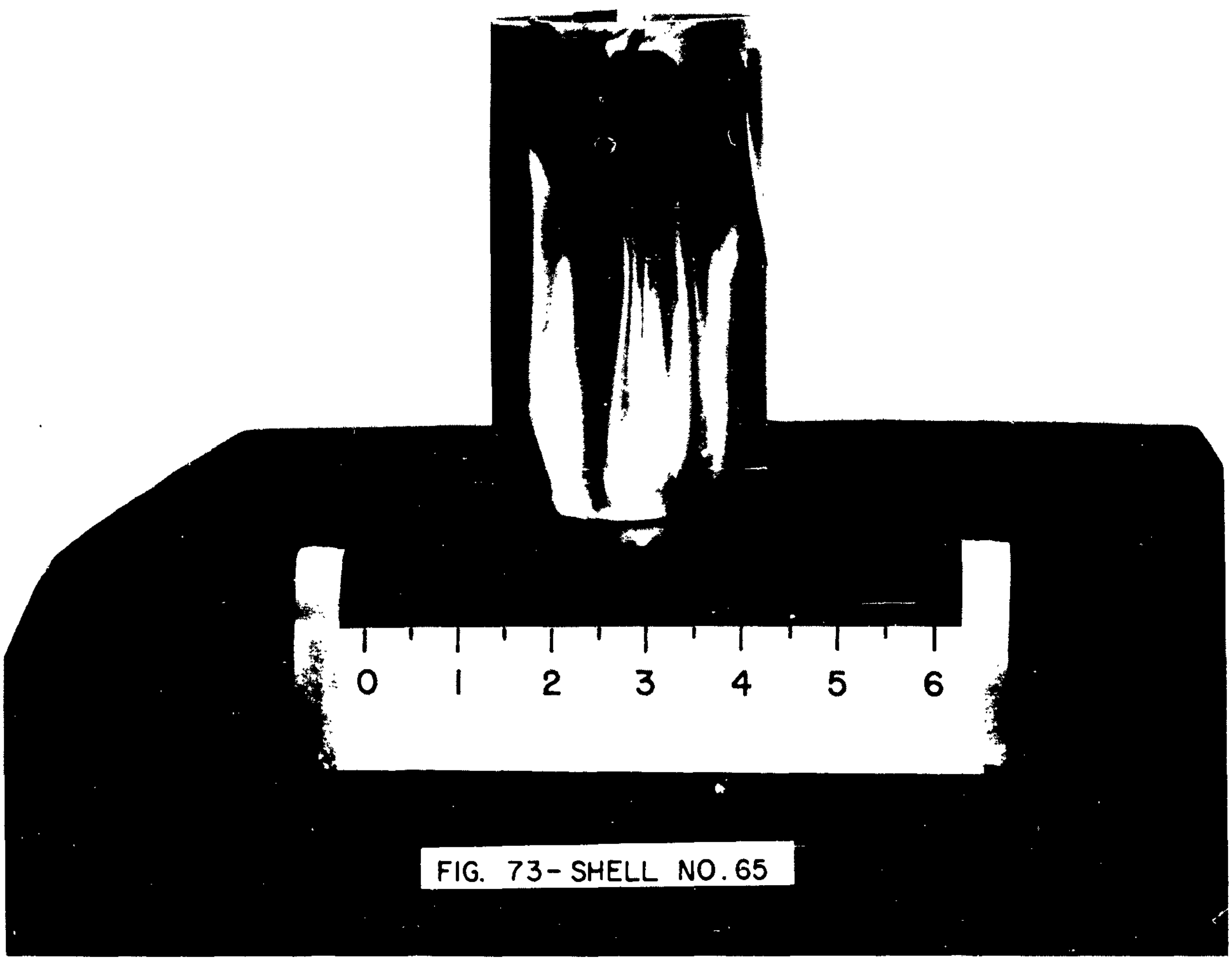

FIG. 73- SHELL NO. 65

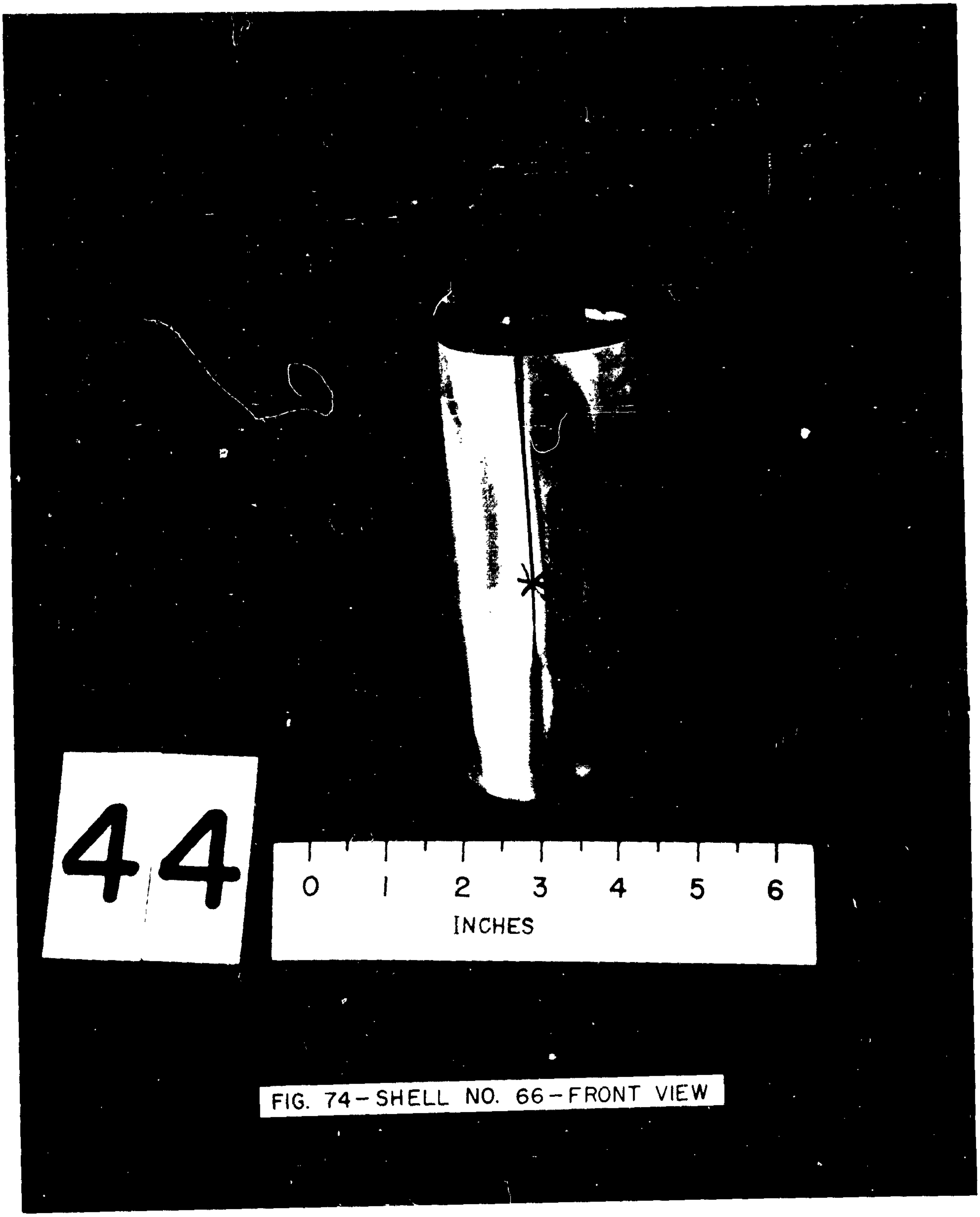

FIG. 74-SHELL NO. 66-FRONT VIEW

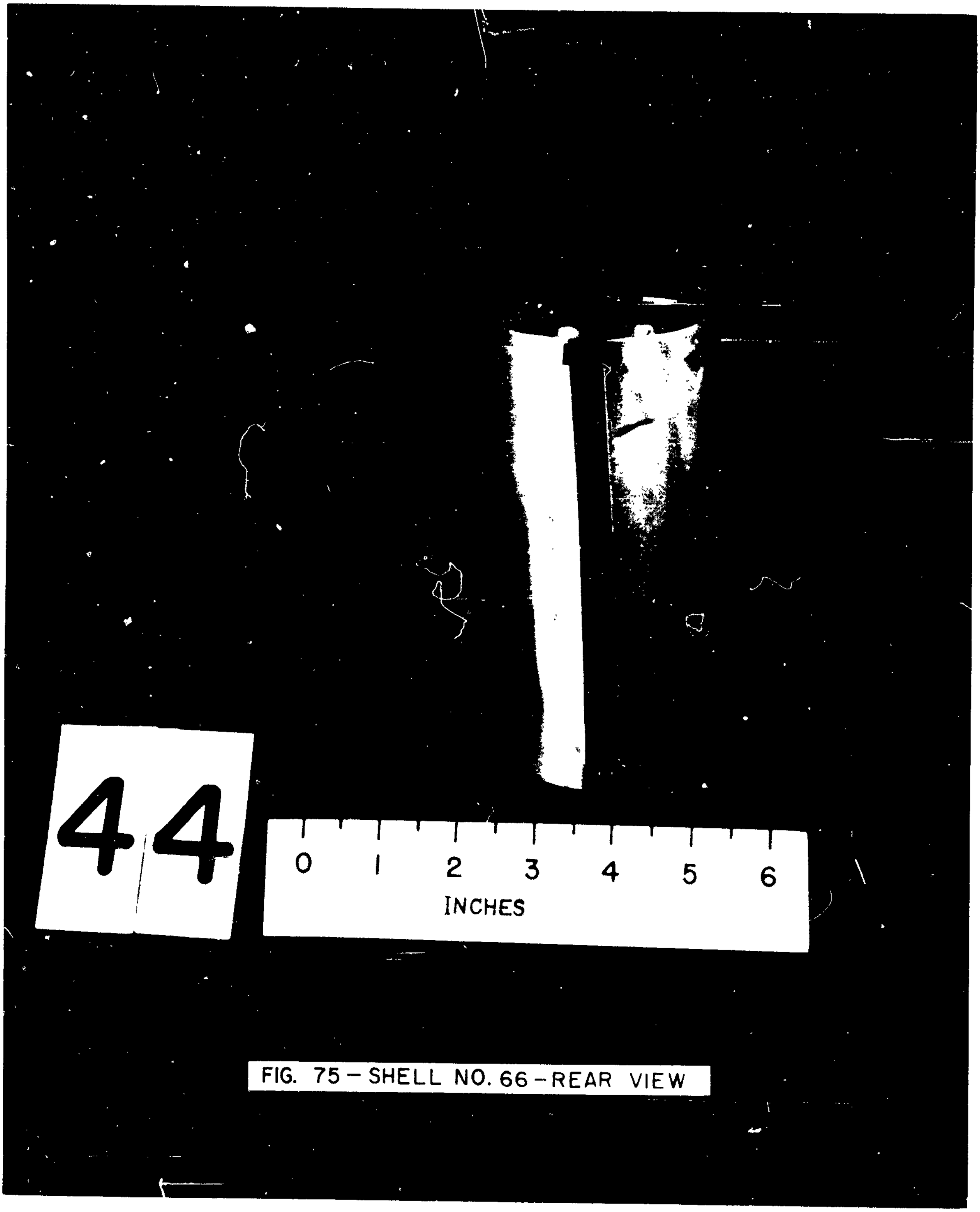

FIG. 75 – SHELL NO. 66 – REAR VIEW

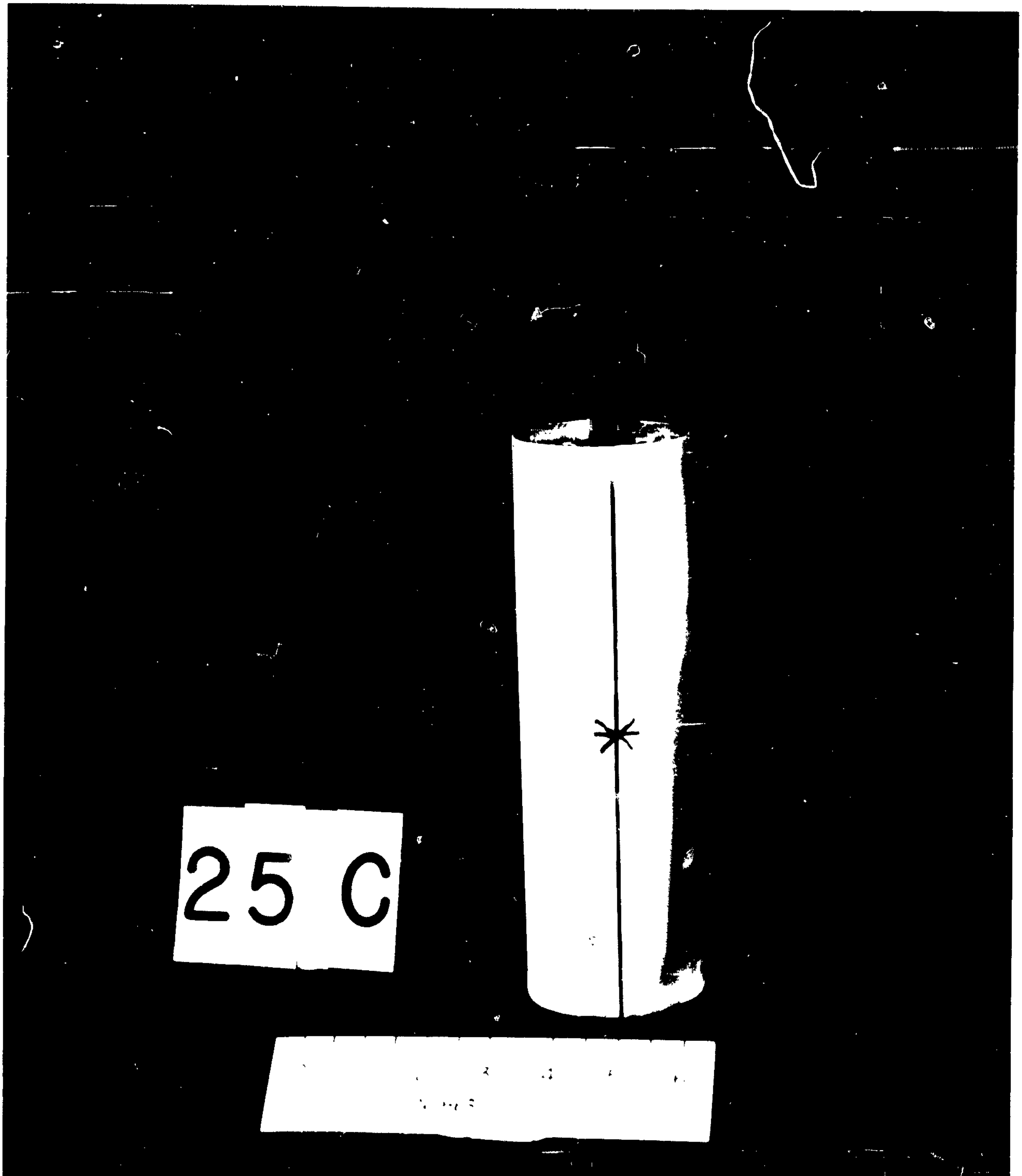

FIG. 76 - SHELL NO. 67 - FRONT VIEW

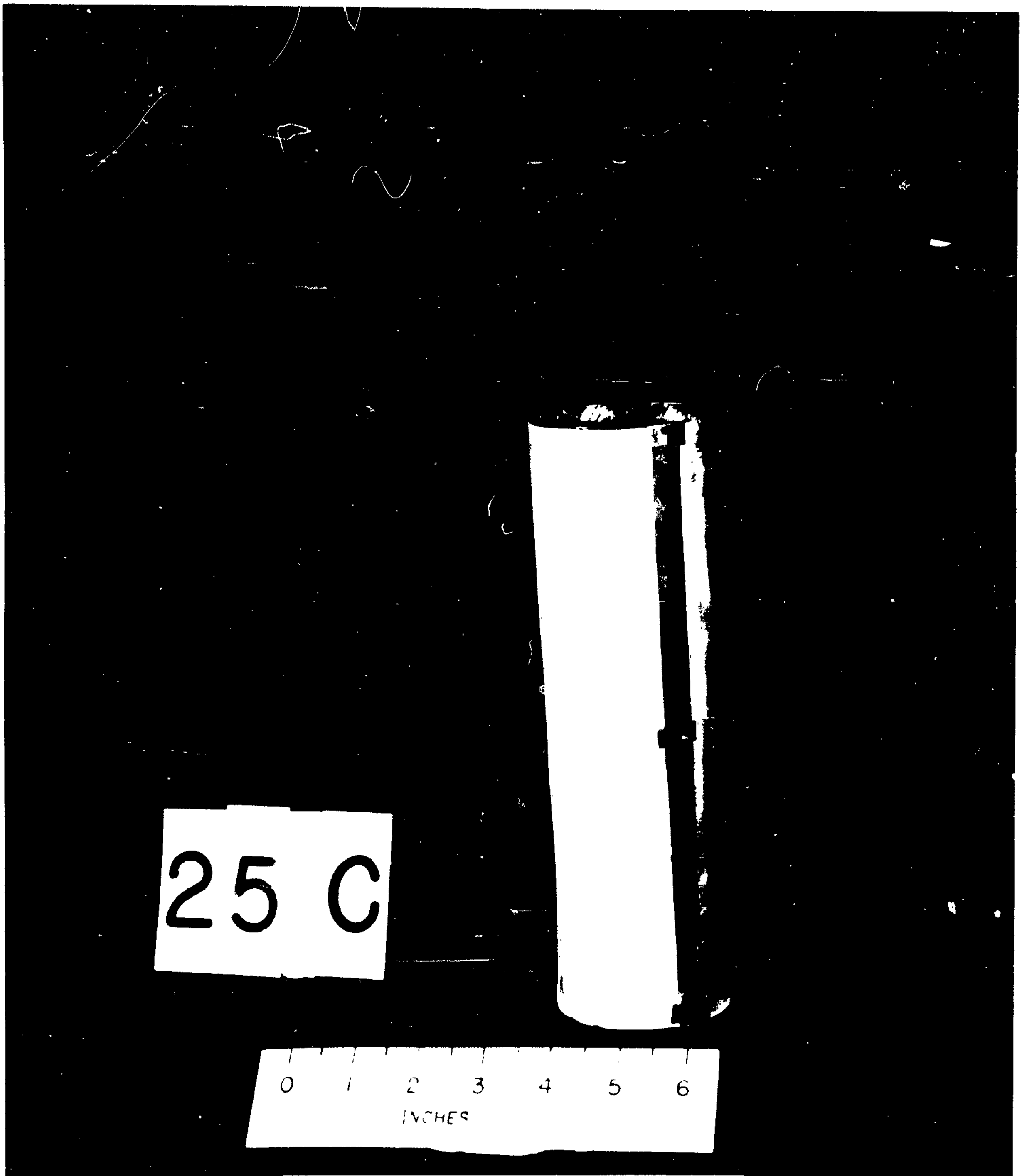

FIG. 77 - SHELL NO. 67 - REAR VIEW

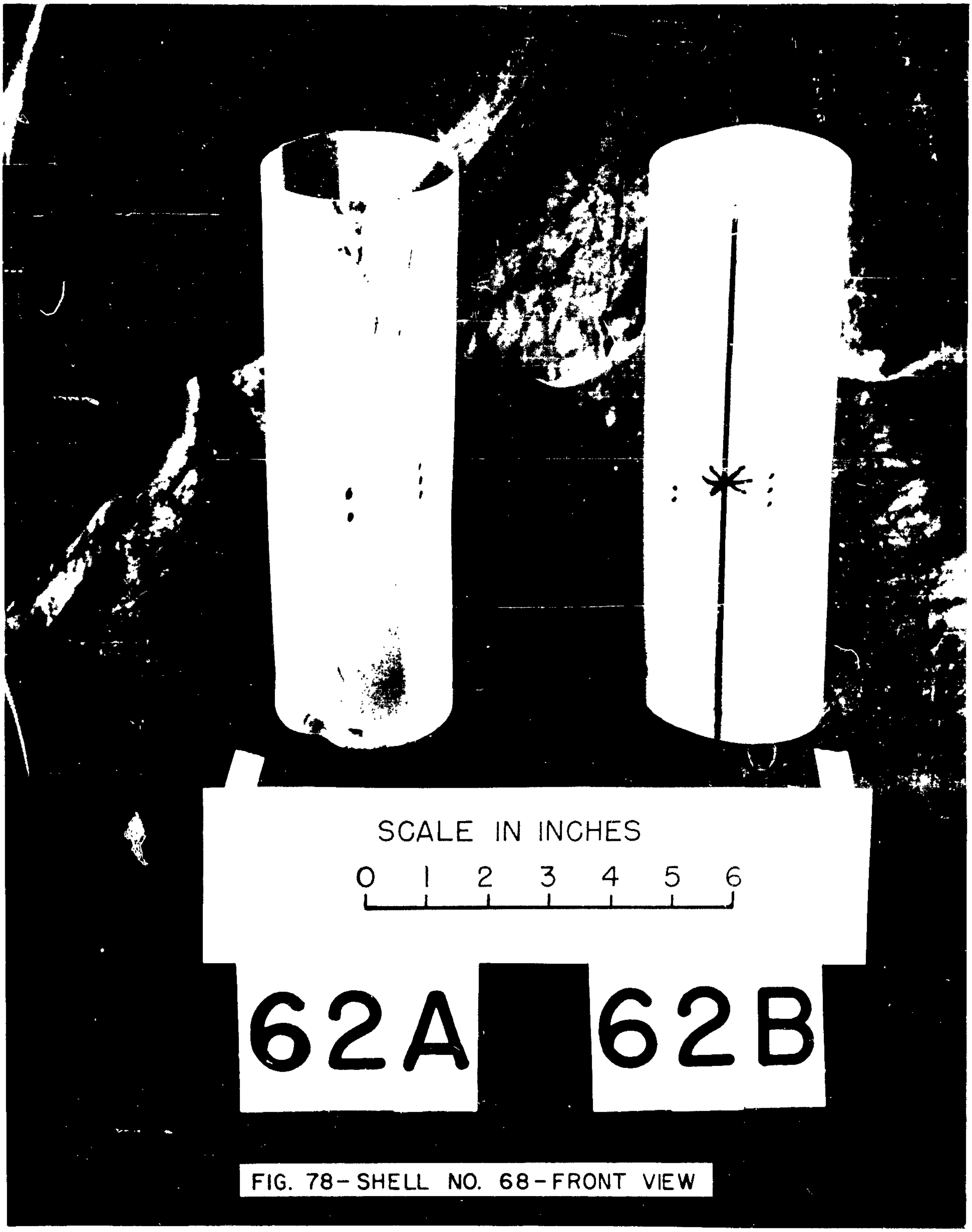

FIG. 78-SHELL NO. 68-FRONT VIEW

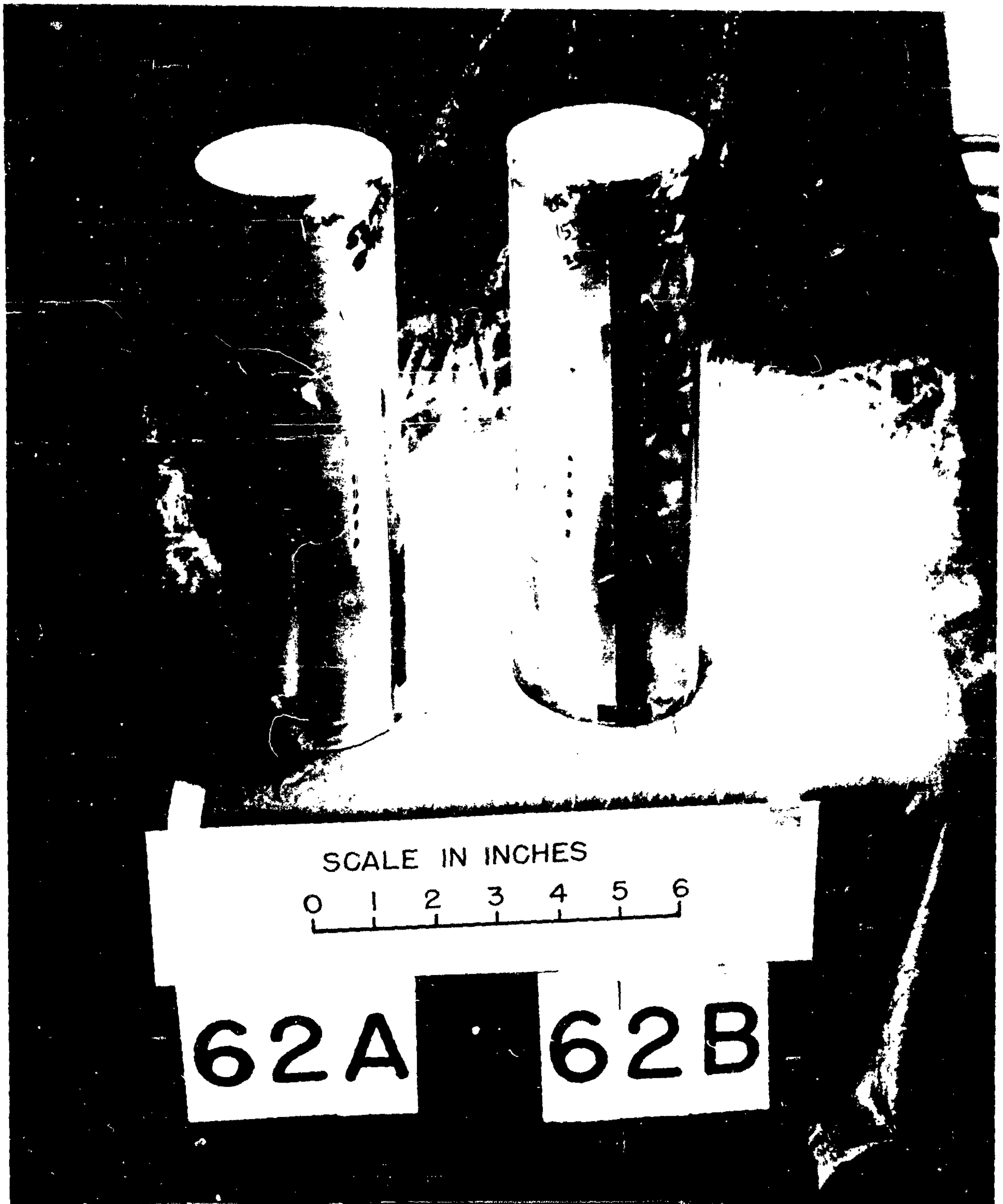

FIG. 79 - SHELL NO. 68 - REAR VIEW

FIG. 80– SHELL NO. 69–FRONT VIEW

FIG. 81 - SHELL NO. 69 - SIDE VIEW

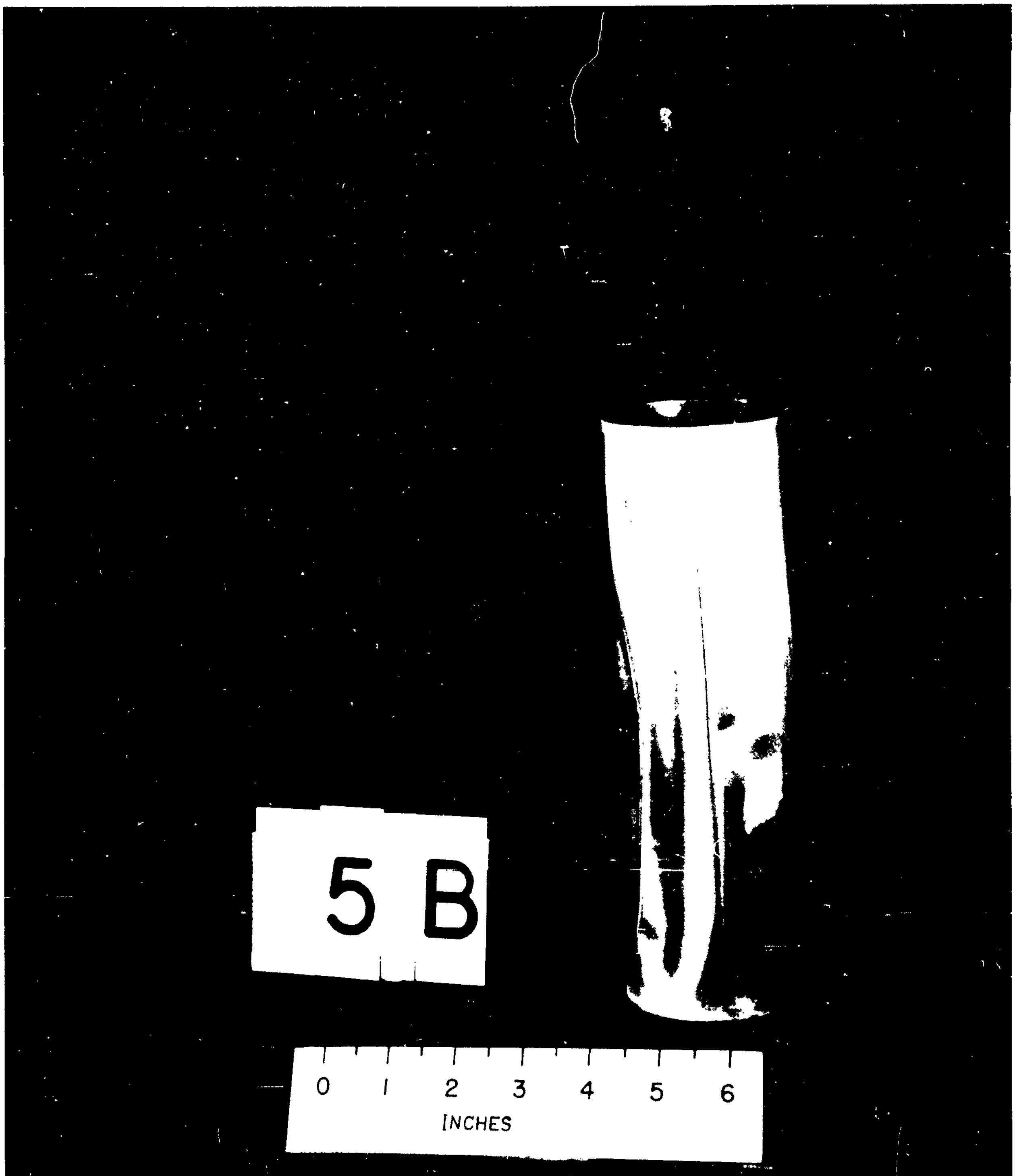

FIG. 82- SHELL NO. 71- SIDE VIEW

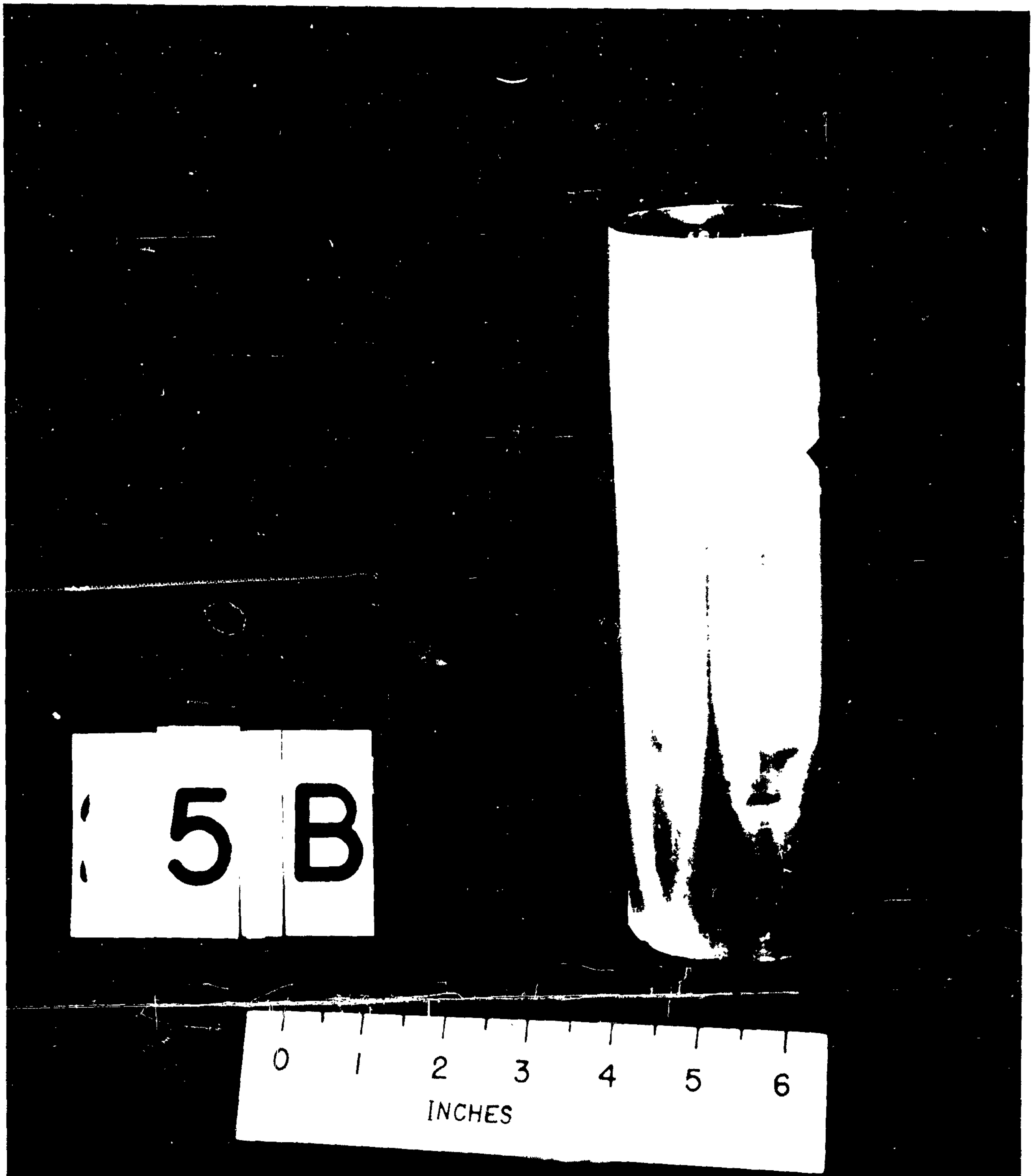

FIG. 83 - SHELL NO. 71 - REAR VIEW

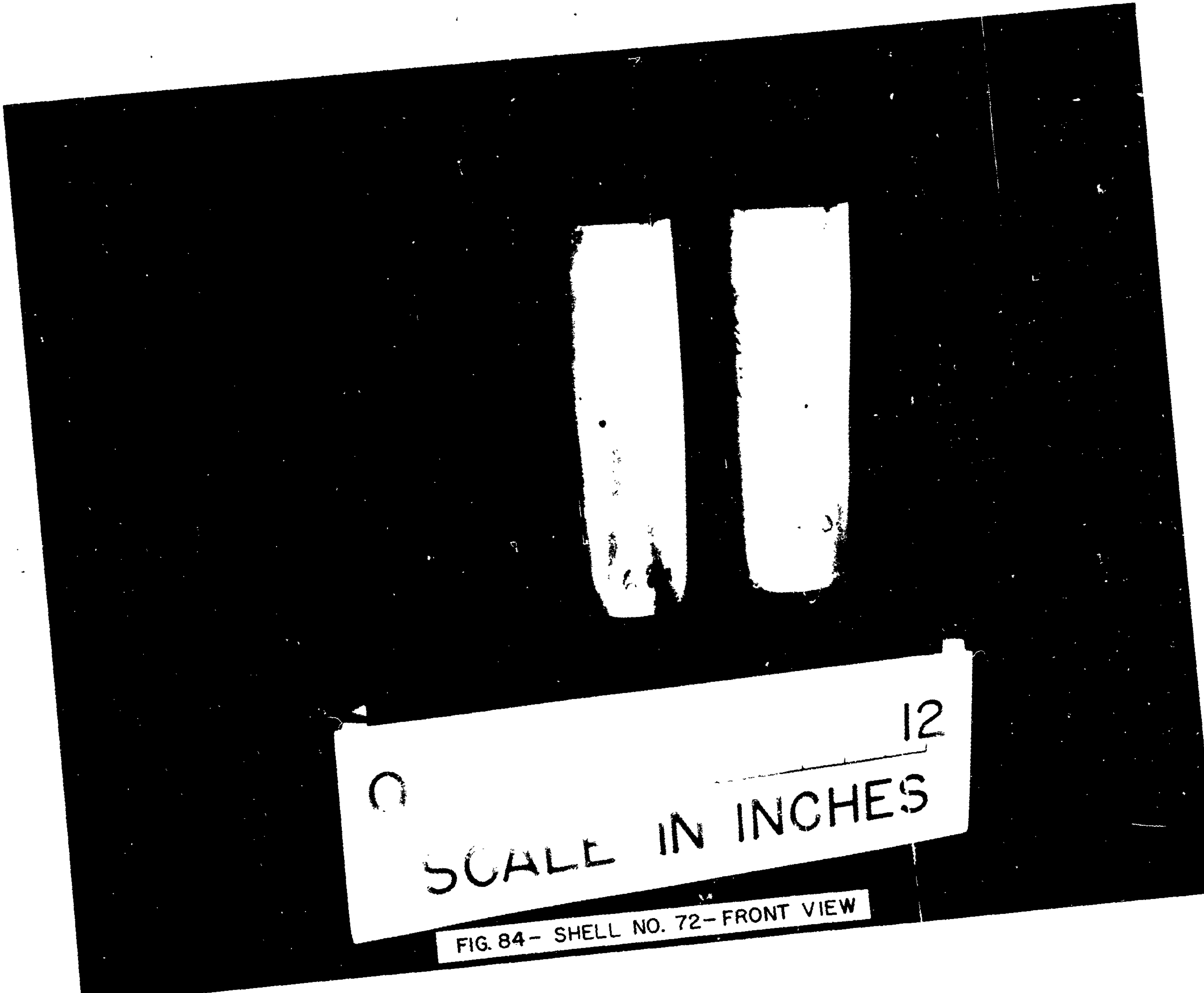

FIG. 84 - SHELL NO. 72 - FRONT VIEW

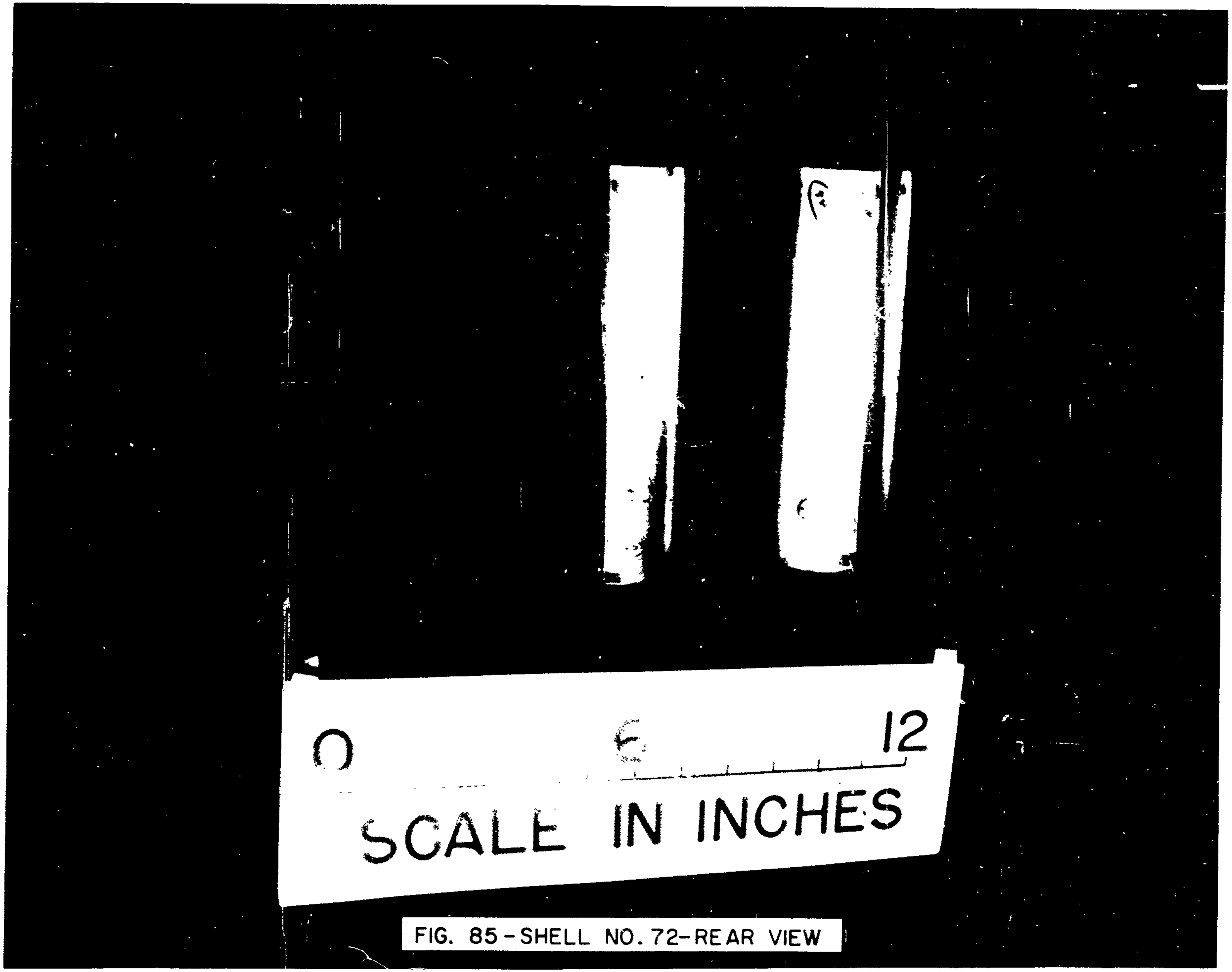

FIG. 85-SHELL NO. 72-REAR VIEW

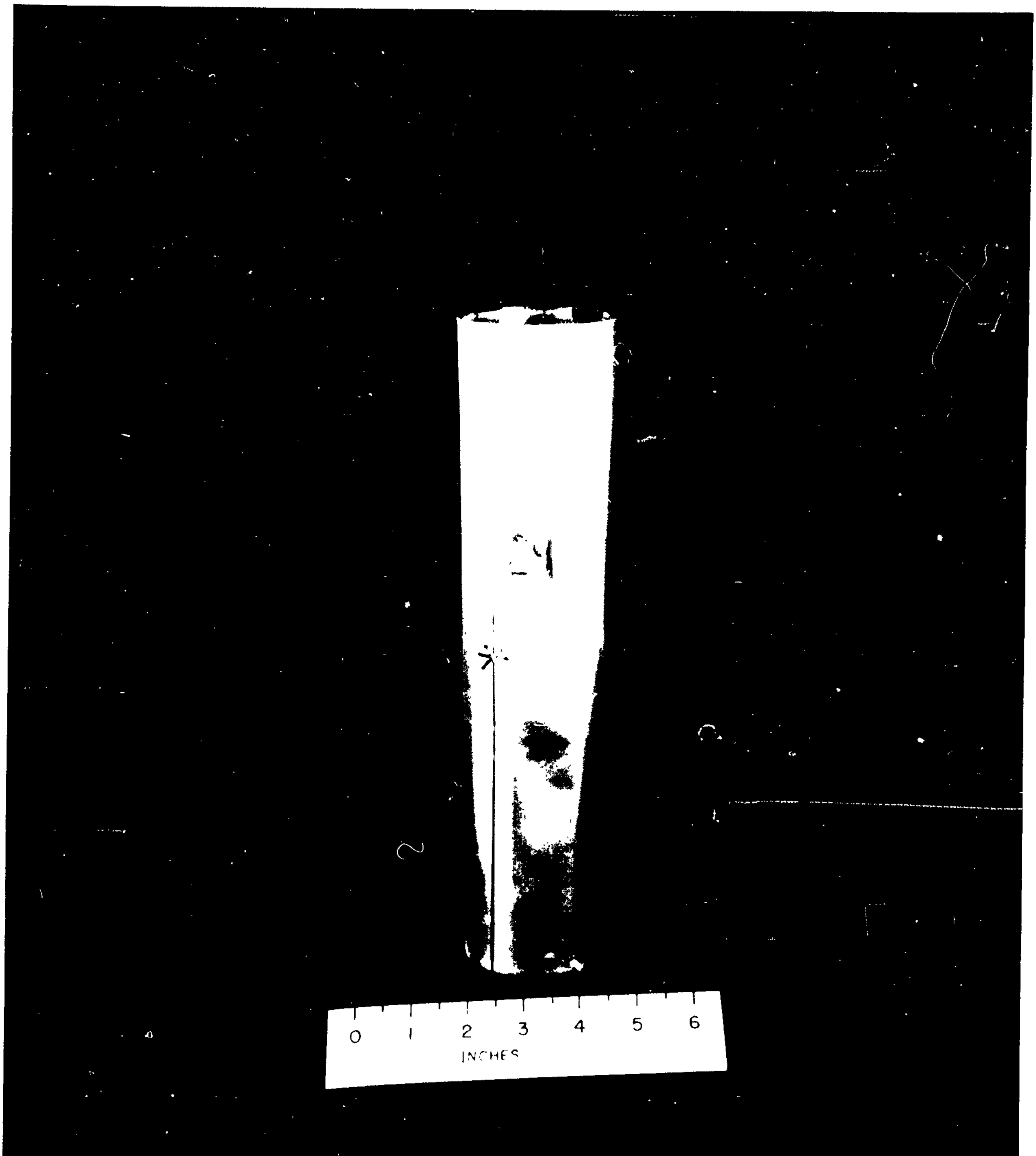

FIG. 86- SHELL NO. 76-FRONT VIEW

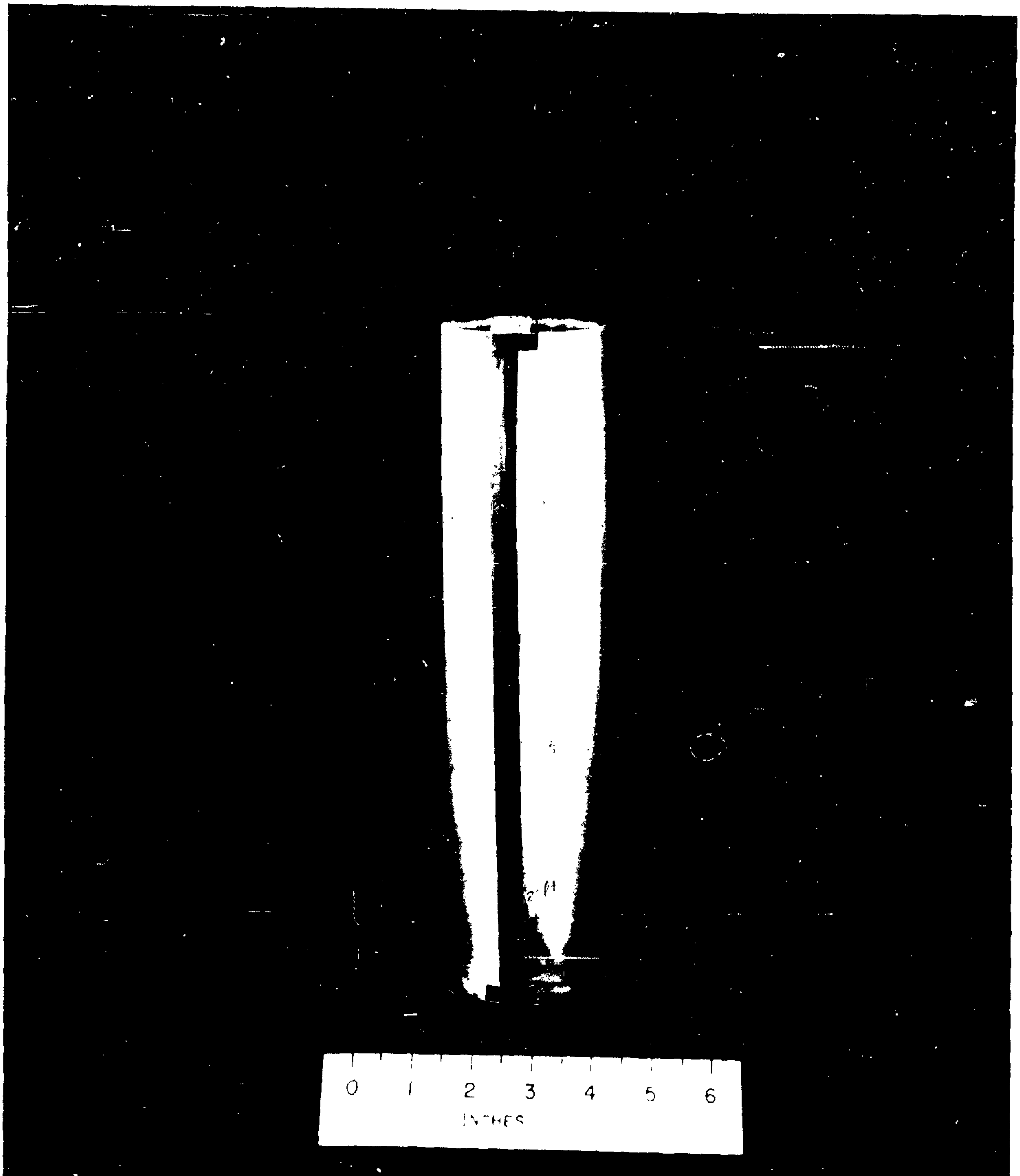

FIG. 87 - SHELL NO. 76- REAR VIEW

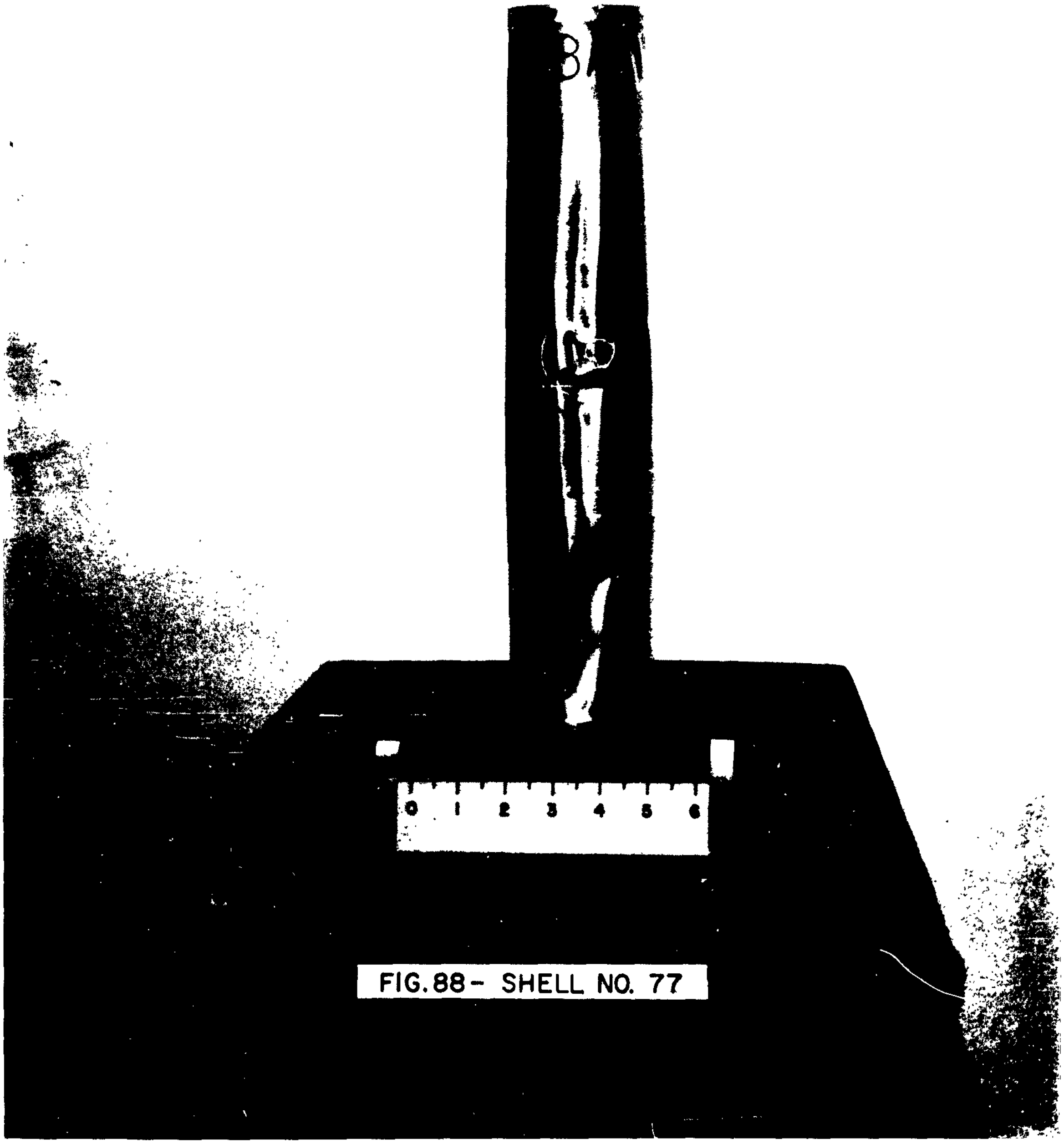

FIG. 88 - SHELL NO. 77

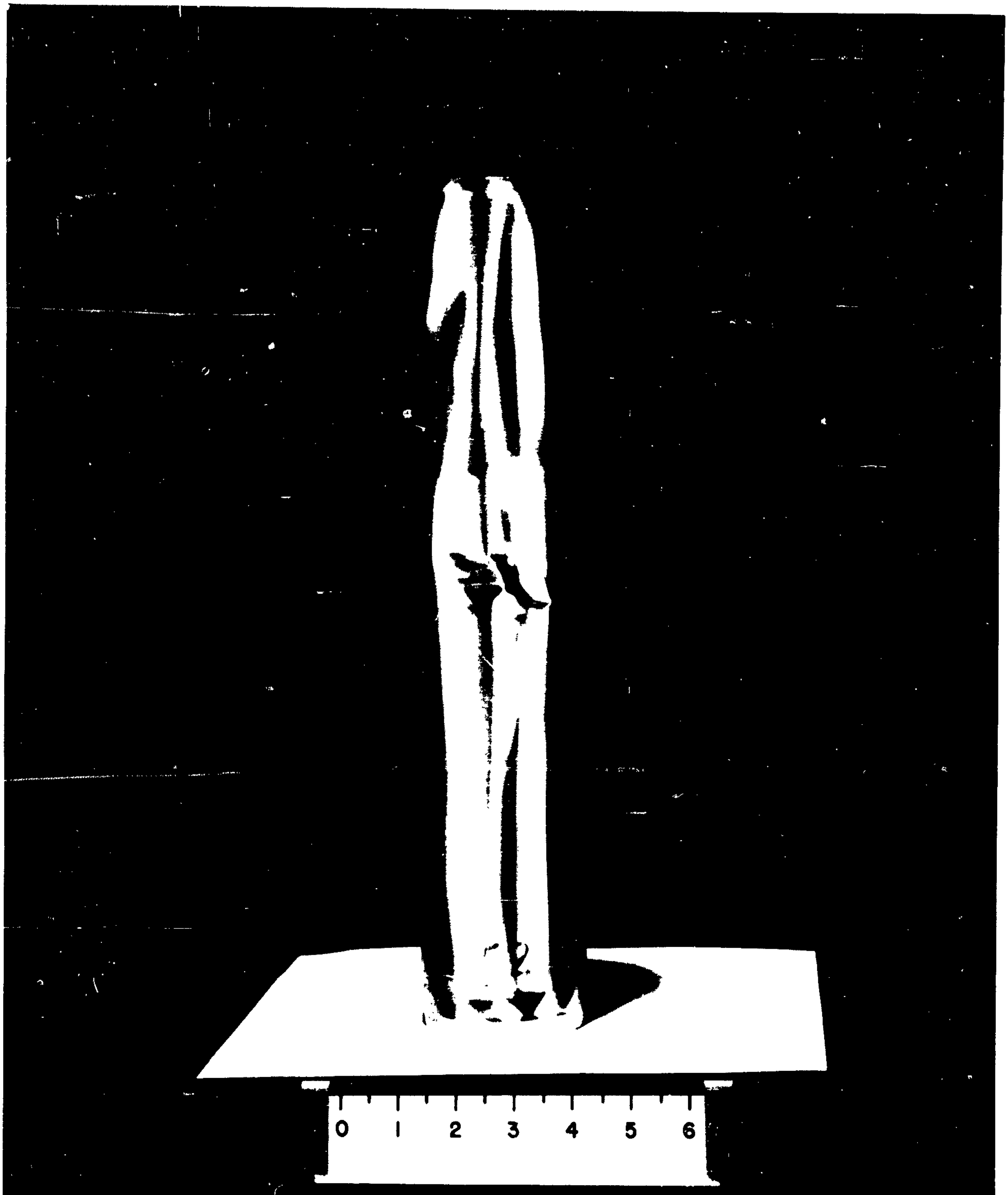

FIG. 89-SHELL NO. 78

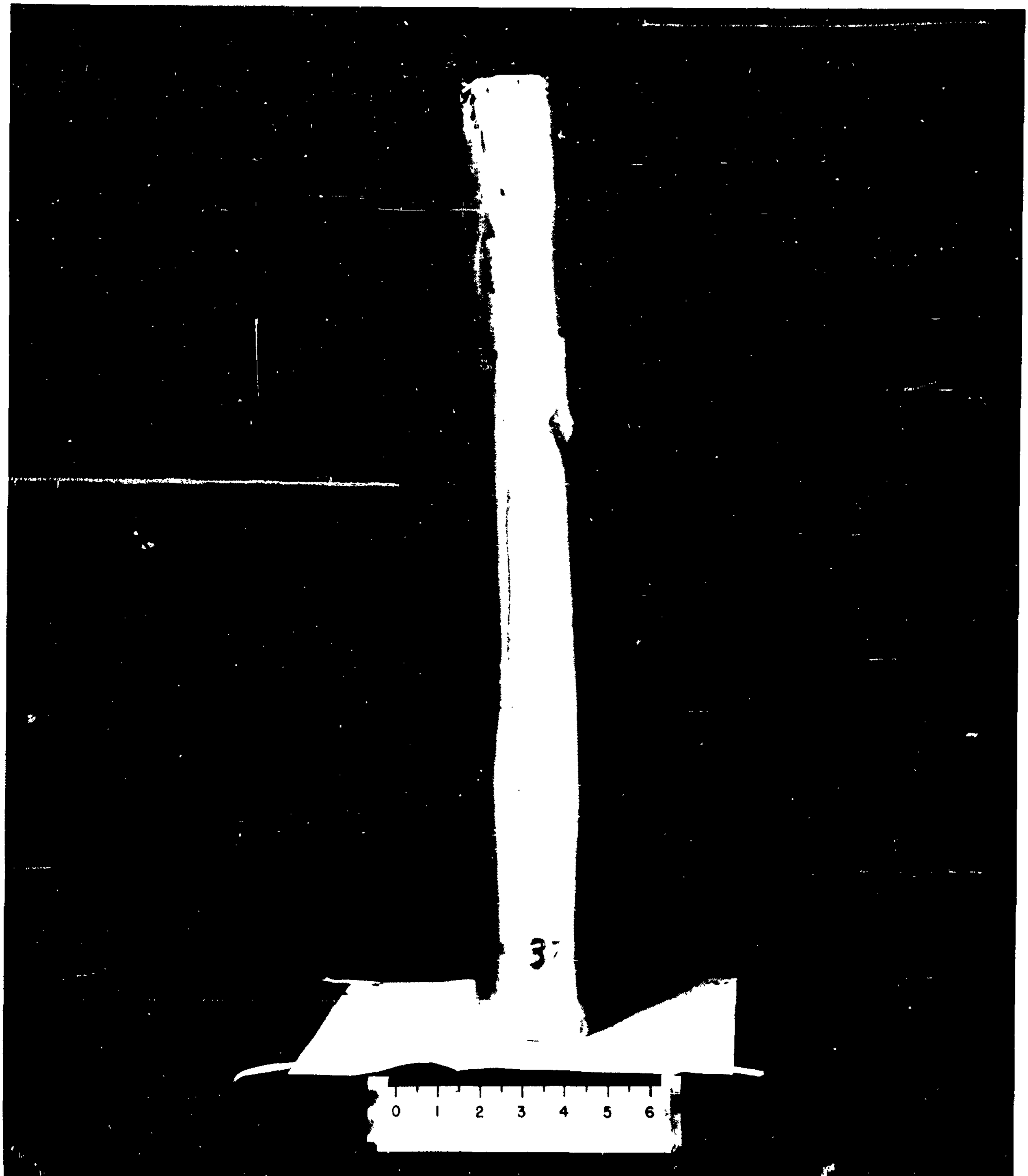

FIG. 90- SHELL NO. 79

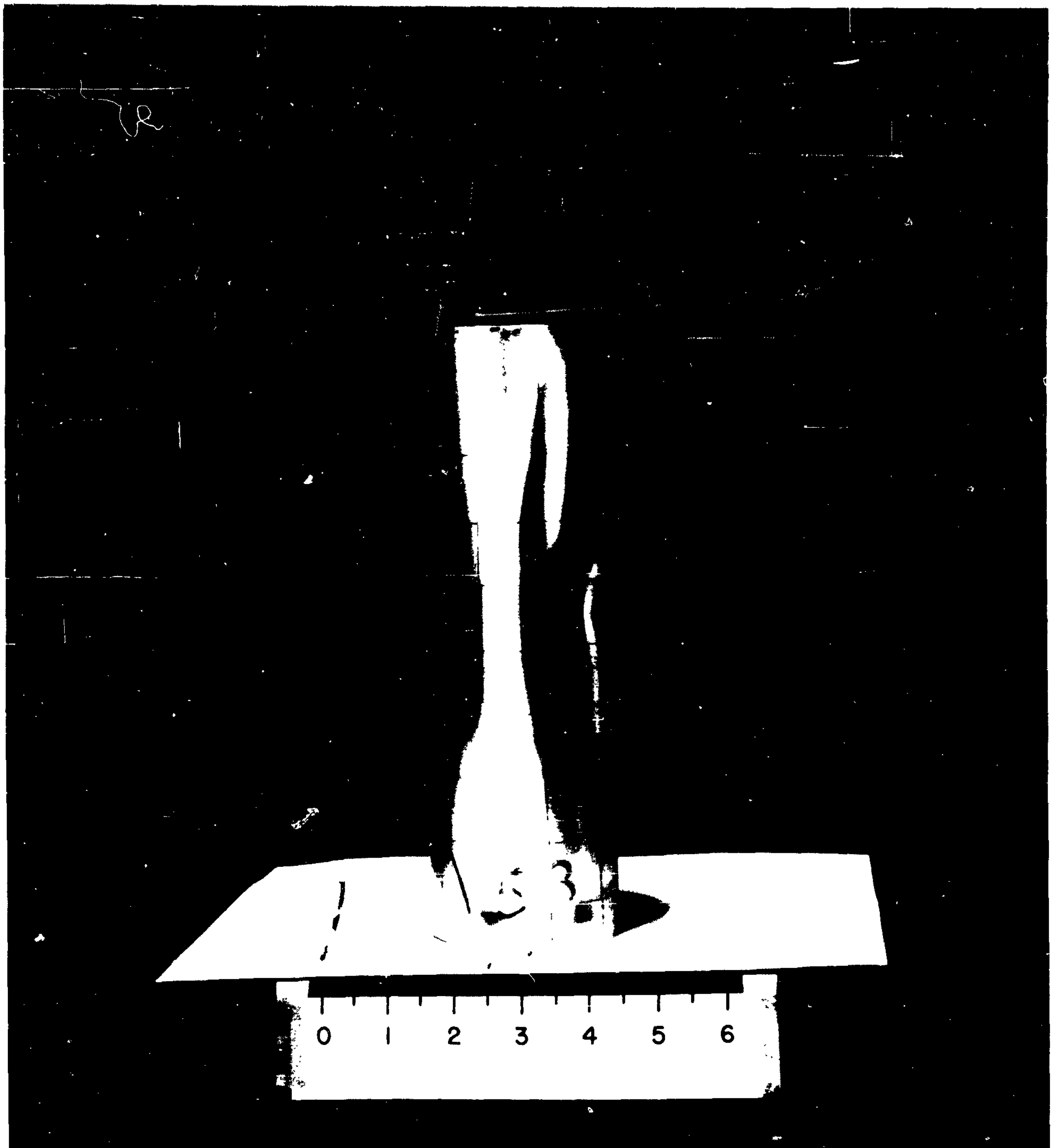

FIG. 91 – SHELL NO. 80 – FRONT VIEW

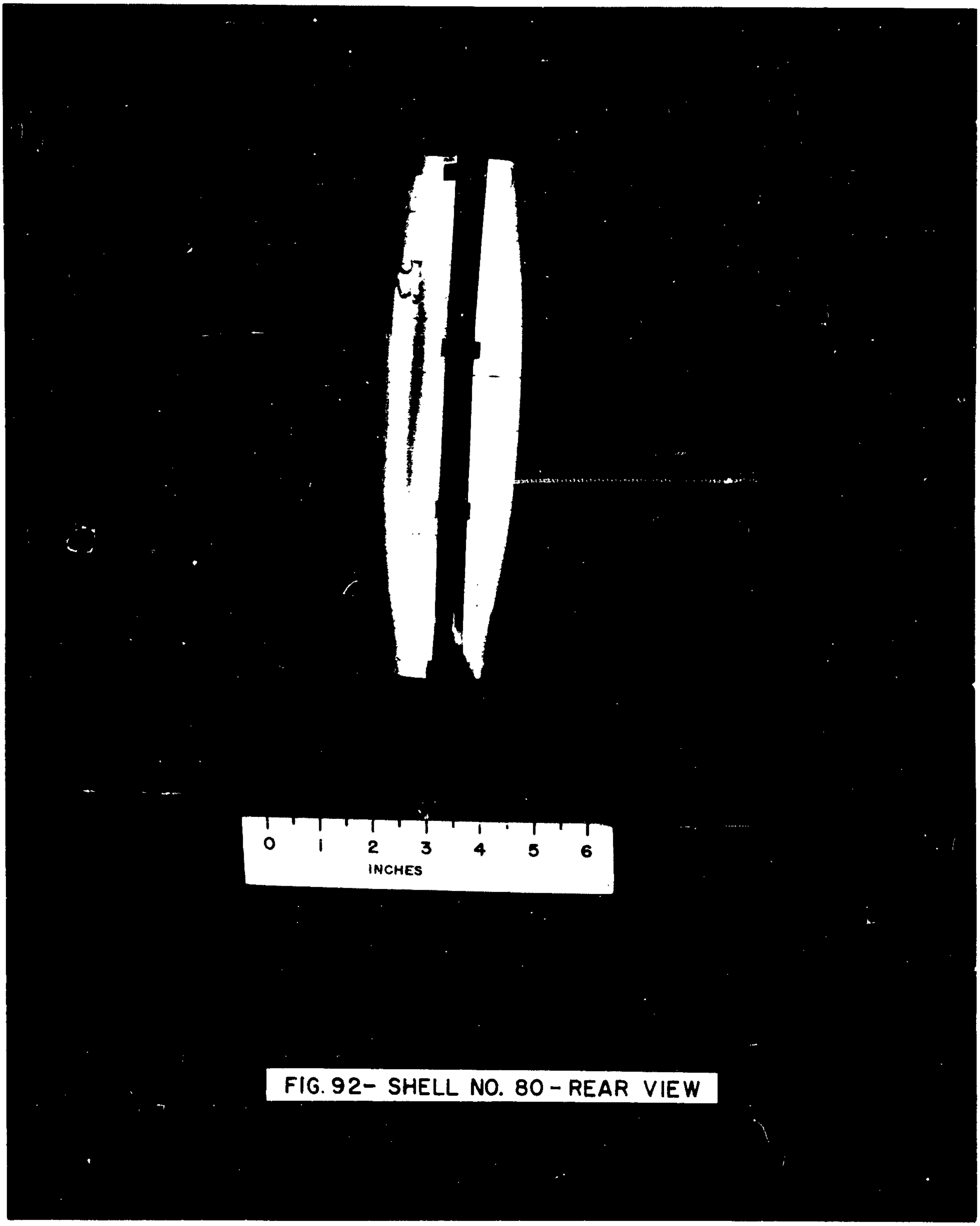

FIG. 92- SHELL NO. 80 - REAR VIEW

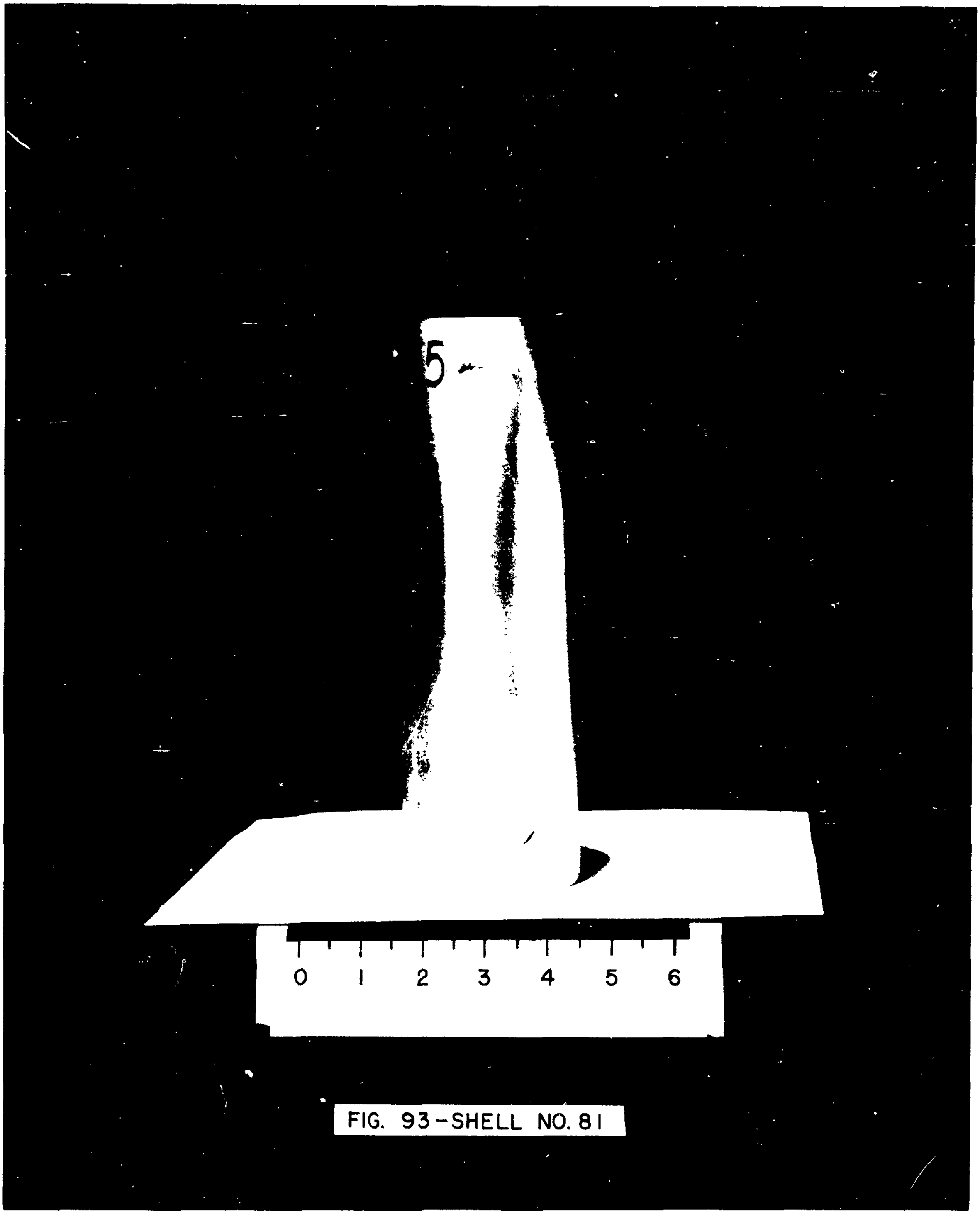

FIG. 93-SHELL NO. 81

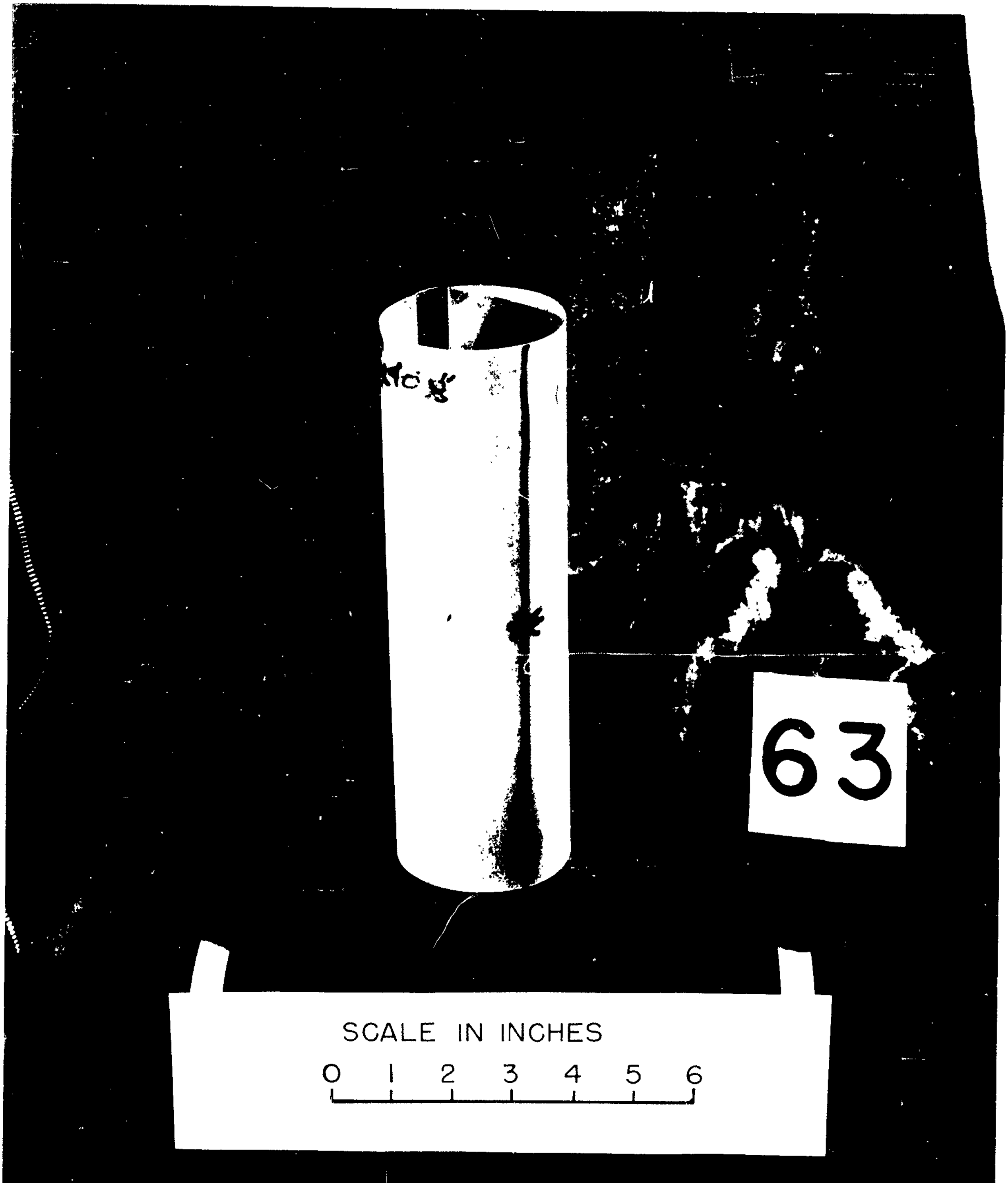

FIG. 94 - SHELL NO. 82

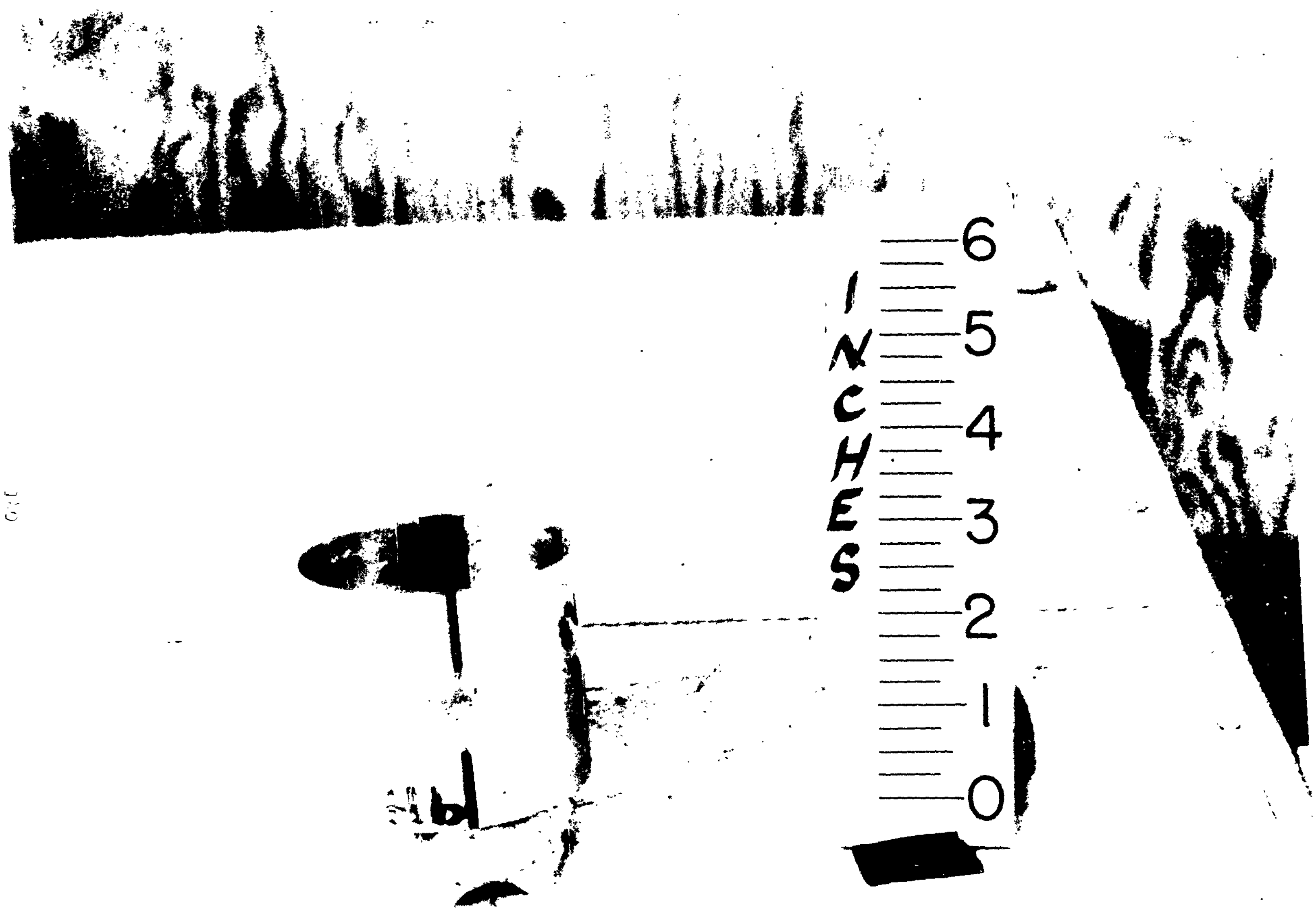

FIG. 95- SHELL NO. 84

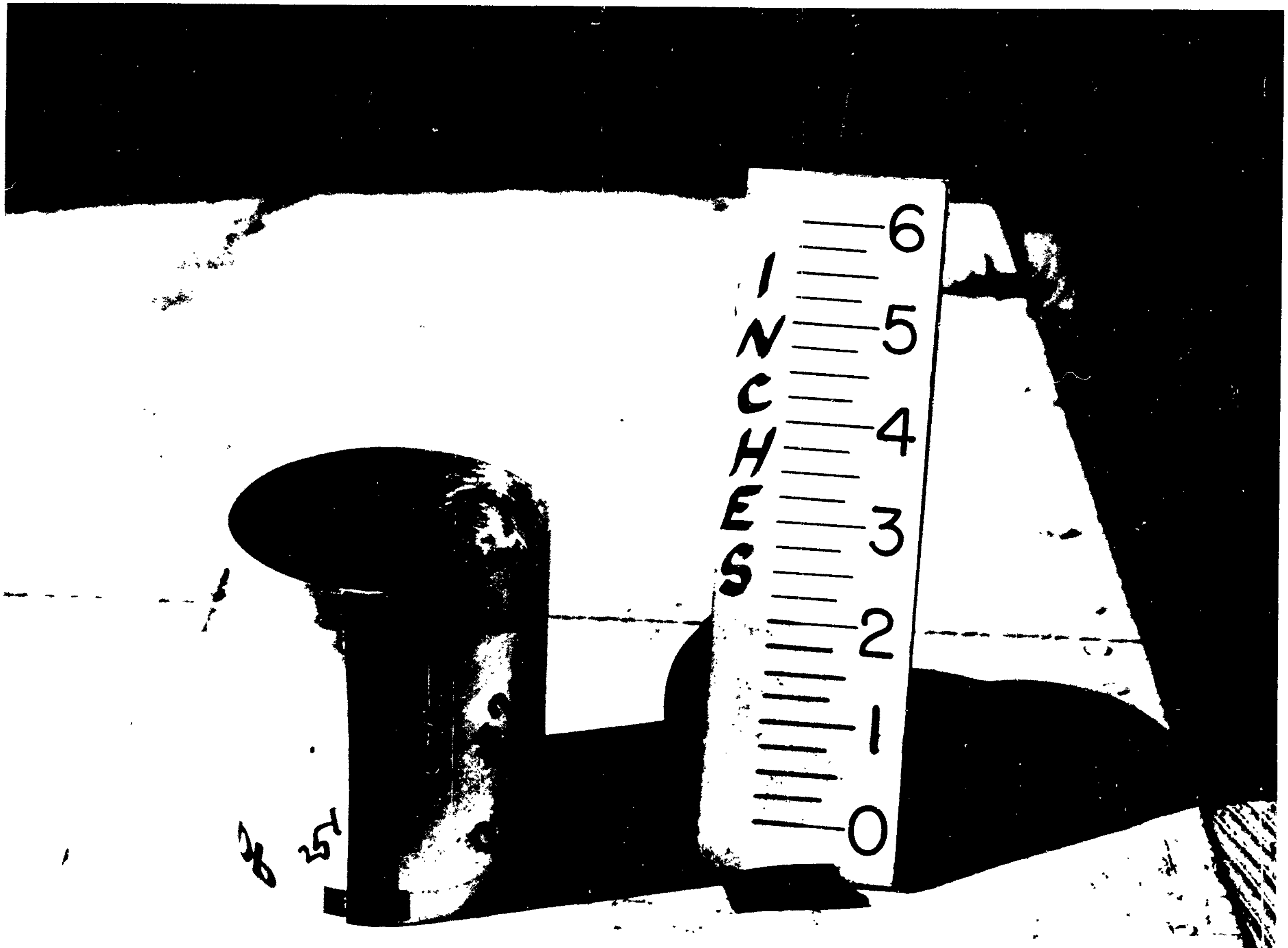

FIG. 96 — SHELL NO. 87

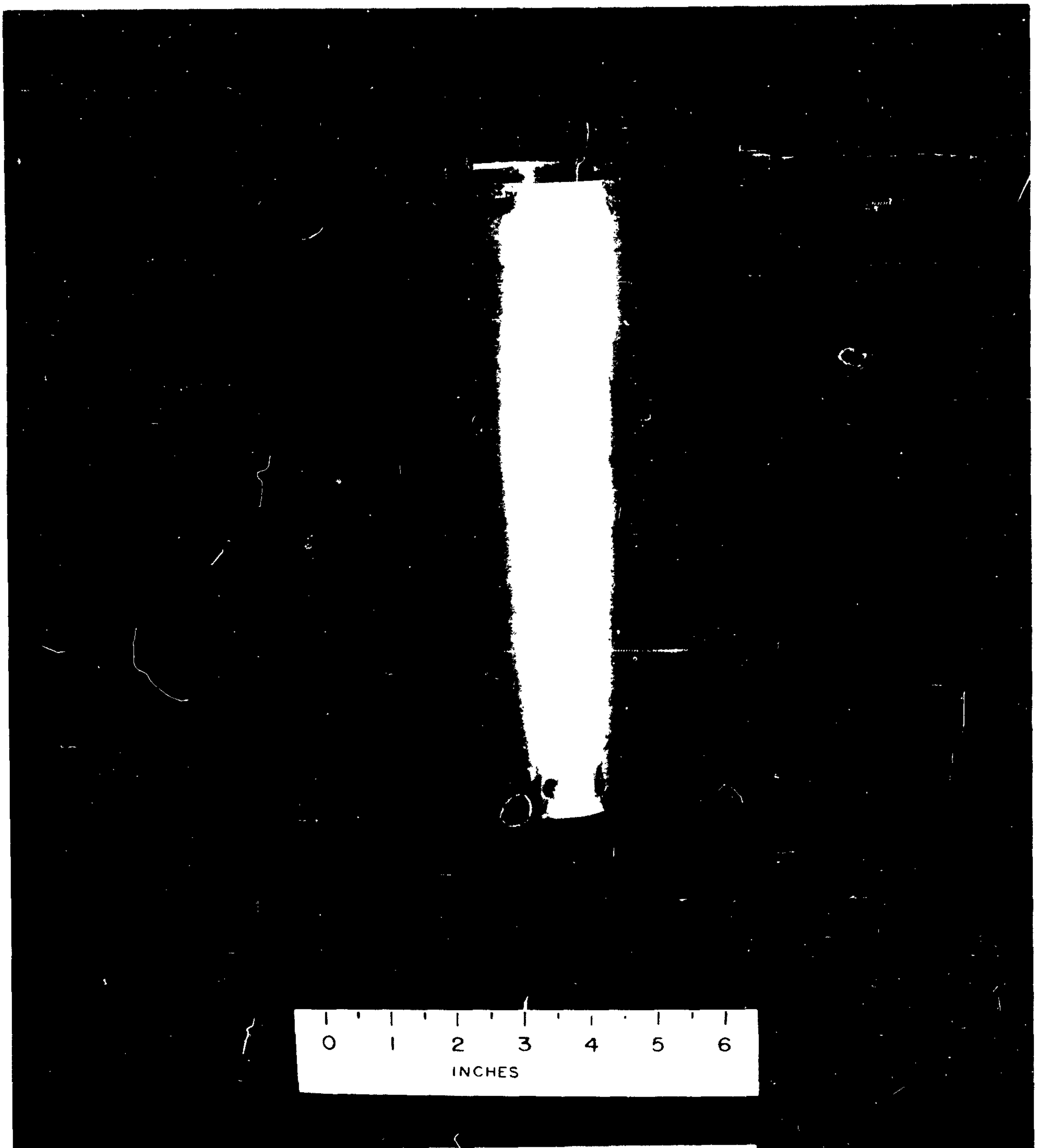

FIG. 97 - SHELL NO. 88 - FRONT VIEW

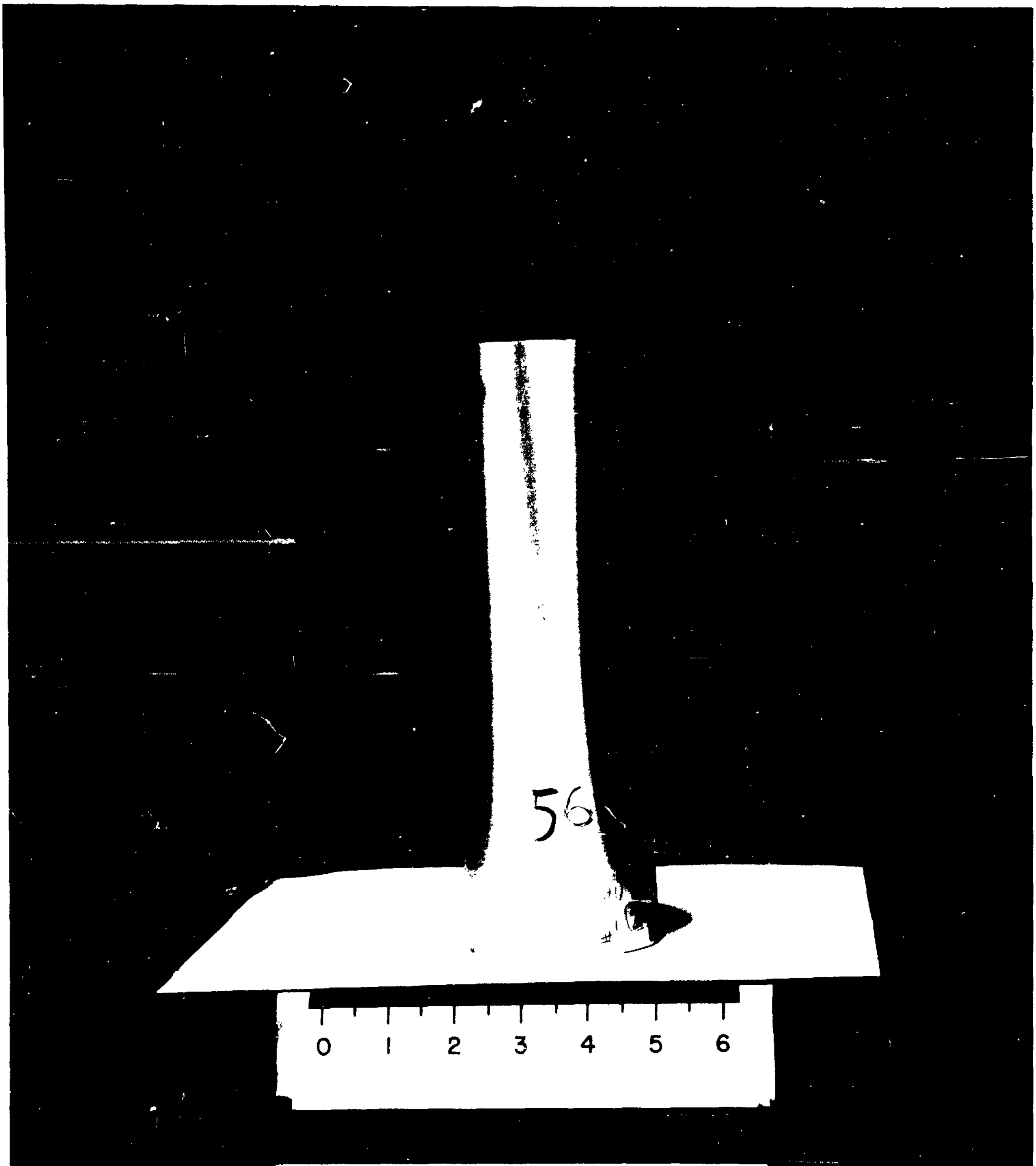

FIG. 98 - SHELL NO. 88- SIDE VIEW

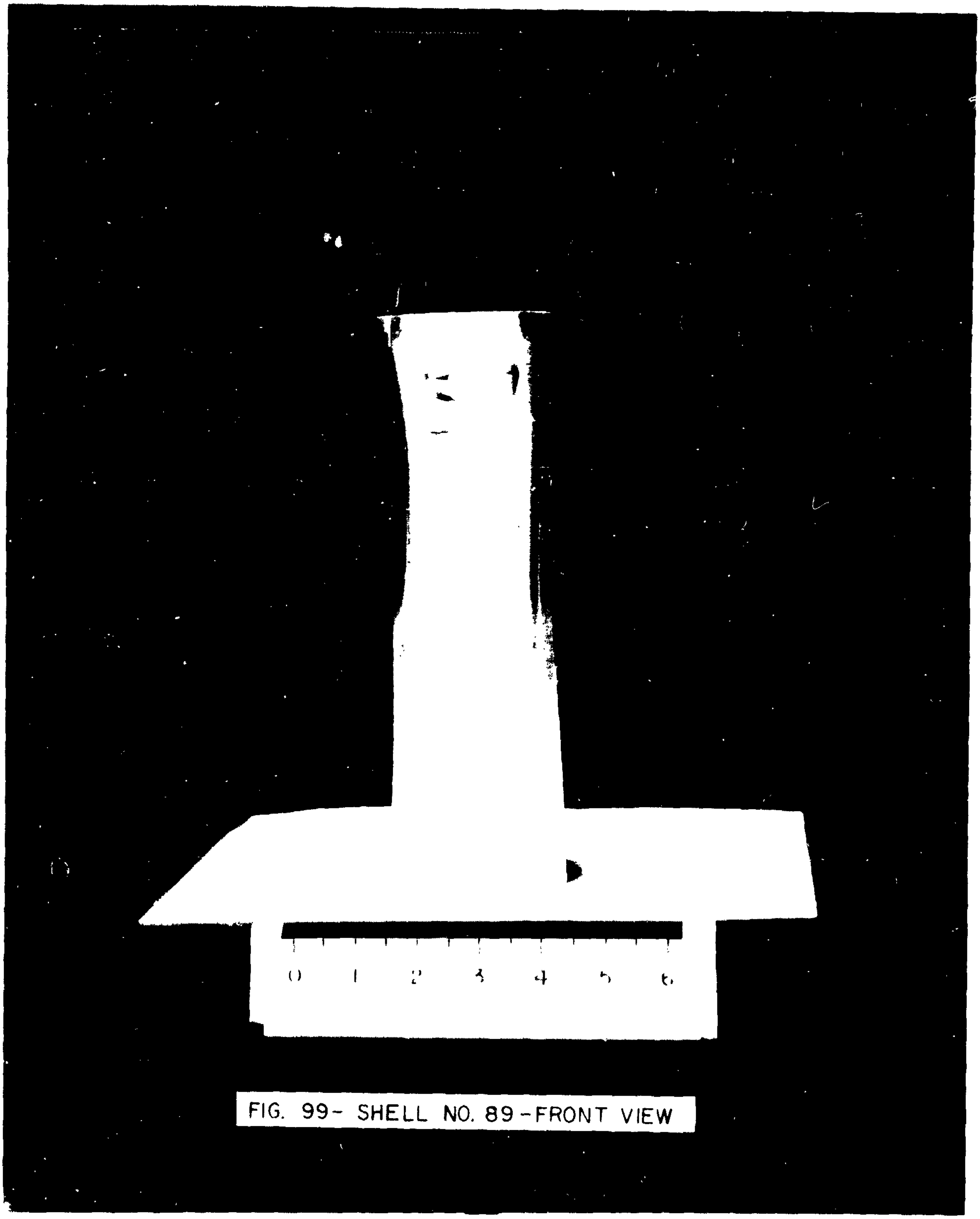

FIG. 99- SHELL NO. 89-FRONT VIEW

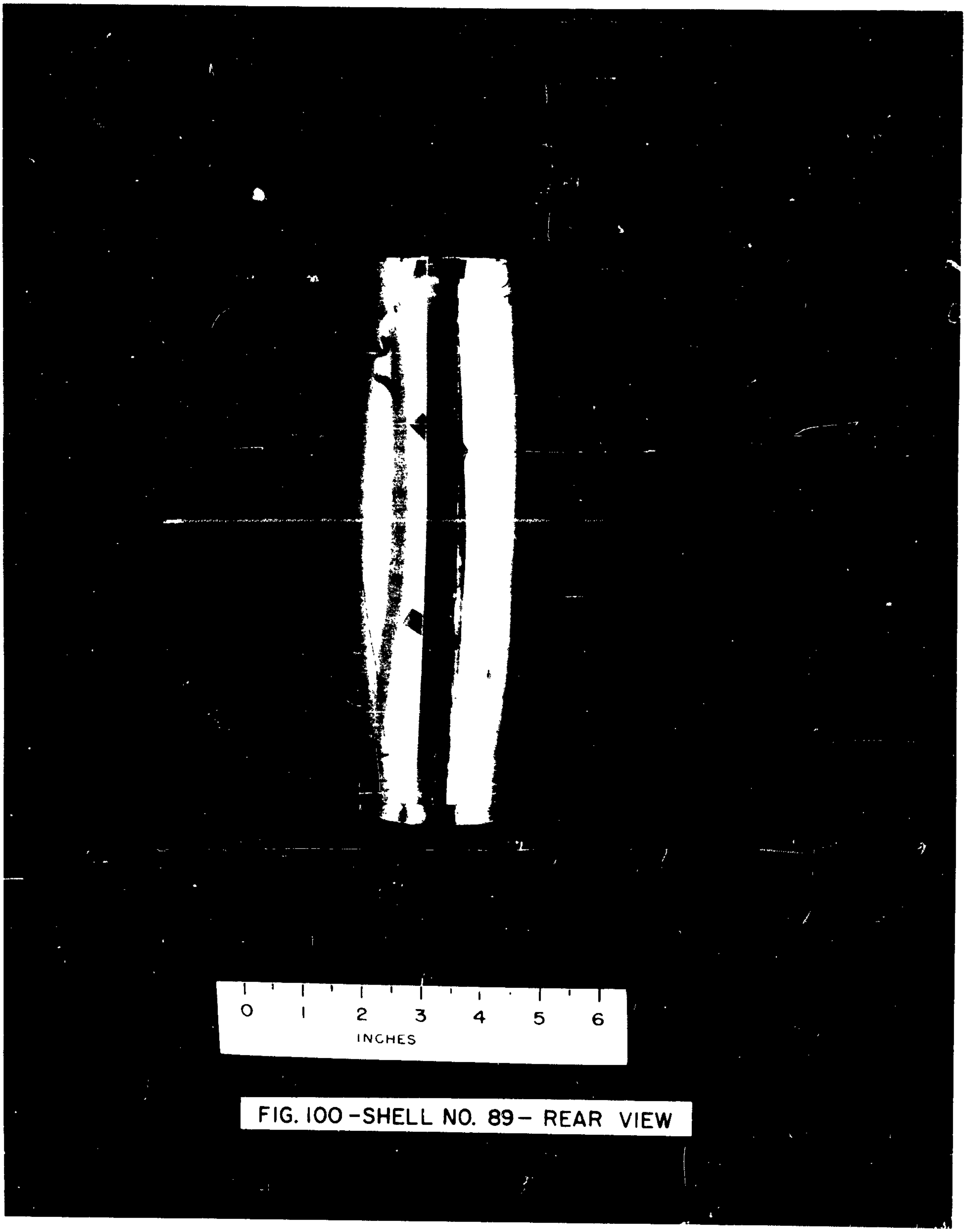

FIG. 100 - SHELL NO. 89 - REAR VIEW

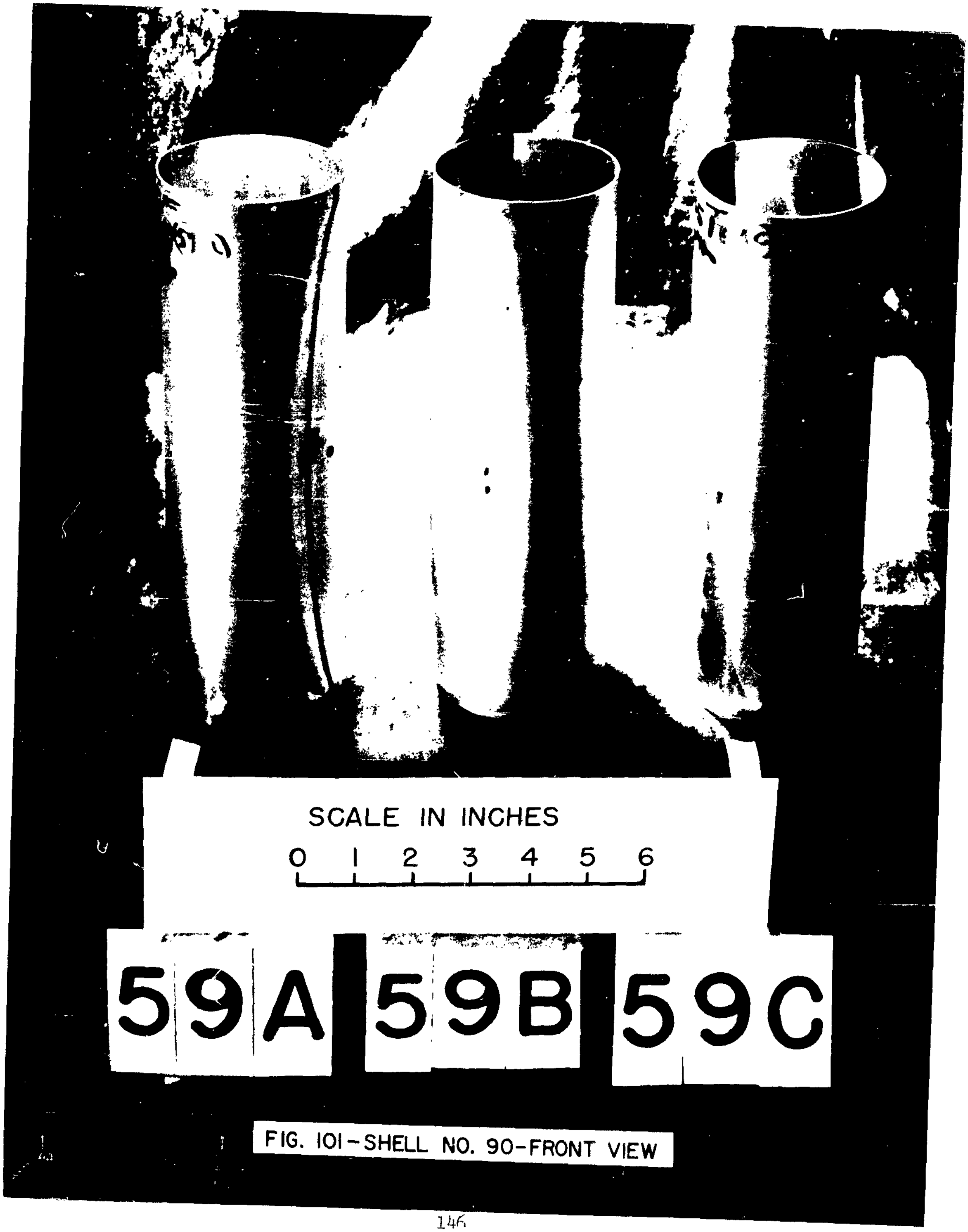

FIG. 101-SHELL NO. 90-FRONT VIEW

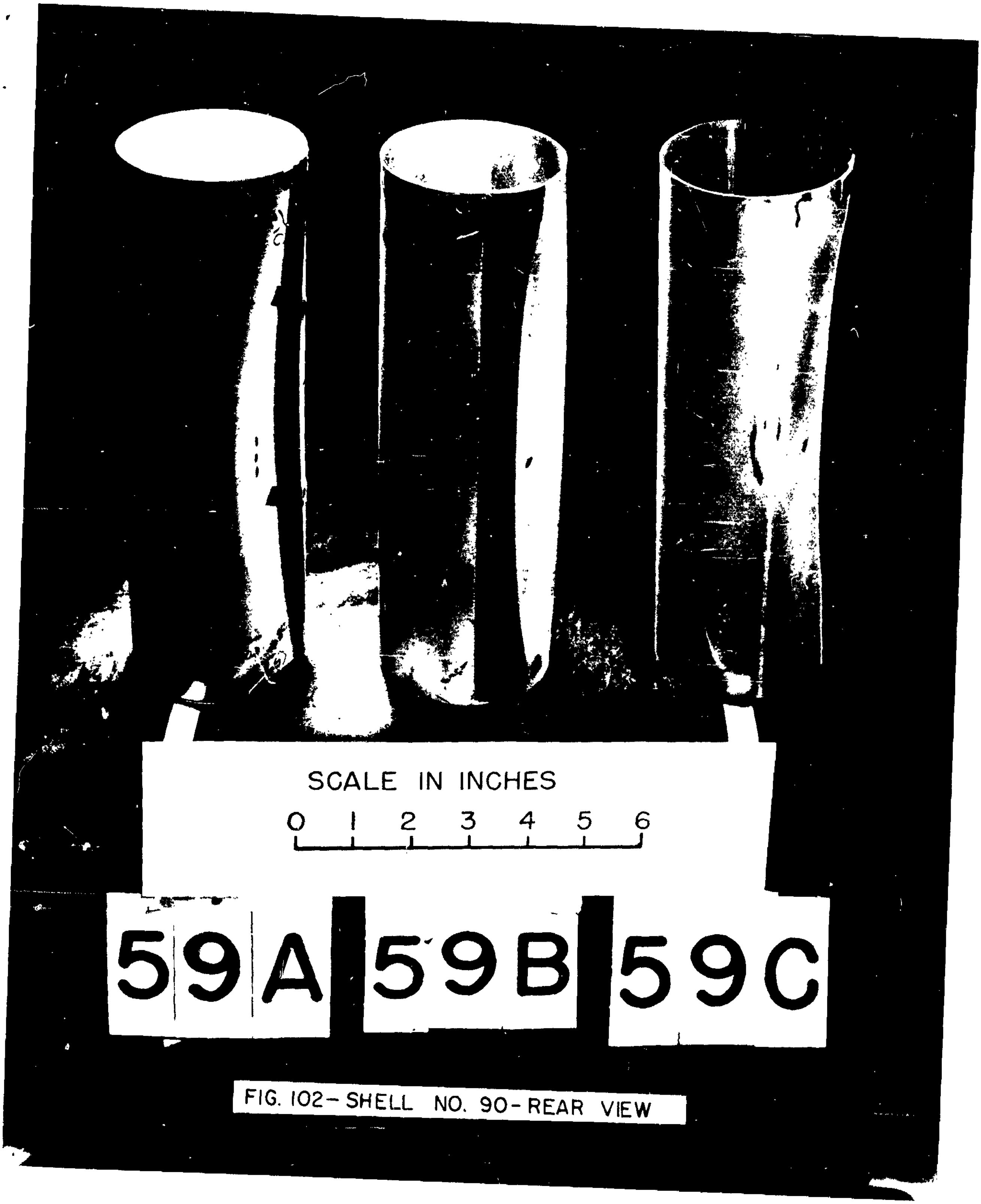

FIG. 102 - SHELL NO. 90 - REAR VIEW

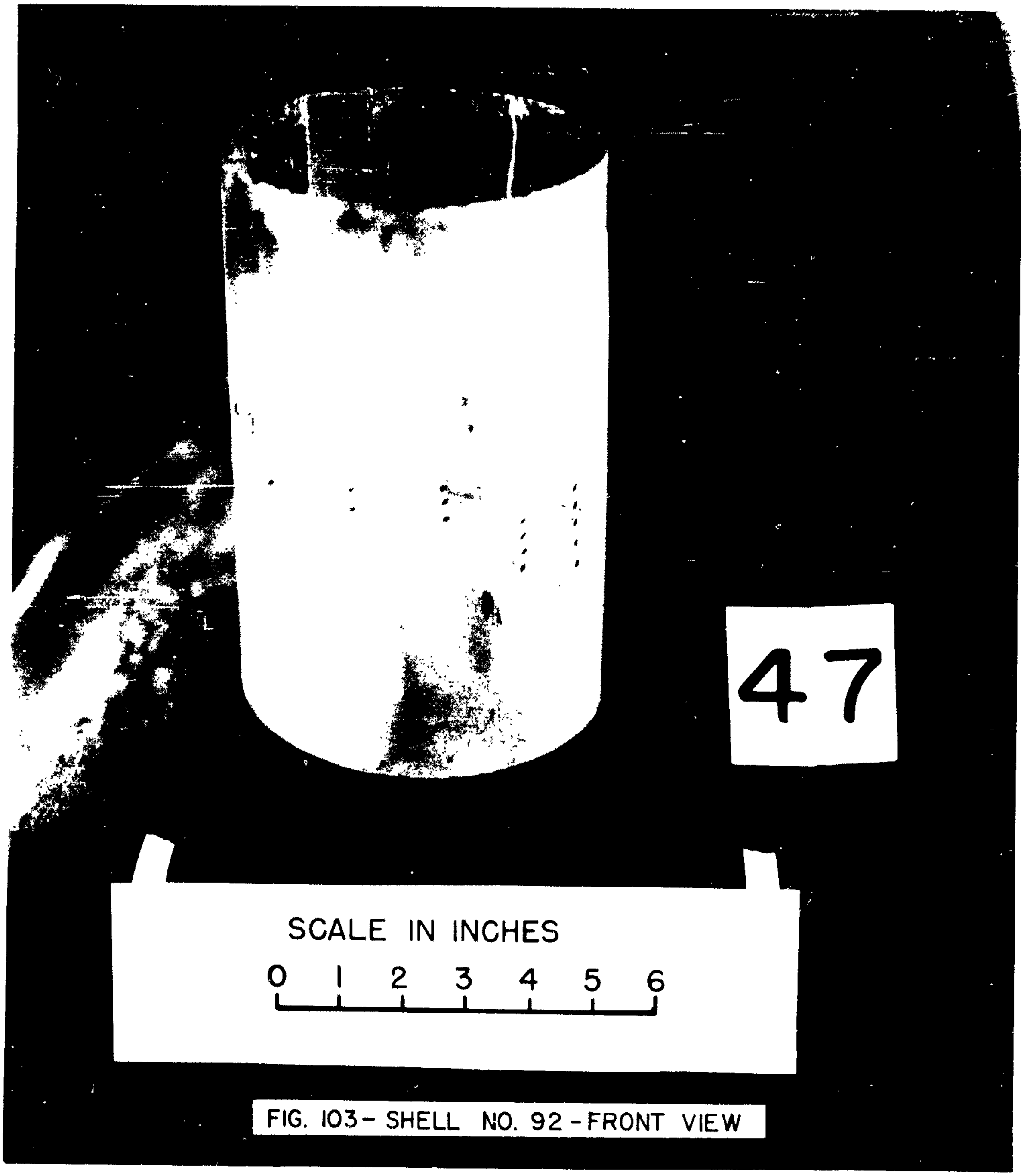

FIG. 103 - SHELL NO. 92 - FRONT VIEW

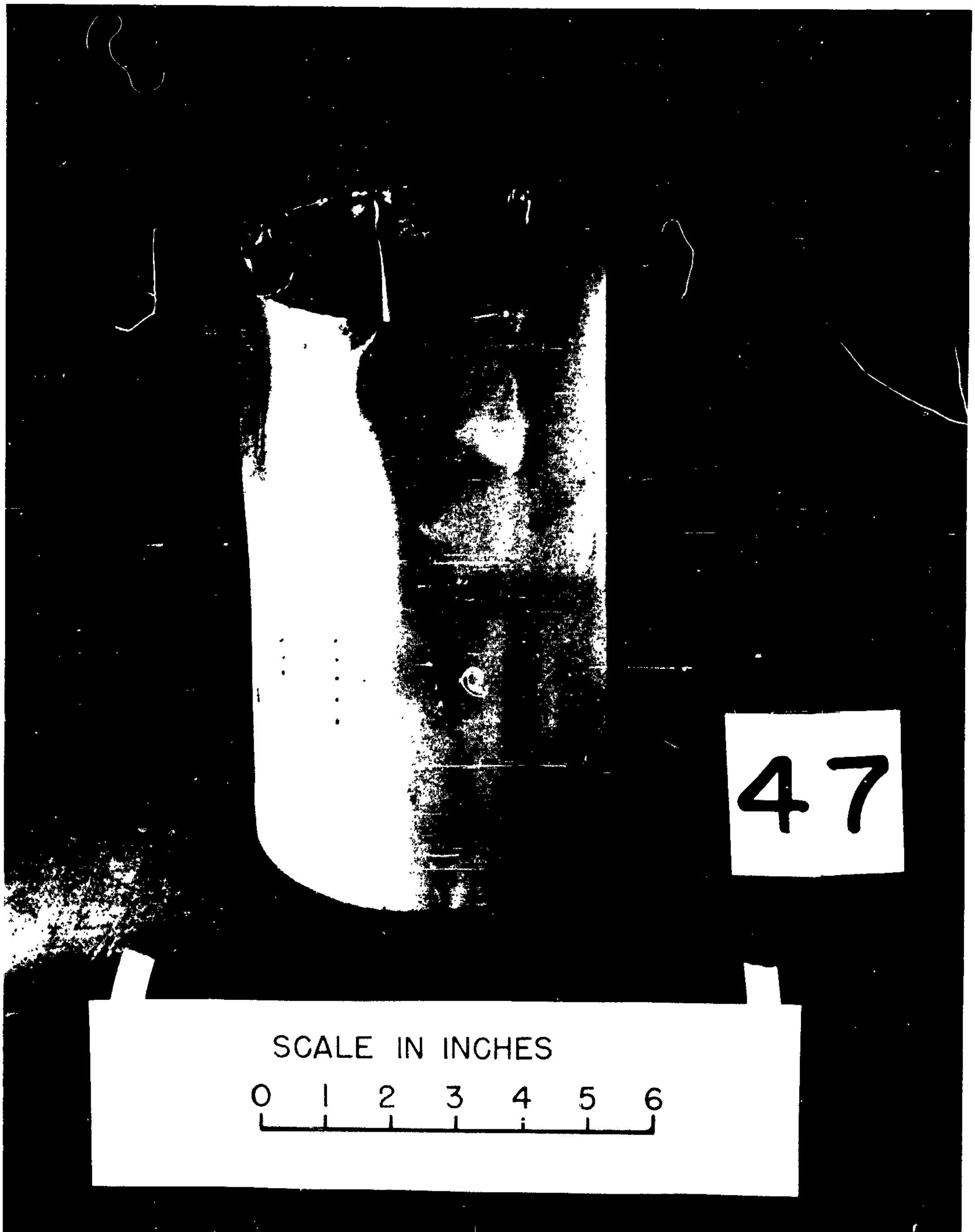

FIG. 104 - SHELL NO. 92 - SIDE VIEW

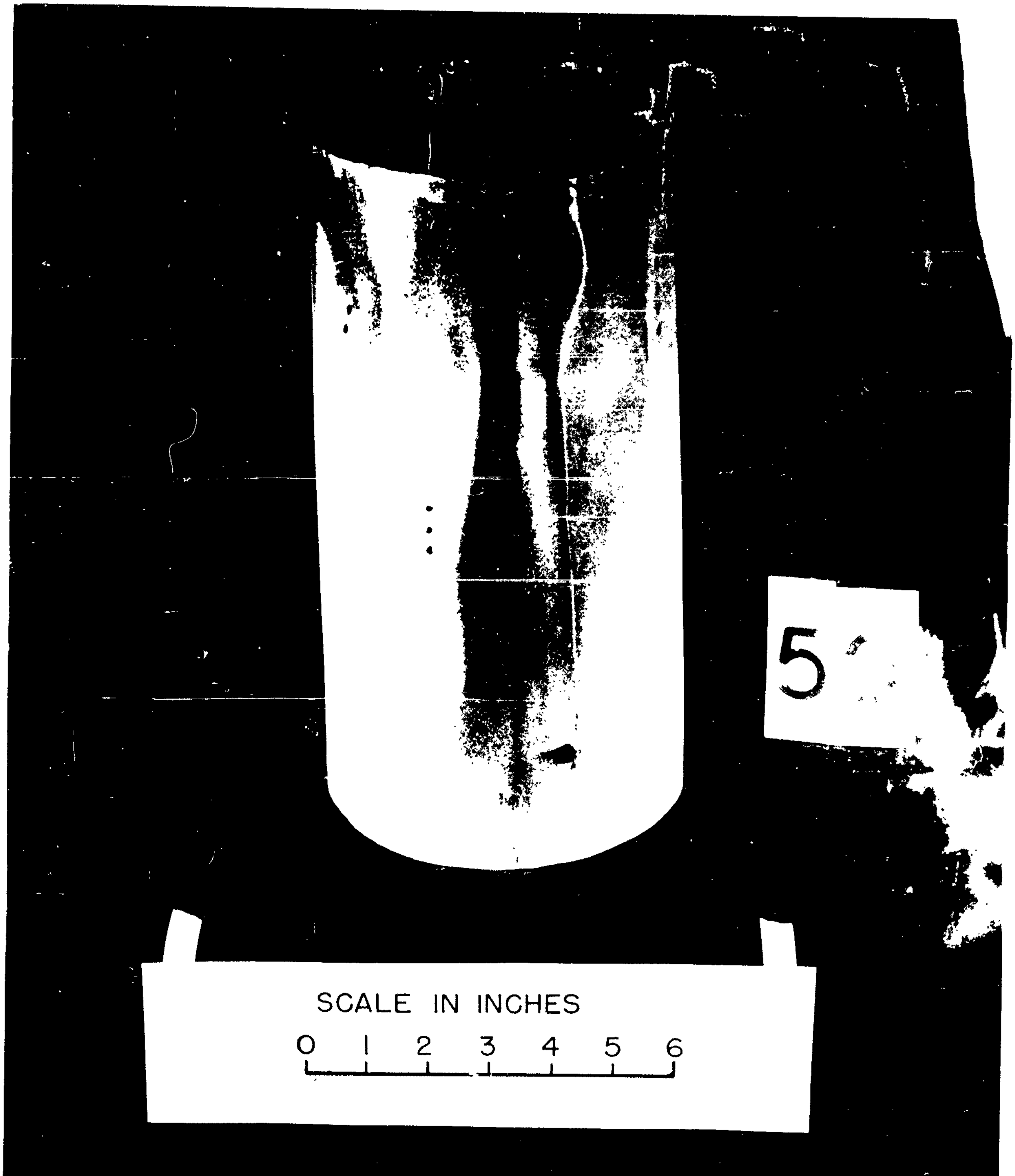

FIG. 105-SHELL NO. 93-FRONT VIEW

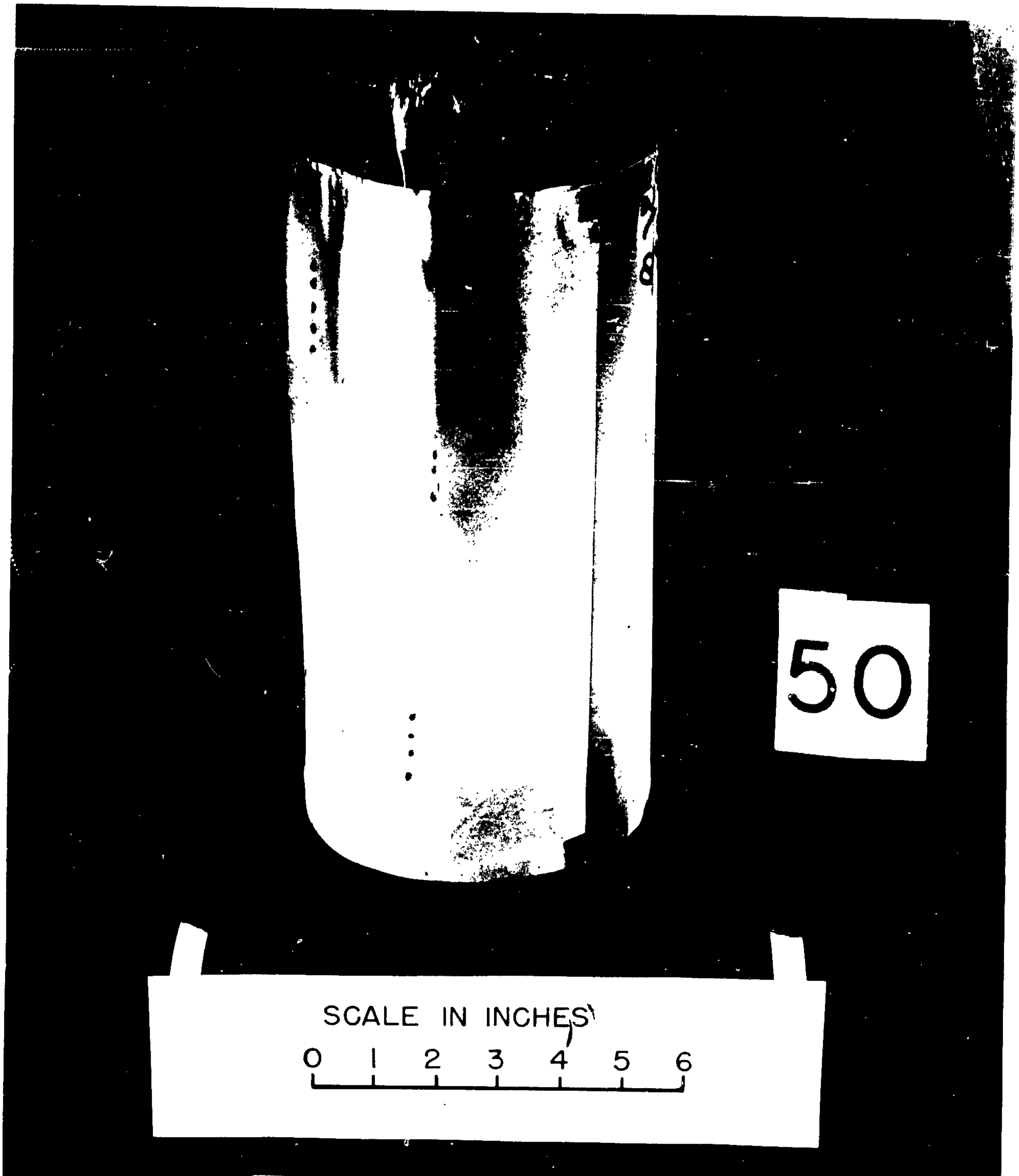

FIG. 106—SHELL NO. 93—REAR VIEW

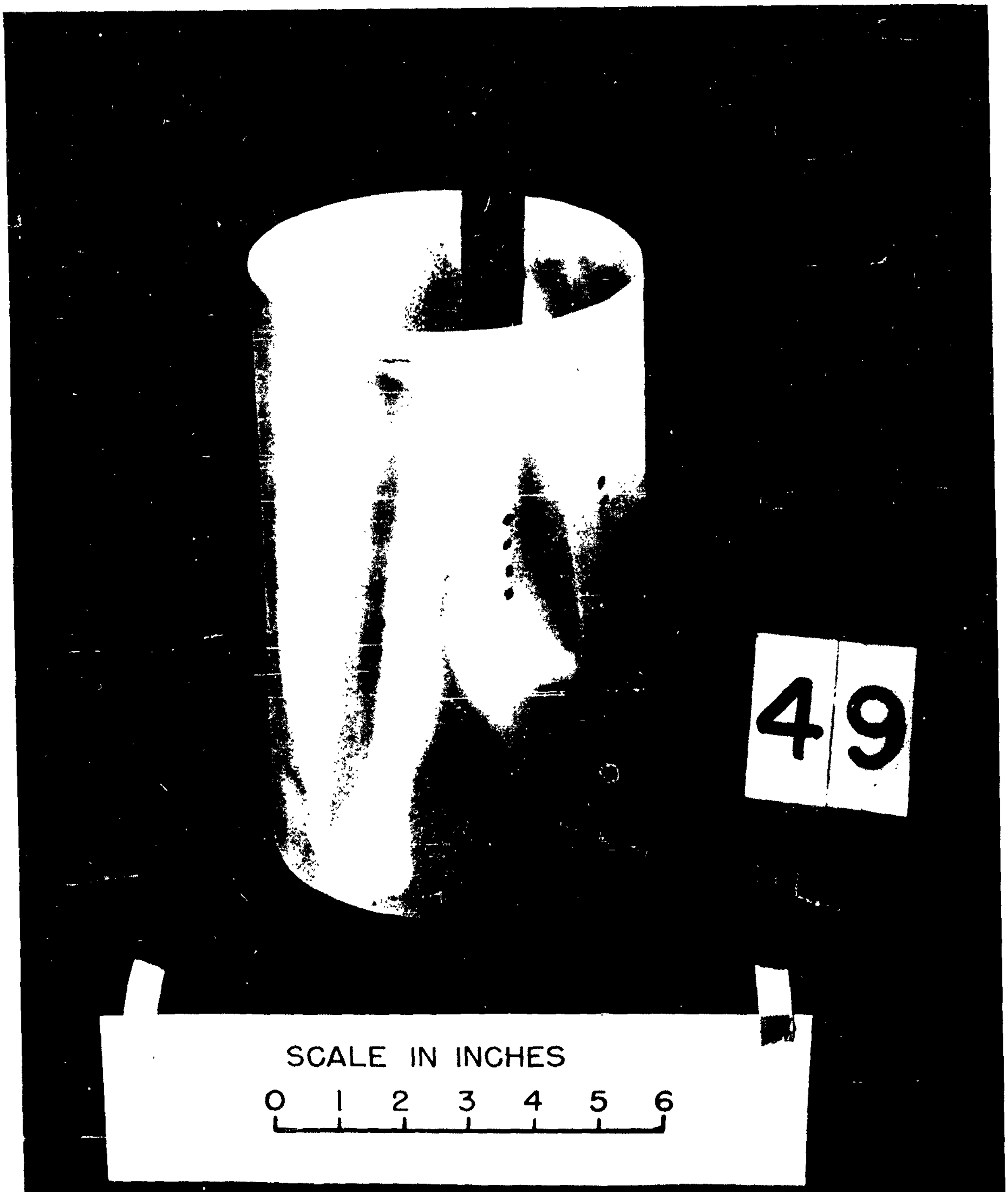

FIG. 107 - SHELL NO. 96 - FRONT VIEW

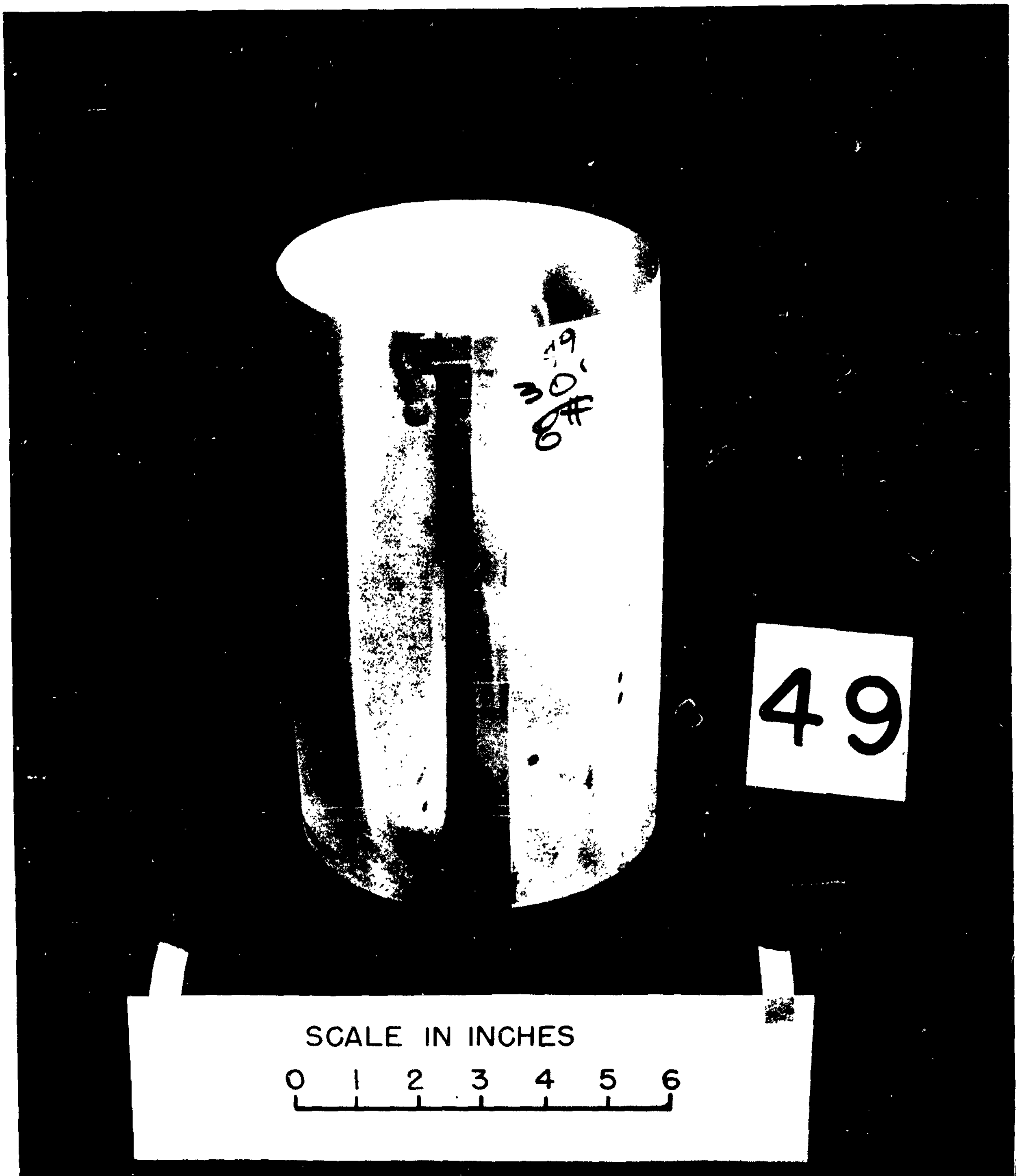

FIG. 108- SHELL NO. 96- REAR VIEW

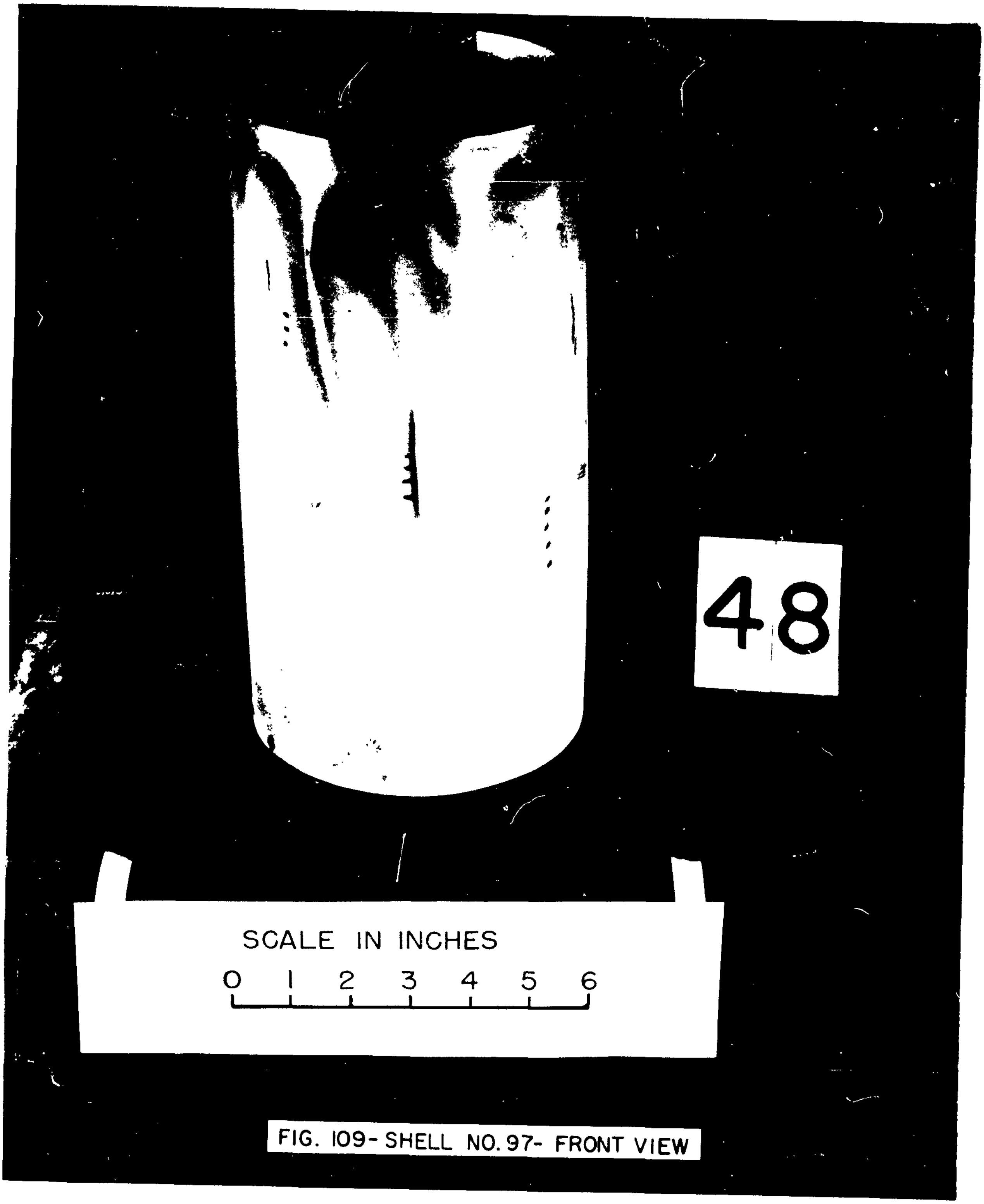

FIG. 109- SHELL NO. 97- FRONT VIEW

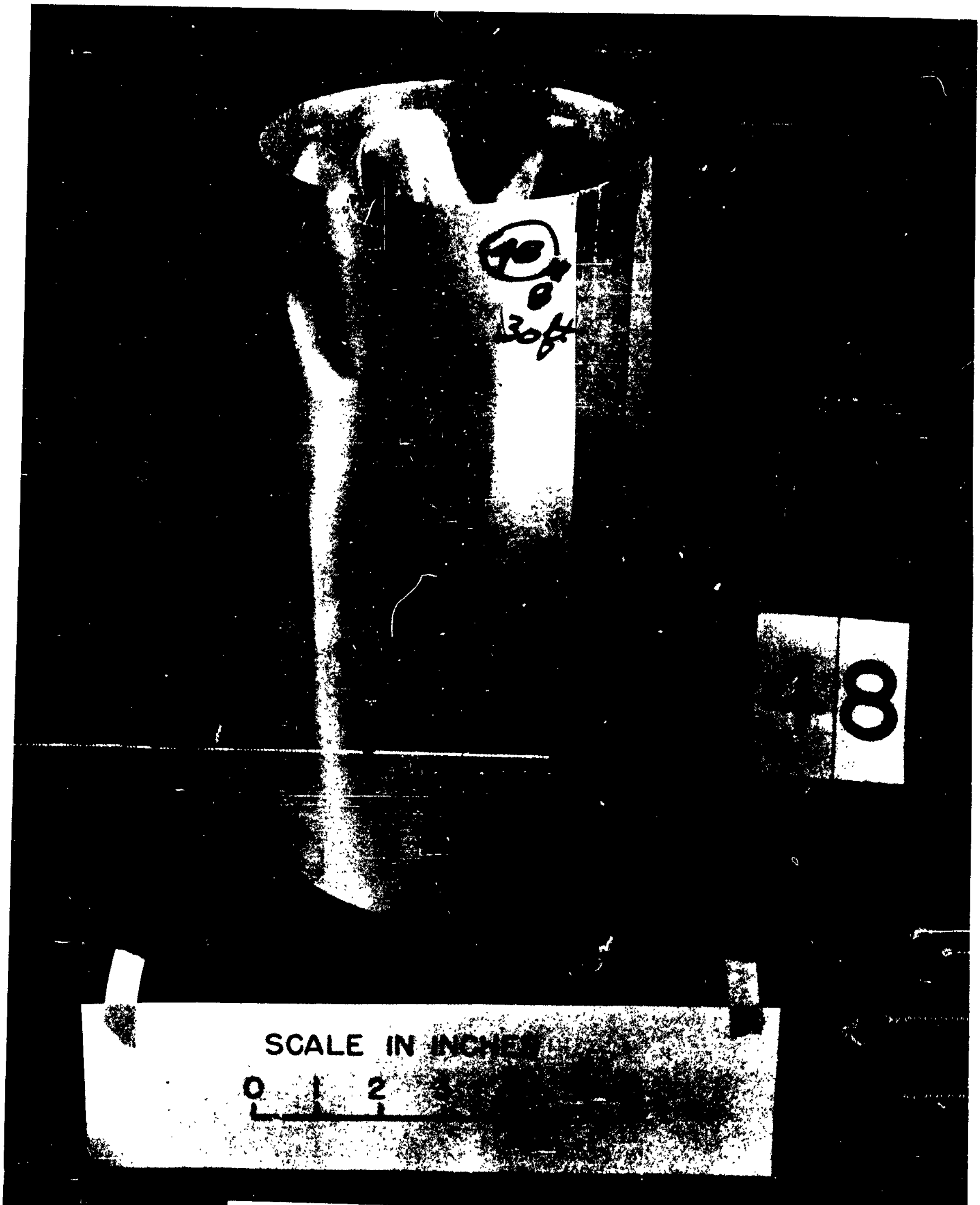

FIG. 110 - SHELL NO. 97 - REAR VIEW

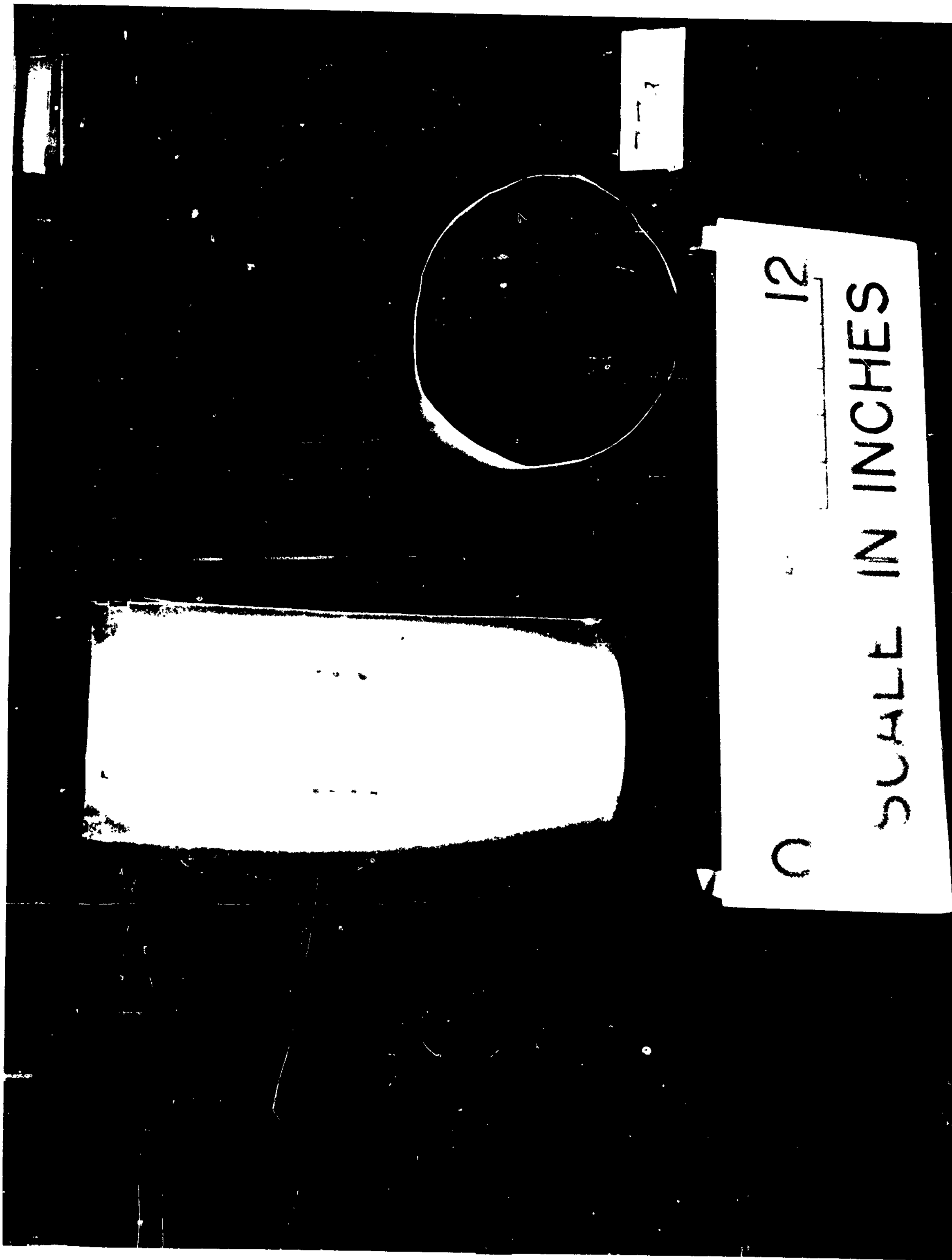

FIG. 111 - SHELL NO. 98 - FRONT VIEW

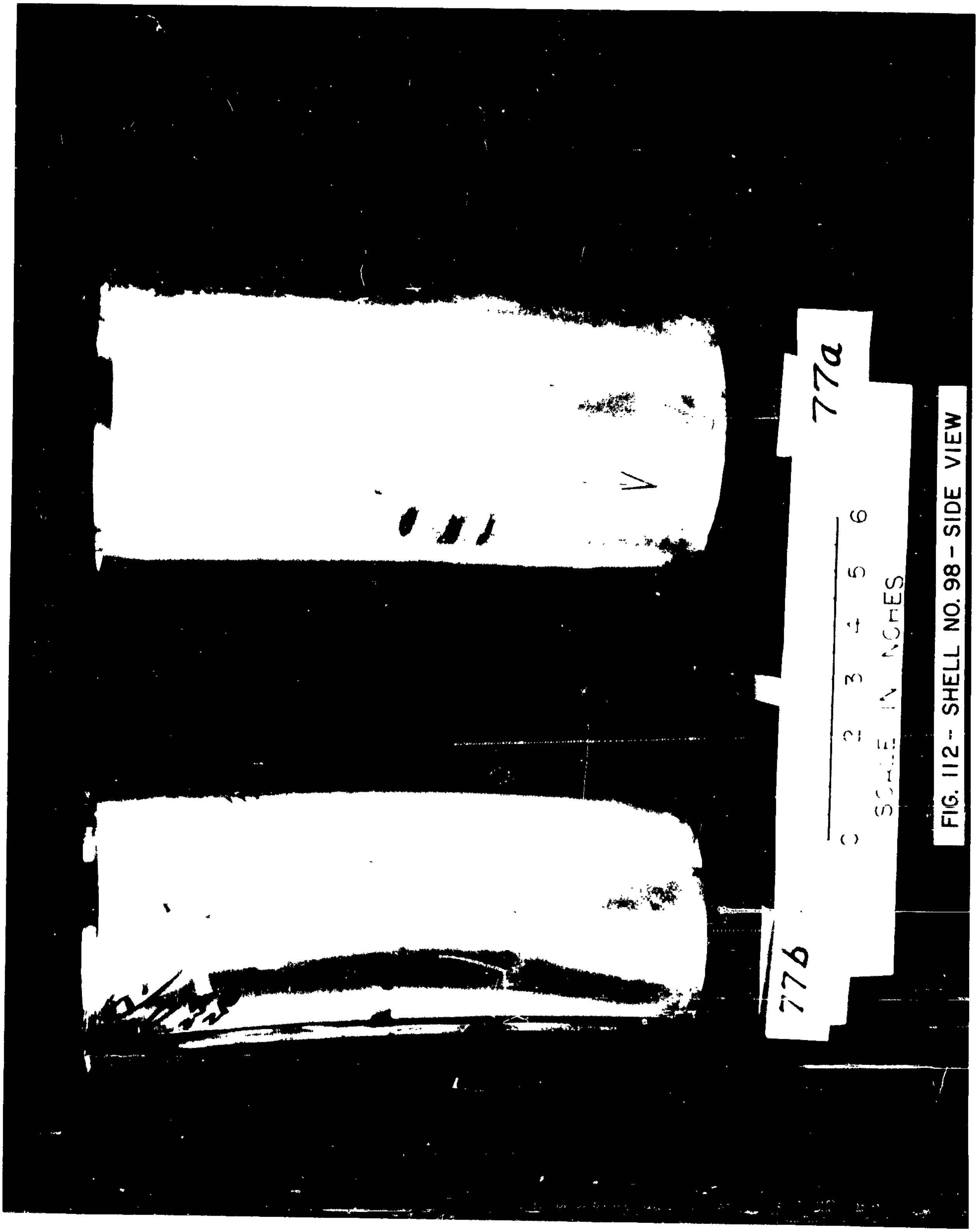

FIG. 112 - SHELL NO. 98 - SIDE VIEW

FIG. 113-SHELL NO.99-FRONT VIEW

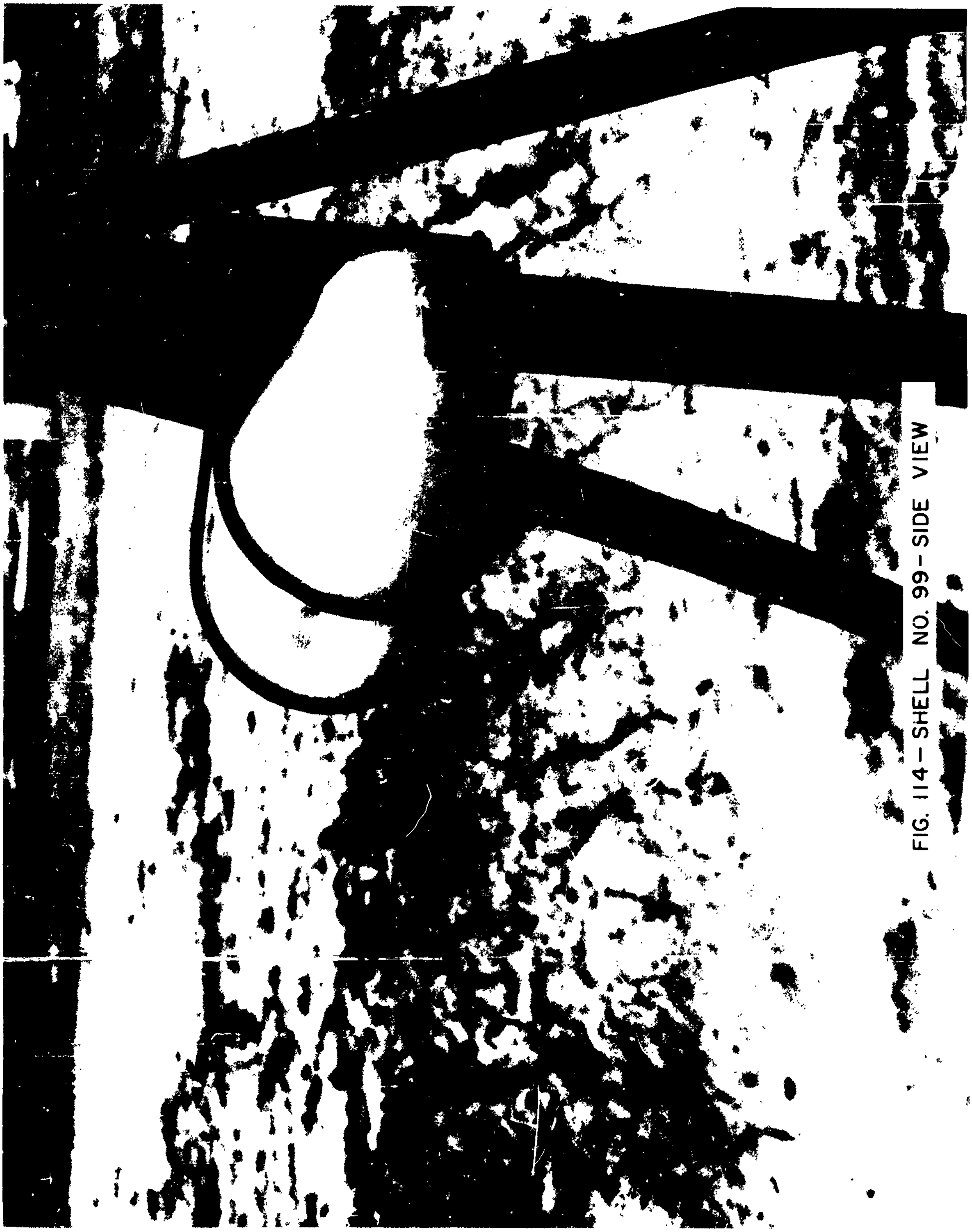

FIG. 114 – SHELL NO. 99 – SIDE VIEW

APPENDIX B

DEFORMATION OF LONGITUDINALLY LOADED SHELLS

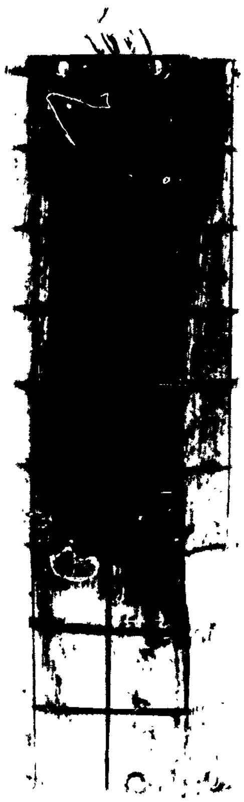

FIG. I - SHELL NO.3b-FRONT VIEW

FIG. 2 – SHELL NO. 3b – END VIEW

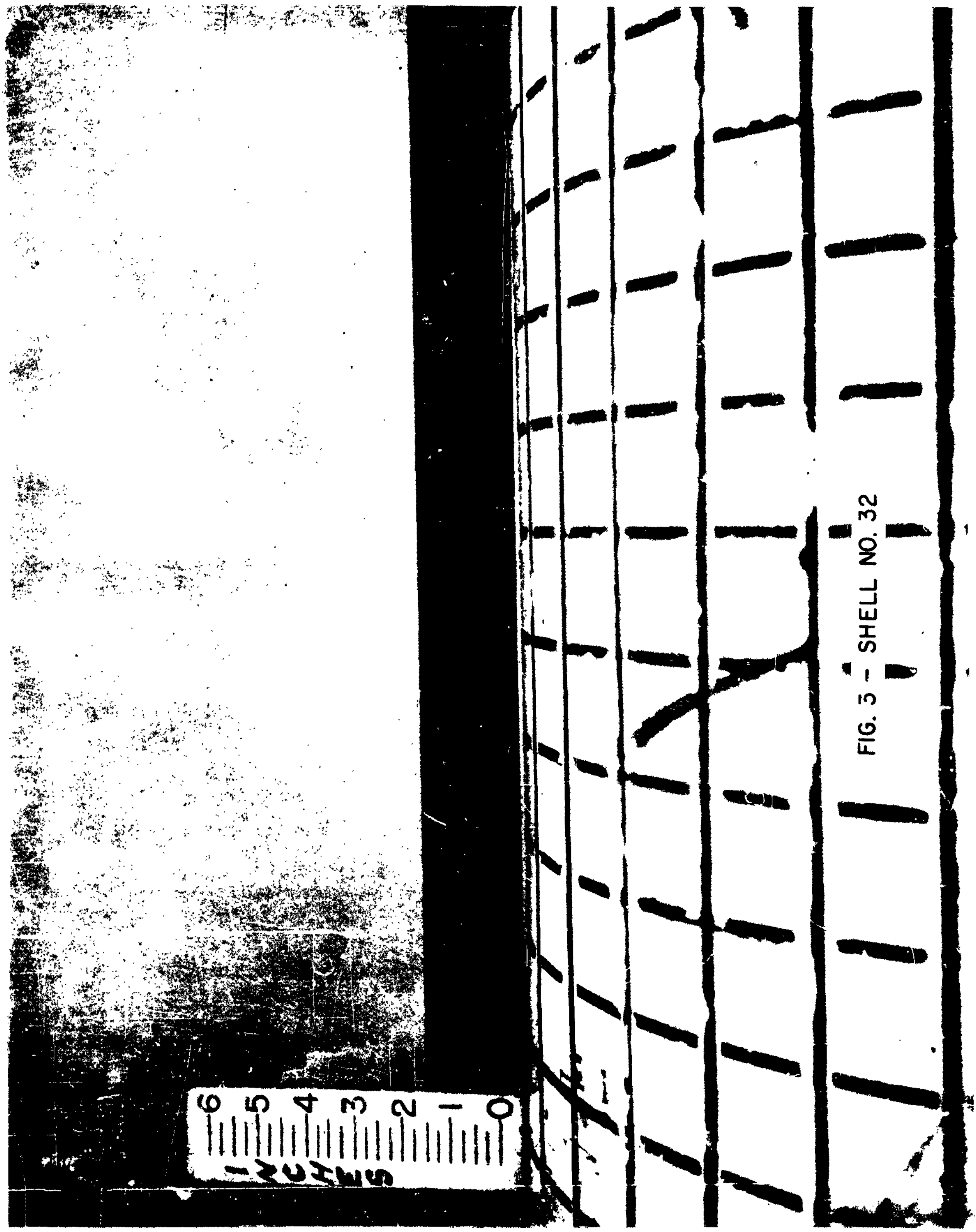

FIG. 3 - SHELL NO. 32

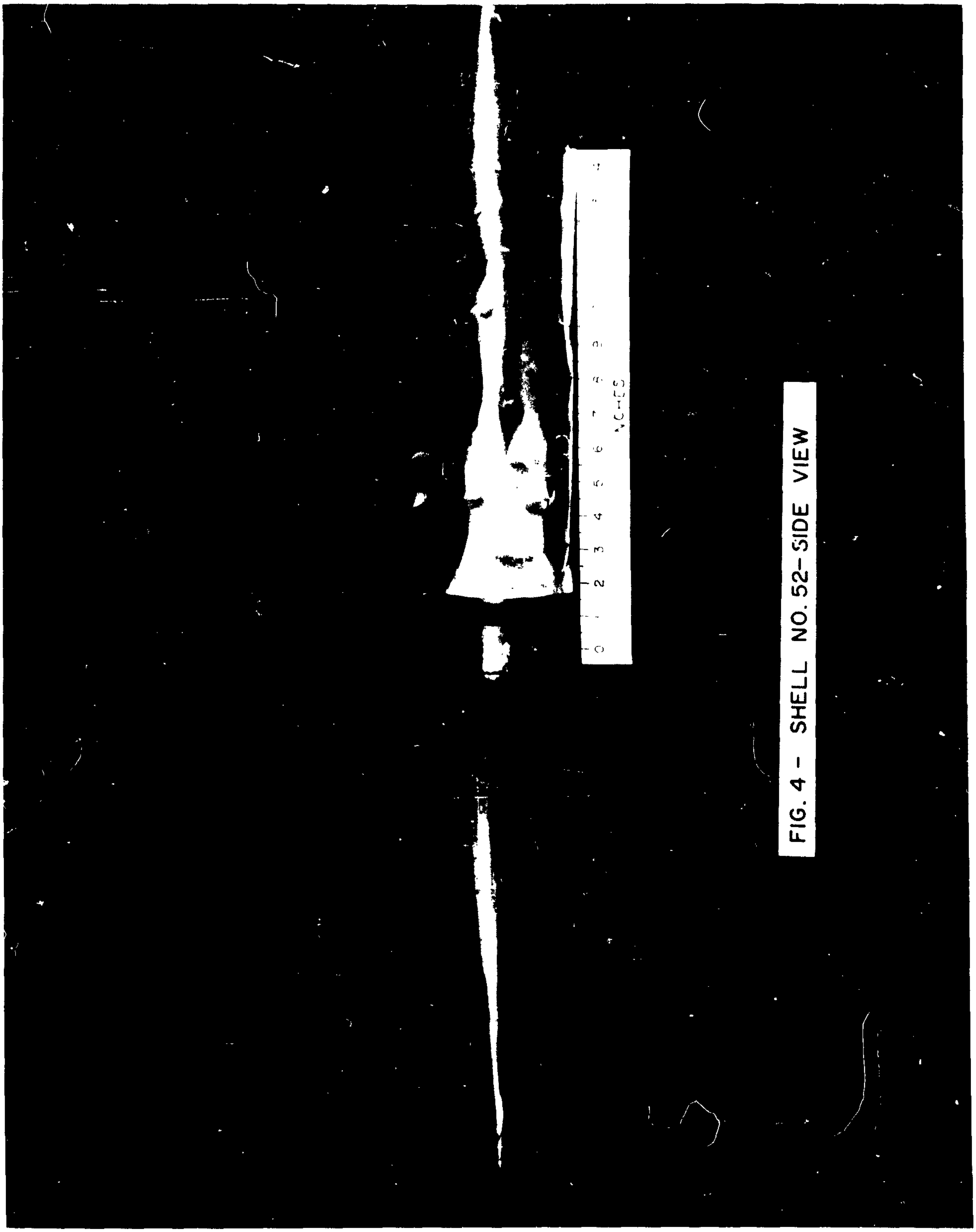

FIG. 4 - SHELL NO. 52- SIDE VIEW

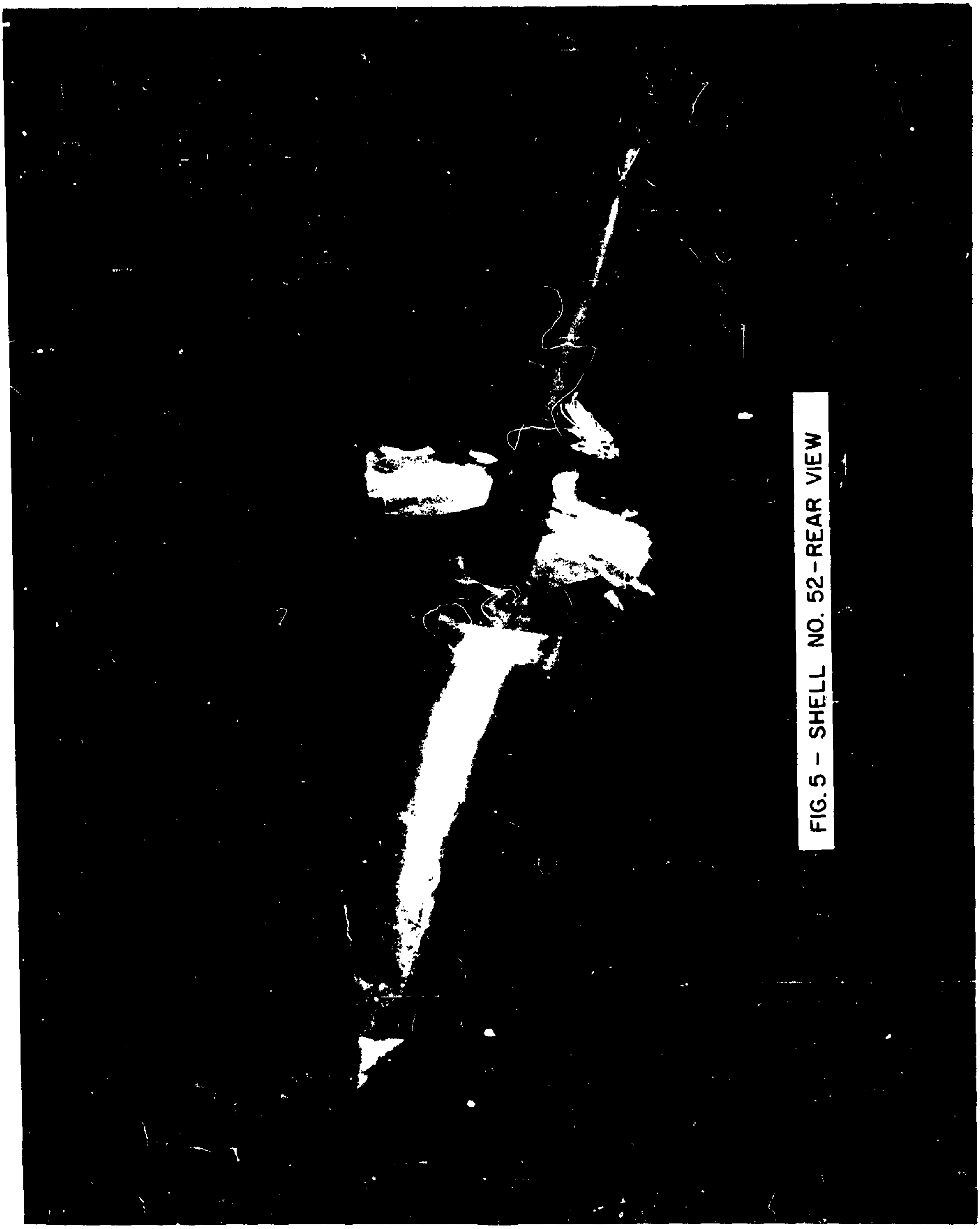

FIG. 5 – SHELL NO. 52-REAR VIEW

FIG. 6 – SHELL NO. 73

FIG. 7 – SHELL NO. 74

REFERENCES

1. Hodge, P. G. Impact Pressure Loading of Rigid-Plastic Cylindrical Shells Polytechnic Institute of Brooklyn Report No. 255, May 1954.

Hodge, P. G. Ultimate Dynamic Load of a Circular Cylindrical Shell Polytechnic Institute of Brooklyn Report No. 265, November 1954.

Hodge, P. G. The Influence of Blast Characteristics on the Final Deformation of Circular Cylindrical Shells Polytechnic Institute of Brooklyn Report No. 266, December 1954.

Sankaranarayanan, R. Dynamic Response of Plastic Circular Cylindrical Shells Under Lateral and Hydrostatic Pressures Polytechnic Institute of Brooklyn Report No. 573, June 1961.

2. Mindlin, R. D. and Bleich, H. H. Response of an Elastic Cylindrical Shell to a Transverse Step Shock Wave Technical Report No. 3, Contract Nonr-266(08), Columbia University, March 1952.

Baron, M. L. and Bleich, H. H. Further Studies of the Response of a Cylindrical Shell to a Transverse Shock Wave Technical Report No. 10, Contract Nonr-266(08), Columbia University, December 1953.

Bleich, H. H. and Dimaggio, F. L. Dynamic Buckling of Submerged Plates and Shells Technical Report No. 12, Contract Nonr-266(08), Columbia University, September 1954.

3. Seide, P., Weingarten, V. I., and Morgan, E. J. Final Report on the Development of Design Criteria for Elastic Stability of Thin Shell Structures Space Technology Laboratories, AFBMD/TR-61-7, December 1960.

Final Report on Buckling of Shells Under Dynamic Loads Final Report, Contract NASr-56, Space Technology Laboratories, October 1961.

4. Radkowski, P. P. et al Studies on the Dynamic Response of Shell Structures and Materials to a Pressure Pulse AVCO Corporation, AFSWC-TR-61-31 (II), July 1961.

5. DeHart, R. C. and Basdekas, N. L. Response of Aircraft Fuselages and Missile Bodies to Blast Loading Southwest Research Institute, ASD-TDR-62 - Preprint, March 1962.

6. Scientific Observations on the Explosion of a 20 Ton TNT Charge, Volume One, General Information and Measurements Report No. 203, Suffield Experimental Station, Ralston, Alberta, September 1961.

7. Goodman, H. J. Compiled Free-Air Blast Data on Bare Spherical Pentolite, BRL Report No. 1092, February 1960.

8. Baker, W. E. and Schuman, W. J. Air Blast Data for Correlation with Moving Airfoil Tests BRL Technical Note No. 1421, August 1961.

9. Kinney, G. F. Explosive Shocks in Air The MacMillan Company, 1962.

10. Cole, R. H. Underwater Explosions Princeton University Press, 1948.

DISTRIBUTION LIST

No. of Copies	Organization
10	Commander Armed Services Technical Information Agency ATTN: TIPCR Arlington Hall Station Arlington, Virginia
2	Chief Defense Atomic Support Agency ATTN: Blast and Shock Division Washington 25, D. C.
1	Commanding General Field Command Defense Atomic Support Agency Sandia Base P. O. Box 5100 Albuquerque, New Mexico
1	Director Defense Research and Engineering (OSD) ATTN: Director/Electronics Washington 25, D. C.
1	Director IDA/Weapon Systems Evaluation Group Room 1E875, The Pentagon Washington 25, D. C.
1	Commanding General U. S. Army Materiel Command ATTN: AMCRD-RS-PE-Bal Research and Development Directorate Washington 25, D. C.
5	Commanding Officer Picatinny Arsenal ATTN: Feltman Research and Engineering Laboratories Dover, New Jersey
1	Commanding Officer Harry Diamond Laboratories ATTN: Technical Information Office, Branch 012 Washington 25, D. C.
1	Commanding General U. S. Army Missile Command ATTN: ORDXM-RFC Redstone Arsenal, Alabama
1	Defense Intelligence Agency ATTN: AP1(K2), Mr. White Washington 25, D. C.
2	Commander U. S. Naval Ordnance Laboratory White Oak Silver Spring 19, Maryland
2	Director U. S. Naval Research Laboratory ATTN: Code 5367 Washington 25, D. C.
1	Commander U. S. Naval Ordnance Test Station ATTN: Army Ordnance Representative NOTS Annex 3202 E. Foothill Boulevard Pasadena 8, California
1	Commander U. S. Naval Missile Center Point Mugu, California
3	Chief Bureau of Naval Weapons ATTN: DIS-33 Department of the Navy Washington 25, D. C.

DISTRIBUTION LIST

No. of Copies	Organization
1	Commander U. S. Naval Ordnance Test Station ATTN: Code 4057 China Lake, California
1	Commander U. S. Naval Weapons Laboratory ATTN: Technical Library Dahlgren, Virginia
1	Commanding Officer Naval Ordnance Laboratory ATTN: Technical Library Corona, California
1	Inspector of Naval Material 428 South Warren Street Syracuse 2, New York
2	Commanding Officer Naval Air Development Center Johnsville, Pennsylvania
1	Chief of Naval Research ATTN: ONR: 439: N. Perrone Washington 25, D. C.
1	Commanding Officer and Director David W. Taylor Model Basin ATTN: Technical Library, Code 142 Washington 7, D. C.
2	Hq., USAF (AFRDC) Washington 25, D. C.
1	RADC Griffiss Air Force Base Rome, New York
1	FTD Wright-Patterson Air Force Base Ohio
1	Headquarters USAF Europe ATTN: Operations Analysis APO 633 New York, New York
1	ASD (ASRSMF-2) Wright-Patterson Air Force Base Ohio
4	ASD (ASRMDS-12) Wright-Patterson Air Force Base Ohio
4	BSD (BSBKR, BSTBK, BSQK, BSTAK) Norton Air Force Base California
2	AFSWC (SWRA) Kirtland Air Force Base Albuquerque, New Mexico
10	Director National Aeronautics and Space Administration ATTN: Mr. R. A. Schmidt, Code MLO Washington 25, D. C.
4	Director National Aeronautics and Space Administration Langley Research Center ATTN: Mr. Harold B. Pierce, Atmospheric Input Section Langley Field, Virginia
2	Marshall Space Flight Center ATTN: Claude Grain/M-P&VE-SD Huntsville, Alabama
2	National Aero Space Administration Manned Space Craft Houston 1, Texas

DISTRIBUTION LIST

No. of Copies	Organization
1	Applied Physics Laboratory ATTN: Col. Hackman 8621 Georgia Avenue Silver Spring, Maryland
1	AVCO Research and Advanced Development Division ATTN: Mr. P. P. Radkowski 201 Lowell Street Wilmington, Massachusetts
1	Avidyne Research, Incorporated ATTN: Dr. N. P. Hobbs 76 Cambridge Street Burlington, Massachusetts
1	Aerospace Corporation ATTN: R. M. Cooper P. O. Box 95085 Los Angeles 45, California
1	Armour Research Foundation Mechanics Research Division ATTN: Dr. E. Sevin 10 West 35th Street Chicago 16, Illinois
2	Aircraft Armaments, Incorporated ATTN: Dr. W. E. Baker Cockeysville, Maryland
1	Boeing Company Seattle 14, Washington
1	Cornell Aeronautical Laboratory P. O. Box 235 Buffalo 21, New York
1	Falcon R&D Company Denver 18, Colorado
2	J. G. Engineering Research Associates 3831 Menlo Drive Baltimore 15, Maryland
1	Lockheed Missile and Space Division ATTN: Mr. J. F. M. Gram Sunnyvale, California
2	Lockheed-Georgia Company ATTN: B. H. Little, Jr. 865 Cobb Drive Marietta, Georgia
1	The Martin Marietta Corporation ATTN: H. R. Fuehrer, MP-109 Sand Lake Road Orlando, Florida
1	The Martin Marietta Company Baltimore 3, Maryland
1	The Martin Marietta Corporation Technical Development Section ATTN: Dr. A. A. Ezra Denver, Colorado
2	The Pennsylvania State University Department of Engineering Mechanics ATTN: Prof. N. Davids University Park, Pennsylvania
1	Republic Aviation Corporation ATTN: Sup. Eng. Library Farmingdale, Long Island, New York
1	Raytheon Company Mail No. 550 Hartwell Road Bedford, Massachusetts

DISTRIBUTION LIST

No. of Copies	Organization
1	Suffield Experimental Station ATTN: J. M. Dewey Ralston, Alberta, Canada
1	Kaman - Nuclear ATTN: D. C. Sachs Garden of Gods Road Colorado Springs, Colorado
1	Space Technology Laboratories ATTN: Dr. J. D. Wood One Space Park Renondo Beach, California
1	Stanford Research Institute Poulter Laboratories Division ATTN: Dr. G. Abrahamson Menlo Park, California
1	Southwest Research Institute Department of Mechanical Sciences ATTN: Dr. H. N. Abramson 8500 Calebra Road San Antonio 6, Texas
2	Massachusetts Institute of Technology ATTN: Dr. E. A. Witmer Dr. J. R. Ruetenik Cambridge 39, Massachusetts
1	University of Chicago Institute for Air Weapons Research Chicago 37, Illinois
10	The Scientific Information Officer Defence Research Staff British Embassy 3100 Massachusetts Avenue, N. W. Washington 8, D. C.
4	Defence Research Member Canadian Joint Staff 2450 Massachusetts Avenue, N. W. Washington 8, D. C.

AD Accession No. ______ UNCLASSIFIED

Ballistic Research Laboratories, APG
THE RESPONSE OF CYLINDRICAL SHELLS TO EXTERNAL BLAST LOADING
William J. Schuman, Jr.

Cylindrical shell - Deformation
Blast effects - Analysis

BRL Memorandum Report No. 1461 March 1963

RDT & E Project No. 1M010501A006
UNCLASSIFIED Report

A method of predicting permanent deformation of thin-walled unstiffened cylindrical shells to external blast loading from charges of high explosives is presented. Empirical relations are derived from a series of firings conducted at Aberdeen Proving Ground against scaled shells. The average deviation between the predicted and the actual blast pressures required for permanent deformation is 12%.

AD Accession No. ______ UNCLASSIFIED

Ballistic Research Laboratories, APG
THE RESPONSE OF CYLINDRICAL SHELLS TO EXTERNAL BLAST LOADING
William J. Schuman, Jr.

Cylindrical shell - Deformation
Blast effects - Analysis

BRL Memorandum Report No. 1461 March 1963

RDT & E Project No. 1M010501A006
UNCLASSIFIED Report

A method of predicting permanent deformation of thin-walled unstiffened cylindrical shells to external blast loading from charges of high explosives is presented. Empirical relations are derived from a series of firings conducted at Aberdeen Proving Ground against scaled shells. The average deviation between the predicted and the actual blast pressures required for permanent deformation is 12%.

AD Accession No. ______ UNCLASSIFIED

Ballistic Research Laboratories, APG
THE RESPONSE OF CYLINDRICAL SHELLS TO EXTERNAL BLAST LOADING
William J. Schuman, Jr.

Cylindrical shell - Deformation
Blast effects - Analysis

BRL Memorandum Report No. 1461 March 1963

RDT & E Project No. 1M010501A006
UNCLASSIFIED Report

A method of predicting permanent deformation of thin-walled unstiffened cylindrical shells to external blast loading from charges of high explosives is presented. Empirical relations are derived from a series of firings conducted at Aberdeen Proving Ground against scaled shells. The average deviation between the predicted and the actual blast pressures required for permanent deformation is 12%.

AD Accession No. ______ UNCLASSIFIED

Ballistic Research Laboratories, APG
THE RESPONSE OF CYLINDRICAL SHELLS TO EXTERNAL BLAST LOADING
William J. Schuman, Jr.

Cylindrical shell - Deformation
Blast effects - Analysis

BRL Memorandum Report No. 1461 March 1963

RDT & E Project No. 1M010501A006
UNCLASSIFIED Report

A method of predicting permanent deformation of thin-walled unstiffened cylindrical shells to external blast loading from charges of high explosives is presented. Empirical relations are derived from a series of firings conducted at Aberdeen Proving Ground against scaled shells. The average deviation between the predicted and the actual blast pressures required for permanent deformation is 12%.